

Construction of C–C, C–N and C–O Bonds on sp^2 / sp^3 Carbon via Radical Pathway

A dissertation submitted in partial fulfillment for the degree of
Doctor of Philosophy

Submitted by

Bilal Ahmad Mir
Roll No. 146122034



Department of Chemistry
Indian Institute of Technology Guwahati
Guwahati-781039, Assam, India
February, 2020

Construction of C–C, C–N and C–O Bonds on sp^2 / sp^3 Carbon via Radical Pathway

Submitted by

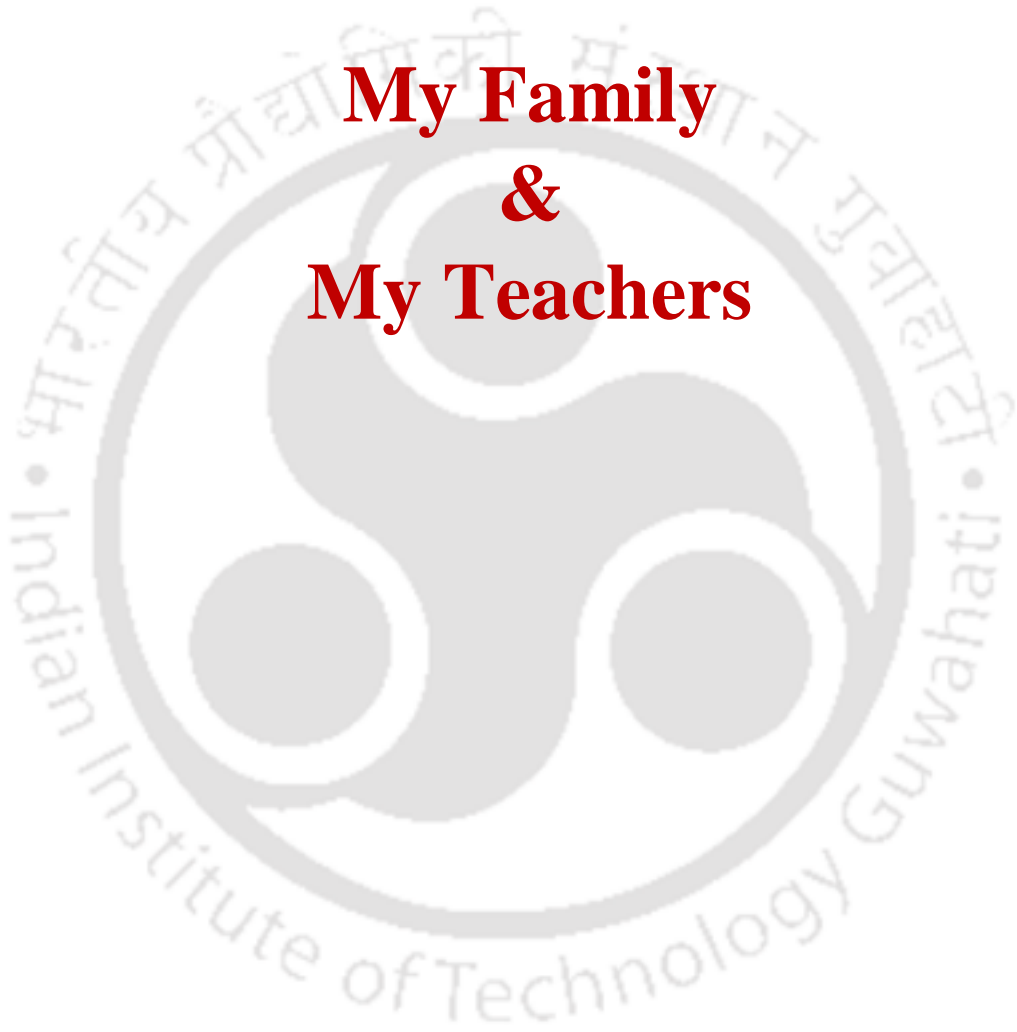
Bilal Ahmad Mir
Roll No. 146122034



Department of Chemistry
Indian Institute of Technology Guwahati
Guwahati-781039, Assam, India
February, 2020

Dedicated to

**My Family
&
My Teachers**





INDIAN INSTITUTE OF TECHNOLOGY GUWAHATI

Department of Chemistry

STATEMENT

I do hereby declare that the matter embodied in this thesis is the result of investigations carried out by me in the Department of Chemistry, Indian Institute of Technology Guwahati, India, under the guidance of Professor Bhisma K. Patel.

In keeping with the general practice of reporting scientific observations, due acknowledgements have been made wherever the work described is based on the findings of other investigators.

February, 2020
IIT Guwahati

Bilal Ahmad Mir



INDIAN INSTITUTE OF TECHNOLOGY GUWAHATI

Department of Chemistry

CERTIFICATE

This is to certify that Bilal Ahmad Mir has been working under my supervision since March, 2015 as a regular registered Ph. D. student. His thesis entitled “**Construction of C–C, C–N and C–O Bonds on sp^2 / sp^3 Carbon via Radical Pathway**” is an authentic record of the results obtained from the research work in the Department of Chemistry, Indian Institute of Technology Guwahati, India. I am forwarding his thesis to submit for the Ph. D. (Science) degree from this institute. I certify that he has fulfilled all the requirements according to the rules of this institute regarding the investigations embodied in his thesis and this work has not been submitted elsewhere for a degree.

February, 2020

Prof. Bhisma K. Patel
(Thesis Supervisor)
Department of Chemistry
IIT Guwahati

ACKNOWLEDGMENT

It is my great pleasure to take this opportunity to express my sincere gratitude to all the people who supported and encouraged me during my Ph. D journey. The successful outcome of my thesis would not have been possible without every each one of you.

First and foremost, with the deepest sense of gratitude, I would like to express my sincere thanks to my supervisor, Prof. Bhisma K. Patel for allowing to be his Ph. D student. His valuable guidance, encouragement, inspiration, creative and scientific ideas helped me a lot to explore the domain of work assembled in this thesis. I am also thankful to him for providing me the freedom to pursue my interests and I find myself privileged to have worked under his valuable guidance.

I would like to acknowledge my sincere gratitude to all my doctoral committee members Dr. Lal M. Kundu, Prof. Subhas C. Pan and Prof. Vaibhav. V. Goud for their timely evaluation of my Ph. D work and insightful suggestions. Thanks to the Chemistry staff for their friendly and cooperative nature. My sincere thanks to the staff of central instruments facility for their help and guidance to various analytical instruments during this period.

I wish to acknowledge my sincere thanks to IIT Guwahati for all the facilities that were made available to me and the MHRD, India for financial support.

Besides, I have been very fortunate to have the company of some wonderful lab seniors like Srimanta da, Arghya da, Ganesh da, Anupal da, Nilufa di, Sourav bhai, Wajid bhai, Ahalya di, Anju di, Suresh anna, Prakash da for their enormous help and support. I am also lucky to have labmates like prasenjit, Amitava, Subhendu, Anjali, Tipu, Ashish, Nikita, Tamanna, Bubul, Hiru, Joy da, Sutapa di, Suman da, Ritush da, Gaurav da and Pakiza di. You all have been very friendly and cooperative under all circumstances. A special thanks to Arghya da, Sourav bhai and Suresh anna for their precious guidance and valuable suggestions that greatly helped me during my Ph. D. I also had the opportunity to work with some enthusiastic M.Sc student like Thazhathethil and B.Sc student like Tamanna.

I would also like to thank you to my friends in IIT Guwahati like Abhishekh, Raman, Rupinder, Ila, Tapasi, Minati, Mustakeem, Nirranjan, Upasana, Renu, Arpita,

Sandeep, Aniruddha, Chandan, Sulender, Muninder, Suhab, Shawaz, Biswajeet, Subhas, Santanu, Saurabh, Maimur, Nazrul, Kuldeep da, Saad bhai, Vijay anna, Adil Bhai, Gattu da, Hemanta da, Somnath da, Fahad bhai. I would like to extend my sincere gratitude to my Kashmiri friends here in IIT Guwahati like Adil, Altaf, Basit, Khalid, Sajjad, Abdul Rehman, Asif, Abid, Waseem, Ajaz bhai, Akter Bhai, Muzzafer bhai, Rayees bhai and Tariq bhai for their unconditional support and love. Thanks to the other research scholars@chem and all my IITG friends, who have shared their thoughts and views with me.

I take this opportunity to thank my B.Sc. and M.Sc. friends like Rayees Rehman, Shahzad, Zubair, Jhangeer, Shabir, Feroz Majeed, Feroz, Rizwan Nabi, Rayees, Muneer, Akbar, Issa, Zameer, Nasir, Amit, Lokesh, Pramood, Amol, Indrajit, Irfan, Adil, Rizwan, Imran, Saqib, Ashraf, Hamid, Bilal, Muzzafer, Bitu, for their help, encouragement and joyful moments spend with them. Thanks to the staff, teachers and students @AGPS Phalgam and TIAI Nasirabad, especially Anurag sir, Farooq sir, Javed sir, Sirtaj sir, Gulzar sir, Muzzafer sir, Syed, Hilal, Abid, Abbas, for having a great time with you people.

No words would suffice to express my feelings for my teachers like Fayaz sir, Khaliq sir, Sadiq sir, Majeed sir, Shabir sir, Suliman sir, Zaffar sir, Farooq sir, Aswar sir, Prasad sir, Kodape madam, Dore madam, Jamode sir, Jaiprakash sir and all other school and college teachers for their insightful ideas, great teaching skills which made my journey smooth. A special thanks go to Kodape madam who inspired and helped me to start my research.

Finally, my deepest gratitude goes to my family for their endless love, unending support, tolerance and blessings throughout my life. I am extremely grateful to my parents, whose sacrifices in every stage of my life motivated me to overcome the hurdles to come up to this stage. I am highly grateful to my two brothers and my two sisters whose constant support, love and encouragement became an integral part of this journey. I am also grateful to my relatives and neighbours for their love, affection and blessings. Still, many names are missing whose contribution and help is worthy to mention.

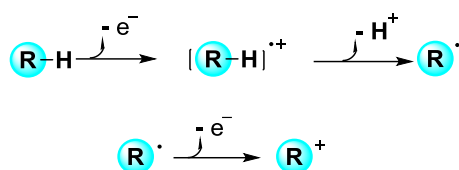
Bilal Ahmad Mir

Abstract

The contents of this thesis have been divided into five chapters based on the results of experimental works performed during the complete course of the research period. The introductory chapter of the thesis presents an overview of the construction of C–C, and C–X (C–N, C–O) bonds via the intermediacy of radicals. All the other chapters emphasize on C–C, C–N and C–O bond formations on sp^2 / sp^3 carbon via a radical pathway involving oxidizing agents. These bond formations (C–C, C–N and C–O) have been achieved via metal-free or metal-catalyzed radical addition and radical substitution. Chapter II describes the copper-catalyzed differential peroxidation of the terminal and internal alkenes using tertiary butyl hydroperoxide. Chapter III demonstrates *tert*-butyl nitrite mediated differential functionalizations of internal alkenes as paths to furoxans and nitroalkenes. Chapter IV illustrates the *tert*-butyl nitrite mediated nitro-nitratation of internal alkenes. Chapter V deals with iron (III)-catalyzed peroxide-mediated C-3 functionalizations of flavones. Each of these chapters comprises of seven subsections which include introduction, literature reports, present work, experimental section, references, spectral data and some selected spectra.

CHAPTER I. Construction of C–C, C–N and C–O Bonds on sp^2 / sp^3 Carbon via Radical Pathway

This chapter gives a layout of the construction of C–C and C–X (X = N, O) bonds on sp^2 / sp^3 carbon via the intermediacy of radicals. The radicals are generally generated by homolytic fission of a covalent bond. Energy in the form of ultraviolet-visible light, heat or some other form of energy is needed to do such homolytic fission. The dissociation energies for homolytic cleavage of the C–C, C–H and C–X bonds are quite high but the relatively weak O–O bonds are cleaved at relatively low temperatures. Some of the methods used for the generation of free radicals are (I) thermolysis (II) photolysis (III) redox reactions. One important aspect of these radical-mediated functionalizations is the generation of a carbocation intermediate by losing two electrons (Scheme I.1).



Scheme I.1. Formation of radical and radical cation via electron transfer

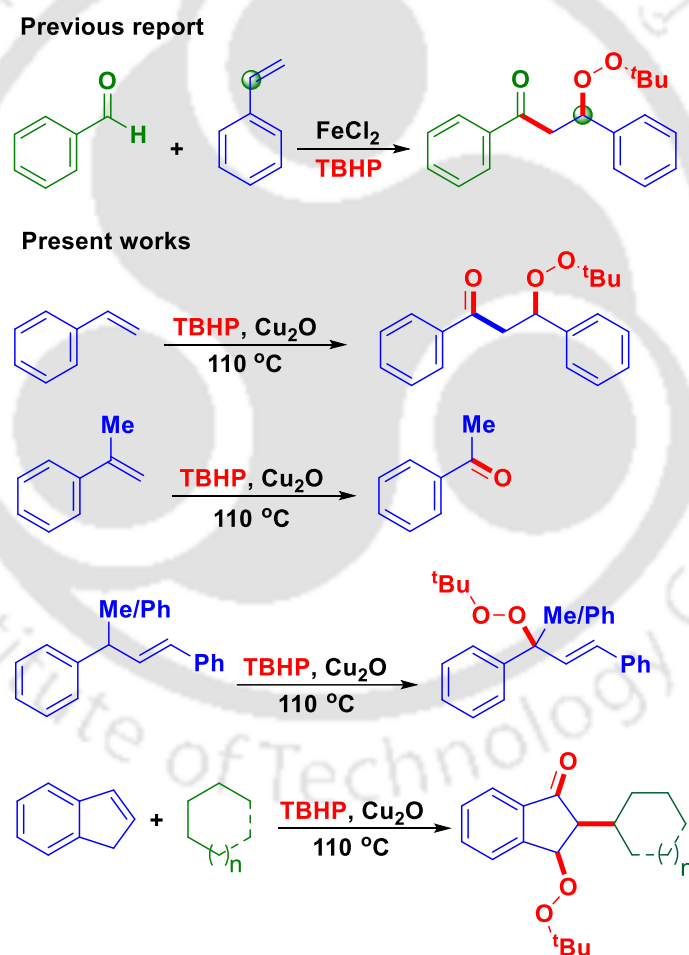
Radicals and radical cations are active intermediates and have a range of properties and reactivities, for example, nucleophilicity, electrophilicity, hydrogen abstraction reactions, and self-coupling reactions. Thus, they are highly reactive. This reactive nature of the free radicals and radical cations gives rise to the formation of new bonds. In organic chemistry, we are generally encountered with the formation of C–C and C–X (X = heteroatom) bonds. There are many useful methods in organic synthesis that have been developed for the construction of C–C and C–X (X = heteroatom) bonds involving radical pathways. These methods generally involve substitution, addition or rearrangement reactions to bring about the desired functionalization. In addition to this, the carbon atom participating in radical-mediated functionalization may be sp, sp² or sp³. In this context, our group has been involved in the construction of new C–C and C–X (X = O, N) bonds and generation of various functionalities via the intermediacy of radicals by using sp² / sp³ carbon.

CHAPTER II. Copper(I) Catalyzed Differential Peroxidation of Terminal and Internal Alkenes Using TBHP

This chapter focuses on the copper(I) catalyzed carbonylation-peroxidation, α-peroxidation and peroxidation-carbonylation-cycloalkylation/cycloetherification of vinyl arenes, internal unsymmetrical alkenes such as (*E*)-prop-2-ene-1,1,3-triyltribenzene and cyclic alkene (indene) respectively.

Di-functionalization of alkenes is significant in the synthetic transformation to build molecular complexity in a single operation. Both intra and intermolecular hetero-di-functionalizations of alkenes have received considerable attention. In contrast to intermolecular processes, intramolecular di-functionalizations are much more selective and thermodynamically favourable. The transition-metal-catalyzed intermolecular di-functionalizations such as carbohalogenation, dihydroxylation, oxyarylation, oxyamination, aminofluorination, aminocyanation, hydro-alkylation, carboboration and

other di-functionalizations are well explored. However, intermolecular di-functionalization of olefins has rarely been explored following the C–H bond functionalization strategy. Carbonylation of alkenes has been developed as one of the powerful methods for the synthesis of carbonyl compounds. But the simultaneous introduction of a carbonyl group and another functional group such as alcohol, amine and peroxide into alkenes is not well explored. Lately, organic peroxides are used as oxidizing agents and initiators for free-radical reactions both in academia and industry. These peroxy compounds are produced and used in various natural and biological processes such as preparation of antimalarial agents, anthelmintics, and antitumor drugs. A Fe(II)-catalyzed carbonylation-peroxidation of olefins is reported via the sp^2 C–H bond functionalization using aldehydes (Scheme II.1).

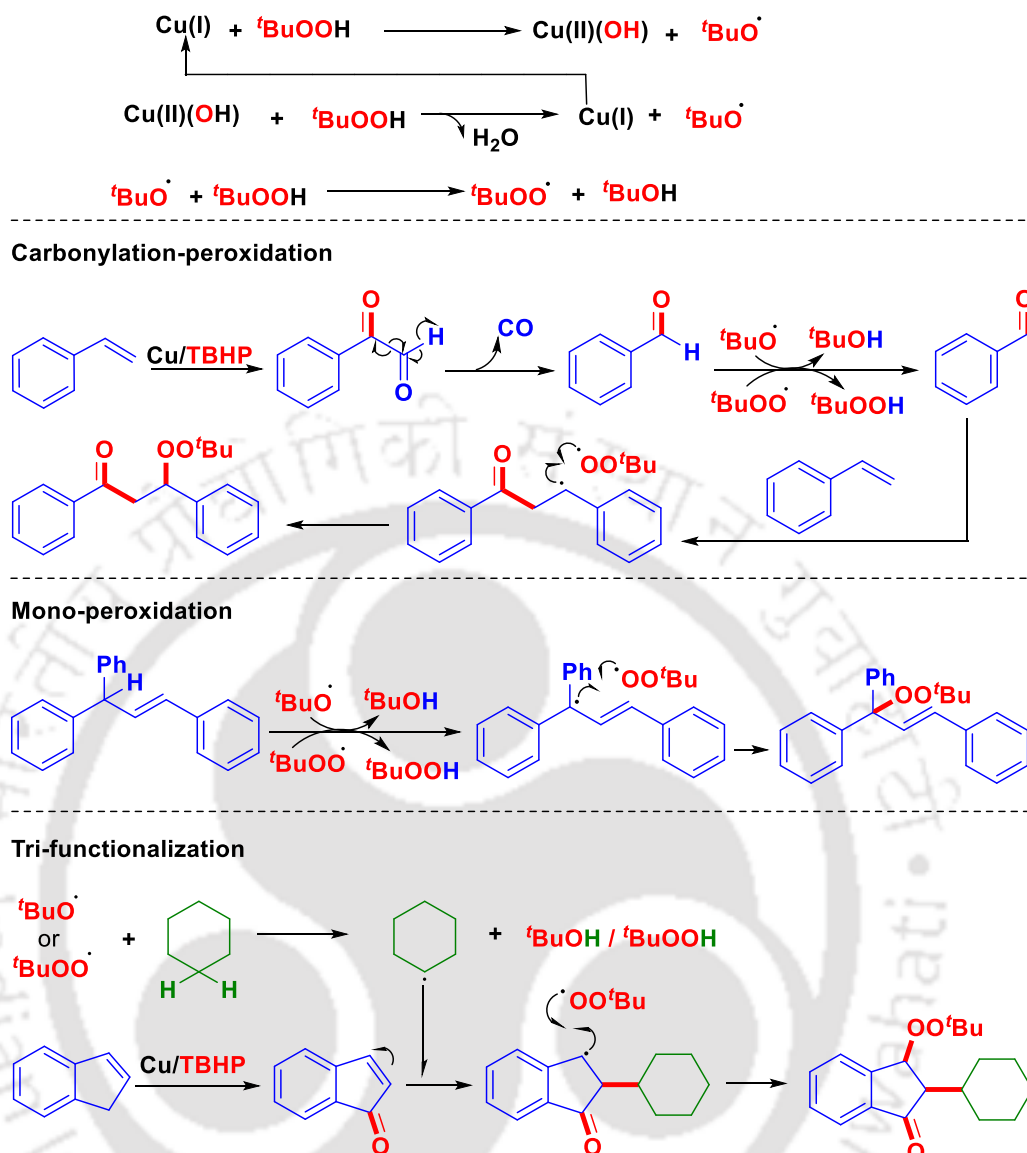


Scheme II.1. Strategies for various peroxidations using TBHP

Earlier our group generated two coupling partners from the same precursor, where one half of alkylbenzene is converted to an aryl carboxyl intermediate and the other half into a benzyl cation leading to the formation of an ester. Thus, we envisaged

that one half of the styrene can be converted to an arylcarboxaldehyde, which can couple with the remaining half of the styrene in the presence of an oxidant TBHP leading to keto-peroxidation as shown in (Scheme II.1).

To attain a suitable reaction condition for the carbonylation-peroxidation various reaction parameters such as catalysts, oxidants and solvents were screened to achieve the maximum possible yield. After a series of experiments, the optimized reaction condition arrived at was Cu₂O (10 mol%), TBHP (3 equiv) at 110 °C in CH₃CN under an air atmosphere. Various vinyl arenes were subjected to optimized reaction conditions. This methodology was found to be compatible with a variety of electron-donating and electron-withdrawing groups in vinyl arenes giving moderate to good yields of their corresponding carbonylation-peroxidation products. However, compared to substrates bearing electron donating groups, electron withdrawing substituents gave better yields. Further, when this strategy was applied to internal alkenes such as (*E*)-prop-2-ene-1,1,3-triyltribenzene and cyclic benzylic internal alkene such as indene both reacted successfully and provided their α -peroxidation and tri-functionalization (peroxidation-carbonylation-cycloalkylation/cycloetherification) products respectively in good to moderate yields. The α -peroxidation was achieved just by changing the number of equivalents of TBHP (from 6 to 3) otherwise identical reaction conditions. Whereas, the tri-functionalization was achieved just by changing the solvent from CH₃CN to cyclohexane otherwise identical reaction conditions. Based on the results / observations of mechanistic investigations, literature reports and DFT calculations, a separate mechanism has been proposed for each of these transformations (Scheme II.2).



Scheme II.2. Plausible mechanisms for various alkene peroxidations

In conclusion, we have demonstrated the differential reactivity of terminal and internal alkenes. A carbonylation-peroxidation of vinyl arenes is achieved in the absence of any carbonyl source. But α -methyl styrenes yielded aryl methyl ketones as the only product. An α -substituted unsymmetrical internal alkene such as but-1-ene-1,3-diylbenzene afforded selective α -peroxidation at the tertiary carbon and not across the double bond under the similar reaction conditions. An internal cyclic alkene such as indene provided peroxidation-carbonylation-cycloalkylation/cycloetherification by switching the solvent system from acetonitrile to cycloalkanes / cyclic ether.

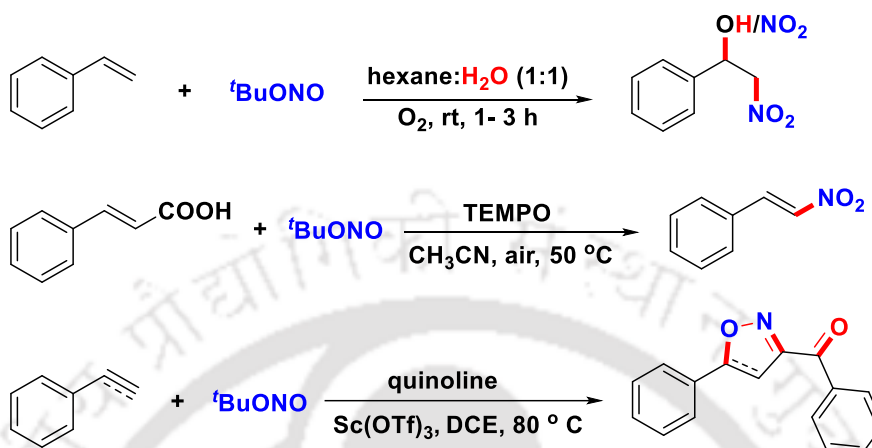
CHAPTER III. *tert*-Butyl Nitrite Mediated Differential Functionalizations of Internal Alkenes: Paths to Furoxans and Nitroalkenes

This chapter demonstrates the synthesis of furoxans and nitroalkenes from (symmetrical and unsymmetrical internal alkenes) and (α,β -unsaturated carboxylic acids and alicyclic alkenes) respectively. These transformations have been achieved by using *tert*-butyl nitrite (TBN), quinoline and $K_2S_2O_8$. Furoxan (or 1,2,5-oxadiazole 2-oxide) is a heterocycle of the isoxazole family and is an important scaffold in medicinal chemistry. Moreover, furoxan derivatives have drawn phenomenal biological and pharmaceutical interests, some of which are reported to have antioxidant, vasodilator, leishmanicidal, anticancer, antibacterial antimalarial, antihistaminic, and anti-HIV activities. Furoxan derivatives are known to release nitric oxide (NO) in the presence of thiol co-factors, thus activating the soluble guanylate cyclase. Consequently, many research groups pursued studies on the development of furoxan-based drugs. However, any organic reagent such as *tert*-butyl nitrite mediated synthesis of furoxans from alkenes is still unexplored. In this regard, synthesis of furoxans from easily accessible and biologically demanding internal alkenes bearing an allylic stereogenic centre may generate potential applications as both stereogenic centre and furoxan moiety are important parts of many biologically active compounds, thus are expected to receive considerable interest from a biological and pharmaceutical point of view.

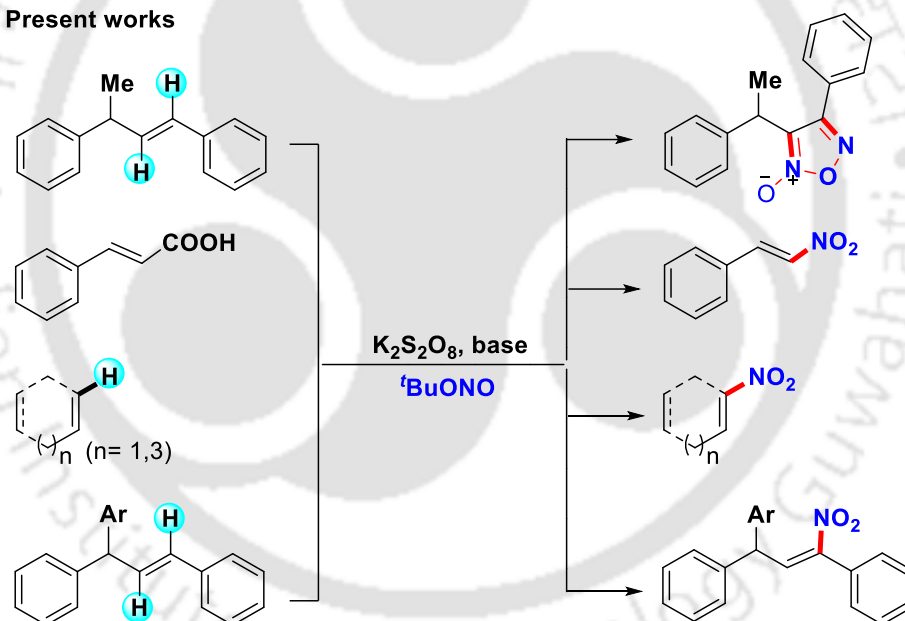
Alkenes which are simple organic molecules have been widely applied in organic synthesis for the construction of a diverse array of complex molecules. One of the finest approaches to build such class of molecules in a single operation is via the direct 1,2- di-functionalization of alkenes. In this context, *tert* butylnitrite (TBN) has emerged as a versatile reagent in organic synthesis. Therefore, it has been employed for various functionalizations such as oxidative nitration of alkenes decarboxylative nitration of α,β -unsaturated carboxylic acids (Scheme III.1, previous works). Recently our group has reported a *tert*-butyl nitrite mediated domino synthesis of isoxazolines and isoxazoles respectively from styrenes and phenylacetylene (Scheme III.1, previous works). However, *tert*-butyl nitrite mediated di-functionalization of any internal olefin is less explored so far. Thus the query arises, whether treatment of an internal alkene with TBN may lead to the formation of similar isoxazoline, furoxans or a completely different

reactivity may drive the formation of some other product? Therefore, we were curious to investigate the reaction of various internal alkenes with TBN (Scheme III.1, present works).

Previous works



Present works

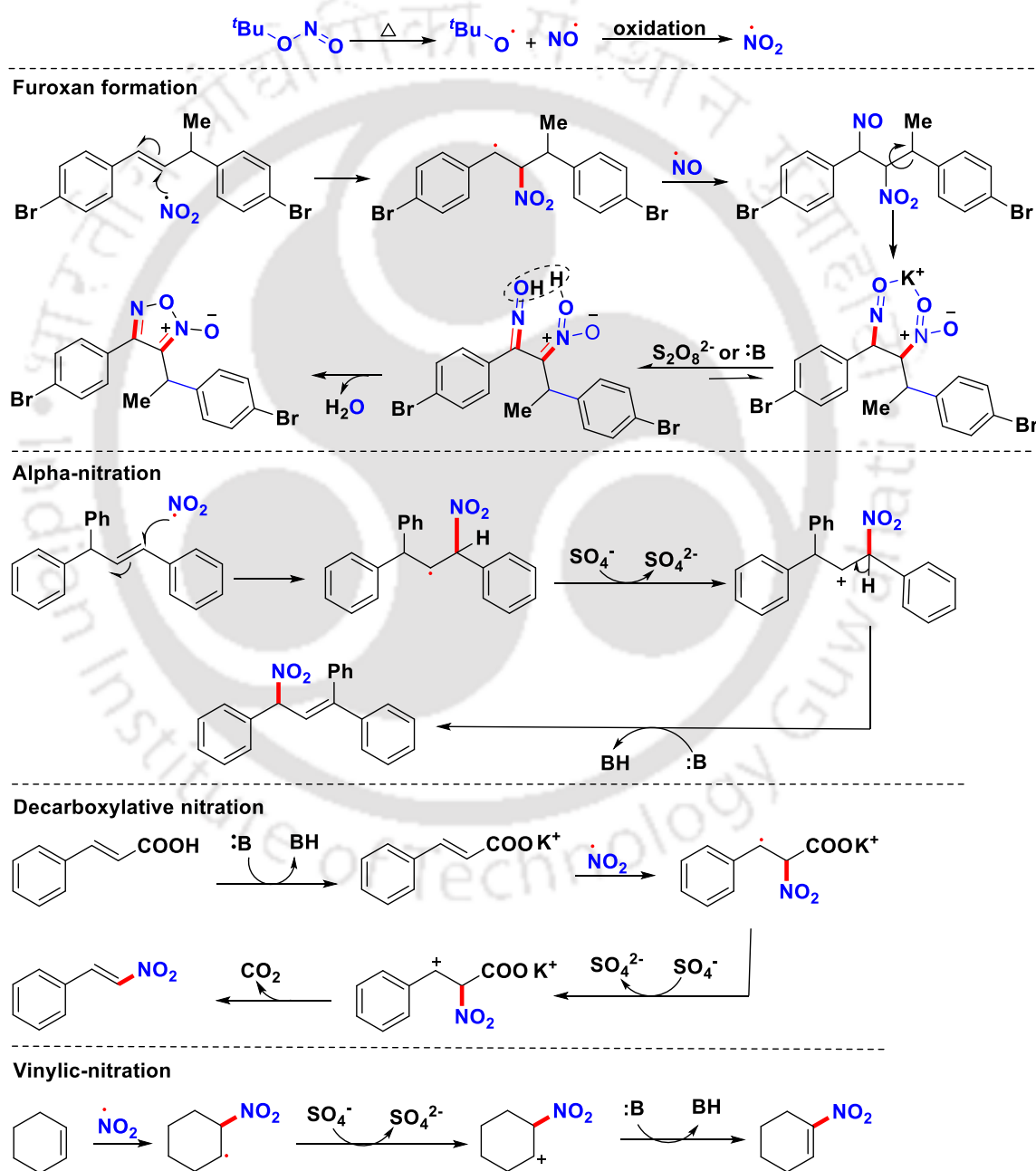


Scheme III.1. Strategies for functionalization of olefins using TBN

Reaction parameters such as catalysts, bases, oxidants, additives and solvents were varied to obtain the optimal conditions for this reaction and it was found that the use of TBN (2 equiv), quinoline (1 equiv), $K_2S_2O_8$ (1 equiv) at 85 °C for 5 h. afforded the maximum possible yield of the desired furoxan and nitroolefin. The optimized conditions were then implemented in the reactions between internal alkenes (symmetrical and unsymmetrical internal alkenes) and (α,β -unsaturated carboxylic acids

and alicyclic alkenes). All these reactions proceeded smoothly providing their respective products in moderate to good yields. Alkenes possessing electron-withdrawing substituents provided higher yields of products than those bearing electron-donating substituents.

Several experimental studies were performed to elucidate the mechanism of this transformations. Based on the observations of these experiments and related literature reports, four plausible mechanisms have been proposed (Scheme III.2).



Scheme III.2. Proposed mechanism for the formation of furoxans and nitrolefins

In conclusion, we have demonstrated the differential reactivity of various alkenes with *tert*-butyl nitrite (TBN). Internal benzylic alkenes such as (*E*)-1,3-diphenyl-1-butene gave furoxan as the exclusive product in the presence of $K_2S_2O_8$, base and TBN. While α,β - their product. In the furoxan formation, TBN is serving as a NO_2 cum NO synthon and as unsaturated esters are inert to TBN but α,β -unsaturated acids under an identical condition undergone a rapid decarboxylation giving nitroalkenes. On the other hand, acyclic internal alkenes yielded nitro alkenes as the sole product, whereas terminal aliphatic alkenes gave isoxazolines as a decarboxylative nitrating agent when the substrates are α,β -unsaturated acids.

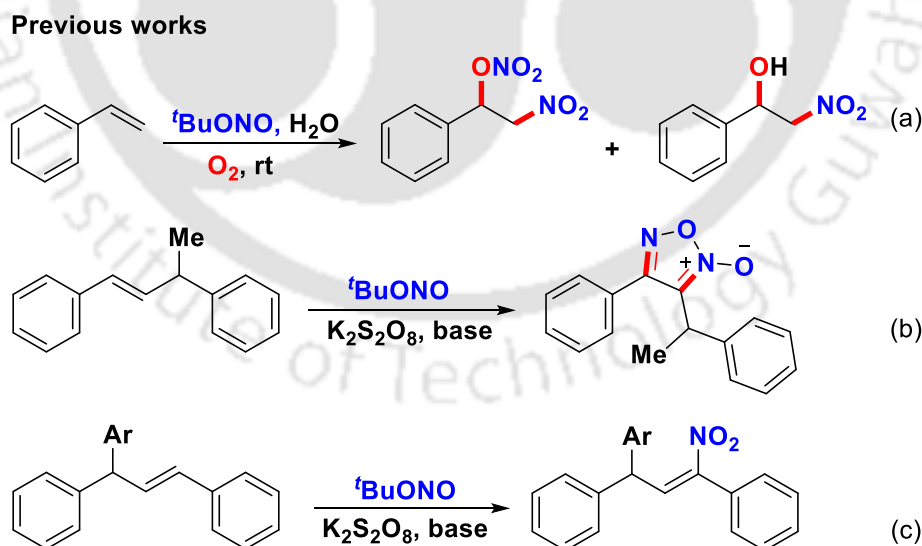
CHAPTER IV. *tert*-Butyl Nitrite Mediated Nitro-Nitratosation of Internal Alkenes

This chapter describes a protocol for the oxidative nitration of unsymmetrical internal alkenes and decarboxylative nitration of α,β -unsaturated carboxylic acids using *tert*-butyl nitrite and molecular oxygen.

The metal-free reagent, *tert*-butyl nitrite (TBN) is emerging as a multi-tasking reagent in various synthetic applications because of its easy availability, easy handling, low cost and stability. Thermolysis of TBN provides NO and $tBuO$ radicals. The former can directly participate in a reaction, whereas both these radicals can initiate several reactions. Due to the intrinsic ability of TBN to activate molecular oxygen it captures dioxygen generating a NO_2 radical, which prompts nitration and many other oxidation processes. Interestingly, the NO radical is a good acceptor of transient radicals thus serving as an efficient radical trapper and source of N and N-O synthons.

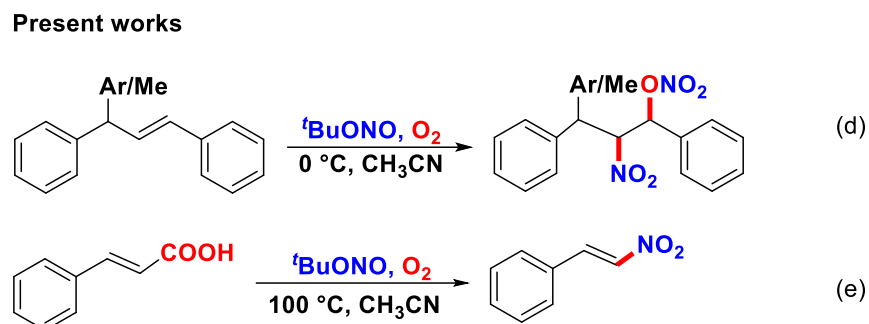
Terminal alkenes such as styrene react differently with TBN depending upon the other additives present in the reaction. Styrenes react with TBN in the presence of Fe(II) catalyst and $NaBH_4$ to give corresponding oximes. Treatment of styrene with TBN in an air atmosphere in toluene at room temperature provided β -nitro alcohol along with nitrated products (Scheme IV.1.a). Styrenes undergo cross-coupling in the presence of metal-based carbene and NO radical (generated *in situ* from the TBN) providing isoxazolines. In this process, styrene serves as a dienophile and undergo [3+2] cycloaddition with the *in situ* generated nitrile oxide intermediate. Following the analogous [3+2] cycloaddition strategy our group obtained symmetrical isoxazolines

from styrenes in the presence of TBN, $\text{Sc}(\text{OTf})_3$ and quinoline. While quinoline did not participate and serve only as a base during the formation of isoxazolines. However, in a Cu-catalyzed process, it took part along with styrene and TBN provided imidazo[1,2-a]quinolines via a three-component process. Here, TBN serves the dual role of an N1 synthon as well as an oxidant. In the absence of any other additives, styrene analogues react with TBN in DMSO providing 1,2,4-oxadiazole-5(4*H*)-ones. Sulfonyl hydrazide as sulfonyl radical and TBN as the NO source adds across styrene double bond to give a bi-functionalized product α -sulfonylethanone oximes, which is mediated by a base. Similarly, α -sulfonylethanone oxime is obtained from styrene, where TOSMIC acts as the sulfonyl source and TBN as the NO source as well as an oxidant. Using sulfinic acids as the sulfonating agent and TBN as the NO source as well as an oxidant a vicinal sulfoximation of styrene has been accomplished. From the above literature reports, it is evident that TBN reacts with styrenes in many ways depending on the reaction conditions and other additives present. On the other hand, internal benzylic and non-benzylic alkenes also react differently with TBN. An interesting synthesis of furoxan is accomplished from benzylic internal alkene using TBN, quinoline and $\text{K}_2\text{S}_2\text{O}_8$ (Scheme IV.1.b). Under a similar condition α,β -unsaturated carboxylic acids and cyclic internal alkene afforded nitroalkenes (Scheme IV.1.c).



Scheme IV.1. Various TBN-mediated functionalizations of alkenes

Cont. Scheme IV.1



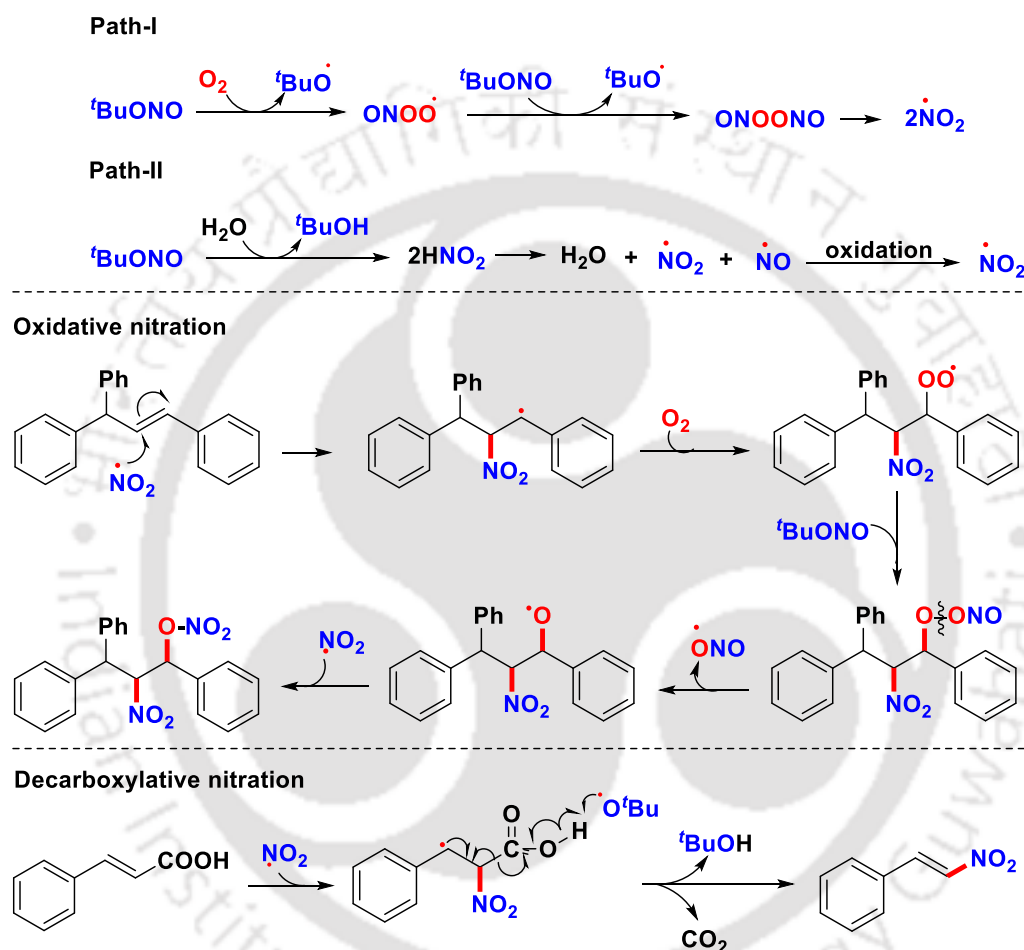
Scheme IV.1. Various TBN-mediated functionalizations of alkenes

In all the above-mentioned cases, the *in situ* generated NO_2 radical attacks at the β -carbon while the NO radical attacks at the α -carbon even though both the radicals coexist in the medium. This attack of NO_2 radical at the β -carbon is in agreement with the computational calculation that shows it is stabilised by around 6 kcal/mole than the attack by NO radical at the same site. However, during furoxan formation, an analogous internal alkene viz. prop-2-ene-1,1,3-triyltriaryl system gave exclusively a mono nitro product where the nitro group is at the benzylic position (α -carbon) (Scheme IV.1.c). This unusual attack of NO_2 at the β -position, prompted us that instead of a terminal alkene (styrene) if an internal alkene such as γ -diaryl substituted or γ -alkyl-aryl-substituted styrene is treated with TBN under an oxygen atmosphere will they react similarly or behave differently giving different products? Further, if mono-nitration takes place will it be at the α or the β -position of the internal benzylic alkenes? Therefore, we were curious to investigate the reaction of various internal alkenes with TBN in an oxygen atmosphere (Scheme IV.1.d, e).

Various reaction parameters such as catalysts, solvents and temperatures were screened to obtain the optimal conditions for this reaction and it was found that the use of TBN (2 equiv) in CH_3CN at $0\text{ }^\circ\text{C}$ were found to be the suitable conditions for our subsequent exploration to extend the scope of this transformation. The optimized conditions were then executed for oxidative nitration of unsymmetrical internal alkenes and to decarboxylative nitration of α,β -unsaturated carboxylic acids just by increasing the temperature to $100\text{ }^\circ\text{C}$ otherwise identical reaction conditions. All the substituted internal alkenes and α,β -unsaturated carboxylic acids served as excellent surrogates toward oxidative nitration and decarboxylative nitration respectively. In particular, those bearing electron-withdrawing groups gave better yields of their respective products

compared to those yields possessing electron-donating groups, in case of both oxidative nitration and decarboxylative nitration.

This elegant and unprecedented transformation is a mechanistic enigma to us and hence systematic investigations were carried out. Based on the results obtained from these control experiments, literature reports and DFT calculations, one plausible mechanism has been proposed for each of these transformations (Scheme III.2).



Scheme IV.2. Proposed mechanism for oxidative and decarboxylative nitration

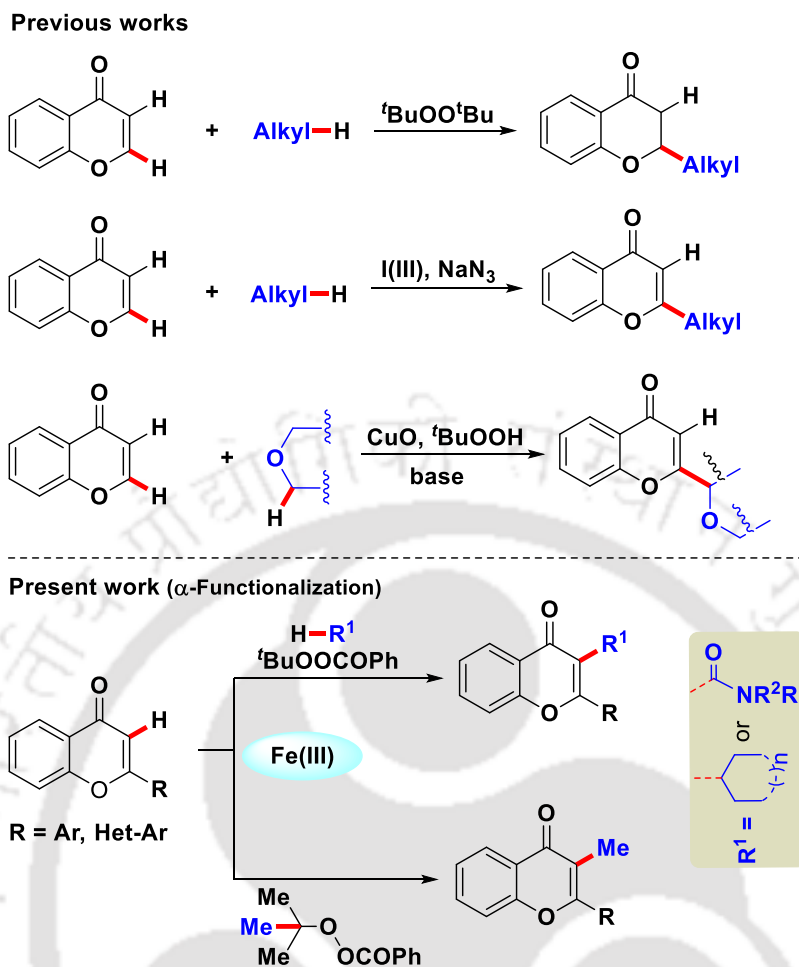
In conclusion, we have demonstrated the differential reactivity of TBN with internal benzylic alkenes in an oxygen atmosphere, which provided nitro-nitrosation products. This result is in contrast to the furoxan formation for the same substrate with TBN but the presence of $\text{K}_2\text{S}_2\text{O}_8$. The γ -diaryl substituted styrenes provided better yields compared to γ -alkyl-aryl-substituted styrenes possible due to anchimeric assistance imparted by the γ -phenyl ring. While α,β -unsaturated esters are inert to TBN but α,β -unsaturated acids provided corresponding nitroalkenes via decarboxylation. Even though

other radical species co-exists in the medium the nitro radical attacks exclusively at the β -carbon in internal benzylic alkenes. A plausible mechanism has been proposed which is supported by DFT calculation.

CHAPTER V. Iron(III) Catalyzed Peroxide Mediated C-3 Functionalizations of Flavones

This chapter deals with iron(III)-catalyzed C-3 functionalization of flavones, which has been achieved using *tert*-butyl peroxybenzoate (TBPB)/potassium persulphate($K_2S_2O_8$) oxidant combinations with a suitable solvent.

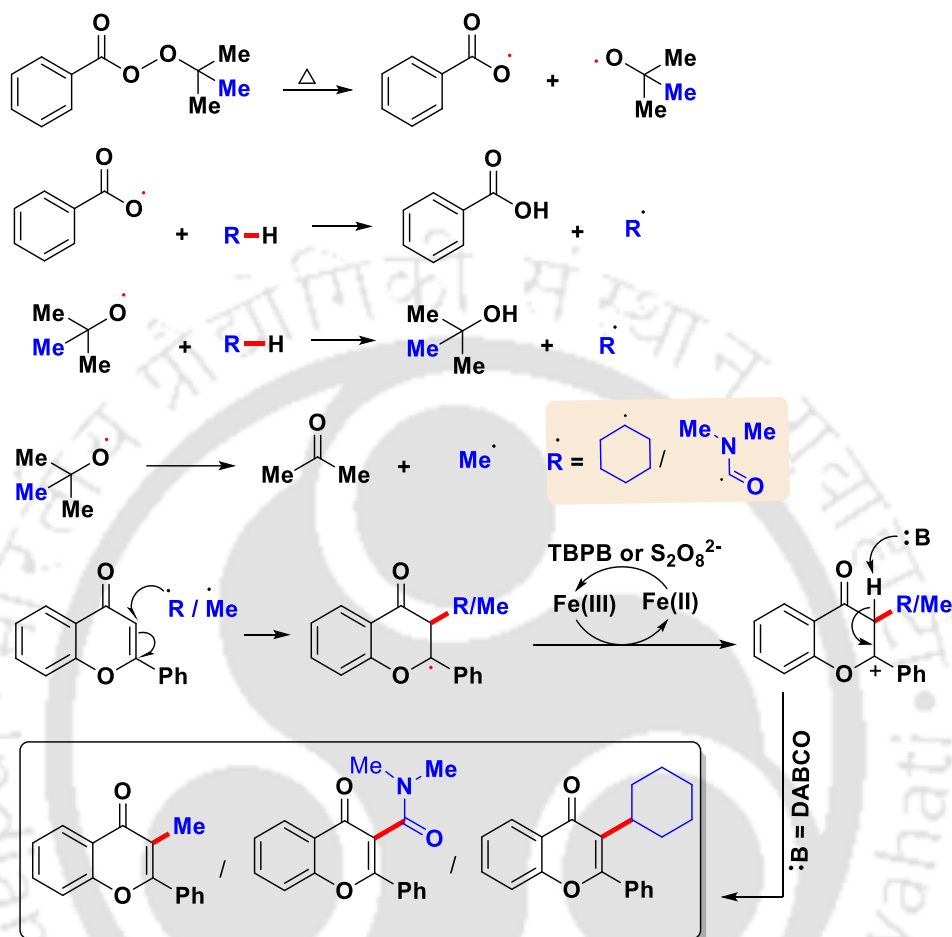
Transition metal-catalyzed C–H functionalization has undergone a renaissance in the past decade for the construction of carbon–carbon (C–C) and carbon–heteroatom (C–X) bonds. In this context cross dehydrogenative coupling (CDC) protocols have emerged as a promising and powerful tool towards the formation of Csp–Csp, Csp–Csp² and Csp²–Csp² bonds. In recent times, this CDC protocol has even made progress for the formation of Csp³–C bonds. In this context, cycloalkanes have been employed for CDC reactions in the absence or presence of transition metal catalysts albeit with limited examples. Aliphatic Csp³–H bonds are the most available natural resource. Thus, methodologies for the direct functionalization of aliphatic Csp³–H bonds will expand the synthetic toolbox, allowing access to value-added products with various important applications. Flavone is an important structural motif, present in many natural products and pharmaceutical molecules having a wide range of biological and pharmaceutical applications. Thus, any further derivatization on this moiety may generate potentially important candidates. To date, there are many examples where chromones have been employed as the coupling partner for regioselective C-2 functionalization (β -functionalization) with arenes, cycloalkanes or cyclic ethers using transition metals, hypervalent iodine or under metal-free conditions (Scheme V.1). However direct C-3 functionalization of chromone has not been reported so far (Scheme V.1). If both C-2 and C-3 positions are available as in the case of chromone, regioselective functionalization can occur at its C-2 site (Scheme V.1, previous reports) but not at the more nucleophilic C-3 site. We speculated that if the C-2 position is substituted with a stabilizing group such as aryl as in flavones, the functionalization might occur at the nucleophilic C-3 site of flavone via a radical pathway (Scheme V.1, present work).



Scheme V.1. Various routes for C-2/C-3 functionalizations of chromones/flavones

Rigorous optimizations were carried out to establish suitable conditions for this transformation. The use of $\text{Fe}(\text{acac})_3$ (20 mol%), DABCO (1 equiv), $\text{K}_2\text{S}_2\text{O}_8$ (1 equiv), TBPB (5–6 M in decane) (3 equiv) at 115 °C gave a modest yield, which was the maximum that could be attained. The yield could not be improved further because of the intrinsic low reactivity of the sp^3 C–H bonds in cyclohexane. Having established the optimal reaction conditions, the present oxidative C-3 cycloalenylation of cycloalkanes was then implemented on cross-couplings between cycloalkanes and a series of substituted flavones. The developed methodology applied to diverse flavones irrespective of the nature of their substituents present, however, the yields were modest in most of the cases. Furthermore, the same optimized reaction conditions were equally applicable to the formamidation and methylation of flavones just by replacing the cycloalkane with formamide in case of formamidation and with chlorobenzene in case of methylation.

Several experimental studies were performed to elucidate the mechanism of this transformation. Based on the observations of these experiments and related literature reports, a plausible mechanism has been proposed (Scheme V.2).



Scheme V.2. A plausible mechanism for C-3 functionalization

In conclusion, we have for the first time demonstrated iron(III) catalyzed C-3 cyclo-alkylation, amidation and methylation of flavones using suitable oxidant / solvent combinations. A broad range of flavones, cycloalkanes and dialkyl-formamides are tolerated under the reaction conditions. The practical advantages of this strategy are the use of solvents such as cyclohexane, dimethylformamide as the reactive coupling partners with flavones. This method offers a novel and convenient route for the synthesis of C-3 functionalized flavones, which can be extended for the synthesis of drugs such as flavoxate and dimeflin.

Contents

Chapter I. Construction of C–C, C–N and C–O Bonds on sp^2 / sp^3 Carbon via Radical Pathway	01
I.1. Introduction	03
I.2. Modes of the Generation of Radicals	04
I.3. Classification	05
I.3.1. Representative examples of radical-mediated C–C bond formation	05
I.3.2. Representative examples of radical-mediated C–N bond formation	07
I.4.3. Representative examples of radical-mediated C–O bond formation	09
I.4. References	12
Chapter II. Copper(I) Catalyzed Differential Peroxidation of Terminal and Internal Alkenes Using TBHP	16
II.1. Introduction	18
II.2. Strategies for Differential Benzylic-Peroxidation	18
II.3. Present Work	21
II.4. Experimental Section	34
II.4.1. General information	34
II.4.2. General procedure for keto-peroxidation, mono-peroxidation and tri-functionalization	35
II.4.3. Mechanistic investigations	36
II.5. References	37
II.6. Spectral Data	40
II.7. Selected Spectra	52
Chapter III. <i>tert</i>-Butyl Nitrite Mediated Differential Functionalizations of Internal Alkenes: Paths to Furoxans and Nitroalkenes	55
III.1. Introduction	57
III.2. Strategies for <i>tert</i> -Butyl Nitrite (TBN) Mediated Functionalizations of Olefins	58
III.3. Present Work	60

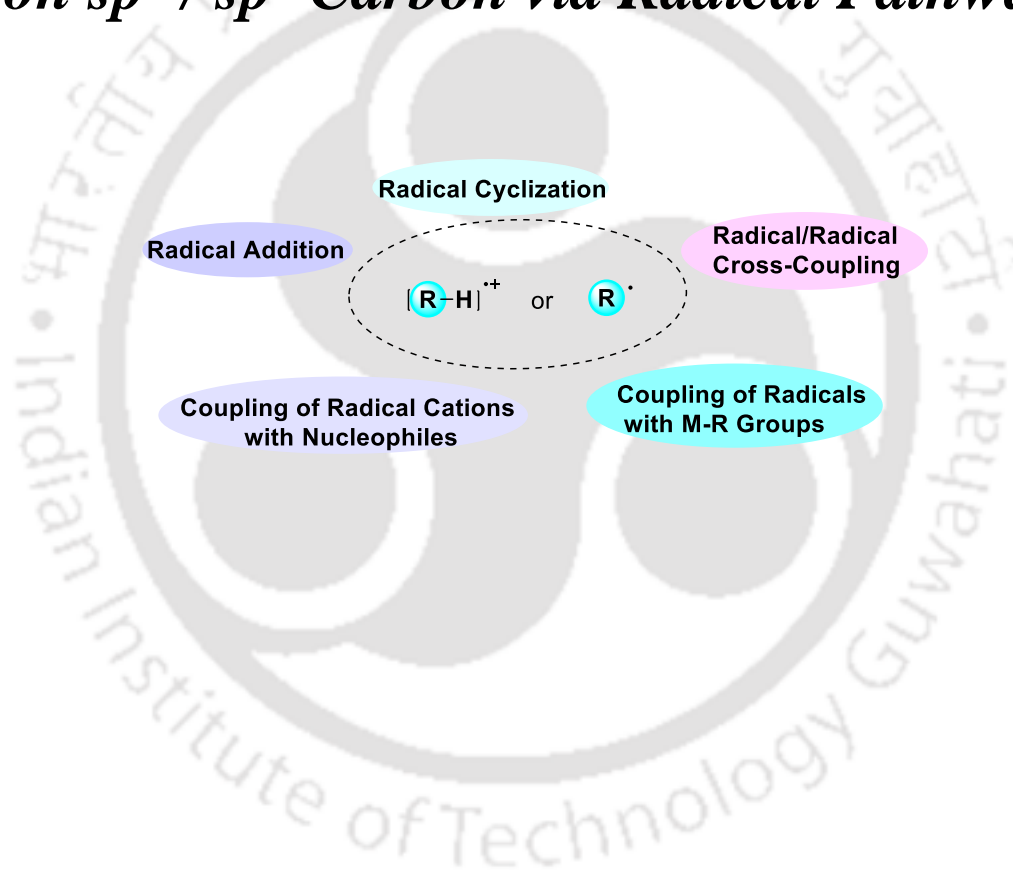
III.4. Experimental Section	72
III.4.1. General information	72
III.4.2. Crystallographic description:	72
III.4.3. General procedure for the synthesis of furoxans and nitrolefins	73
III.4.4. Mechanistic investigation	74
III.5. References	74
III.6. Spectral Data	77
III.7. Selected Spectra	86
Chapter IV. <i>tert</i>-Butyl Nitrite Mediated Nitro-Nitratosation of Internal Alkenes	89
IV.1. Introduction	91
IV.2. Strategies for <i>tert</i> -Butyl Nitrite (TBN) Mediated Functionalizations of Alkenes	91
IV.3. Present Work	94
IV.4. Experimental Section	104
IV.4.1. General information	104
IV.4.2. Crystallographic description	105
IV.4.3. General procedure for oxidative nitration and decarboxylative nitration	105
IV.4.3. Mechanistic investigation	106
IV.5. References	107
IV.6. Spectral Data	109
IV.7. Selected Spectra	119
Chapter V. Iron(III) Catalyzed Peroxide Mediated C-3 Functionalizations of Flavones	122
V.1. Introduction	124
V.2. Strategies for α / β -Functionalizations of Chromones	124
V.3. Present Work	127
V.4. Experimental Section	136
V.4.1. General information	136

V.4.2. Crystallographic description	136
V.4.3. General procedure for the synthesis of α -functionalized flavones	137
V.4.4. Mechanistic investigation	138
V.5. References	139
V.6. Spectral Data	141
V.7. Selected Spectra	151
Publications	154



CHAPTER I

Construction of C–C, C–N and C–O Bonds on sp^2 / sp^3 Carbon via Radical Pathway

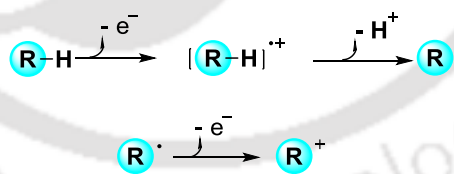


CHAPTER I

I. Construction of C–C, C–N and C–O Bonds on sp^2 / sp^3 Carbon via Radical Pathway

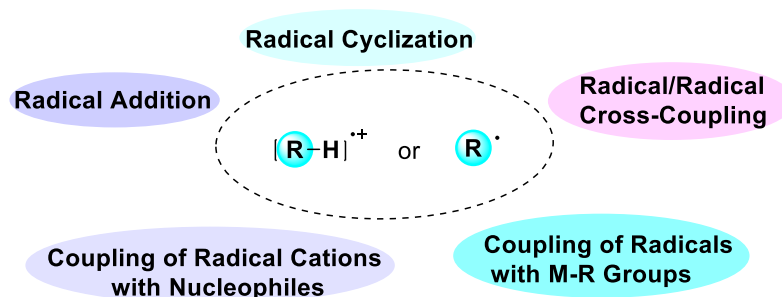
I.1. Introduction

In recent decades, various strategies have been applied both in the industry as well as in academia to construct carbon–carbon and carbon–heteroatom bonds.^[1] The advanced cross-coupling strategies have been successfully applied to the synthesis of commercially important products.^[2] Despite the tremendous advances, it has many drawbacks such as the use of stoichiometric organometallic reagents, or pre-functionalized components which increases the number of synthetic steps. One of the approaches to address this problem is to utilize radical-mediated direct functionalization. Direct functionalization via a radical pathway has emerged as a promising approach towards molecular construction with high atom- and step-economy.^[3] Unlike the transition-metal-catalyzed C–H functionalization reactions, where C–M (Pd, Rh, Ru, etc.) species are believed to be formed, serving as the key intermediates in coupling reactions,^[4–6] C–H bond activation in radical-mediated functionalization occurs via the loss of one proton with one electron, simultaneously forming a radical, that is involved in single-electron transfer processes.^[7] The radical can further go through oxidation and loss of one electron to generate a cation intermediate. The radical and radical cation can serve as key intermediates in such functionalizations. (Scheme I.1.1)



Scheme I.1.1. Formation of radical and radical cation via electron transfer

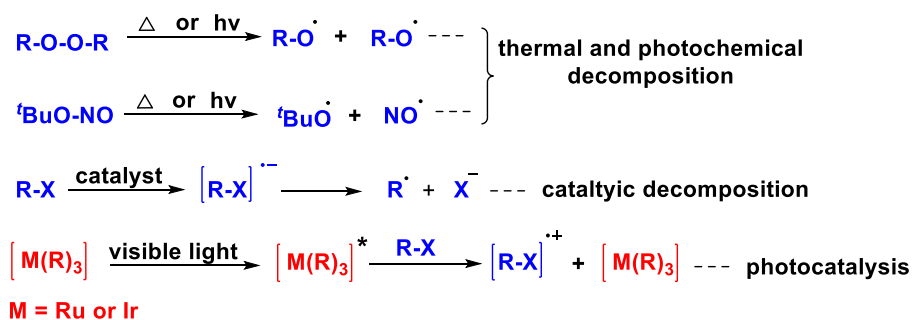
One important aspect of these radical-mediated functionalizations is the generation of a carbocation intermediate by losing two electrons which will then react with another nucleophile.^[8,9] Radicals and radical cations are active intermediates and have a range of properties and reactivities,^[10] for example, nucleophilicity, electrophilicity, hydrogen abstraction reactions, and self-coupling reactions; a variety of reactions via radical processes have been developed recently (Scheme I.1.2).



Scheme I.1.2. Representative reaction types of radical functionalization

I.2. Modes of the Generation of Radicals

Radicals are significant as they mediate the reactions that are otherwise considered either to be impossible or difficult to achieve with cations and anions. Therefore, they react with most of the organic molecules whether inert or activated.^[3] This distinguishing feature of radicals can be attributed to their highly reactive nature to get stability. Thus, it becomes equally important to know how to generate these reactive species? Radicals are generally produced via thermal, photochemical or catalytic decomposition of organic peroxides,^[11a] *tert*-butyl nitrite,^[11b,c] or by photo-catalysis^[11d] (Scheme I.2.1). The peroxides generally used in radical reactions are organic peroxides, such as alkyl hydroperoxides, aryl hydroperoxides, ketone peroxides, dialkyl peroxides, diacyl peroxides, peroxy esters, peroxydicarbonates, peroxyacetals, and inorganic peroxides which act as radical initiators. The peroxides and *tert*-butyl nitrite produce radical species via homolytic fission under mild conditions and promote radical reactions. However, in photocatalysis, the radical formation is initiated by a photocatalyst. As most organic compounds do not absorb visible light efficiently that has limited their application in photochemical synthesis. Therefore, a photocatalyst is often utilized as a sensitizer in organic molecules to carry out required photochemical reactions. The use of visible light sensitization has reduced the side reaction often associated with photochemical reactions conducted with high energy UV light. Some of the commonly used photocatalysts include Ru and Ir polypyridyl complexes that absorb in the visible-light region.



Scheme I.2.1. Various modes of radical generation

I.3. Classification

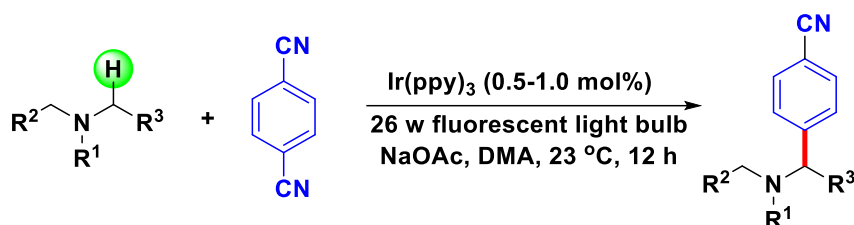
The reactive nature of the radicals and radical cations gives rise to the formation of new bonds. In organic chemistry, we are generally encountered with the formation of C–C and C–X (X = heteroatom) bonds. In this regard, the present chapter aims to define the research on radical-mediated C–C and C–X bond formation by using peroxides and *tert*-butyl nitrite. Specifically, the construction of C–C, C–N and C–O bond formation and generation of various functionalities via the intermediacy of radicals utilizing sp^2 and sp^3 carbon.

I.3.1 Representative Examples of Radical-Mediated C–C Bond Formation

The carbon–carbon bond formation is the most fundamental transformation in synthetic organic chemistry. Nowadays, several novel synthetic methodologies have been developed, especially the radical-mediated C–C bond formation which affords aryl, alkyl, alkenyl, di-functionalized and cyano products. Reactions pertinent to each of these categories are exemplified below.

Radical-Mediated Arylation via sp^2 and sp^3 Carbon

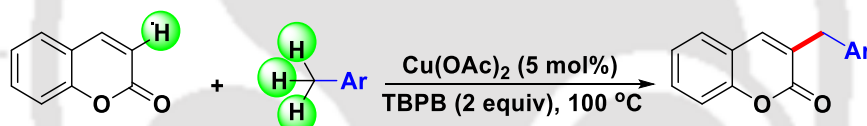
In 2011, MacMillan and co-workers developed a C–H arylation of amines with benzonitriles by using Ir(ppy)_3 as a catalyst and NaOAc as the base under a 26W fluorescent light source via a radical-radical cross-coupling (Scheme I.3.1.1).^[11e] In the same year, β -arylation of saturated aldehydes and ketones via a radical pathway has been disclosed.^[12] Similarly, arylation was achieved by using other arylation sources such as 2-Halobenzodiazoles^[13] and arylborates.^[14]



Scheme I.3.1.1 Ir-catalyzed arylation involving sp^3 carbon

Radical-Mediated Alkylation via sp^2 and sp^3 Carbon

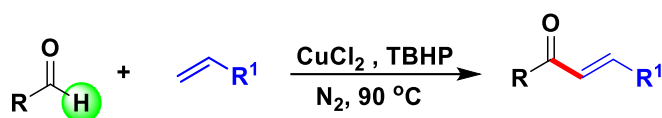
In this context, Duan group reported that coumarin substrates in the presence of $\text{Cu}(\text{OAc})_2$ and *tert*-butylperoxy benzoate (TBPB) and methylarenes, provided regioselective α -benzylation at the sp^2 C–H sites (Scheme I.3.1.2).^[15] Similar type of α -benzylation of α,β -unsaturated carbonyl compounds with toluene derivatives has been achieved in the presence of triethyl borane (Et_3B).^[16] In the presence of NaN_3 and hypervalent iodine, chromones afforded a selective alkylation.^[17] Using di-*tert*-butyl peroxide (DTBP) β -alkylation of chromones was reported.^[18] Alkylation has also been reported by using other alkyl sources such as ethers,^[19] peroxides^[20] and alcohols.^[21]



Scheme I.3.1.2. Cu-catalyzed benzylation of coumarins

Radical-Mediated Alkenylation via sp^2 and sp^3 Carbon

Lei and co-workers reported a copper-catalyzed oxidative radical cross-coupling between alkenes and aldehydes (Scheme I.3.1.3).^[22] In the presence of CuI , KI and DTBP radical alkenylation of ethers^[23] and thioethers^[24] with alkenes were reported. Likewise, alkenylation has been achieved by using other alkenylation sources such as alkynes,^[25] enones,^[26] α,β -unsaturated carboxylic acids,^[27] β -nitrostyrenes,^[28] β -halostyrenes.^[29]

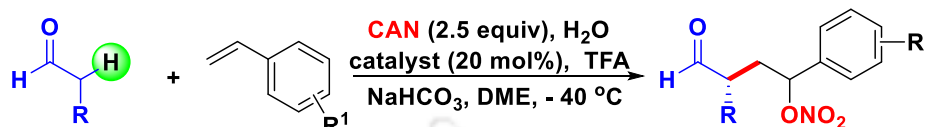


Scheme I.3.3. Cu-catalyzed alkenylation of aldehydes

Radical-Mediated Di-functionalizations via sp^2 and sp^3 Carbon

MacMillan and co-workers achieved the difunctionalization of styrenes via radical C–H activation. This di-functionalization was achieved by using imidazolidinone as the

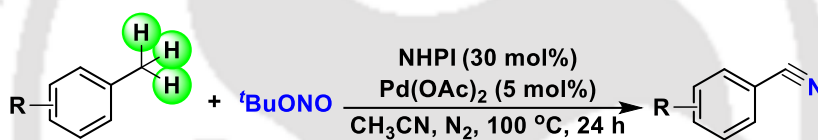
SOMO catalyst and ceric ammonium nitrate as an oxidant (Scheme I.3.1.4).^[30] By using TBHP as an oxidant, di-functionalization of alkenes with aldehydes was achieved.^[31] Similar type of di-functionalization was reported by Klusman *et al.* when the aldehyde was replaced by ketone.^[32] Vinyl arenes^[33] and allylic alcohols^[34] have afforded a similar type of di-functionalization known as oxy-alkylation via a radical pathway.



Scheme I.3.1.4. Imdazolidinone catalyzed oxy-alkylation of styrenes with aldehydes

Radical-Mediated Cyanation via sp^3 Carbon

In 2013, Wang and co-workers reported a TBN mediated palladium(II)-catalyzed oxidation of the benzyl C–H bond to directly convert methylarenes into aromatic nitriles via a radical pathway (Scheme I.3.1.5).^[35] In this process, TBN serves the dual role of an oxidant as well as a source of nitrogen.



Scheme I.3.1.5. Pd-catalyzed cyanation of methylarene

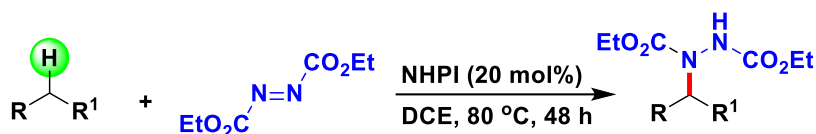
I.3.2. Representative Examples of Radical-Mediated C–N Bond Formation

With more efforts focusing on radical-radical cross-coupling, research has not been confined to C–C bond formation; several methodologies have been developed to construct C–N bonds. Representative examples of various forms of C–N bond formations are shown below.

Radical-Mediated Amination via sp^2 and sp^3 Carbon

A direct C–H amination of a radical amination of $C(sp^3)$ –H bonds was developed by Inoue and co-workers employing N-hydroxyphthalimide (NHPI) as a catalyst and dialkyl azodicarboxylate as the trapping agent (Scheme I.3.2.1).^[36] In this strategy, benzylic, propargylic, and aliphatic C–H bonds can be easily tolerated. Direct $C(sp^3)$ –H amination of benzocyclic amines using the Ir catalyst has been achieved through the addition of α -aminoalkyl radicals to azodicarboxylate esters.^[37] Amination has also been reported by using

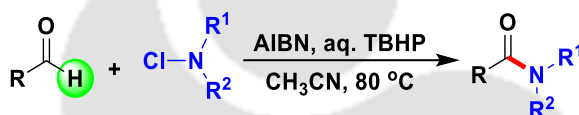
other sources of amination such as anilines,^[38] imidazoles,^[39] ammonia,^[40] pyridine,^[41] alkyl amines.^[42]



Scheme I.3.2.1. NHPI-catalyzed intermolecular amination involving sp^3 carbon

Radical-Mediated Amidation via sp^2 Carbon

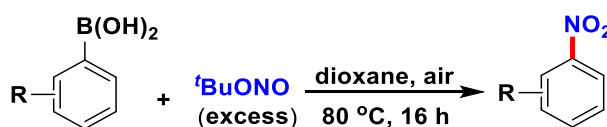
The synthesis of amides using TBHP mediated and AIBN-catalyzed amidation of aldehydes with N-chloroamines has been disclosed by Singh group (Scheme I.3.2.2).^[43] In the presence of TBHP, Hartwig and coworkers also reported a copper-catalyzed intermolecular amidation and imidation of unactivated alkanes, affording the corresponding N-alkyl products.^[44]



Scheme I.3.2.2. AIBN-catalyzed amidation of aldehydes with N-chloroamines

Radical-Mediated Nitration via sp^2 Carbon

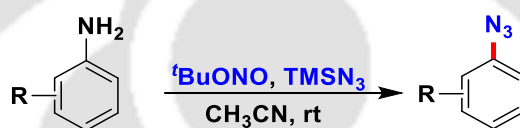
Besides wide range applications of TBN, it can also serve as a nitrating agent participating in various nitration reactions. In this context, an efficient method for the synthesis of nitro compounds by treating phenylboronic acids with an excess of TBN has been reported by Beller and co-workers (Scheme I.3.2.3).^[45] Similarly, alkenes,^[46] phenols,^[47] sulphonamides,^[48] undergone nitration by using TBN as a nitrating agent. Apart from TBN, ceric ammonium nitrate (CAN) along with NaNO_2 has also been used as a source of nitration. In this direction, Hwu *et al.* reported that alkenes could be nitrated with excess sodium nitrite in the presence of CAN and acetic acid in chloroform.^[49] He also showed that the same reagent combination can be used for the ultrasonic nitration of allylsilanes.^[50] Simultaneous nitration and acetamidation has been achieved in acetonitrile using CAN and sodium nitrite.^[51]



Scheme I.3.2.3. TBN-mediated sp^2 C-H nitration of phenylboronic acids

Radical-Mediated Azidation via sp^2 and sp^3 Carbon

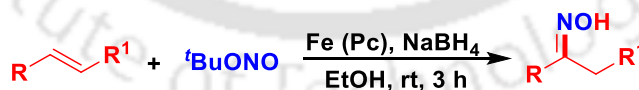
An efficient TBN-enabled azidation of anilines with the aid of azidotrimethylsilane was disclosed by Moses and co-workers (Scheme I.3.2.4).^[52] The reaction was having good functional group tolerance. In presence of Zhdankin azidoiodane reagent Chen and co-workers introduced visible-light-induced Ru-catalyzed azidation of aliphatic tertiary C–H bonds.^[53] Analogous to this, Greaney and co-workers reported an azidation of benzylic C–H groups by a copper photoredox catalyst and the Zhdankin azidoiodane reagent.^[54] A photoinduced C(sp^3)–H azidation was also reported by using tosyl azide as the azide source.^[55] Azidation of olefinic substrates like stilbene, acenaphthalene, cinnamic acids, esters, and amides has been reported through CAN promoted addition of azide radicals to olefins.^[56]



Scheme I.3.2.4. TBN-mediated sp^2 C–H azidation of aniline

Radical-Mediated Oximation via sp^2 and sp^3 Carbon

In 2009, Beller and co-workers reported an iron-catalyzed oximation of alkenes in the presence of NaBH_4 to have access to the oximes (Scheme I.3.2.5).^[57] Oximation and aminooximation of vicinal unactivated alkenes were developed by Han and co-workers using TBN, in which TBN was employed not only as of the iminoxyl radical initiator but also the carbon radical trap.^[58] In the presence of TBN Yang and co-workers developed a Brønsted acid-catalyzed benzylic C–H oximation of aza-arenes to afford the oximes in moderate to good yields.^[59]



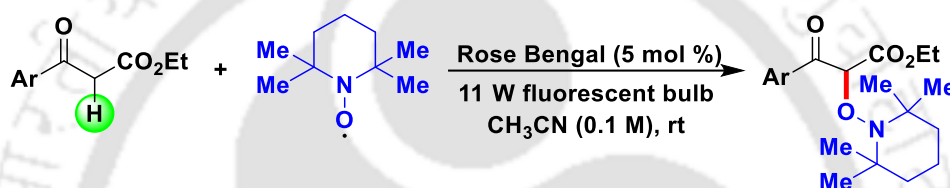
Scheme I.3.2.5. TBN-mediated oximation of alkenes involving sp^2 carbon

I.3.3. Representative Examples of Radical-Mediated C–O Bond Formation

The direct oxidative cross-coupling of hydrocarbons with oxy-compounds has emerged as a promising method for the construction of C–O bonds. The C–O bond installations *via* the intermediacy of radicals occur in several ways; the common forms being oxyamination, esterification, hydroxylation and alkoxylation. Representative examples of various forms of C–O bond formations are discussed below.

Radical-Mediated Oxyamination via sp^3 Carbon

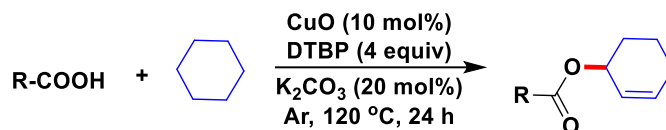
The 2,2,6,6-tetramethylpiperidine-1-oxyl radical (TEMPO), is a well-known persistent radical. Therefore, it is possible to achieve the selective coupling of several radicals with TEMPO for the construction of C–O bonds. In this connection, the Tan group developed a visible-light-induced α -oxyamination reaction between TEMPO and 1,3-dicarbonyl compounds using rose bengal as the photocatalyst (Scheme I.3.3.1).^[60] It may be mentioned here, that this metal-free reaction also proceeds smoothly in the water. A strongly electron-deficient aromatic β -ketoester reacts to faster reaction than electron-rich substrates. No reaction has been observed with alkyl ketones. Latter, Deng and co-workers also reported a Cu-mediated α -oxyamination of 1,3-dicarbonyl compounds with TEMPO and its derivatives as oxygen sources.^[61]



Scheme I.3.3.1. Rose bengal-catalyzed oxyamination involving sp^3 carbon

Radical-Mediated Esterification via sp^3 Carbon

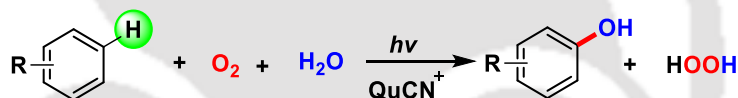
Li and co-workers developed a copper-catalyzed oxidative coupling of alkanes and carboxylic acids for the selective synthesis of allylic esters (Scheme I.3.3.2).^[62] Around the same time, Chaudhuri and co-workers also reported a copper-catalyzed oxidative cross-dehydrogenative coupling for the construction of α -acyloxy ethers from cyclic ethers and carboxylic acids.^[63] In this work, *tert*-butyl hydroperoxide (TBHP) was used as the oxidant under atmospheric conditions. Iron-catalyzed oxidative esterification between carboxylic acids and unactivated C-(sp^3)-H bonds from symmetric and asymmetric ethers, that proceeds through a radical mechanism involving a diiron(III) intermediate was reported by Han and co-workers.^[64] Further, a directing-group-assisted copper-catalyzed oxidative esterification of phenols with aldehydes was developed by Xuan and co-workers.^[65] In addition to this, an NHC-catalyzed amino-esterification of aldehydes with TEMPO as the oxidant was disclosed by the Studer group.^[66]



Scheme I.3.3.2. Cu-catalyzed esterification of cycloalkanes

Radical-Mediated Hydroxylation via sp^2 and sp^3 Carbon

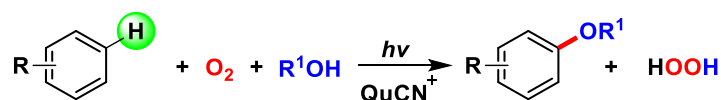
In the presence of 3-cyano-1-methylquinolinium ion (QuCN^+) photosensitizer, Fukuzumi and coworkers reported an efficient photocatalytic method for the selective oxygenation of benzene to phenol with dioxygen (O_2) and water (H_2O) (Scheme I.3.3.3).^[67] The photocatalytic oxygenation of benzene to phenol under visible-light conditions was further improved by using 2,3-dichloro-5,6-dicyano-*p*-benzoquinone (DDQ) as the photosensitizer.^[68] Later on, a photocatalytic cross-coupling strategy for aromatic C–H functionalization, via a combination of photocatalysis and cobalt catalysis, was utilized for benzene hydroxylation by Wu and co-workers.^[69] Again Fukuzumi and co-workers reported metal-free photocatalyzed oxygenation of cycloalkane to achieve cyclohexanone, cyclohexanol, and hydrogen peroxide in 2011.^[70]



Scheme I.3.3.3 Pd-catalyzed ortho-hydroxylation of arylcarboxylic acids

Radical-Mediated Alkoxylation via sp^2 Carbon

Fukuzumi and coworkers have reported an efficient photocatalytic method for the selective oxygenation of benzene to alkoxy benzene with dioxygen (O_2) and alcohol (ROH) (Scheme I.3.3.4). They disclosed that the highly oxidizing 3-cyano-1-methylquinolinium ion (QuCN^+) can act as an efficient photosensitizer to achieve the single-electron oxidation of benzene to generate a radical cation. Through this intermediate, aryl C–H functionalization of benzene and other arenes was achieved with nucleophiles such as alcohols using O_2 as the oxidant.^{[66]Δ}



Scheme I.3.3.4. Cu-catalyzed ortho-alkoxylation of arylcarboxylates

I.4. References

- [1] a) F. Monnier and M. Taillefer, *Angew. Chem. Int. Ed.*, **2009**, *48*, 6954-6971; b) G. Evano, N. Blanchard and M. Toumi, *Chem. Rev.*, **2008**, *108*, 3054-3131; c) J. P. Corbet and G. Mignani, *Chem. Rev.*, **2006**, *106*, 2651-2710; d) A. Correa, O. G. Mancheño and C. Bolm, *Chem. Soc. Rev.*, **2008**, *37*, 1108-1117; e) S. Würtz and F. Glorius, *Acc. Chem. Res.*, **2008**, *41*, 1523-1533; f) S. V. Ley and A. W. Thomas, *Angew. Chem. Int. Ed.*, **2003**, *43*, 5400-5449.
- [2] a) W. Carruthers and I. Coldham, *Modern Methods of Organic Synthesis*, Cambridge University Press, Cambridge, **2004**, pp. 45-67; b) D. M. Huryn, in *Comprehensive Organic Synthesis*, Vol. 1 (Eds.: B. M. Trost and I. Fleming), Pergamon, Oxford, **1991**, pp. 49-75; c) T. Banno, Y. Hayakawa and M. Umeno, *J. Organomet. Chem.*, **2002**, *653*, 288-291.
- [3] a) Y. Hong, G. Zhang, H. Wang, Z. Huang, J. Wang, A. K. Singh, A. Lei *Chemical Reviews* **2017**, *117*, 9016-9085; b) A. Gunay, K. H. Theopold, *Chem. Rev.* **2010**, *110*, 1060-1081; (c) C. L. Sun, B.-J. Li, Z.-J. Shi, *Chem. Rev.* **2011**, *111*, 1293-1314.
- [4] P. B. Arockiam, C. Bruneau, P. H. Dixneuf, *Chem. Rev.* **2012**, *112*, 5879-5918.
- [5] D. A. Colby, Bergman, R. G. J. A. Ellman, *Chem. Rev.* **2010**, *110*, 624-655.
- [6] C. Liu, H. Zhang, W. Shi, A. Lei, *Chem. Rev.* **2011**, *111*, 1780-1824.
- [7] C. Liu, D. Liu, A. Lei, *Acc. Chem. Res.* **2014**, *47*, 3459-3470
- [8] S. A. Girard, T. Knauber, C. J. Li, *Angew. Chem., Int. Ed.* **2014**, *53*, 74-100.
- [9] M. K. Singh, H. K. Akula, S. Satishkumar, L. Stahl,; M. K. Lakshman, *ACS Catal.* **2016**, *6*, 1921-1928.
- [10] H. Togo, *Advanced Free Radical Reactions for Organic Synthesis, 1st ed.*; Elsevier: Amsterdam, Boston, **2004**.
- [11] a) I. A. Yaremenko, V. A. Vil, D. V. Demchuk, A. O. Terent'ev, *Beilstein J. Org. Chem.*, **2016**, *12*, 1647-1748; b) P. Li, X. Jia, *Synthesis*, **2018**, *50*, 711-722; c) N. G. Khaligh, *Curr. Org. Chem.*, **2018**, *22*, 1120-1138; d) J. M. R. Narayanam, C. R. J. Stephenson, *Chem. Soc. Rev.*, **2011**, *40*, 102-113; e) A. McNally, C. K. Prier, D. W. MacMillan, *Science* **2011**, *334*, 1114-1117.
- [12] M. T. Pirnot, D. A. Rankic, D. B. Martin, D. W. MacMillan, *Science* **2013**, *339*, 1593-1596.
- [13] C. K. Prier, D. W. C. MacMillan, *Chem. Sci.* **2014**, *5*, 4173-4178.
- [14] D. Liu, Y. Li, X. Qi, C. Liu, Y. Lan, A. Lei, *Org. Lett.* **2015**, *17*, 998-1001.

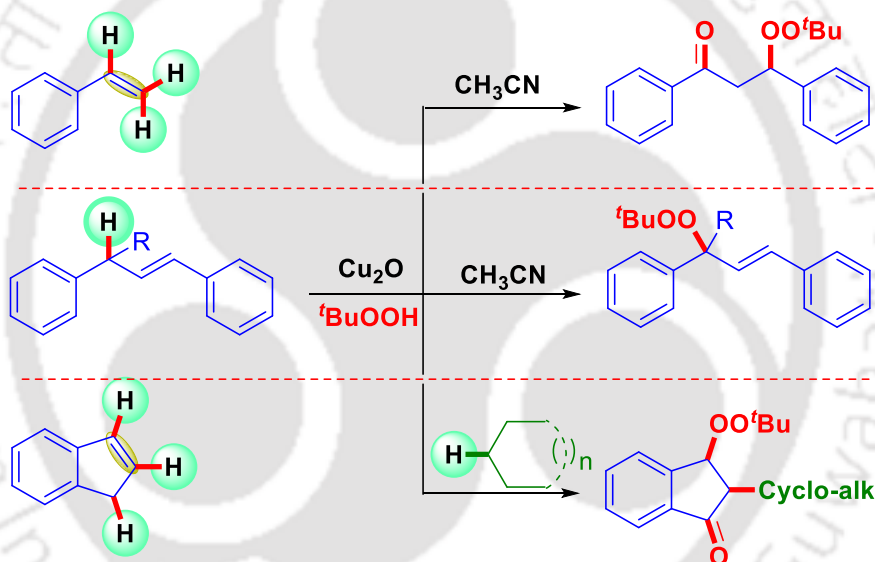
- [15] S. L. Zhou, L. N. Guo, X.-H. Duan, *Eur. J. Org. Chem.* **2014**, 2014, 8094-8100.
- [16] M. Ueda, E. Kondoh, Y. Ito, H. Shono, M. Kakiuchi, Y. Ichii, T. Kimura, T. Miyoshi, T. Naito, O. Miyata, *Org. Biomol. Chem.* **2011**, 9, 2062-2064.
- [17] R. Narayan, A. P. Antonchick, *Chem. Eur. J.* **2014**, 20, 4568-4572.
- [18] J. Zhao, H. Fang, P. Qian, J. Han, Y. Pan, *Org. Lett.* **2014**, 16, 5342-5345.
- [19] B. Niu, W. Zhao, Y. Ding, Z. Bian, C. U. Jr. Pittman, A. Zhou, H. Ge, *J. Org. Chem.* **2015**, 80, 7251-7257.
- [20] a) P. Z. Zhang, J. A. Li, L. Zhang, A. Shoberu, J. P. Zou, W. Zhang, *Green Chem.* **2017**, 19, 919-923; b) S. Guo, Q. Wang, Y. Jiang, J. T. Yu, *J. Org. Chem.* **2014**, 79, 11285-11289.
- [21] S. Y. Zhang, Y. Q. Tu, C. A. Fan, F. M. Zhang, L. Shi, *Angew. Chem., Int. Ed.* **2009**, 48, 8761-8765.
- [22] J. Wang, C. Liu, J. Yuan, A. Lei, *Angew. Chem., Int. Ed.* **2013**, 52, 2256-2259.
- [23] D. Liu, C. Liu, H. Li, A. Lei, **2014**, 50, 3623-3626.
- [24] H. Cao, D. Liu, C. Liu, X. Hu, A. Lei, *Org. Biomol. Chem.* **2015**, 13, 2264-2266.
- [25] a) Z. Q. Liu, L. Sun, J. G. Wang, J. Han, Y. K. Zhao, B. Zhou, *Org. Lett.* **2009**, 11, 437-439; b) C. D. Lu, X. Tusun, *Synlett* **2013**, 24, 1693-1696; c) J. Li, J. Zhang, H. Tan, D. Z. Wang, *Org. Lett.* **2015**, 17, 2522-2525.
- [26] G. Qin, X. Chen, L. Yang, H. Huang, *ACS Catal.* **2015**, 5, 2882-2885.
- [27] a) Z. Cui, X. Shang, X.-F. Shao, Z.-Q. Liu, *Chem. Sci.* **2012**, 3, 2853-2858; b) J. X. Zhang, Y. J. Wang, W. Zhang, N. X. Wang, C. B. Bai, Y. L. Xing, Y. H. Li; J. L. Wen, *Sci. Rep.* **2015**, 4, 7446; c) Z. Liu, L. Wang, D. Liu, Z. Wang, *Synlett* **2015**, 26, 2849-2852.
- [28] S. Guo, Y. Yuan, J. Xiang, *New J. Chem.* **2015**, 39, 3093-3097.
- [29] A. Solvhoj, A. Ahlburg, R. Madsen, *Chem. -Eur. J.* **2015**, 21, 16272-16279.
- [30] T. H. Graham, C. M. Jones, N. T. Jui, D. W. MacMillan, *J. Am. Chem. Soc.* **2008**, 130, 16494-16495.
- [31] a) W. Liu, Y. Li, K. Liu, Z. Li, *J. Am. Chem. Soc.* **2011**, 133, 10756-10759; b) J. Li, D. Z. Wang, *Org. Lett.* **2015**, 17, 5260-5263.
- [32] B. S. Chaput, J. Demaerel, H. Engler, M. Klussmann, *Angew. Chem., Int. Ed.* **2014**, 53, 8737-8740
- [33] a) K. Cheng, L. Huang, Y. Zhang, *Org. Lett.* **2009**, 11, 2908-2911; b) H. Sun, Y. Zhang, F. Guo, Z. Zha, Z. Wang, *J. Org. Chem.* **2012**, 77, 3563-3569; c) X. W. Lan, N. X. Wang,

- W. Zhang, J. L. Wen, C. B. Bai, Y. Xing, Y. H. Li, *Org. Lett.* **2015**, *17*, 4460-4463; d) W. Zhang, N. X. Wang, C. B. Bai, Y. J. Wang, X. W. Lan, Y. Xing, Y. H. Li, J. L. Wen, *Sci. Rep.* **2015**, *5*, 15250; e) P. Du, H. Li, Y. Wang, J. Cheng, X. Wan, *Org. Lett.* **2014**, *16*, 6350-6353; f) J. Zhang, J. Jiang, D. Xu, Q. Luo, H. Wang, J. Chen, H. Li, Y. Wang, X. Wan, *Chem., Int. Ed.* **2015**, *54*, 1231-1235.
- [34] a) X. Q. Chu, H. Meng, Y. Zi, X. P. Xu, S. J. Ji, *Chem. Commun.* **2014**, *50*, 9718-9721; b) A. Bunescu, Q. Wang, J. Zhu, *Angew. Chem., Int. Ed.* **2015**, *54*, 3132-3135; c) R. J. Song, Y. Q. Tu, D. Y. Zhu, F. M. Zhang, S. H. Wang, *Chem. Commun.* **2015**, *51*, 749-752.
- [35] Z. B. Shu, Y. X. Ye, Y. F. Deng, Y. Zhang, J. B. Wang, *Angew. Chem. Int. Ed.* **2013**, *52*, 10573-10576.
- [36] Y. Amaoka, S. Kamijo, T. Hoshikawa, M. Inoue, *J. Org. Chem.* **2012**, *77*, 9959-9969.
- [37] Y. Miyake, K. Nakajima, Y. Nishibayashi, *Chem. - Eur. J.* **2012**, *18*, 16473-16477.
- [38] a) Y. Zhao, B. Huang, C. Yang, W. Xia, *Org. Lett.* **2016**, *18*, 3326-3329; b) R. T. Gephart, D. L. Huang, M. J. B. Aguila, G. Schmidt, A. Shahu, T. H. Warren, *Angew. Chem., Int. Ed.* **2012**, *51*, 6488-6492.
- [39] a) N. A. Romero, K. A. Margrey, N. E. Tay, D. A. Nicewicz, *Science* **2015**, *349*, 1326-1330; b) T. Morofuji, A. Shimizu, J. Yoshida, *J. Am. Chem. Soc.* **2014**, *136*, 4496-4499.
- [40] Y. W. Zheng, B. Chen, P. Ye, K. Feng, W. Wang, Q. Y. Meng, L. Z. Wu, C. H. Tung, *J. Am. Chem. Soc.* **2016**, *138*, 10080-10083.
- [41] T. Morofuji, A. Shimizu, J. Yoshida, *J. Am. Chem. Soc.* **2013**, *135*, 5000-5003.
- [42] T. Morofuji, A. Shimizu, J. Yoshida, *J. Am. Chem. Soc.* **2015**, *137*, 9816-9819.
- [43] R. Vanjari, T. Guntreddi, K. N. Singh, *Green Chem.* **2014**, *16*, 351-356.
- [44] B. L. Tran, B. Li, M. Driess, J. F. Hartwig, *J. Am. Chem. Soc.* **2014**, *136*, 2555-2563.
- [45] X. F. Wu, J. Schranck, H. Neumann, M. Beller, *Chem. Commun.* **2011**, *47*, 12462-12463.
- [46] a) T. Taniguchi, A. Yajima, H. Ishibashi, *Adv. Synth. Catal.* **2011**, *353*, 2643-2647; b) T. Taniguchi, Y. Sugiura, T. Hatta, A. Yajima, H. Ishibashi, *Chem. Commun.* **2013**, *49*, 2198-2200.
- [47] D. Koley, O. C. Colón, S. N. Savinov, *Org. Lett.* **2009**, *11*, 4172-4175.
- [48] B. Kilpatrick, M. Heller, S. Arns, *Chem. Commun.* **2013**, *49*, 514-516.
- [49] J. R. Hwu, K. L. Chen, S. J. Ananthan, *Chem. Soc., Chem. Commun.* **1994**, 1425-1426.
- [50] J. R. Hwu, K. L. Chen, S. Ananthan, H. V. Patel, *Organometallics* **1996**, *15*, 499-505.
- [51] M. V. R. Reddy, B. Mehrotra, Y. D. Vankar, *Tetrahedron Lett.* **1995**, *36*, 4861-4864.

- [52] K. Barral, A. D. Moorhouse, J. E. Moses, *Org. Lett.* **2007**, *9*, 1809-1811.
- [53] Y. Wang, G. X. Li, G. Yang, G. He, G. Chen, *Chem. Sci.* **2016**, *7*, 2679-2683.
- [54] P. T. Rabet, G. Fumagalli, S. Boyd, M. F. Greaney, *Org. Lett.* **2016**, *18*, 1646-1649.
- [55] S. Kamijo, M. Watanabe, K. Kamijo, K. Tao, T. Murafuji, *Synthesis* **2015**, *48*, 115-121.
- [56] a) M. Hu, J. H. Fan, Y. Liu, X. H. Ouyang, R. J. Song, J. H. Li, *Angew. Chem., Int. Ed.* **2015**, *54*, 9577-9580; b) V. Nair, T. G. George, *Tetrahedron Lett.* **2000**, *41*, 3199-3201.
- [57] S. Prateeptongkum, I. Jovel, R. Jackstell, N. Vogl, C. Weckbeckerb, M. Beller, *Chem. Commun.* **2009**, 1990-1992.
- [58] X. X. Peng, Y. J. Deng, X. L. Yang, L. Zhang, W. Yu, B. Han, *Org. Lett.* **2014**, *16*, 4650-4653.
- [59] X. Gao, F. Zhang, G. J. Deng, L. Yang, *Org. Lett.* **2014**, *16*, 3364-3367.
- [60] H. Liu, W. Feng, C. W. Kee, Y. Zhao, D. Leow, Y. Pan, C. H. Tan, *Green Chem.* **2010**, *12*, 953-956.
- [61] X. Luo, Z. L. Wang, J.-H. Jin, X. L. An, Z. Shen, W. P. Deng, *Tetrahedron* **2014**, *70*, 8226-8230.
- [62] C. Y. Wang, R. J. Song, W. T. Wei, J. H. Fan, J. H. Li, *Chem. Commun.* **2015**, *51*, 2361-2363.
- [63] D. Talukdar, S. Borah, M. K. Chaudhuri, *Tetrahedron Lett.* **2015**, *56*, 2555-2558.
- [64] J. Zhao, H. Fang, W. Zhou, J. Han, Y. Pan, *J. Org. Chem.* **2014**, *79*, 3847-3855.
- [65] Y. Zheng, W. B. Song, L. J. Xuan, *Org. Biomol. Chem.* **2015**, *13*, 10834-10843.
- [66] J. Guin, S. De Sarkar, S. Grimme, A. Studer, *Angew. Chem., Int. Ed.* **2008**, *47*, 8727-8730.
- [67] K. Ohkubo, T. Kobayashi, S. Fukuzumi, *Angew. Chem., Int. Ed.* **2011**, *50*, 8652-8655.
- [68] K. Ohkubo, A. Fujimoto, S. Fukuzumi, *J. Am. Chem. Soc.* **2013**, *135*, 5368-5371.
- [69] Y. W. Zheng, B. Chen,; P. Ye, K. Feng, W. Wang, Q. Y. Meng, L. Z. Wu, C. H. Tung, *J. Am. Chem. Soc.* **2016**, *138*, 10080-10083.
- [70] K. Ohkubo, A. Fujimoto, S. Fukuzumi, *Chem. Commun.* **2011**, *47*, 8515-8517.

CHAPTER II

Copper(I) Catalyzed Differential Peroxidation of Terminal and Internal Alkenes Using TBHP



ABSTRACT: Terminal and internal alkenes react contrarily with tert-butyl hydroperoxide (TBHP) giving different products. A Cu(I) catalysed decarbonylative C–C bond formation followed by a carbonylation-peroxidation of vinyl arenes has been achieved using tert-butyl hydroperoxide (TBHP) as the oxidant in acetonitrile solvent. Whereas, α -methyl styrenes yielded aryl methyl ketones and the α -substituted unsymmetrical internal alkenes afforded selective α -peroxidation under the identical reaction conditions. Concurrent regioselective peroxidation-carbonylation-cycloalkylation/cyclo-etherification of internal cyclic alkene such as indene is achieved by switching the solvent system from acetonitrile to cycloalkanes / cyclic ether. All these reactions proceed via radical paths generating interesting peroxy-compounds.

CHAPTER II

II. Copper(I) Catalyzed Differential Peroxidation of Terminal and Internal Alkenes Using TBHP

II.1. Introduction

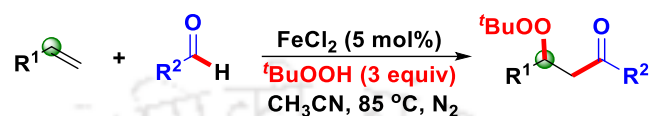
Construction of C–C or C–X bonds via a radical pathway in targeted synthesis has undergone a renaissance in modern organic synthesis.^[1] In this direction, alkenes which are simple organic molecules have been widely applied in organic synthesis for the construction of a diverse array of complex molecules. One of the finest approaches to build such class of molecules in a single operation is via the direct 1,2-di-functionalization of alkenes. Both intra and intermolecular hetero-di-functionalization of alkenes have received considerable attention. In contrast to intermolecular processes, intramolecular di-functionalization are much more selective and thermodynamically favourable. The transition-metal-catalyzed intermolecular di-functionalization such as carbohalogenation,^[2] dihydroxylation,^[3] oxyarylation,^[4] oxyamination,^[5] aminofluorination,^[6] aminocyanation,^[7] hydro-alkylation,^[8] carboboration,^[9] and other di-functionalization^[10] are well explored. However, intermolecular di-functionalization of olefins has rarely been explored following the radical-mediated C–H bond functionalization strategy. Carbonylation of alkenes has been developed as one of the powerful methods for the synthesis of carbonyl compounds.^[11] But the simultaneous introduction of a carbonyl group and another functional group such as alcohol, amine, and peroxide into alkenes is not well explored.^[12]

II.2. Strategies for Differential Benzylic-Peroxidation

Lately, organic peroxides have been used as oxidising agents and initiators for free-radical reactions both in academia and industry. These peroxy-compounds are produced and used in various natural and biological processes such as preparation of antimalarial agents,^[5d-f] anthelmintics,^[12g] and antitumor drugs.^[12h,i] A survey of the literature entails that of the formation of benzylic-peroxy-compounds, a plethora of methods have been recently reported using TBHP mediated radical approach.

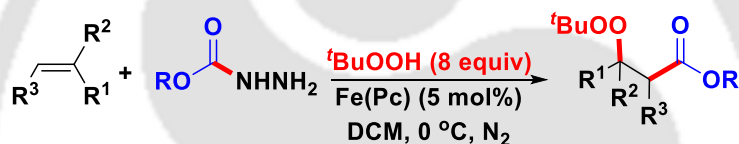
In this context, intermolecular differential peroxidation of olefins has rarely been explored following radical-mediated approach. Recently a Fe(II)-catalyzed carbonylation-

peroxidation of olefins was reported via a radical pathway using aldehydes and *tert*-butyl hydroperoxide (TBHP) (Scheme II.2.1).^[13a] This carbonylation-peroxidation product has been utilized by the same group for the synthesis of (\pm) clavilactones A, B^[13b] and D.^[13c] Complimentary asymmetric carbofunctionalization of olefins using aldehydes has been demonstrated by MacMillan *et al.* following the concept of singly occupied molecular orbital (SOMO).^[13d,e]



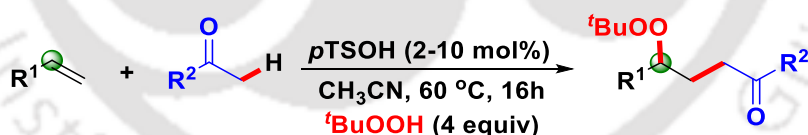
Scheme II.2.1. Strategy for carbonylation-peroxidation involving sp^2 C–H bond

Again in 2015, Li group reported a Fe-catalyzed alkoxy-carbonylation-peroxidation of alkenes with carbazates and T-Hydro.^[14a] This strategy was used for the synthesis of a variety of β -ester peroxides (Scheme II.2.2).



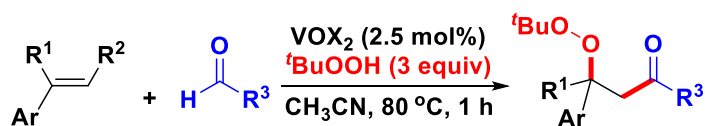
Scheme II.2.2. Strategy for carbonylation-peroxidation involving sp^2 C–H bond

Klussmann *et al.* have reported *p*-toluenesulfonic acid (*p*TsOH) catalyzed oxidative keto-peroxidation of olefins using ketones and TBHP (Scheme II.2.3).^[14b]



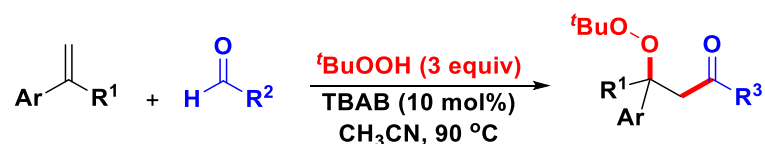
Scheme II.2.3. Strategy for keto-peroxidation involving sp^2 C–H bond

Chen and co-workers reported a vanadium catalyzed carbonylation-peroxidation of styrenes using aldehydes and TBHP. In this three-component reaction, radical addition takes place between a nucleophilic alkene and electrophilic aldehyde followed by coupling with *tert*-butoxy radical (Scheme II.2.4).^[14c]



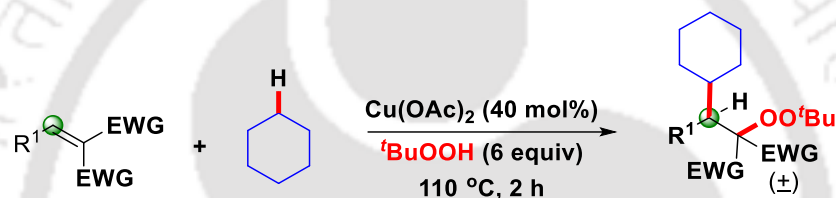
Scheme II.2.4. Strategy for carbonylation-peroxidation involving sp^2 C–H bond

Wang *et al.* reported a tetra-*n*-butylammonium bromide (TBAB)-catalyzed carbonylation-peroxidation of styrenes using aldehydes and TBHP.^[14d] In this metal-free approach, the various styrenes have been treated with aldehyde and TBHP to achieve a variety of β -peroxy compounds (Scheme II.2.5)



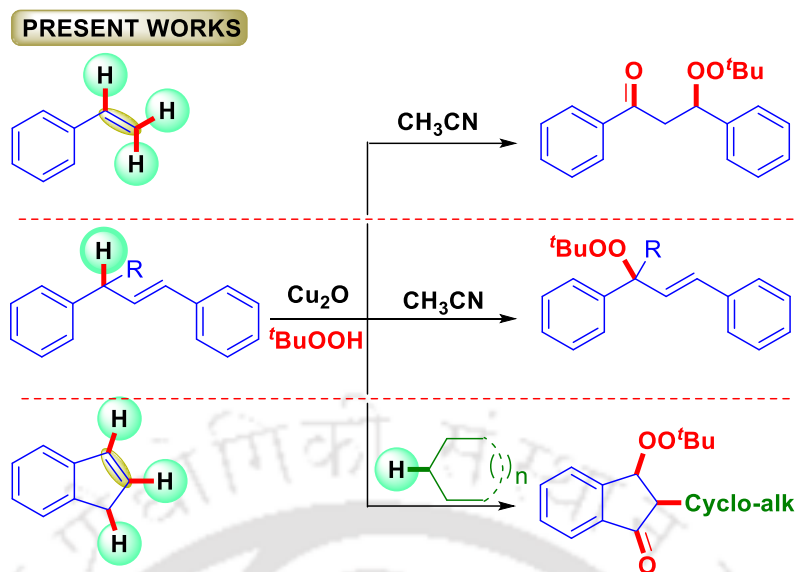
Scheme II.2.5. Strategy for carbonylation-peroxidation involving sp^2 C–H bond

Recently, our group reported a Cu(I)-catalyzed cycloalkylation-peroxidation. In this alkene di-functionalization, various coumarins have been treated with cycloalkanes and TBHP to access a variety of cycloalkylation-peroxidation products (Scheme II.2.6).^[14e]



Scheme II.2.6. Strategy for cycloalkylation-peroxidation involving sp^2 C–H bond

In this context an obvious query arises as to whether this differential peroxidation can be achieved without the presence of another functionality such as aldehyde, ketone or activating group such as carbonyl, ester etc.? Taking cues from the literature and our recent success on TBHP mediated radical functionalizations.^[15] We contemplated that treating only simple alkenes with TBHP can lead us to differential peroxidation, where TBHP can play the dual role of an activator and peroxidation source (Scheme II.2.7).



Scheme II.2.7. Strategies for differential benzylic peroxidation

II.3. Present Work

Although carbonylation-peroxidation, keto-peroxidation and alkylation-peroxidation strategies are reported using carbonyl compounds and activated alkenes, the differential peroxidation of unactivated olefins using only TBHP has never been investigated so far.

Optimization of Reaction Conditions. To execute our strategy on styrene, an initial reaction was carried out by employing styrene (**1**) (1.0 mmol), *tert*-butyl hydroperoxide (**a**) (3.0 mmol), and catalyst $\text{Cu}(\text{OAc})_2$ (10 mol%) in chlorobenzene (2.0 mL) at 110 °C. A new product (**1a**) was isolated in 58% yield (entry 1, Table II.3.1) which was subjected to spectroscopic analysis (^1H and ^{13}C NMR) and comparison of the spectra with the literature,¹² the structure of the product was revealed to be 3-(*tert*-butylperoxy)-1,3-diphenylpropan-1-one (**1a**). Interestingly, this 3-(*tert*-butylperoxy)-1,3-diphenylpropan-1-one (**1a**) has peroxide linkage similar to the most potent anti-malarial drugs such as artemisinin, artemether, dihydroartemisinin and cardamom peroxide (Fig. II.3.1).^[16]

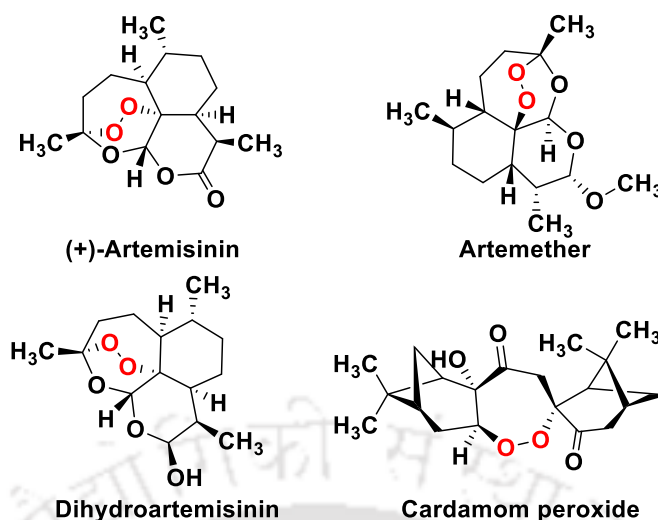
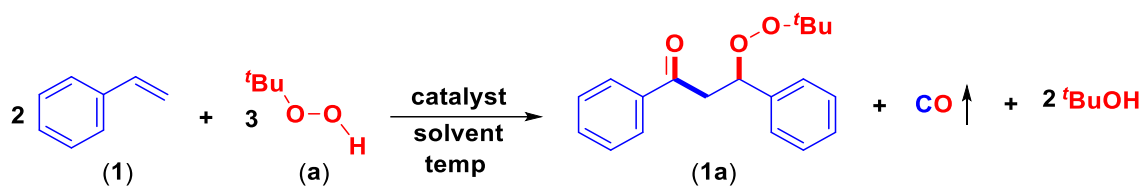


Figure II.3.1. Some potent anti-malarial drugs having peroxy linkage

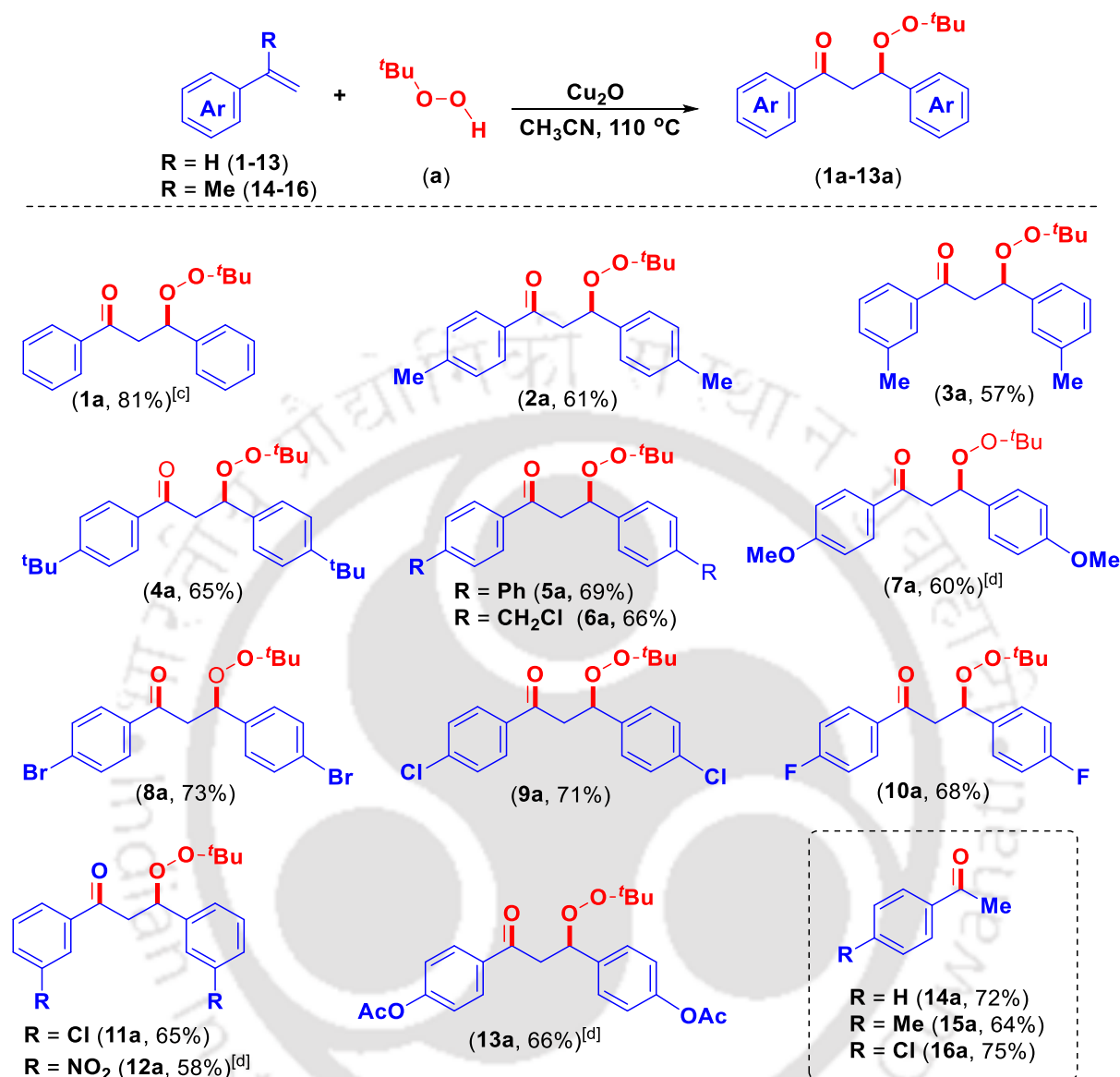
Encouraged by this preliminary success and to arrive at the best possible yield, other reaction parameters such as catalysts, solvents, temperatures were varied. As can be seen from Table II.3.1, among various Cu(I) and Cu(II)-catalysts tested (entries 2-5, Table II.3.1) the catalyst Cu₂O was found to be the best in terms of yield in chlorobenzene solvent. Keeping the catalyst Cu₂O and its quantity fixed, screening of various solvents such as CH₃CN, DCE, cyclohexane, DMSO and DMF (entries 6-10, Table II.3.1) the former (entry 6, Table II.3.1) was found to be the ideal. The reaction when carried out at higher (120 °C) or a lower (100 °C) temperature (entries 11-12, Table II.3.1) reduced the yield of the product (**1a**) marginally compared to the reaction at 110 °C. Keeping the catalyst, solvent and temperature fixed, the yield remained unchanged (81%) using 8 equiv of TBHP, but the yield dropped to 64% using 4 equiv of TBHP (entries 13-14, Table II.3.1). Similarly, keeping all other parameters identical, a marginal improvement in the yield (82%) was observed when the catalyst loading was increased to 15 mol% (entry 15, Table II.3.1) but the yield reduced to 66% using 5 mol% of the catalyst (entry 16, Table II.3.1). A control experiment in the absence of catalyst delivered a trace amount of the desired product (entry 17, Table II.3.1). Thus, it was found that the use of styrene (**1**) (1.0 mmol), *tert*-butyl hydroperoxide (TBHP) (**a**) (3.0 mmol), Cu₂O (10 mol%) in acetonitrile (2.0 mL) at 110 °C for 2 h (entry 6, Table II.3.1) is the ideal reaction condition to achieve (**1a**).

Table II.3.1. Optimization of reaction conditions^[a-d]

Entry	Catalyst (mol%)	Oxidant (equiv)	Solvent (2.0 mL)	Yield (%) ^[b]
1	Cu(OAc) ₂ (10)	TBHP (6)	PhCl	58
2	Cu(OTf) ₂ (10)	TBHP (6)	PhCl	51
3	CuI (10)	TBHP (6)	PhCl	67
4	CuCl (10)	TBHP (6)	PhCl	65
5	Cu ₂ O (10)	TBHP (6)	PhCl	73
6	Cu₂O (10)	TBHP (6)	CH₃CN	81
7	Cu ₂ O (10)	TBHP (6)	DCE	55
8	Cu ₂ O (10)	TBHP (6)	Cyclohexane	49
9	Cu ₂ O (10)	TBHP (6)	DMSO	00
10	Cu ₂ O (10)	TBHP (6)	DMF	00
11	Cu ₂ O (10)	TBHP (6)	CH ₃ CN	78 ^[c]
12	Cu ₂ O (10)	TBHP (6)	CH ₃ CN	72 ^[d]
13	Cu ₂ O (10)	TBHP (8)	CH ₃ CN	81
14	Cu ₂ O (10)	TBHP (4)	CH ₃ CN	64
15	Cu ₂ O (15)	TBHP (6)	CH ₃ CN	82
16	Cu ₂ O (5)	TBHP (6)	CH ₃ CN	66
17	-	TBHP (6)	CH ₃ CN	07

^[a]Reaction condition: Styrene (1) (1.0 mmol) and *tert*-butyl hydroperoxide (a) (3.0 mmol) at 110 °C for 2 h. ^[b]Isolated yields. ^[c]Temperature 120 °C. ^[d]Temperature 100 °C.

After successful carbonylation-peroxidation, various styrenes were investigated under the optimized reaction condition. Styrenes possessing moderately electron-donating groups such as *p*-Me (2), *m*-Me (3), *p*-*t*Bu (4), *p*-Ph (5) and *p*-CH₂Cl (6) provided their corresponding products (2a, 61%), (3a, 57%), (4a, 65%), (5a, 69%) and (6a, 66%) in the modest yields (Scheme II.3.1). Styrene possessing a strongly electron-donating group such as *p*-OMe reacted

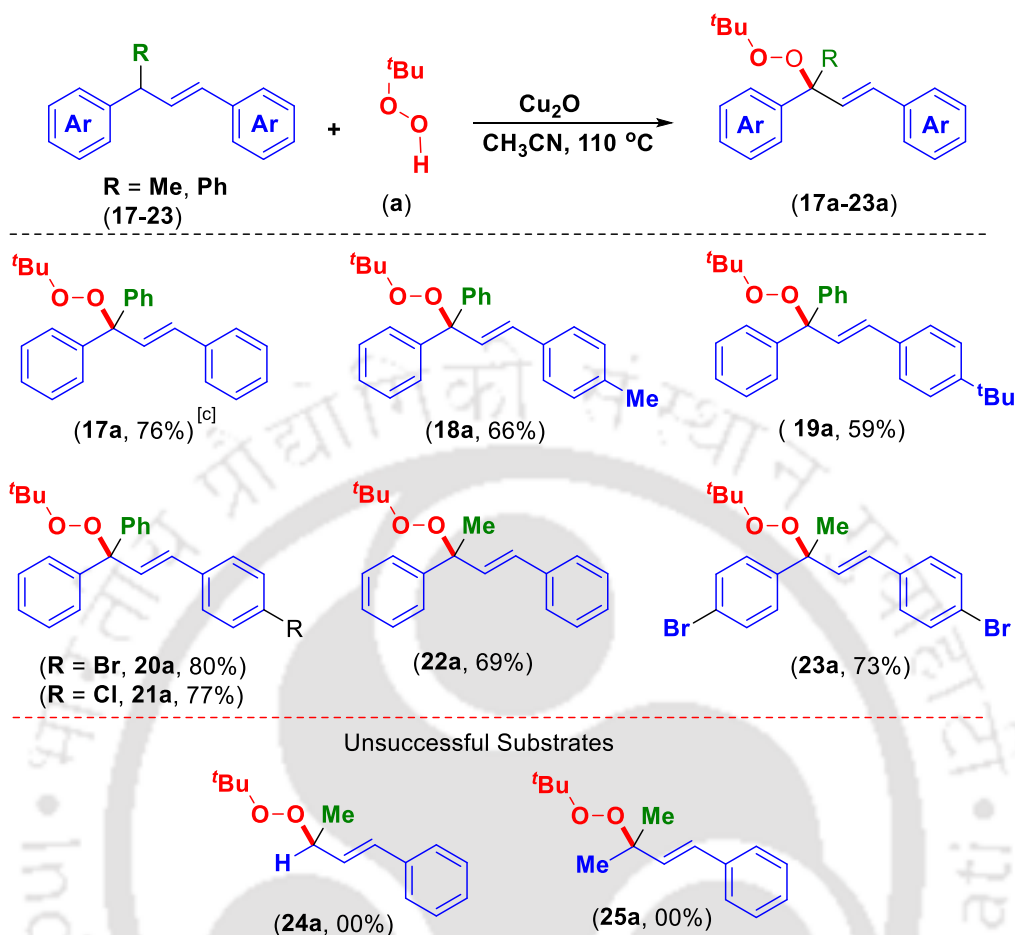
Scheme II.3.1. Carbonylation-peroxidation substrate scope^[a-d]

^[a]Reaction conditions: alkene 1-16 (1.0 mmol) and *tert*-butyl hydroperoxide (a) (3.0 mmol) at 110 °C for 2 h in CH₃CN. ^[b]Isolated yield. ^[c]Yield reported for 20 mmol scale (67%). ^[d] Freshly prepared styrenes were used.

successfully providing the corresponding product (**7a**) in 60% yield. On the other hand, the presence of moderately electron-withdrawing groups on styrenes such as *p*-Br (**8**), *p*-Cl (**9**), *p*-F (**10**) and *m*-Cl (**11**) yielded their respective products (**8a**, 73%), (**9a**, 71%), (**10a**, 68%) and (**11a**, 65%) in moderate yields (Scheme II.3.1). Styrenes having strong electron-withdrawing *m*-NO₂ (**12**) and *p*-OAc (**13**) groups reacted successfully giving their corresponding keto-peroxidation products in moderate yields. The yield of the product (**1a**) dropped to (67%) when a gram scale (1.99 g, 20 mmol) reaction was performed under an identical reaction condition

(Scheme II.3.1). To check whether the α -methyl styrene (**14**) would undergo similar carbonylation-peroxidation, it was subjected to an identical reaction condition. The reaction did not provide any carbonylation-peroxidation product rather yielded acetophenone in 72% yield, suggesting the essential requirement of benzylic sp^2 C–H bond for the process. Thus, this is one of the useful methods for the preparation of aryl methyl ketone. Two other α -methyl styrenes namely, one possessing an electron-donating *p*-Me (**15**) and the other an electron-withdrawing group *p*-Cl (**16**) both provided their aryl methyl ketones (**15a**, 64%) and (**16a**, 75%) in moderate yields (Scheme II.3.1). This result is not surprising and similar transformation has been observed using TBHP in the presence of other catalysts.^[17]

After the successful carbonylation-peroxidation of styrenes, we were curious to investigate the fate of substituted internal alkenes such as (*E*)-prop-2-ene-1,1,3-triyltribenzene (**17**) under the present reaction condition. The HRMS analysis of the product suggests the loss of a proton and addition of 88 mass unit indicating a possible peroxidation (–OO^tBu). Further, the spectroscopic (¹H and ¹³C NMR) analysis of the new product revealed its structure to be (*E*)-(1-(*tert*-butylperoxy)prop-2-ene-1,1,3-triyl)tribenzene (**17a**) which was isolated in 76% yield (Scheme II.3.2). Here, the peroxidation is not at the double bond, rather it is taking place at the tertiary benzylic site. The radical generated at this tertiary site is benzylic as well as allylic and also α -to the other phenyl group, thus is expected to be much more stable than the other possible secondary benzylic radical. Thus, in spite of steric hindrance, the peroxidation is taking place regioselectively at this benzylic tertiary position. This trend in the regioselective peroxidation was demonstrated with four other substrates. The substrate possessing a moderately electron-donating group such as *p*-Me (**18**) and *p*-^tBu (**19**) in the phenyl ring and the other two substrates having moderately electron-withdrawing groups such as *p*-Br (**20**), *p*-Cl (**21**) all provided their peroxo products (**18a**, 66%), (**19a**, 59%), (**20a**, 80%) and (**21a**, 77%) in modest to good yields. This strategy was equally successful even when the phenyl group is replaced with a methyl group as has been demonstrated for substrates (**22**) and (**23**) yielding their peroxo products (**22a**, 69%) and (**23a**, 73%) respectively. When the phenyl group at the allylic position is replaced with hydrogen (a mono-methyl) or methyl (*i.e.* a di-methyl part), the peroxidation was completely unsuccessful giving numerous products (Scheme II.3.2). The yield of the product (**17a**) dropped to 68% when a gram scale (1.22 g, 5 mmol) reaction was performed under an identical reaction condition (Scheme II.3.2).

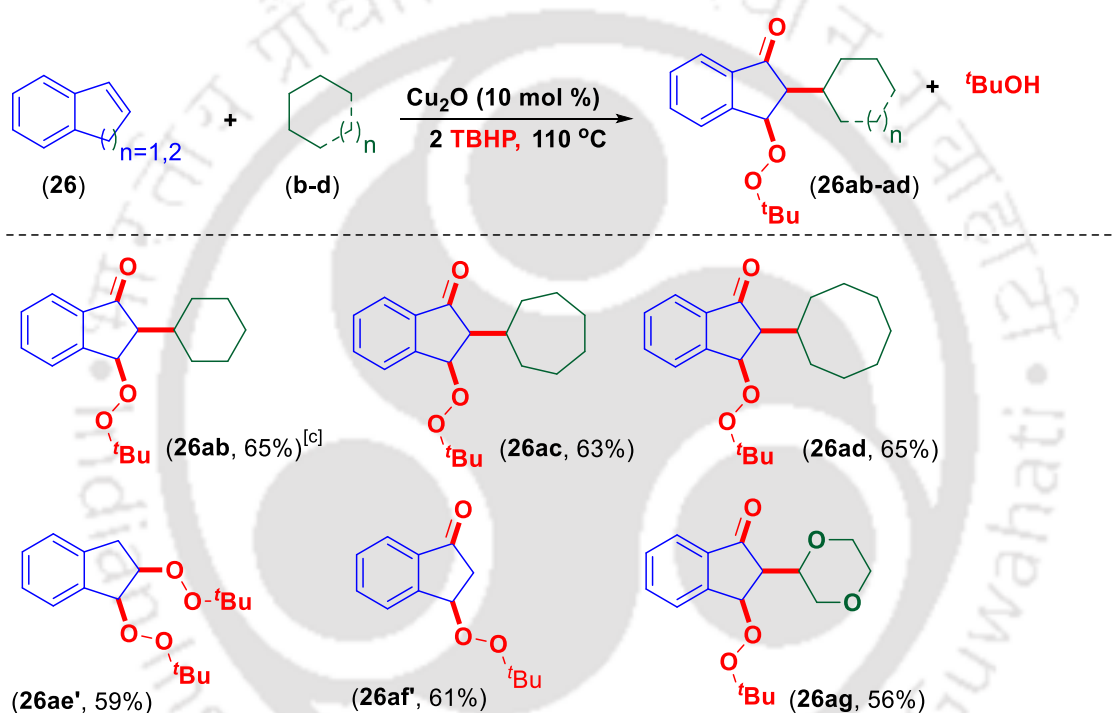
Scheme II.3.2. Selective-peroxidation of substrates^[a-c]

^[a]Reaction conditions: alkene **16-23** (0.5 mmol), and *tert*-butyl hydroperoxide (**a**) (1.5 mmol) at 110 °C for 2 h in CH₃CN. ^[b]Isolated yields. ^[c]Yield reported for 5 mmol scale (68%).

As can be seen from Scheme II.3.1 and Scheme II.3.2, terminal and internal alkenes react differently giving two types of products. The non-cyclic benzylic internal alkenes underwent successful peroxidation at the available allylic position which however is dictated by the stability of the radicals formed (Scheme II.3.2). Thus, the query arises what will happen if a cyclic benzylic internal alkene such as indene (**26**) which has a benzylic/vinylic position? With this objective indene (**26**) was subjected to the present condition. The substrate indene (**26**) was fully consumed but gave a multitude of inseparable products in CH₃CN solvent. Interestingly, by switching the solvent from CH₃CN to cyclohexane (**b**) under otherwise identical reaction condition gave cyclohexylation-peroxidation-benzylic oxidation product (**26ab**) in 35% yield. The structure along with the regioselectivity of the product (**26ab**) has been confirmed by ¹H, ¹³C, COSY, NOESY, and NOE NMR spectroscopic techniques. After

a series of optimization, it was found that by changing the number of TBHP equiv from 3 to 6 resulted in the formation of an improved yield (66%) of the product (Scheme II.3.3). This type of cycloalkane functionalization is in agreement with our previous work, where substituted coumarin undergoes cycloalkylation-peroxidation under a similar condition.^[14e] This tri-functionalization strategy was successfully extended to higher cycloalkanes such as cycloheptane (**c**), cyclooctane (**d**). Both the cycloalkanes coupled successfully with indene (**26**) affording tri-functionalized products (**26ac**) and (**26ad**) in moderate yields of 63% and 65% respectively (Scheme II.3.3).

Scheme II.3.3. Indene tri-functionalization^[a-c]



^[a]Reaction conditions: alkene **26** (0.5 mmol), and *tert*-butyl hydroperoxide (**a**) (3.0 mmol) at 110 °C for 3 h in cyclohexane. ^[b]Isolated Yields. ^[c]Yield reported for 10 mmol scale (57%).

However, when an indene (**26**) was treated with cyclopentane (**e**), the desired tri-functionalized cyclopentylated product (**26ae**) was formed in trace amount which was detected only by HRMS analysis (Fig. II.3.2). However, a diperoxy product of indene (**26ae'**) could be isolated in 59% yield (Scheme II.3.3). Similar to cycloalkanes, cyclic ethers are amenable to form radical adjacent to an oxygen atom. Thus, when this strategy was extended to a cyclic ether such as THF (**f**), the tri-functionalized product (**26af**) could not be isolated due to the formation of a multitude of uncharacterized products but could be detected by HRMS analysis of the inseparable column fraction (Figure II.3.3), interestingly, a keto-peroxidation product

(**26af'**) was isolated in 64% yield. However, another cyclic ether dioxane (**g**) gave the tri-functionalized product (**26ag**) in 57% isolated yield (Scheme II.3.3).

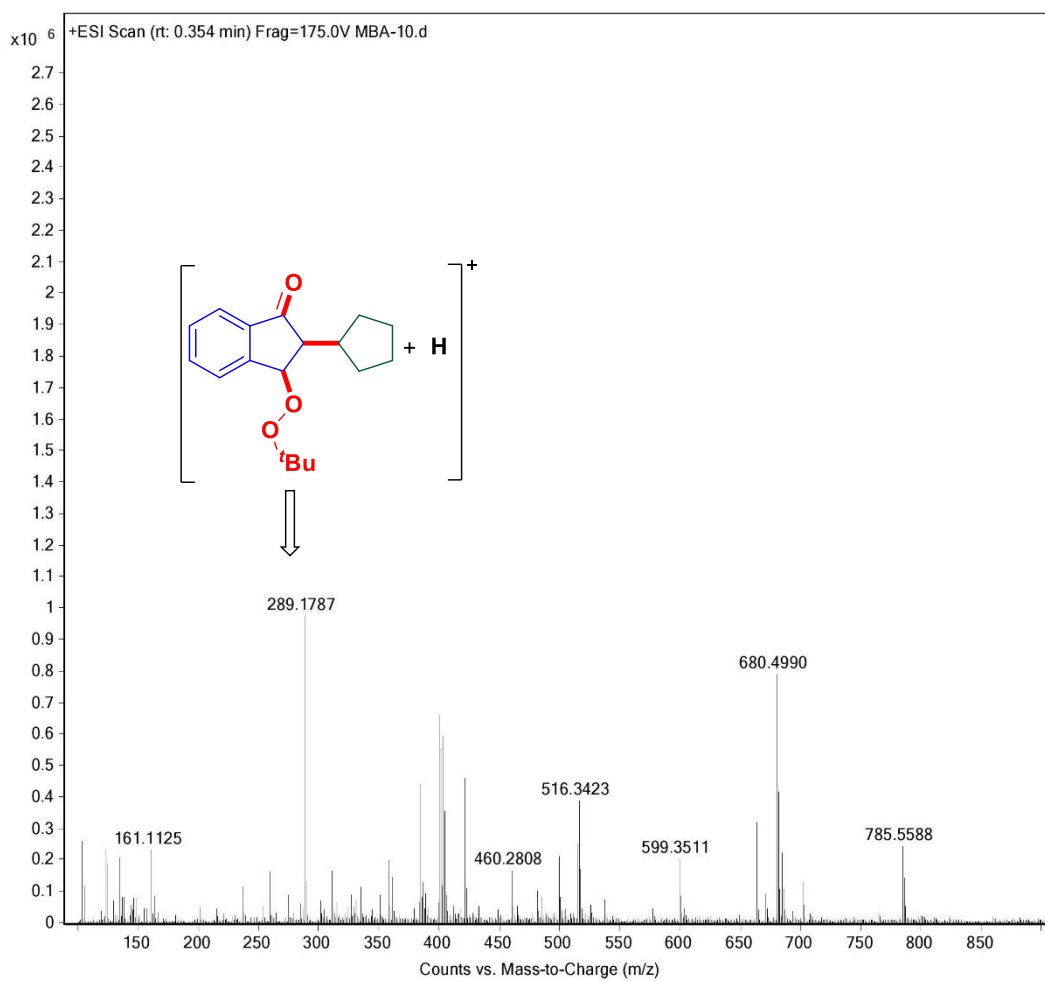


Figure II.3.2. HRMS spectrum of inseparable column fraction.

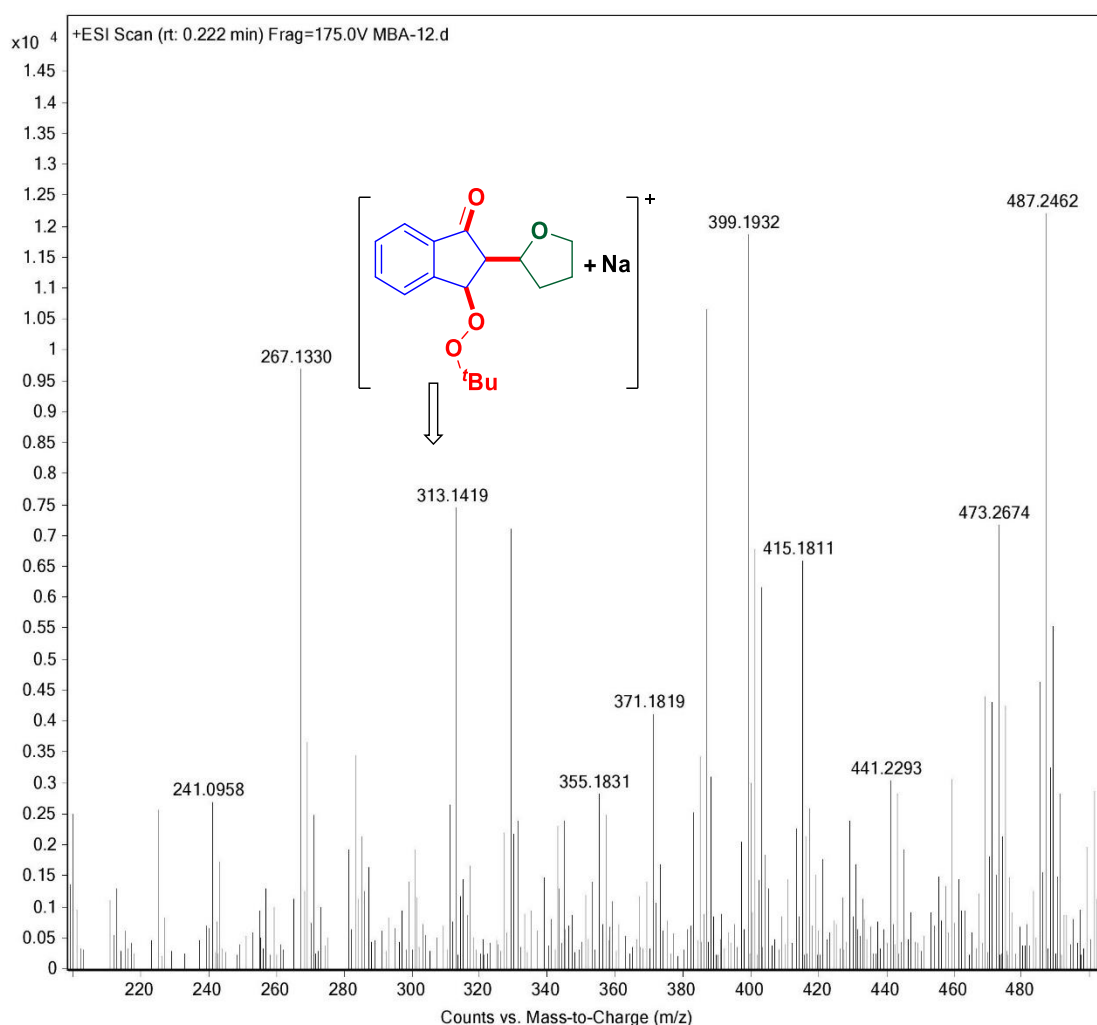
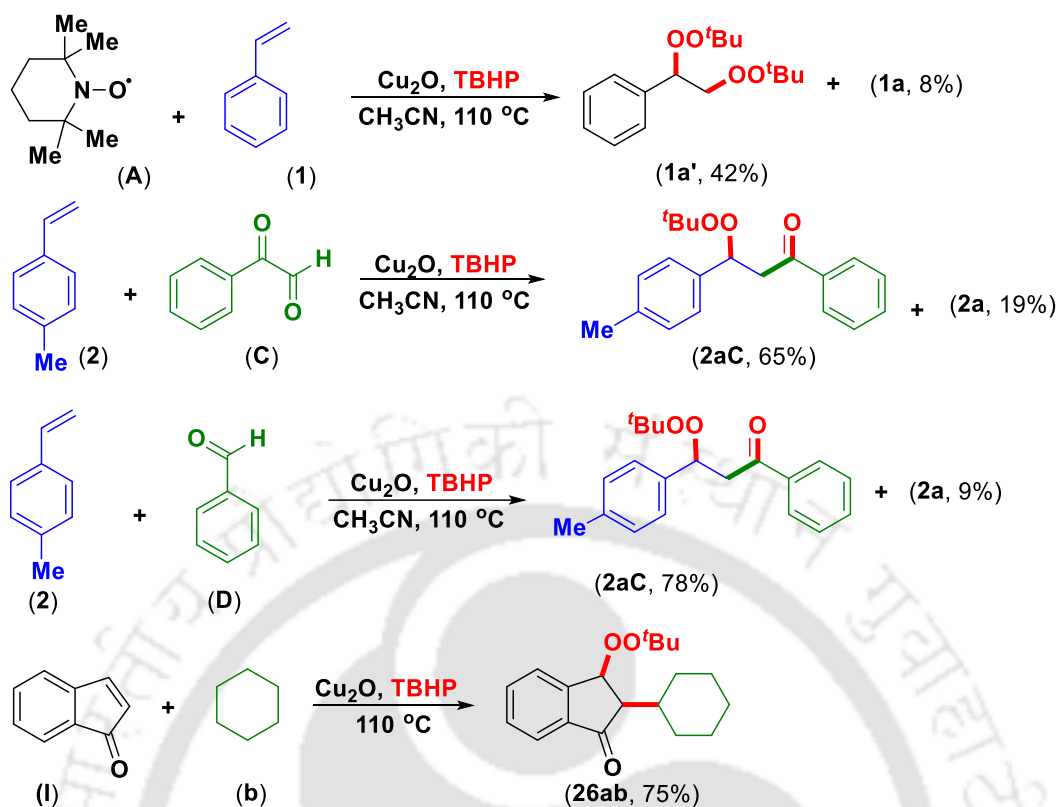


Figure II.3.3. HRMS spectrum of inseparable column fraction

Several control experiments were conducted to elucidate a plausible reaction mechanism for these transformations. When a typical reaction between styrene (**1**) and TBHP (**a**) was carried out under an identical condition, but in the presence of a radical scavenger 2,2,6,6-tetramethylpiperidine-1-oxyl (**A**) (TEMPO, 1 equiv), only a trace amount of the product (**1a**) was obtained along with the formation a substantial amount of side product (**1a'**) (Scheme II.3.4).



Scheme II.3.4. Some controlled experiments

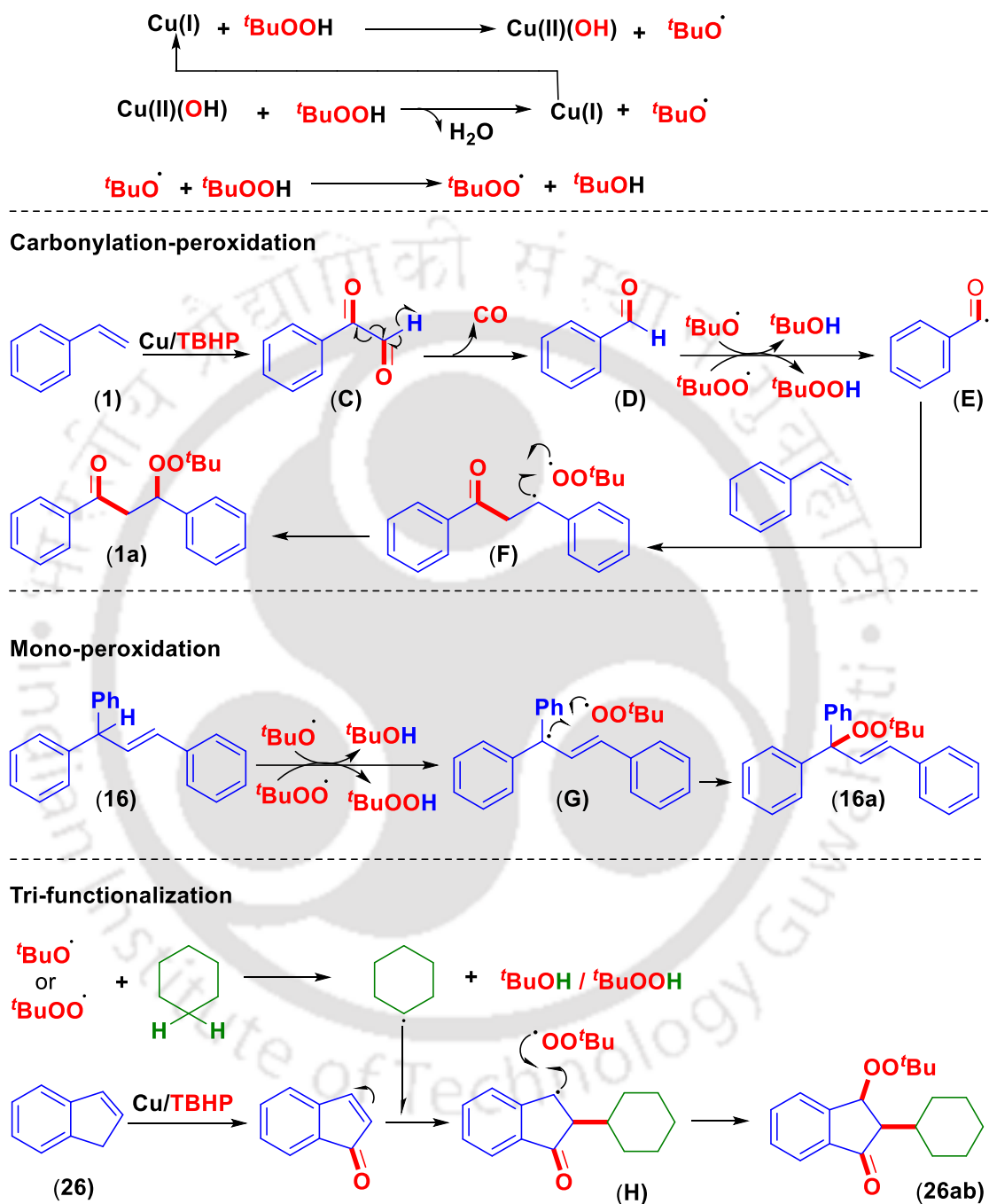
It seems the reaction is proceeding via a radical mechanism, that is the generation of *tert*-butoxy radical (${}^t\text{BuOO}^\cdot$), which on reaction with styrene (**1**) gave the product (**1a'**). Similar di-peroxidation product (**1a'**) is well known in the literature.^[18a] The *tert*-butoxy radical (${}^t\text{BuOO}^\cdot$) cannot be trapped with TEMPO as it will result in the formation of a species having three consecutive oxygen which will be unstable under the reaction temperature (110 °C). The reaction of styrene with TBHP gives phenyl glyoxal (**C**), and benzaldehyde (**D**),^[18b,c] which decomposed in the presence of a metal catalyst to an aroyl radical (ArCO^\cdot) which perhaps couple with the styrene to give the product (**1a**). When *p*-Me styrene (**2**) was reacted with phenyl glyoxal (**C**) under the present reaction condition it gave two coupled keto-peroxy products (**2aC**, 65%) and (**2a**, 19%) (Scheme II.3.4). The product **2aC** was obtained in higher percentage (65%) because of the coupling of aroyl radical (ArCO^\cdot) generated by the easy decomposition of phenyl glyoxal (**C**) with *p*-Me styrene (**2**), thereby supporting the intermediacy of (**C**). Further, when *p*-Me styrene (**2**) was reacted with benzaldehyde (**D**) it again gave two keto-peroxy products (**2aC**, 78%) and (**2a**, 9%) (Scheme II.3.4). The product **2aC** was yet again obtained in higher percentage (78%) because of the coupling of aroyl

(ArCO \cdot) obtained by the C–H bond cleavage of benzaldehyde (**C**) with *p*-Me styrene (**2**), thereby confirming the intermediacy of benzaldehyde (**D**).^[18d] Phenyl glyoxal (**C**), on decomposition, gives benzaldehyde with the concurrent release of CO.^[19a-c] Here, the release of CO from the reaction has been confirmed by spot test using PdCl₂-phosphomolybdic acid (PMA) strip, supporting the decarbonylation path.

The results of the above experiments and related literature reports,^[18b,c] convey the operation of the following paths for the carbonylation-peroxidation (Scheme II.3.5), mono-peroxidation and tri-functionalization (Scheme II.3.5).

The Cu(I)-assisted cleavage of *tert*-butyl hydroperoxide (TBHP) generates 'BuO \cdot ' radical and Cu(II) species in the medium. The Cu(II) species on reaction with another equivalent of TBHP produce 'BuOO \cdot ' radical and Cu(I) for further reaction.^[20a] This 'BuOO \cdot ' radical can also be generated by the action of TBHP and 'BuO \cdot ' radical. On the other hand, styrene (**1**) in the presence of Cu/TBHP is converted to benzaldehyde (**D**) via the intermediacy of phenyl glyoxal (**C**) (Scheme II.3.5).^[18b-d] The PhCO \cdot radical (**E**) generated from benzaldehyde (**D**) reacts with the unreacted part of styrene (**a**) to give a benzylic radical intermediate (**F**), which subsequently couples with 'BuOO \cdot ' radical to provide the desired product (**1a**). So far as mono-peroxidation of internal alkene, but-1-ene-1,3-diylbenzene (**16**) is concerned, the peroxidation is not taking place at the double bond, rather it is happening at the tertiary benzylic site (Scheme II.3.6). Here, the 'BuO \cdot ' or 'BuOO \cdot ' radical species abstract the tertiary proton of (**17**) to generate a radical intermediate (**G**) which is doubly benzylic as well as allylic, thus is much more stable than the other possible secondary benzylic radicals that may form by the direct attack of 'BuOO \cdot ' radical at the double bond. Thus, preferential peroxidation is taking place regioselectively at this benzylic tertiary position despite steric hindrance to giving the product (**17a**). The mechanism for the formation of tri-functionalization of indene is depicted in Scheme II.3.6. The *in situ* generated radical species 'BuO \cdot ' or 'BuOO \cdot ' as shown in (Scheme II.3.6) abstract a proton from the cycloalkane to generate a cycloalkyl radical species (**H**). The benzylic CH₂ of the indene (**26**) is oxidized to C=O in the presence of Cu/TBHP to give α,β -unsaturated ketone (**I**). The cyclohexyl radical (**H**) attacks at the α -carbon of (**I**) generating a benzylic radical (**J**).^[20b] This has been confirmed when a 1*H*-inden-1-one (**I**) was reacted with cyclohexane and TBHP under the optimized reaction condition, it resulted in the exclusive formation of product (**26ab**) in an improved yield of 75% thereby suggesting its intermediacy (Scheme II.3.4). Finally, a radical cross-coupling between 'BuOO \cdot ' benzylic radical (**J**) furnish the cycloalkyl-

peroxy product (**26ab**) (Scheme II.3.5). Similar peroxidation at the α - and cyclohexylation at the β -positions has been documented in the literature.^[14e,20b]



Scheme II.3.5. Plausible mechanism for various peroxidations

Even though both *tert*-butylperoxy and cyclohexyl radicals exist in the medium in this regioselective cycloalkylation-peroxidation process, the peroxidation is preferentially taking place at the benzylic position and the cycloalkylation at the C-2- position. No reverse attack is observed in any of the cases. To understand the origin of regioselectivity, density functional (DFT) studies were carried out which is depicted in Figure II.3.4.

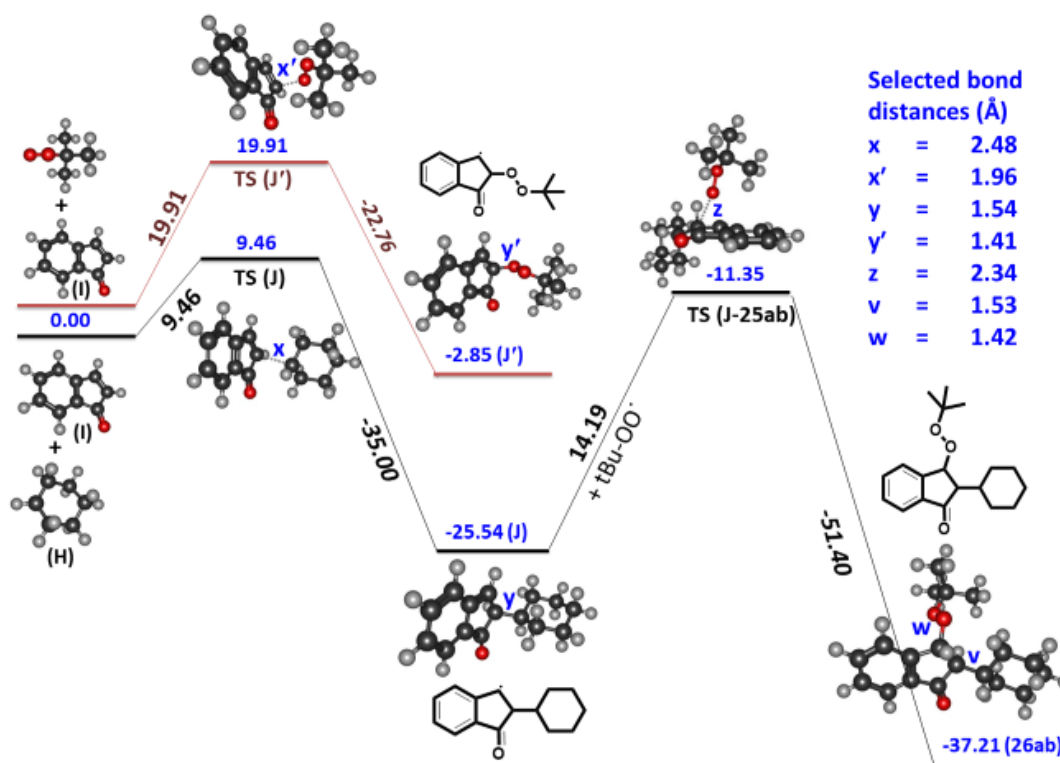


Figure II.3.4. Calculated energy profile diagram for the reaction with two paths considered. The relative energies from DFT calculations are in kcal mol^{-1} and bond lengths in Å , done at M06/6-31g+(d,p) level of theory

Theoretical calculations have been performed at the M06 level of theory using a 6-31+G(d,p) basis set for the atoms present in the system as implemented in the GAUSSIAN 09 program package. Frequency calculations have been performed on all the modelled structures using the same level of theory. The optimized structures for transition states, intermediates and the products are depicted in the energy profile diagram with some selected geometric parameters (Figure II.3.4). Two possible ways to proceed with the reaction have been investigated: the C-2-position of the indene can be attacked by an *in situ* generated cyclohexyl radical (**H**) which passes through a barrier height of $9.46 \text{ kcal mol}^{-1}$ and forms intermediate (**J**).

Alternately, the attack of *tert*-butylperoxy radical at the non-benzylic position (C-2) passes through a barrier height of 19.91 kcal.mol⁻¹, forming intermediate (**J'**). It could be seen from (Figure II.3.4), the energy of activation required to proceed with ^tBuOO[•] is 10.45 kcal.mol⁻¹ higher as compared to one attacked by cyclohexyl radical (**H**). Intermediate (**J**) is more stable than (**J'**) by 12.24 kcal.mol⁻¹. Thus, the reaction proceeding with ^tBuOO[•] as attacking nucleophile is less favourable and its possibility has been ruled out. The length of bonds (x,y) shown in Figure II.3.4, reveals the formation of a bond between the reactant and the incoming cyclohexyl radical. In the transition state, the bond length of x is of 2.48 Å indicating interaction with the incoming moiety. This bond (y) has shortened to a length of 1.54 Å in species (**J**), indicating the formation of a C–C bond. Subsequently, the incoming radical ^tBuOO[•] attack at position C-3 of the intermediate (**J**), forming a stable product (**26ab**) with an energy release of -51.40 kcal.mol⁻¹ after crossing a barrier height of 14.19 kcal mol⁻¹. (Figure II.3.4.).^[21]

In conclusion, we have demonstrated the differential reactivity of terminal and internal alkenes. A carbonylation-peroxidation of vinyl arenes is achieved in the absence of any carbonyl source. Vinyl arenes undergo decarbonylative C–C bond formation followed by a concurrent carbonylation-peroxidation catalyzed by Cu(I) and *tert*-butyl hydroperoxide (TBHP) but α -methyl styrenes yielded aryl methyl ketones as the only product. An α -substituted unsymmetrical internal alkene such as but-1-ene-1,3-diylbenzene afforded selective α -peroxidation at the tertiary carbon and not across the double bond under the identical reaction conditions which is governed by the stability of tertiary radical. An internal cyclic alkene such as indene provided peroxidation-carbonylation-cycloalkylation/cycloetherification by switching the solvent system from acetonitrile to cycloalkanes/cyclic ether. Plausible reaction mechanisms have been proposed for each of these transformations. Thus a variety of organic peroxy compounds can be generated via radical-mediated peroxidation of internal and terminal alkenes which may find useful applications in medicinal chemistry.

II.4. Experimental Section

II.4.1. General Information. All the reagents were commercial grade and purified according to the established procedures. Organic extracts were dried over anhydrous sodium sulphate. Solvents were removed in a rotary evaporator under reduced pressure. Silica gel (100-200 mesh size) was used for the column chromatography. Reactions were monitored by TLC

on silica gel 60 F₂₅₄ (0.25 mm). NMR spectra were recorded in CDCl₃ with tetramethylsilane as the internal standard for ¹H NMR (400 and 600 MHz) and in for ¹³C NMR (101 and 151 MHz) CDCl₃ as the internal standard. HRMS spectra were recorded using +ESI (TOF) mode. IR spectra were recorded in KBr or neat.

II.4.2. Synthesis of Keto-Peroxidation, mono-Peroxidation and tri-Functionalization Products

II.4.2. General Procedure for the Synthesis of 3-(*tert*-Butylperoxy)-1,3-diphenylpropan-1-one (1a) from Styrene (1) and *tert*-Butyl hydroperoxide (a): To an oven-dried 10.0 mL round bottom flask fitted with a reflux condenser was added styrene (**1**) (114.4 μL, 1.0 mmol), *tert*-butyl hydroperoxide (**a**) (600 μL, 3.0 mmol), Cu₂O (14.0 mg, 0.1 mmol), and acetonitrile (2.0 mL). The reaction mixture was stirred in an oil bath for 2 h at 110 °C. The reaction mixture was cooled to room temperature, admixed with ethyl acetate (25.0 mL) and the organic layer was washed with water (2.0 x 10.0 mL). The organic layer was dried over anhydrous sodium sulfate (Na₂SO₄), and the solvent was evaporated under reduced pressure. The resulting crude product was purified over a column of silica gel (hexane / ethyl acetate, 99.5:0.5) to give pure 3-(*tert*-butylperoxy)-1,3-diphenylpropan-1-one (**1a**) (121 mg, yield 81%). The identity and purity of the product were confirmed by spectroscopic analysis.

II.4.2. General Procedure for the Synthesis of (*E*)-(3-(*tert*-Butylperoxy)but-1-ene-1,3-diyl)dibenzene (22a) from (*E*)-But-1-ene-1,3-diyl)dibenzene (22) and *tert*-Butyl hydroperoxide (a): To an oven-dried 10.0 mL round bottom flask fitted with a reflux condenser was added (*E*)-but-1-ene-1,3-diyl)dibenzene (**22**) (104 mg, 0.5 mmol), *tert*-butyl hydroperoxide (**a**) (600 μL, 3.0 mmol), Cu₂O (7.0 mg, 0.05 mmol), and acetonitrile (2.0 mL). The reaction mixture was stirred in an oil bath for 2 h at 110 °C. The reaction mixture was cooled to room temperature, admixed with ethyl acetate (25.0 mL) and the organic layer was washed with water (2.0 x 10.0 mL). The organic layer was dried over anhydrous sodium sulfate (Na₂SO₄), and the solvent was evaporated under reduced pressure. The resulting crude product was purified over a column of silica gel (hexane / ethyl acetate, 99.5:0.5) to give pure (*E*)-(3-(*tert*-butylperoxy)but-1-ene-1,3-diyl)dibenzene (**22a**) (102 mg, yield 69%). The identity and purity of the product were confirmed by spectroscopic analysis.

II.4.2. General Procedure for the Synthesis of 3-(*tert*-Butylperoxy)-2-cyclohexyl-2,3-dihydro-1*H*-inden-1-one (26ab) from Indene (26) and *tert*-Butyl hydroperoxide (a): To an oven-dried 10.0 mL round bottom flask fitted with a reflux condenser was added indene (26) (58 μ L, 0.5 mmol), *tert*-butyl hydroperoxide (a) (600 μ L, 3.0 mmol), Cu₂O (7.0 mg, 0.05 mmol), and cyclohexane (2.0 mL). The reaction mixture was stirred in an oil bath for 3 h at 110 °C. The reaction mixture was cooled to room temperature, admixed with ethyl acetate (25.0 mL) and the organic layer was washed with water (2.0 x 10.0 mL). The organic layer was dried over anhydrous sodium sulfate (Na₂SO₄), and the solvent was evaporated under reduced pressure. The resulting crude product was purified over a column of silica gel (hexane / ethyl acetate, 99:1.0) to give pure 2-(*tert*-butylperoxy)-3-cyclohexyl-2,3-dihydro-1*H*-inden-1-one (26ab) (100 mg, yield 66%). The identity and purity of the product were confirmed by spectroscopic analysis.

II.4.3. Mechanistic Investigations

II.4.3. Determine the Extrusion of CO from the Reaction: For the detection of the evolution of carbon monoxide (CO), a strip containing PdCl₂ and PMA (phosphomolybdic acid) was hanged from the neck of the reaction flask (Figure II.4.3). The initial yellow colour of the strip before the reaction (Figure II.4.3) turned blue after 2 h of the reaction progress (Figure II.4.3). This colour change confirms the extrusion of CO from the reaction.



PdCl₂-PMA test strip
before the reaction



PdCl₂-PMA test strip
after the reaction

Figure II.4.3

Carbonylation-Peroxidation of Styrene in the Presence of Radical Scavenger TEMPO: In an oven-dried 25.0 mL round bottom flask styrene (**1**) (114.4 μ L, 1.0 mmol), *tert*-butyl hydroperoxide in decane (5-6 M) (**a**) (600 μ L, 3.0 mmol), Cu₂O (14.0 mg, 0.1 mmol), TEMPO (156 mg, 1.0 mmol) and acetonitrile (2.0 mL) each of were added. The flask was fitted to a condenser and the reaction mixture was stirred in a preheated oil bath at 110 °C for 2 h. The reaction after 2 h afforded the *bis*-peroxy product (**1a'**) in 42% yield along with paltry yield (~8%) of the desired product (**1a**).

II.5. References

- [1] a) G. Dyker, *Handbook of C-H Transformations: Applications in Organic Synthesis*; Wiley-VCH: Weinheim, **2005**; b) J.-Q. Yu, Z.-J. Shi, *C-H Activation*; Springer: Berlin, Germany, **2010**; c) X. Chen, K. M. Engle, D.-H. Wang and J.-Q. Yu, *Angew. Chem. Int. Ed.* **2009**, *48*, 5094-5115; d) T. W. Lyons and M. S. Sanford, *Chem. Rev.* **2010**, *110*, 1147-1169; e) D. A. Colby, R. G. Bergman and J. A. Ellman, *Chem. Rev.* **2010**, *110*, 624-655; f) J. Wencel-Delord, T. Droge, F. Liu and F. Glorius, *Chem. Soc. Rev.* **2011**, *40*, 4740-4761; (g) S. H. Cho, J. Y. Kim, J. Kwak and S. Chang, *Chem. Soc. Rev.* **2011**, *40*, 5068-5083; h) C.-L. Sun, B. J. Li and Z.-J. Shi, *Chem. Rev.*, **2011**, *111*, 1293-1314; i) L. Ackermann, *Chem. Rev.* **2011**, *111*, 1315-1345; j) C. J. Li, *Acc. Chem. Res.* **2009**, *42*, 335-344; k) S. A. Girard, T. Knauber and C.-J. Li, *Angew. Chem. Int. Ed.* **2014**, *53*, 74-100; l) J. A. Ashenurst, *Chem. Soc. Rev.* **2010**, *39*, 540-548.
- [2] a) D. Kalyani, M. S. Sanford, *J. Am. Chem. Soc.* **2008**, *130*, 2150-2151; b) D. Kalyani, A. D. Satterfield, M. S. Sanford, *J. Am. Chem. Soc.* **2010**, *132*, 8419-8427.
- [3] K. H. Jensen, J. D. Webb, M. S. Sigman, *J. Am. Chem. Soc.* **2010**, *132*, 17471-17481.
- [4] S. Kirchberg, R. Fröhlich, A. Studer, *Angew. Chem. Int. Ed.* **2010**, *49*, 6877-6880.
- [5] Y. Xie, J. Hu, P. Xie, B. Qian, H. Huang, *J. Am. Chem. Soc.* **2013**, *135*, 18327-18330.
- [6] S. Qiu, T. Xu, J. Zhou, Y. Guo, G. Liu, *J. Am. Chem. Soc.* **2010**, *132*, 2856-2857.
- [7] Y. Miyazaki, N. Ohta, K. Semba, Y. Nakao, *J. Am. Chem. Soc.* **2014**, *136*, 3732-3735.
- [8] V. Chudasama, R. J. Fitzmaurice, S. Caddick, *Nat. Chem.* **2010**, *2*, 592-596.
- [9] I. Kageyuki, I. Osaka, K. Takaki, H. Yoshida, *Org. Lett.* **2017**, *19*, 830-833.
- [10] a) H. Egami, T. Yoneda, M. Uku, T. Ide, Y. Kawato, Y. Hamashima, *J. Org. Chem.* **2016**, *81*, 4020-4030; b) S. R Chowdhury, I. U. Hoque, S. Maity, *Chem. Asian J.* **2018**, *13*, 2824-2828; c) U. Hoque, S. Maity, S. Roy Chowdhury, *J. Org. Chem.* **2019**, *84*, 3025-3035.

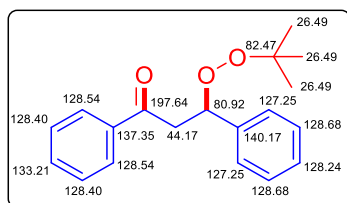
- [11] Reviews: a) A. Brennführer, H. Neumann, M. Beller, *Angew. Chem. Int. Ed.* **2009**, *48*, 4114-4133; b) C.-H. Jun, E.-A. Jo, J.-W. Park, *Eur. J. Org. Chem.* **2007**, 1869-1881; c) C. H. Schiesser, U. Wille, H. Matsubara, I. Ryu, *Acc. Chem. Res.* **2007**, *40*, 303-313; d) M. Beller, J. Seayad, A. Tillack, H. Jiao, *Angew. Chem. Int. Ed.* **2004**, *43*, 3368-3398; e) T. Morimoto, K. Kakiuchi, *Angew. Chem. Int. Ed.* **2004**, *43*, 5580-5588; f) G. Kiss, *Chem. Rev.* **2001**, *101*, 3435-3456.
- [12] a) T. Taniguchi, Y. Sugiura, H. Zaimoku, H. Ishibashi, *Angew. Chem. Int. Ed.* **2010**, *49*, 10154-10157; b) T. A. Cernak, T. H. Lambert, *J. Am. Chem. Soc.* **2009**, *131*, 3124-3125; c) T. Punniyamurthy, B. Bhatia, J. Iqbal, *J. Org. Chem.* **1994**, *59*, 850-853; d) I. A. Yaremenko, V. A. Vil, D. V. Demchuk, A. O. Terent'ev, *Beilstein J. Org. Chem.* **2016**, *12*, 1647-1748; e) F. W. Muregi, A. Ishih, *Drug Dev. Res.* **2010**, *71*, 20-32; f) J. L. Vennerstrom, H. N. Fu, W. Y. Ellis, A. L. Ager, J. K. Wood, S. L. Andersen, L. Gerena, W. K. Milhous, *J. Med. Chem.* **1992**, *35*, 3023-3027; g) K. Ingram, I. A. Yaremenko, I. B. Krylov, L. Hofer, A. O. Terent'ev, J. Keiser, *J. Med. Chem.* **2012**, *55*, 8700-8711; h) G. H. Posner, J. D'Angelo, P. MO'Neill, A. Mercer, *Expert Opin. Ther. Patents.* **2006**, *16*, 1665-1672; i) V. M. Dembitsky, T. A. Glorizova, V. V. Poroikov, *Mini-Rev. Med. Chem.* **2007**, *7*, 571-589; j) M. Nakanishi, C. Bolm, *Adv. Synth. Catal.* **2007**, *349*, 861-864; k) B. Orlinska, J. Zawadiak, D. Gilner, *Appl. Catal., A* **2005**, *287*, 68-74; l) Y. Watanabe, K. Ohta, S. Suyama, *Bull. Chem. Soc. Jpn.* **1992**, *65*, 2063-2066; m) J. Zawadiak, D. Gilner, R. Mazurkiewicz, B. Orlinska, *Appl. Catal., A* **2001**, *205*, 239-243.
- [13] a) W. Liu, Y. Li, K. Liu, Z. Li, *J. Am. Chem. Soc.* **2011**, *133*, 10756-10759; b) L. Lv, B. Shen, Z. Li, *Angew. Chem. Int. Ed.* **2014**, *53*, 4164-4167; c) L. Lv, B. B. Snider, Z. Li, *J. Org. Chem.* **2017**, *82*, 5487-5491; d) T. H. Graham, C. M. Jones, N. T. Jui, D. W. C. MacMillan, *J. Am. Chem. Soc.* **2008**, *130*, 16494-16495; e) N. T. Jui, J. A. O. Garber, F. G. Finelli, D. W. C. MacMillan, *J. Am. Chem. Soc.* **2012**, *134*, 11400-11403.
- [14] a) Z. Zong, S. Lu, W. Wanga, Z. Li, *Tetrahedron Lett.* **2015**, *56*, 6719-6721; b) B. S. Chaput, J. Demaerel, H. Engler, M. Klussmann, *Angew. Chem. Int. Ed.* **2014**, *53*, 8737-8740; c) W. C. Yang, S. S. Weng, A. Ramasamy, G. Rajeshwaren, Y. Y. Liao, C. T. Chen, *Org. Biomol. Chem.* **2015**, *13*, 2385-2392; d) Y. Yao, Z. Wang, B. Wang, *Org. Chem. Front.* **2018**, *5*, 2501-2504; e) A. Banerjee, S. K. Santra, A. Mishra, N. Khatun, B. K. Patel, *Org. Biomol. Chem.* **2015**, *13*, 1307-1312.

- [15] a) A. Gogoi, A. Modi, S. Guin, S. K. Rout, D. Das, B. K. Patel, *Chem. Commun.*, **2014**, 50, 10445-10447; b) S. K. Rout, S. Guin, K. K. Ghara, A. Banerjee and B. K. Patel, *Org. Lett.*, **2012**, 14, 3982-3985; c) S. K. Rout, S. Guin, A. Banerjee, N. Khatun, A. Gogoi, B. K. Patel, *Org. Lett.*, **2013**, 15, 4106-4109; d) G. Majji, S. Guin, A. Gogoi, S. K. Rout, B. K. Patel, *Chem. Commun.*, **2013**, 49, 3031-3033.
- [16] a) C. Zhu and S. P. Cook, *J. Am. Chem. Soc.* **2012**, 134, 13577-13579; b) X. Hu and T. J. Maimone, *J. Am. Chem. Soc.*, **2014**, 136, 5287-5290.
- [17] a) M. M. Hossain, W. K. Huang, H. J. Chen, P. H. Wang, S. G. Shyu, *Green Chem.* **2014**, 16, 3013-3017; b) M. M. Hossain, S. G. Shyu, *Tetrahedron* **2014**, 70, 251-255; c) M. Jafarpour, M. Ghahramaninezhad, A. Rezaeifard, *RSC Adv.*, **2014**, 4, 1601-1608.
- [18] a) A. O. Terent'ev, Y. M. Sharipov, I. B. Krylov, D. V. Gaidarenko, G. I. Nikishin, *Org. Biomol. Chem.* **2015**, 13, 1439-1445; b) S. K. Rout, S. Guin, A. Gogoi, G. Majji, B. K. Patel, *Org. Lett.* **2014**, 16, 1614-1617; c) G. Majji, S. Guin, S. K. Rout, A. Behera, B. K. Patel, *Chem. Commun.* **2014**, 50, 12193-12196; d) N. Khatun, A. Banerjee, S. K. Santra, A. Behera, B. K. Patel, *RSC Adv.* **2014**, 4, 54532-54538.
- [19] a) F. Feigl, V. Anger, *Spot Tests in Inorganic Analysis* 6th editions; Elsevier, pp. 169; b) L. Wang, X. Ren, J. Yu, Y. Jiang, J. Cheng, *J. Org. Chem.* **2013**, 78, 12076-12081; c) S. K. Santra, A. Banerjee, P. R. Mohanta, B. K. Patel, *J. Org. Chem.* **2016**, 81, 6066-6074.
- [20] a) S. K. Rout, S. Guin, W. Ali, A. Gogoi, B. K. Patel, *Org. Lett.* **2014**, 16, 3086-3089; b) Y. Lan, C. Yang, Y.-H. Xu, T.-P. Loh, *Org. Chem. Front.* **2017**, 4, 1411-1415.
- [21] Y. Zhao, D. G. Truhlar, The M06 suite of density functionals for main group thermochemistry, thermochemical kinetics, noncovalent interactions, excited states, and transition elements, *Theor. Chem. Acc.* **2008**, 120, 215-241; b) Gaussian 09, Revision D.01, M. J. Frisch, G. W. Trucks, H. B. Schlegel, G. E. Scuseria, M. A. Robb, J. R. Cheeseman, G. Scalmani, V. Barone, B. Mennucci, G. A. Petersson, H. Nakatsuji, M. Caricato, X. Li, H. P. Hratchian, A. F. Izmaylov, J. Bloino, G. Zheng, J. L. Sonnenberg, M. Hada, M. Ehara, K. Toyota, R. Fukuda, J. Hasegawa, M. Ishida, T. Nakajima, Y. Honda, O. Kitao, H. Nakai, T. Vreven, J. A. Montgomery, Jr., J. E. Peralta, F. Ogliaro, M. Bearpark, J. J. Heyd, E. Brothers, K. N. Kudin, V. N. Staroverov, R. Kobayashi, J. Normand, K. Raghavachari, A. Rendell, J. C. Burant, S. S. Iyengar, J. Tomasi, M. Cossi, N. Rega, J. M. Millam, M. Klene, J. E. Knox, J. B. Cross, V. Bakken, C. Adamo, J. Jaramillo, R. Gomperts, R. E. Stratmann, O. Yazyev, A. J. Austin, R. Cammi, C. Pomelli, J. W. Ochterski, R. L. Martin, K.

Morokuma, V. G. Zakrzewski, G. A. Voth, P. Salvador, J. J. Dannenberg, S. Dapprich, A. D. Daniels, Ö. Farkas, J. B. Foresman, J. V. Ortiz, J. Cioslowski, D. J. Fox, Gaussian, Inc., Wallingford CT, 2009.

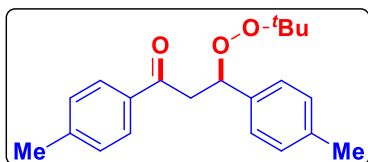
II.6. Spectral Data

3-(*tert*-Butylperoxy)-1,3-diphenylpropan-1-one (1a):

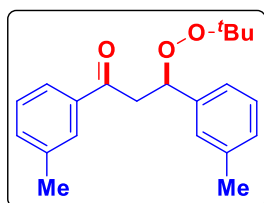


Colourless oil, (121 mg, 81%). ^1H NMR (CDCl_3 , 400 MHz) δ 7.95 (d, 2H, $J = 7.2$ Hz), 7.55 (t, 1H, $J = 7.4$ Hz), 7.47–7.42 (m, 4H), 7.35 (t, 2H, $J = 7.4$ Hz), 7.30 (d, 1H, $J = 7.2$ Hz), 5.60 (t, 1H, $J = 6.4$ Hz), 3.77 (dd, 1H, $J = 16.4$, 7.2 Hz), 3.21 (dd, 1H, $J = 16.0$, 6.0 Hz), 1.16 (s, 9H) ppm. ^{13}C NMR (CDCl_3 , 101 MHz) δ 197.64, 140.17, 137.35, 133.21, 128.68, 128.54, 128.40, 128.24, 127.25, 82.47, 80.92, 44.17, 26.49 ppm. IR (KBr, cm^{-1}): 2979, 1687, 1450, 1360, 1198, 751, 694; HRMS (ESI/Q-TOF) m/z : $[\text{M} + \text{Na}]^+$ Calcd for $\text{C}_{19}\text{H}_{22}\text{NaO}_3$ 321.1461; found 321.1466.

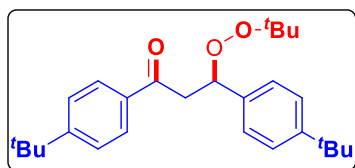
3-(*tert*-Butylperoxy)-1,3-di-*p*-tolylpropan-1-one (2a):



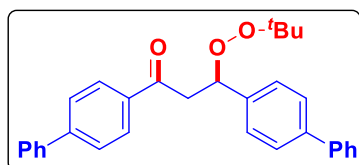
Yellow gummy, (100 mg, 61%). ^1H NMR (CDCl_3 , 400 MHz) δ 7.84 (d, 2H, $J = 8.0$ Hz), 7.32 (d, 2H, $J = 8.0$ Hz), 7.24 (d, 2H, $J = 8.0$ Hz), 7.15 (d, 2H, $J = 7.6$ Hz), 5.55 (t, 1H, $J = 6.6$ Hz), 3.76 (dd, 1H, $J = 16.0$, 6.8 Hz), 3.19 (dd, 1H, $J = 16.0$, 6.0 Hz), 2.40 (s, 3H), 2.33 (s, 3H), 1.16 (s, 9H) ppm. ^{13}C NMR (CDCl_3 , 101 MHz) δ 197.40, 143.98, 137.99, 137.06, 134.86, 129.34, 129.24, 128.52, 127.27, 82.45, 80.88, 43.91, 26.50, 21.78, 21.35 ppm. IR (KBr, cm^{-1}): 2977, 2928, 1684, 1606, 1512, 1362, 1271, 1195, 1019, 810, 756; HRMS (ESI/Q-TOF) m/z : $[\text{M} + \text{Na}]^+$ Calcd for $\text{C}_{21}\text{H}_{26}\text{NaO}_3$ 349.1774; found 349.1783.

3-(*tert*-Butylperoxy)-1,3-di-*m*-tolylpropan-1-one (3a):

Gummy, (93 mg, 57%). ^1H NMR (CDCl_3 , 400 MHz) δ 7.75 (d, 2H, $J = 7.6$ Hz), 7.35–7.23 (m, 3H), 7.23 (d, 3H, $J = 3.6$ Hz), 5.59–5.53 (m, 1H), 3.76 (dd, 1H, $J = 16.3$, 7.1 Hz), 3.18 (dd, 1H, $J = 16.0$, 6.8 Hz), 2.40 (s, 3H), 2.35 (s, 3H), 1.17 (s, 9H) ppm. ^{13}C NMR (CDCl_3 , 101 MHz) δ 197.89, 140.03, 138.41, 138.11, 137.33, 133.94, 129.04, 128.92, 128.52, 128.42, 127.94, 125.61, 124.32, 82.55, 80.94, 44.23, 26.49, 21.61, 21.47 ppm. IR (KBr, cm^{-1}): 2978, 2927, 1683, 1606, 1654, 1362, 1195, 783, 702; HRMS (ESI/Q-TOF) m/z : $[\text{M} + \text{Na}]^+$ Calcd for $\text{C}_{21}\text{H}_{26}\text{NaO}_3$ 349.1774; found 349.1778.

1,3-bis(4-(*tert*-Butyl)phenyl)-3-(*tert*-butylperoxy)propan-1-one (4a):

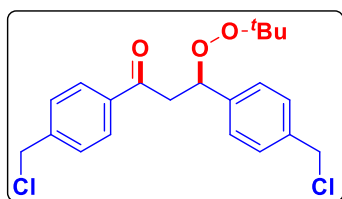
Gummy, (124 mg, 65%). ^1H NMR (CDCl_3 , 400 MHz) δ 7.89 (d, 2H, $J = 8.4$ Hz), 7.46 (d, 2H, $J = 8.4$ Hz), 7.35 (bs, 4H), 5.59 (t, 1H, $J = 6.4$ Hz), 3.77 (dd, 1H, $J = 16.4$, 6.8 Hz), 3.21 (dd, 1H, $J = 16.4$, 10.4 Hz), 1.33 (s, 9H), 1.30 (s, 9H), 1.18 (s, 9H) ppm. ^{13}C NMR (CDCl_3 , 101 MHz) δ 197.45, 156.91, 151.05, 137.02, 134.82, 128.35, 126.97, 125.59, 125.46, 82.33, 80.91, 44.01, 35.24, 34.69, 31.48, 31.23, 26.53 ppm. IR (KBr, cm^{-1}): 2965, 1759, 1685, 1601, 1452, 1361, 1198, 1019, 831, 752, 696; HRMS (ESI/Q-TOF) m/z : $[\text{M} + \text{K}]^+$ Calcd for $\text{C}_{27}\text{H}_{38}\text{KO}_3$ 449.2453; found 449.2441.

1,3-di([1,1'-Biphenyl]-4-yl)-3-(*tert*-Butylperoxy)propan-1-one (5a):

Yellow solid, (311 mg, 69%), m. p. 100–104 °C. ^1H NMR (400 MHz, CDCl_3) δ 8.05 (d, $J = 8.4$ Hz, 2H), 7.69 (d, $J = 8.4$ Hz, 2H), 7.58–7.64 (m, 6H), 7.52 (d, $J = 8.4$ Hz, 2H), 7.49–7.40 (m, 5H), 7.35 (t, $J = 7.2$ Hz, 1H), 5.67 (t, $J = 6.4$ Hz, 1H), 3.85 (dd, $J = 16.4$, 6.8 Hz, 1H), 3.29 (dd, $J = 16.0$, 6.0 Hz, 1H), 1.21 (s, 9H) ppm. ^{13}C NMR (101

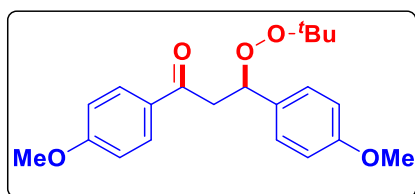
MHz, CDCl₃) δ 197.19, 145.92, 141.17, 140.97, 139.96, 139.15, 135.98, 129.09, 129.01, 128.87, 128.38, 127.70, 127.43, 127.40, 127.35, 127.33, 127.26, 82.29, 81.05, 44.12, 26.54 ppm. IR (KBr, cm⁻¹): 2974, 2924, 1664, 1599, 1484, 1405, 1360, 1196, 870, 760, 690. HRMS (ESI/Q-TOF) m/z: [M + Na]⁺ Calcd for C₃₁H₃₀NaO₃ 473.2187; found 473.2192.

3-(*tert*-Butylperoxy)-1,3-bis(4-(chloromethyl)phenyl)propan-1-one (6a):

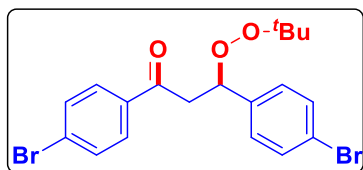


Brownish gummy, (130 mg, 66%). ¹H NMR (CDCl₃, 400 MHz) δ 7.94 (d, 2H, *J* = 8.3 Hz), 7.47 (d, 2H, *J* = 8.3 Hz), 7.40 (dd, 4H, *J* = 20.1, 8.2 Hz), 5.59 (t, 1H, *J* = 6.5 Hz), 4.61 (s, 2H), 4.58 (s, 2H), 3.74 (dd, 1H, *J* = 16.3, 7.1 Hz), 3.18 (dd, 1H, *J* = 16.3, 5.9 Hz), 1.16 (s, 9H) ppm. ¹³C NMR (CDCl₃, 101 MHz) δ 196.79, 142.63, 140.49, 137.43, 137.09, 128.84, 128.83, 128.81, 127.58, 81.97, 81.05, 46.08, 45.39, 44.18, 26.49 ppm. IR (KBr, cm⁻¹): 2982, 2881, 1691, 1362, 1267, 1196; HRMS (ESI/Q-TOF) m/z: [M + Na]⁺ Calcd for C₂₁H₂₄Cl₂NaO₃ 417.0995; found 417.0968.

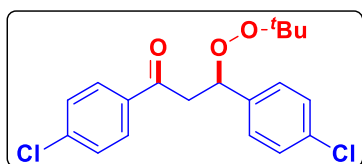
3-(*tert*-Butylperoxy)-1,3-bis(4-methoxyphenyl)propan-1-one (7a):



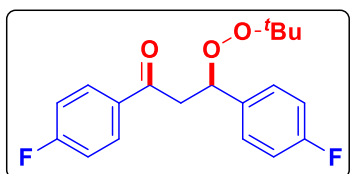
Gummy, (215 mg, 60%). ¹H NMR (400 MHz, CDCl₃) δ 7.94 (d, *J* = 9.2 Hz 2H), 7.35 (d, 2H, *J* = 8.8 Hz), 6.94–6.86 (m, 4H), 5.52 (t, 1H, *J* = 6.6 Hz), 3.86 (s, 3H), 3.79 (s, 3H), 3.75 (dd, 1H, *J* = 16.0, 6.4 Hz), 3.19 (dd, 1H, *J* = 16.0, 6.0 Hz), 1.17 (s, 9H) ppm. ¹³C NMR (101 MHz, CDCl₃) δ 196.33, 163.61, 159.57, 132.10, 130.67, 130.46, 128.68, 113.9, 113.8, 82.34, 80.83, 55.60, 55.36, 43.51, 26.51 ppm. IR (KBr, cm⁻¹): 2975, 2839, 1675, 1602, 1512, 1255, 1174, 1030, 831, 739; HRMS (ESI/Q-TOF) m/z: [M + Na]⁺ Calcd for C₂₁H₂₆NaO₅ 381.1672; found 381.1679.

1,3-bis(4-Bromophenyl)-3-(tert-butylperoxy)propan-1-one (8a):

Gummy, (167 mg, 73%). ^1H NMR (CDCl_3 , 400 MHz) δ 7.88 (d, 2H, $J = 8.8$ Hz), 7.43 (d, 2H, $J = 7.2$ Hz), 7.37–7.31 (m, 4H), 5.53 (t, 1H, $J = 6.6$ Hz), 3.70 (dd, 1H, $J = 16.0, 6.8$ Hz), 3.12 (dd, 1H, $J = 16.4, 6.0$ Hz), 1.15 (s, 9H) ppm. ^{13}C NMR (CDCl_3 , 101 MHz) δ 196.10, 139.90, 138.60, 135.50, 134.09, 129.80, 129.08, 128.79, 128.60, 81.65, 81.10, 43.93, 26.47 ppm. IR (KBr, cm^{-1}): 2980, 2880, 1689, 1589, 1490, 1401, 1362, 1091, 823; HRMS (ESI/Q-TOF) m/z : $[\text{M} + \text{K}]^+$ Calcd for $\text{C}_{19}\text{H}_{20}\text{Br}_2\text{KO}_3$ 492.9411; found 492.9418.

3-(tert-Butylperoxy)-1,3-bis(4-chlorophenyl)propan-1-one (9a):

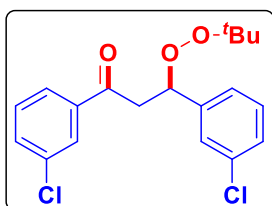
Gummy, (130 mg, 71%). ^1H NMR (CDCl_3 , 400 MHz) δ 7.80 (d, 2H, $J = 4.8$ Hz), 7.59 (d, 2H, $J = 8.8$ Hz), 7.46 (d, 2H, $J = 8.4$ Hz), 7.30 (d, 2H, $J = 8.4$ Hz), 5.52 (t, 1H, $J = 6.6$ Hz), 3.68 (dd, 1H, $J = 16.4, 7.2$ Hz), 3.11 (dd, 1H, $J = 16.4, 6.0$ Hz), 1.15 (s, 9H) ppm. ^{13}C NMR (CDCl_3 , 101 MHz) δ 196.20, 139.12, 135.86, 132.15, 132.05, 131.71, 130.73, 129.87, 122.23, 81.64, 81.08, 43.85, 26.45 ppm. IR (KBr, cm^{-1}): 2979, 2881, 1691, 1585, 1486, 1362, 1195, 1071, 1009; HRMS (ESI/Q-TOF) m/z : $[\text{M} + \text{Na}]^+$ Calcd for $\text{C}_{19}\text{H}_{20}\text{Cl}_2\text{NaO}_3$ 389.0682; found 389.0678.

3-(tert-Butylperoxy)-1,3-bis(4-fluorophenyl)propan-1-one (10a):

Gummy, (114 mg, 68%). ^1H NMR (CDCl_3 , 400 MHz) δ 7.93–7.92 (m, 1H), 7.82 (d, 1H, $J = 8.0$ Hz), 7.55–7.52 (m, 1H), 7.42–7.38 (m, 3H), 7.31–7.29 (m, 2H), 5.54 (dd, 1H, $J = 7.2, 5.6$ Hz), 3.69 (dd, 1H, $J = 20.4, 32.0$ Hz), 3.12 (dd, 1H, $J = 16.4, 5.6$ Hz), 1.16 (s, 9H) ppm. ^{13}C NMR (101 MHz, CDCl_3) δ 195.87, 167.23, 164.70, 163.93, 161.48, 135.83 (d, $J = 3.2$ Hz), 133.68 (d, $J = 3.0$ Hz),

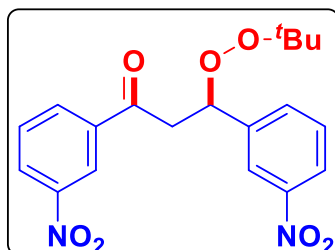
131.87 (d, $J = 9.4$ Hz), 131.03 (d, $J = 9.3$ Hz), 128.98 (d, $J = 8.2$ Hz), 115.94, 115.72 (d, $J = 15.0$ Hz), 115.36, 81.76, 81.01, 43.93, 26.47 ppm. ^{19}F (CDCl_3 , 377 MHz): δ -105.59–105.81 (m), 114.52–114.78 (m) ppm. IR (KBr, cm^{-1}): 2979, 2932, 1724, 1687, 1600, 1509, 1411, 1364, 1226, 1156, 834; HRMS (ESI/Q-TOF) m/z : $[\text{M} + \text{Na}]^+$ Calcd for $\text{C}_{19}\text{H}_{20}\text{F}_2\text{NaO}_3$ 357.1273; found 357.1283

3-(*tert*-Butylperoxy)-1,3-bis(3-chlorophenyl)propan-1-one (11a):



Yellow gummy, (119 mg, 65%). ^1H NMR (400 MHz, CDCl_3) δ 7.93 (t, 1H $J = 1.8$ Hz), 7.83–7.81 (m, 1H), 7.55–7.52 (m, 1H), 7.42–7.38 (m, 2H), 7.31–7.27 (m, 3H), 5.54 (t, 1H $J = 6.4$ Hz), 3.69 (dd, 1H, $J = 19.6, 7.2$ Hz), 3.12 (dd, 1H, $J = 17.6, 5.6$ Hz), 1.16 (s, 9H); ^{13}C NMR (CDCl_3 , 101 MHz) δ 195.89, 142.18, 138.59, 135.11, 134.47, 133.33, 130.08, 129.89, 128.53, 128.47, 127.27, 126.46, 125.37, 81.51, 81.21, 44.10, 26.44; IR (KBr, cm^{-1}): 2978, 2683, 1687, 1609, 1414, 1363, 1195, 1017, 680; HRMS (ESI/Q-TOF) m/z : $[\text{M} + \text{Na}]^+$ Calcd for $\text{C}_{19}\text{H}_{20}\text{Cl}_2\text{NaO}_3$ 389.0682; found 389.0686.

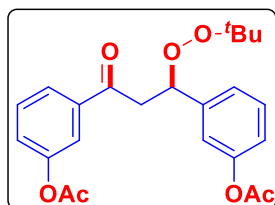
3-(*tert*-Butylperoxy)-1,3-bis(3-nitrophenyl)propan-1-one (12a):



Gummy, (225 mg, 58%). ^1H NMR (400 MHz, CDCl_3) δ 8.80 (s, 1H), 8.45 (d, 1H, $J = 8.0$ Hz), 8.33 (s, 1H), 8.30 (d, 1H, $J = 8.0$ Hz), 8.19 (d, 1H, $J = 8.4$ Hz), 7.80 (d, 1H, $J = 7.6$ Hz), 7.71 (t, 1H, $J = 8.0$ Hz), 7.57 (t, 1H, $J = 8.0$ Hz), 5.69 (t, 1H, $J = 6.6$ Hz), 3.82 (dd, 1H, $J = 16.4, 6.8$ Hz), 3.25 (dd, 1H, $J = 16.8, 5.6$ Hz), 1.16 (s, 9H) ppm. ^{13}C NMR (101 MHz, CDCl_3) δ 194.56, 142.24, 138.09, 133.87, 133.42, 130.17, 129.66, 127.87, 123.41, 123.33, 122.16, 81.52, 80.91, 44.00, 26.44 ppm. IR (KBr, cm^{-1}): 3088, 1700, 1689, 1530, 1351; HRMS (ESI/Q-TOF)

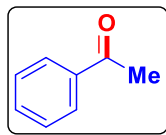
m/z: $[M + H]^+$ Calcd for $C_{19}H_{21}N_2O_7$ 389.1343; found 389.1349.

1-(*tert*-Butylperoxy)-3-oxopropane-1,3-diylbis(4,1-phenylene) diacetate (13a):



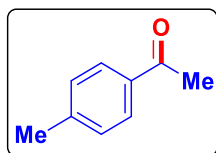
Colorless solid, (273 mg, 66%), m. p. 90–94 °C. 1H NMR (400 MHz, $CDCl_3$) δ 7.99 (d, 2H, $J = 8.4$ Hz), 7.44 (d, 2H, $J = 8.4$ Hz), 7.19 (d, 2H, $J = 8.4$ Hz), 7.08 (d, 2H, $J = 8.4$ Hz), 5.59 (t, 1H, $J = 6.4$ Hz), 3.73 (dd, 1H, $J = 16.4, 6.2$ Hz), 3.16 (dd, 1H, $J = 16.4, 6.0$ Hz), 2.32 (s, 3H), 2.29 (s, 3H), 1.16 (s, 9H) ppm. ^{13}C NMR (101 MHz, $CDCl_3$) δ 196.22, 169.59, 168.96, 154.55, 150.53, 137.72, 134.79, 130.01, 128.30, 121.91, 121.65, 81.73, 81.07, 44.12, 26.47, 21.29 ppm. IR (KBr, cm^{-1}): 3439, 2924, 2853, 1383, 1022, 742; HRMS (ESI/Q-TOF) m/z: $[M + NH_4]^+$ Calcd for $C_{23}H_{30}NO_7$ 432.2017; found 432.2027.

Acetophenone (14a):



Colorless liquid, (87 mg, 72%). 1H NMR ($CDCl_3$, 400 MHz) δ 7.95 (d, 2H, $J = 8.0$ Hz), 7.53 (t, 1H, $J = 7.8$ Hz), 7.44 (t, 2H, $J = 7.6$ Hz), 2.58 (s, 3H) ppm. ^{13}C NMR ($CDCl_3$, 101 MHz) δ 198.09, 137.13, 133.09, 128.57, 128.29, 26.57 ppm. IR (KBr, cm^{-1}): 3062, 1685, 1594, 1444, 1359, 1263, 1179, 1021, 760, 690, 589; HRMS (ESI/Q-TOF) m/z: $[M + NH_4]^+$ Calcd for $C_8H_{12}NO$ 138.0913; found 138.0921.

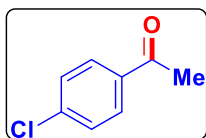
1-(*p*-Tolyl)than-1-one (15a):



Colorless liquid, (86 mg, 64%). 1H NMR ($CDCl_3$, 400 MHz) δ 7.85 (d, 2H, $J = 8.2$ Hz), 7.24 (d, 2H, $J = 8.0$ Hz), 2.56 (s, 3H), 2.40 (s, 3H) ppm. ^{13}C NMR ($CDCl_3$, 101 MHz) δ 197.82, 143.88, 134.76, 129.27, 128.46, 26.51, 21.63 ppm. IR (KBr, cm^{-1}): 3065, 1683, 1596, 1447, 1361, 1263, 1179, 1021, 760, 690, 592; HRMS (ESI/Q-TOF)

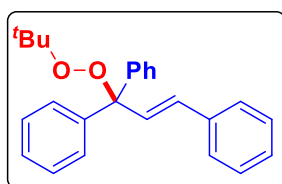
m/z: $[M + H]^+$ Calcd for $C_9H_{11}O$ 135.0804; found 135.0814.

1-(4-Chlorophenyl)ethan-1-one (16a):



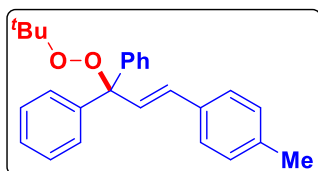
Colorless liquid, (120 mg, 75%). 1H NMR ($CDCl_3$, 400 MHz) δ 7.89 (d, 2H, $J = 8.5$ Hz), 7.42 (d, 2H, $J = 8.5$ Hz), 2.58 (s, 3H) ppm. ^{13}C NMR ($CDCl_3$, 101 MHz) δ 196.84, 139.60, 135.51, 129.79, 128.94, 26.58 ppm. IR (KBr, cm^{-1}): 3069, 1686, 1589, 1451, 1363, 1264, 1182, 1021, 764, 693, 595; HRMS (ESI/Q-TOF) m/z: $[M + K]^+$ Calcd for C_8H_7ClKO 192.9817; found 192.9830.

(E)-(1-(tert-Butylperoxy)prop-2-ene-1,1,3-triyl)tribenzene (17a):



Yellow gummy, (133 mg, 74%). 1H NMR ($CDCl_3$, 400 MHz) δ 7.80 (d, 1H, $J = 7.2$ Hz), 7.58 (t, 1H, $J = 7.4$ Hz), 7.49 (d, 1H, $J = 8.0$ Hz), 7.39–7.36 (m, 4H), 7.33–7.32 (m 3H), 7.25 (d, 5H, $J = 4.8$ Hz), 6.34 (d, 1H, $J = 9.6$ Hz), 5.41 (d, 1H, $J = 9.6$ Hz), 1.18 (s, 9H) ppm. ^{13}C NMR ($CDCl_3$, 101 MHz) δ 144.65, 141.63, 140.05, 139.45, 132.55, 130.20, 130.11, 128.89, 128.73, 128.57, 128.42, 128.28, 128.27, 128.03, 127.78, 127.61, 127.57, 127.45, 83.24, 80.45, 26.59 ppm. IR (KBr, cm^{-1}): 3059, 3028, 2977, 2928, 1661, 1598, 1492, 1477, 1385, 1362, 1276, 1195, 758, 697, 638; HRMS (ESI/Q-TOF) m/z: $[M + H]^+$ Calcd for $C_{25}H_{27}O_2$ 359.2006; found 359.2015.

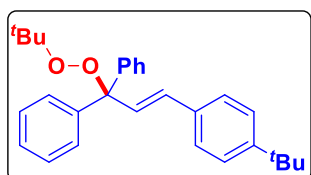
(E)-(1-(tert-Butylperoxy)-3-(p-tolyl)prop-2-ene-1,1-diyl)dibenzene (18a):



Yellow gummy, (123 mg, 66%). 1H NMR ($CDCl_3$, 400 MHz) δ 7.38–7.34 (m, 4H), 7.24–7.21 (m, 7H), 7.14 (d, 3H, $J = 8.0$ Hz), 6.36 (d, 1H, $J = 9.6$ Hz), 5.37 (d, 1H, $J = 9.6$ Hz), 2.34 (s, 3H), 1.17 (s, 9H) ppm. ^{13}C NMR ($CDCl_3$, 101 MHz) δ 144.35, 141.69, 139.49, 137.86, 136.89, 130.13, 129.31, 128.24, 127.72, 127.68, 127.60, 127.51,

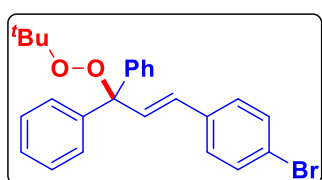
127.41, 83.11, 80.44, 26.59, 21.37 ppm. IR (KBr, cm^{-1}): 2976, 2925, 1663, 1493, 1446, 1360, 1273, 1194, 1015, 812, 762, 699; HRMS (ESI/Q-TOF) m/z : $[\text{M} + \text{Na}]^+$ Calcd for $\text{C}_{26}\text{H}_{28}\text{NaO}_2$ 395.1982; found 395.1998.

(E)-(3-(4-(tert-Butyl)phenyl)-1-(tert-butylperoxy)prop-2-ene-1,1-diyl)dibenzene (19a):



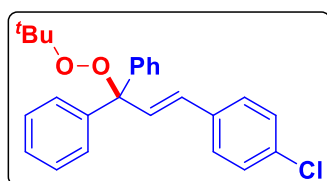
Gummy, (116 mg, 56%). ^1H NMR (600 MHz, CDCl_3) δ 7.40–7.33 (m, 5H), 7.29–7.23 (m, 9H), 6.37 (d, 1H, $J = 9.6$ Hz), 5.40 (d, 1H, $J = 9.6$ Hz), 1.31 (s, 9H), 1.18 (s, 9H) ppm. ^{13}C NMR (151 MHz, CDCl_3) δ 150.97, 144.31, 141.68, 139.48, 138.38, 136.62, 130.17, 128.23, 127.79, 127.70, 127.59, 127.48, 127.11, 125.55, 82.99, 80.52, 34.70, 31.47, 26.58 ppm. IR (KBr, cm^{-1}): 2979, 2923, 1669, 1486, 1442, 1365, 1273, 1199, 1015, 818, 752, 689; HRMS (ESI/Q-TOF) m/z : $[\text{M} + \text{NH}_4]^+$ Calcd for $\text{C}_{29}\text{H}_{38}\text{NO}_2$ 432.2897; found 432.2913.

(E)-(3-(4-Bromophenyl)-1-(tert-butylperoxy)prop-2-ene-1,1-diyl)dibenzene (20a):



Gummy, (173 mg, 79%). ^1H NMR (CDCl_3 , 400 MHz) δ 7.45 (d, 3H, $J = 8.4$ Hz), 7.37 (d, 3H, $J = 7.6$ Hz), 7.26 (bs, 2H), 7.23–7.17 (m, 6H), 6.24 (d, 1H, $J = 9.6$ Hz), 5.35 (d, 1H, $J = 9.5$ Hz), 1.17 (s, 9H) ppm. ^{13}C NMR (CDCl_3 , 101 MHz) δ 145.23, 141.40, 139.42, 139.26, 131.69, 129.98, 129.10, 128.38, 128.33, 127.97, 127.74, 127.61, 126.52, 121.91, 82.64, 80.54, 26.58 ppm. IR (KBr, cm^{-1}): 3027, 1656, 1587, 1527, 1492, 1452, 1333, 1070, 1012, 732, 698; HRMS (ESI/Q-TOF) m/z : $[\text{M} + \text{Na}]^+$ Calcd for $\text{C}_{25}\text{H}_{25}\text{BrNaO}_2$ 459.0930; found 459.0947.

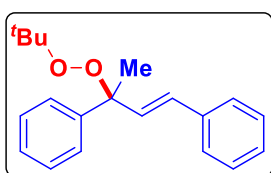
(E)-(1-(tert-Butylperoxy)-3-(4-chlorophenyl)prop-2-ene-1,1-diyl)dibenzene (21a):



Reddish gummy, (151 mg, 77%). ^1H NMR (CDCl_3 , 400 MHz) δ 7.38 (d, 3H, $J = 7.2$ Hz), 7.30 (d, 4H, $J = 8.4$ Hz), 7.25 (bs, 3H), 7.24–7.21 (m, 4H), 6.25 (d, 1H, $J = 9.6$ Hz),

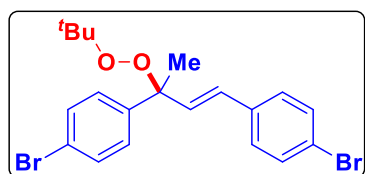
5.37 (d, 1H, $J = 9.6$ Hz), 1.17 (s, 9H) ppm. ^{13}C NMR (CDCl_3 , 101 MHz) δ 145.16, 141.38, 139.24, 138.82, 133.73, 129.97, 128.76, 128.74, 128.37, 128.32, 127.96, 127.72, 127.60, 126.57, 82.58, 80.56, 26.56 ppm. IR (KBr, cm^{-1}): 3031, 1653, 1604, 1559, 1511, 1333, 1232, 1161, 835, 704; HRMS (ESI/Q-TOF) m/z : $[\text{M} + \text{Na}]^+$ Calcd for $\text{C}_{25}\text{H}_{25}\text{ClNaO}_2$ 415.1435; found 415.1449.

(3-(*tert*-Butylperoxy)but-1-ene-1,3-diyl)dibenzene (22a):



Colourless oil, (102 mg, 69%). ^1H NMR (600 MHz, CDCl_3) δ 7.49 (d, 2H, $J = 7.2$ Hz), 7.40 (d, 2H, $J = 7.2$ Hz), 7.35–7.30 (m, 4H), 7.28–7.21 (m, 2H), 6.52 (dd, 2H, $J = 39.6, 16.2$ Hz), 1.79 (s, 3H), 1.25 (s, 9H) ppm. ^{13}C NMR (CDCl_3 , 151 MHz) δ 144.30, 137.16, 134.03, 129.96, 128.67, 128.09, 127.68, 127.25, 126.69, 126.53, 83.76, 79.42, 26.88, 24.70 ppm. IR (KBr, cm^{-1}): 2988, 2935, 1891, 1736, 1677, 1578, 1486, 1394, 1263, 1072, 1026, 1007, 927, 913, 861, 807, 757, 735, 731, 718, 667, 645; HRMS (ESI/Q-TOF) m/z : $[\text{M} + \text{K}]^+$ Calcd for $\text{C}_{20}\text{H}_{24}\text{KO}_2$ 335.1408.; found 335.1416.

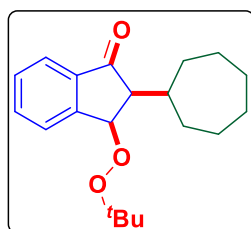
(*E*)-4,4'-(3-(*tert*-Butylperoxy)but-1-ene-1,3-diyl)bis(bromobenzene) (23a):



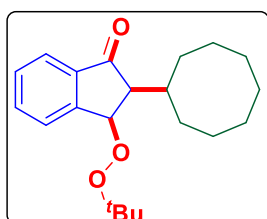
Yellow gummy, (161 mg, 71%). ^1H NMR (CDCl_3 , 400 MHz) δ 7.64–7.42 (m, 4H), 7.34 (d, 2H, $J = 6.0$ Hz), 7.25 (d, 2H, $J = 5.6$ Hz), 6.43 (dd, 2H, $J = 36.0, 11.2$ Hz), 1.75 (s, 3H), 1.23 (s, 9H) ppm. ^{13}C NMR (CDCl_3 , 101 MHz) δ 143.09, 135.78, 133.99, 131.80, 131.20, 129.29, 128.43, 128.22, 121.64, 121.34, 83.39, 79.65, 26.82, 24.63 ppm. IR (KBr, cm^{-1}): 2978, 2930, 1900, 1726, 1687, 1588, 1486, 1394, 1263, 1072, 1026, 1009, 930, 909, 858, 803, 755, 745, 739, 718, 681, 668, 644; HRMS (ESI/Q-TOF) m/z : $[\text{M} + \text{NH}_4]^+$ Calcd for $\text{C}_{20}\text{H}_{26}\text{Br}_2\text{O}_2$ 470.0325; found 470.0337.

3-(*tert*-Butylperoxy)-2-cyclohexyl-2,3-dihydro-1*H*-inden-1-one (26ab):

Yellow gummy, (98 mg, 65%). ^1H NMR (CDCl_3 , 400 MHz) δ 7.81 (d, 1H, $J = 8.0$ Hz), 7.73 (d, 1H, $J = 7.6$ Hz), 7.64 (td, 1H, $J = 7.6, 1.1$ Hz), 7.49 (t, 1H, $J = 7.4$ Hz), 5.45 (d, 1H, $J = 2.4$ Hz), 2.66 (dd, 1H, $J = 4.4, 2.8$ Hz), 2.11–2.04 (m, 1H), 1.79–1.74 (m, 2H), 1.66 (d, 2H, $J = 7.6$ Hz), 1.41 (d, 1H, $J = 11.2$ Hz), 1.35–1.30 (m, 2H), 1.27 (s, 9H), 1.22 (d, 1H, $J = 3.6$ Hz), 1.15–1.10 (m, 2H) ppm. ^{13}C NMR (CDCl_3 , 101 MHz) δ 205.88, 151.09, 138.00, 134.87, 129.91, 127.84, 123.23, 82.21, 80.56, 58.32, 38.94, 31.32, 29.23, 26.75, 26.69, 26.47, 26.35 ppm. IR (KBr, cm^{-1}): 2977, 1717, 1601, 1449, 1362, 1194, 751; HRMS (ESI/Q-TOF) m/z : $[\text{M} + \text{H}]^+$ Calcd for $\text{C}_{19}\text{H}_{27}\text{O}_3$ 303.1955; found 303.1981.

3-(*tert*-Butylperoxy)-2-cycloheptyl-2,3-dihydro-1*H*-inden-1-one (26ac):

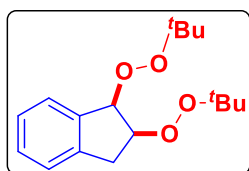
Gummy, (100 mg, 63%). ^1H NMR (CDCl_3 , 400 MHz) δ 7.84 (d, 1H, $J = 8.0$ Hz), 7.74 (d, 1H, $J = 7.6$ Hz), 7.64 (t, 1H, $J = 8.0$ Hz), 7.49 (t, 1H, $J = 7.6$ Hz), 5.45 (d, 1H, $J = 2.4$ Hz), 2.69 (t, 1H, $J = 3.2$ Hz), 2.33–2.27 (m, 1H), 1.80–1.71 (m, 2H), 1.53–1.47 (m, 3H), 1.41–1.29 (m, 5H), 1.28 (s, 9H), 1.27 (d, 2H, $J = 2.8$ Hz) ppm. ^{13}C NMR (CDCl_3 , 101 MHz) δ 205.67, 151.43, 138.06, 134.87, 129.84, 127.86, 123.28, 82.36, 80.58, 59.37, 40.34, 33.31, 30.82, 28.00, 27.76, 27.49, 27.33, 26.70 ppm. IR (KBr, cm^{-1}): 2924, 2858, 1602, 1460, 1362, 1254, 1021, 754; HRMS (ESI/Q-TOF) m/z : $[\text{M} + \text{H}]^+$ Calcd for $\text{C}_{20}\text{H}_{29}\text{O}_3$ 317.2111; found 317.2133.

3-(*tert*-Butylperoxy)-2-cyclooctyl-2,3-dihydro-1*H*-inden-1-one (26ad):

Red gummy, (107 mg, 65%). ^1H NMR (CDCl_3 , 400 MHz) δ 7.84 (d, 1H, $J = 7.6$ Hz), 7.74 (d, 1H, $J = 7.6$ Hz), 7.64 (t, 1H, $J = 7.0$ Hz), 7.48 (t, 1H, $J = 7.4$ Hz), 5.43 (d, 1H,

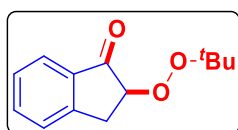
$J = 2.8$ Hz), 2.68 (t, 1H, $J = 3.2$ Hz), 2.45–2.38 (m, 1H), 1.76–1.68 (m, 4H), 1.54–1.51 (m, 3H), 1.44–1.31 (m, 5H), 1.28 (s, 9H), 1.26 (s, 2H) ppm. ^{13}C NMR (CDCl_3 , 101 MHz) δ 205.67, 151.54, 138.17, 134.84, 129.81, 127.85, 123.26, 82.48, 80.58, 59.97, 37.84, 32.49, 30.06, 26.72, 26.64, 26.59, 26.21, 26.19, 26.02 ppm. IR (KBr, cm^{-1}): 2921, 1718, 1602, 1464, 1362, 1195, 1021, 754; HRMS (ESI/Q-TOF) m/z : $[\text{M} + \text{H}]^+$ Calcd for $\text{C}_{21}\text{H}_{31}\text{O}_3$ 331.2268; found 331.2273.

1,2-bis(*tert*-Butylperoxy)-2,3-dihydro-1*H*-indene (26ae'):

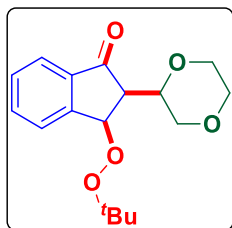


Yellow gummy, (88 mg, 59%). ^1H NMR (CDCl_3 , 400 MHz) δ 7.48 (d, 1H, $J = 7.6$ Hz), 7.29 (d, 1H, $J = 6.0$ Hz), 7.22 (t, 2H, $J = 6.0$ Hz), 5.52 (d, 1H, $J = 1.6$ Hz), 4.99–4.96 (m, 1H), 3.36 (dd, 1H, $J = 17.2, 6.8$ Hz), 2.95 (dd, 1H, $J = 17.2, 2.4$ Hz), 1.28 (s, 9H), 1.26 (s, 9H) ppm. ^{13}C NMR (CDCl_3 , 101 MHz) δ 142.81, 138.27, 129.49, 126.92, 126.87, 125.20, 89.61, 86.61, 80.68, 80.56, 35.85, 26.59 ppm. IR (KBr, cm^{-1}): 2976, 1717, 1466, 1341, 1195, 1020, 874, 751; HRMS (ESI/Q-TOF) m/z : $[\text{M} + \text{NH}_4]^+$ Calcd for $\text{C}_{17}\text{H}_{30}\text{NO}_4$ 312.2169; found 312.2143.

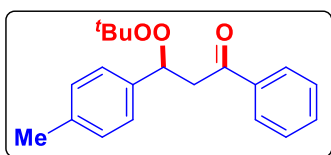
2-(*tert*-Butylperoxy)-2,3-dihydro-1*H*-inden-1-one (26af'):



Brownish gummy, (67 mg, 61%). ^1H NMR (CDCl_3 , 400 MHz) δ 7.75 (d, 1H, $J = 7.6$ Hz), 7.59 (t, 1H, $J = 7.6$ Hz), 7.38 (dd, 2H, $J = 16.0, 8.0$ Hz), 4.38 (dd, 1H, $J = 7.6, 4.8$ Hz), 3.48 (dd, 1H, $J = 16.8, 8.0$ Hz), 2.99 (dd, 1H, $J = 16.4, 4.8$ Hz), 1.34 (s, 9H) ppm. ^{13}C NMR (CDCl_3 , 101 MHz) δ 205.08, 150.80, 135.41, 134.92, 127.85, 126.63, 124.30, 75.33, 74.26, 36.77, 28.49 ppm. IR (KBr, cm^{-1}): 2971, 2925, 1723, 1664, 1606, 1366, 1265, 1193, 951, 752; HRMS (ESI/Q-TOF) m/z : $[\text{M} + \text{H}]^+$ Calcd for $\text{C}_{13}\text{H}_{17}\text{O}_3$ 221.1172; found 221.1199.

3-(*tert*-Butylperoxy)-2-(1,4-dioxan-2-yl)-2,3-dihydro-1*H*-inden-1-one (26ag):

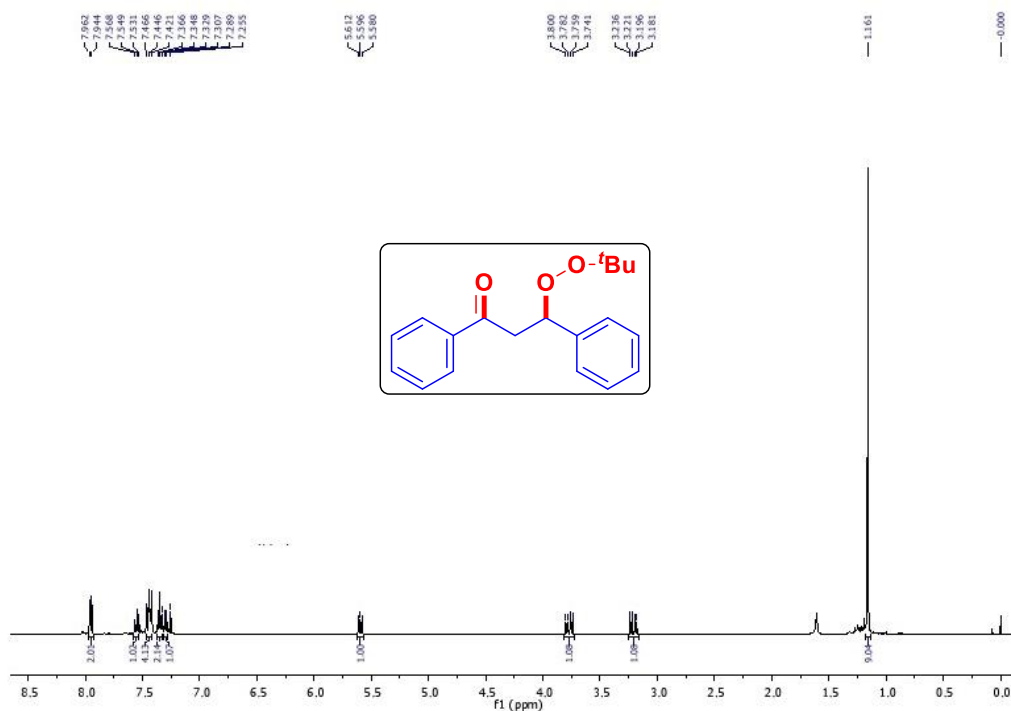
Brownish gummy, (86 mg, 56%). ^1H NMR (CDCl_3 , 400 MHz) δ 7.81–7.75 (m, 2H), 7.67 (t, 1H, $J = 7.4$ Hz), 7.50 (t, 1H, $J = 7.6$ Hz), 5.80 (d, 1H, $J = 2.4$ Hz), 3.90–3.84 (m, 2H), 3.73–3.59 (m, 5H), 2.73 (t, 1H, $J = 2.6$ Hz), 1.29 (s, 9H) ppm. ^{13}C NMR (CDCl_3 , 101 MHz) δ 202.76, 150.94, 137.38, 135.21, 129.92, 127.42, 123.60, 80.79, 80.30, 74.20, 69.77, 67.27, 66.54, 54.61, 26.69 ppm. IR (KBr, cm^{-1}): 2975, 2858, 1722, 1604, 1461, 1362, 1286, 1195, 1119, 876, 756, 616; HRMS (ESI/Q-TOF) m/z : $[\text{M} + \text{H}]^+$ Calcd for $\text{C}_{17}\text{H}_{23}\text{O}_5$ 307.1540; found 307.1563.

3-(*tert*-Butylperoxy)-1-phenyl-3-(*p*-tolyl)propan-1-one (2aC):

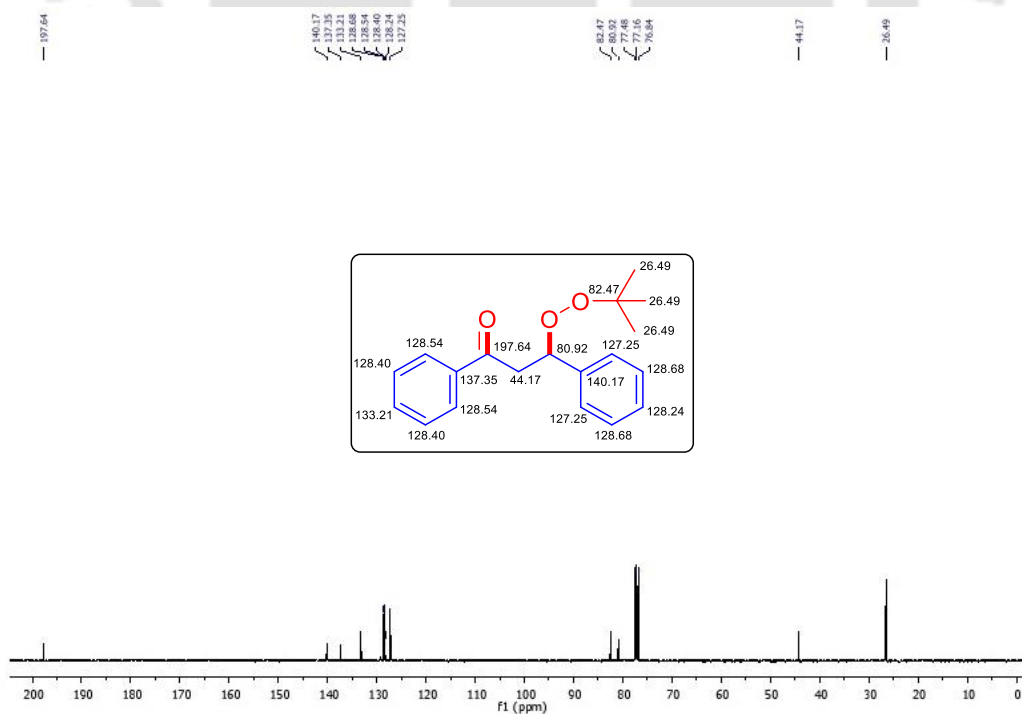
Gummy, (102 mg, 65%). ^1H NMR (400 MHz, CDCl_3) δ 7.95 (d, 2H, $J = 7.2$ Hz), 7.56 (t, 1H, $J = 7.4$ Hz), 7.44 (t, 2H, $J = 7.6$ Hz), 7.32 (d, 2H, $J = 8.0$ Hz), 7.16 (d, 2H, $J = 8.0$ Hz), 5.56 (t, 1H, $J = 6.6$ Hz), 3.79 (dd, 1H, $J = 16.4$, 7.2 Hz), 3.21 (dd, 1H, $J = 16.0$, 6.0 Hz), 2.33 (s, 3H), 1.16 (s, 9H) ppm. ^{13}C NMR (101 MHz, CDCl_3) δ 197.77, 138.02, 137.32, 136.95, 133.16, 129.24, 128.75, 128.63, 128.37, 127.26, 82.40, 80.86, 44.05, 26.47, 26.38, 21.32 ppm. HRMS (ESI/Q-TOF) m/z : $[\text{M} + \text{Na}]^+$ Calcd for $\text{C}_{20}\text{H}_{24}\text{NaO}_3$ 335.1618; found 335.1645.

II.7. Spectra

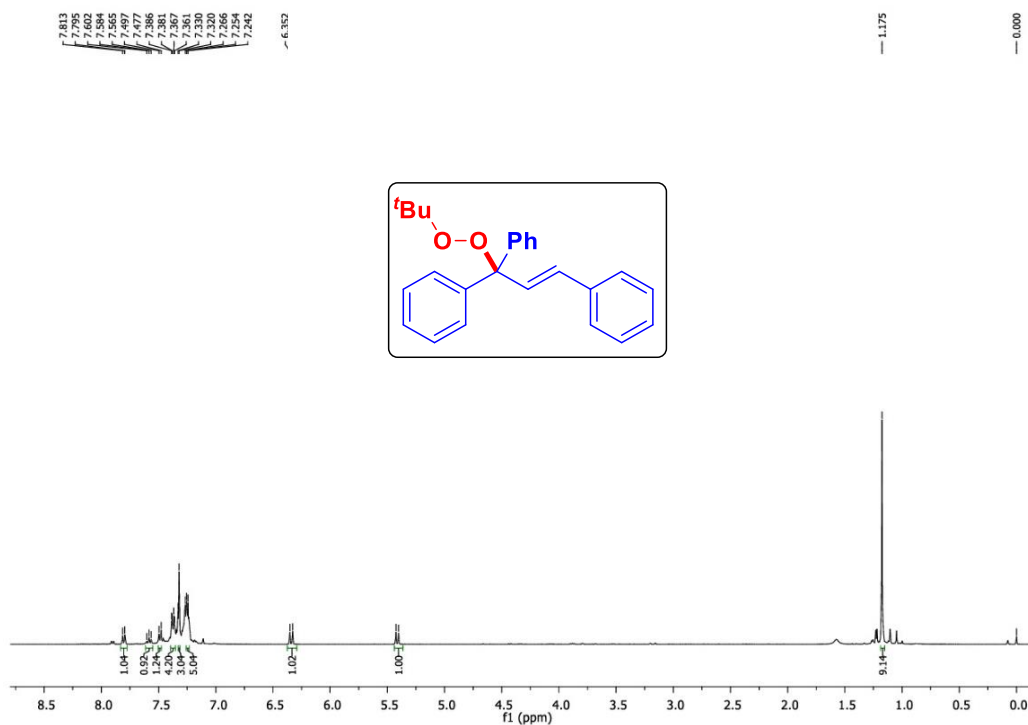
3-(*tert*-Butylperoxy)-1,3-diphenylpropan-1-one (1a): ^1H NMR (400 MHz, CDCl_3)



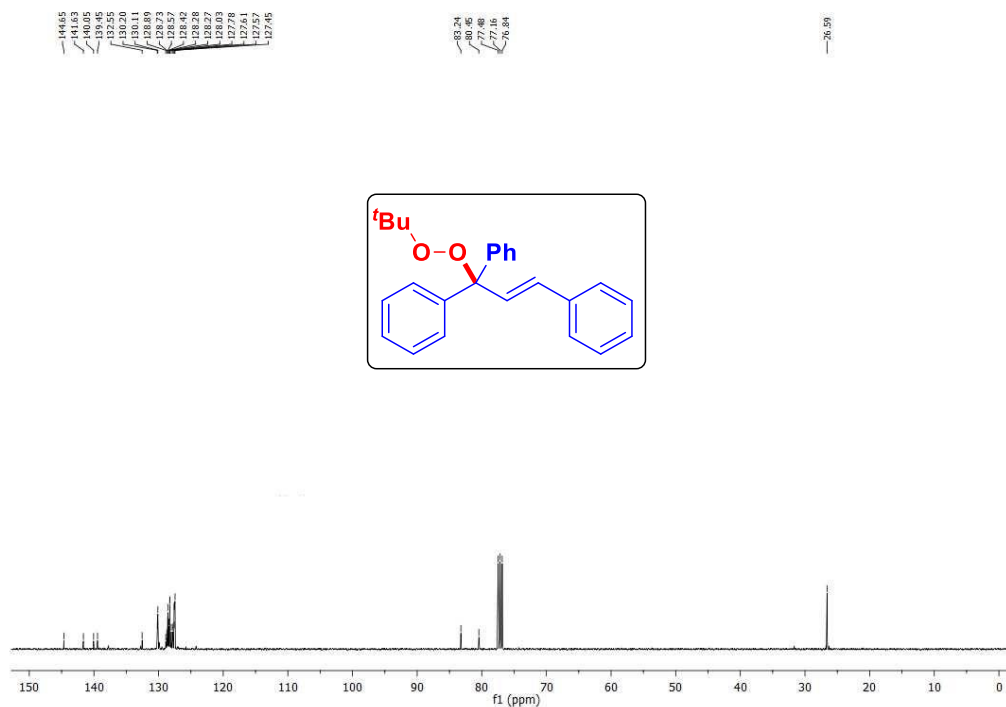
3-(*tert*-Butylperoxy)-1,3-diphenylpropan-1-one (1a): ^{13}C NMR (101 MHz, CDCl_3)

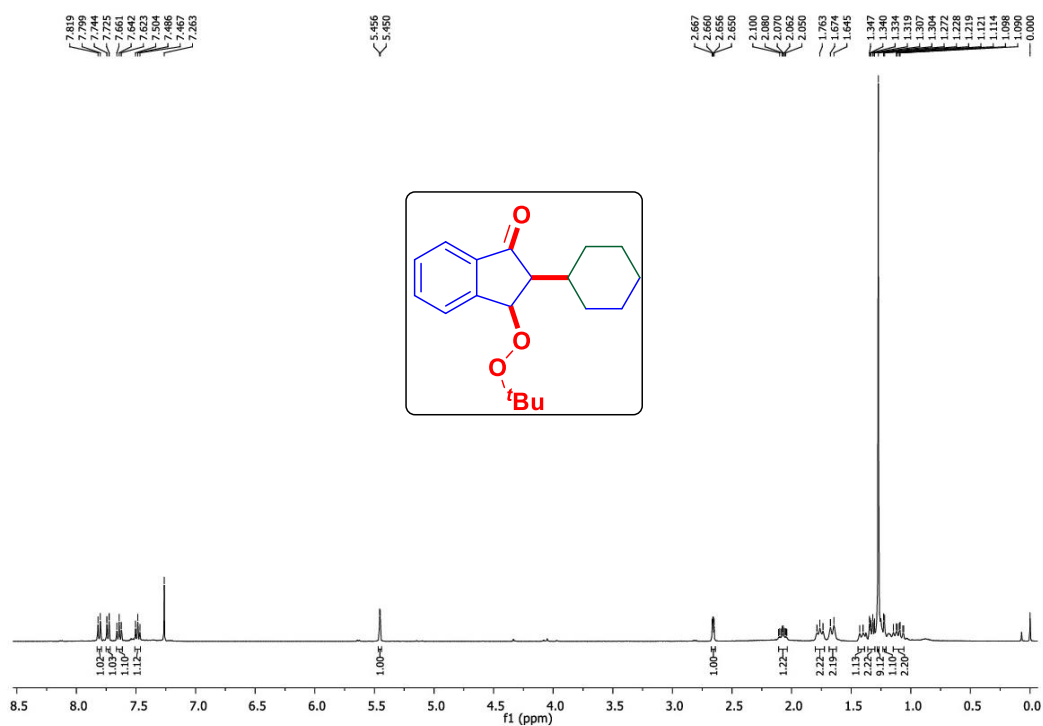
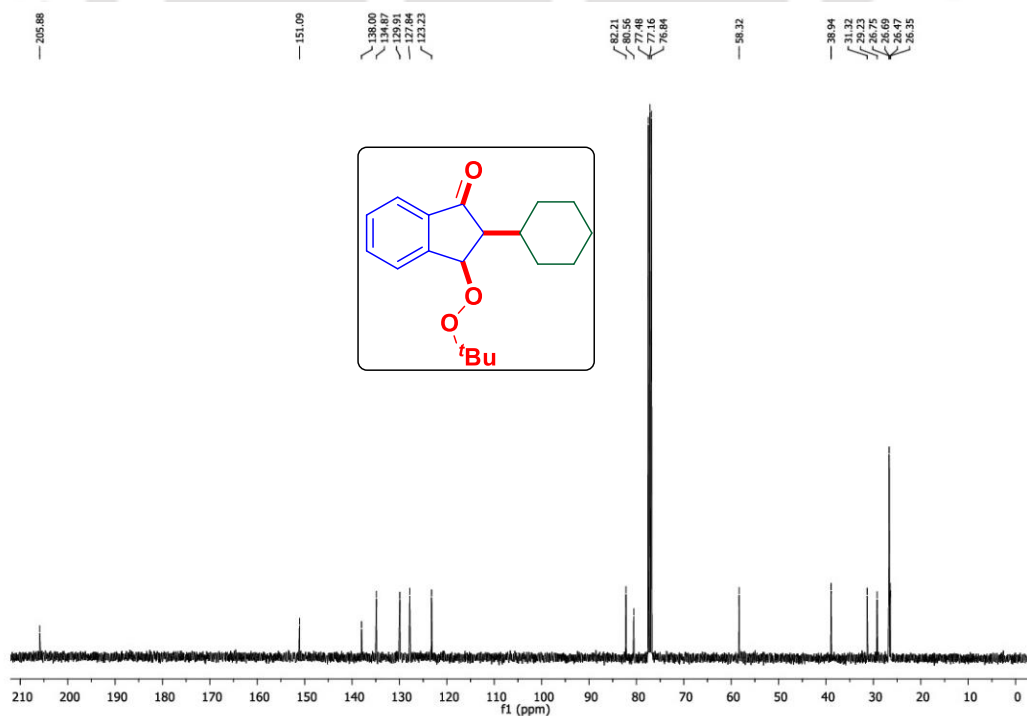


(E)-1-(tert-Butylperoxy)prop-2-ene-1,1,3-triyltribenzene (17a): ^1H NMR (400 MHz, CDCl_3)



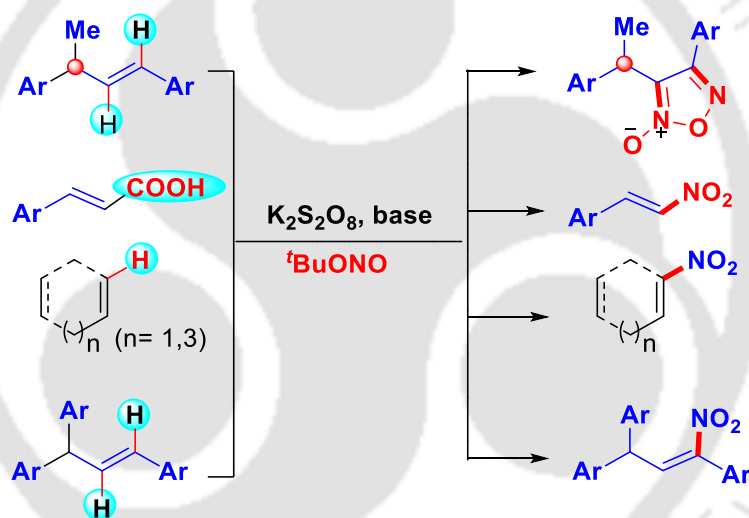
(E)-1-(tert-Butylperoxy)prop-2-ene-1,1,3-triyltribenzene (17a): ^{13}C NMR (101 MHz, CDCl_3)



3-(*tert*-Butylperoxy)-2-cyclohexyl-2,3-dihydro-1*H*-inden-1-one (26ab): ¹H NMR (400 MHz, CDCl₃)**3-(*tert*-Butylperoxy)-2-cyclohexyl-2,3-dihydro-1*H*-inden-1-one (26ab): ¹³C NMR (101 MHz, CDCl₃)**

CHAPTER III

tert-Butyl Nitrite Mediated Differential Functionalizations of Internal Alkenes: Paths to Furoxans and Nitroalkenes



ABSTRACT: *tert-Butyl nitrite (TBN) reacts differently with various internal alkenes leading to interesting and useful products. Synthesis of 1,2,5-oxadiazole-N-oxides (furoxans) has been achieved from internal alkenes using tert-butyl nitrite (TBN), quinoline and $K_2S_2O_8$. Under an identical reaction condition α,β -unsaturated carboxylic acids and cyclic and acyclic internal alkenes both afforded nitroalkenes as the sole product via decarboxylative and direct nitration path respectively.*

CHAPTER III**III. *tert*-Butyl Nitrite Mediated Differential Functionalizations of Internal Alkenes: Paths to Furoxans and Nitroalkenes****III.1. Introduction**

Furoxan (or 1,2,5-oxadiazole 2-oxide) is a heterocycle of the isoxazole family and is an important scaffold in medicinal chemistry.^[1] Derivatives of furoxans or furoxan *N*-oxides are of significant importance in organic synthesis, since they are an integral part of several potential therapeutic agents such as furoxans-praziquantel,^[2a] *N*-acyl derivatives of furoxans,^[2b] furoxans-phthalimide,^[2c] furoxanyl-*N*-acylhydraxones,^[2d] furoxanylacyl-salicylic acid,^[2e] furoxan-farnesylthiosalicylic acid,^[2f] furoxans amodiaquine,^[2g] furoxans-phenylsulfonyl,^[2h] 4-furoxanyl nitron,^[2i] furoxan-chalcones,^[2j] furoxan-fenoterol,^[2k] furoxan-oleanolic acid,^[2l] furoxans-dibenzoyl,^[2m] furoxan-ibuprofen,^[2n] etc. Moreover, furoxan derivatives have drawn phenomenal biological and pharmaceutical interests, some of which are reported to have antioxidant,^[3a] vasodilator,^[3a] leishmanicidal,^[3b] anticancer,^[3c] antibacterial,^[2i] antimalarial,^[2i] antihistaminic,^[3d] and anti-HIV^[3e] activities. Furoxan derivatives are known to release nitric oxide (NO) in the presence of thiol co-factors, thus activating the soluble guanylate cyclase.^[1,4] Consequently, many research groups pursued studies on the development of furoxan-based drugs.^[5] Selected furoxan derivatives possessing potential pharmaceutical applications are shown in Figure III.1.1.^[2i,3a,5c,6] However, any organic reagent such as *tert*-butyl nitrite mediated synthesis of furoxans from alkenes is still unexplored. In this regard, synthesis of furoxans from easily accessible and biologically demanding internal alkenes bearing an allylic stereogenic centre may generate potential applications as both stereogenic centres^[8a] and furoxan moiety^[8b,c] are important parts of many biologically active compounds, thus are expected to receive considerable interest from biological and pharmaceutical point of view.

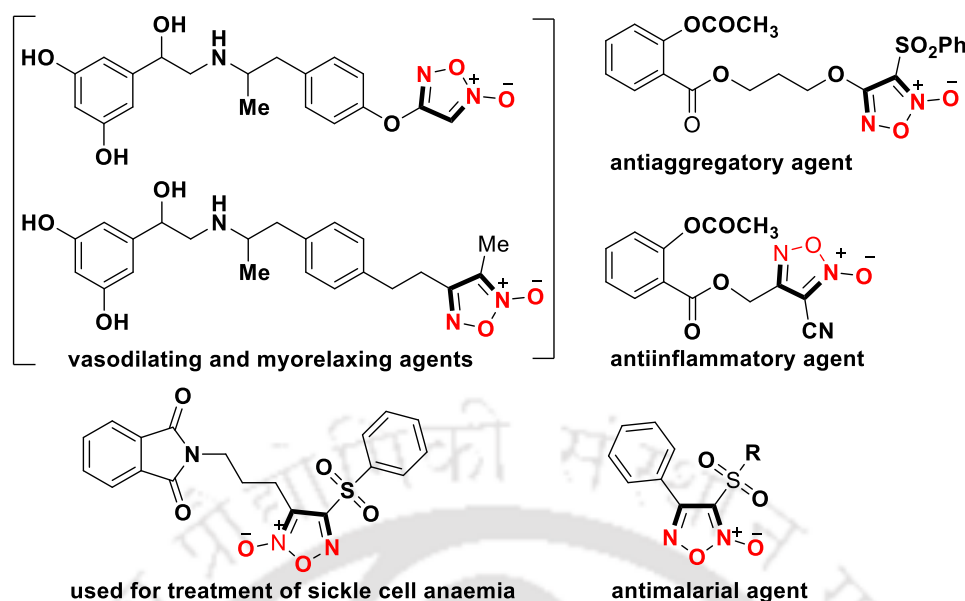


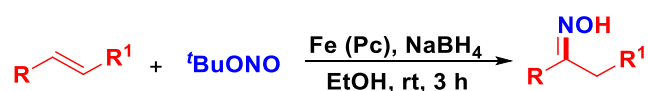
Figure III.1.1. Some representative bioactive furoxans

III.2. Strategies for *tert*-Butyl Nitrite (TBN) Mediated Functionalizations of Olefins

Alkenes which are simple organic molecules have been widely applied in organic synthesis for the construction of a diverse array of complex molecules. One of the finest approaches to build such class of molecules in a single operation is via the direct functionalization of olefins. In this connection, *tert*-butyl nitrite (TBN) has emerged as a versatile reagent in organic synthesis.^[9a] Therefore, it has been widely employed for different types of alkene functionalizations. These functionalizations can be broadly divided into two types *viz* (i) mono-functionalizations and (ii) di-functionalizations. Some of the recent advances in each of these categories are summarized below.

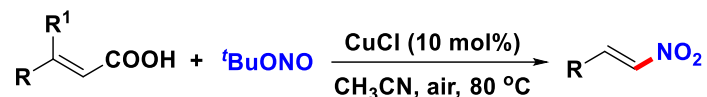
(i) Mono-functionalizations

In this context, Beller disclosed Fe(II)-catalyzed synthesis of oximes from vinylarenes. This synthesis was accomplished in the presence of *tert*-butyl nitrite and NaBH₄ to access different oxime analogues in moderate to good yields (Scheme III.2.1).^[9b]



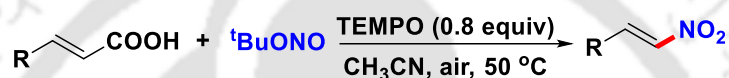
Scheme III.2.1. TBN-mediated oximation of alkenes

Prabhu *et al.* reported a *tert*-butyl nitrite-mediated nitro-decarboxylation of cinnamic acids. This nitrative decarboxylation was achieved using Cu(I) as the catalyst to access a variety of nitrolefins (Scheme III.2.2).^[9c]



Scheme III.2.2. TBN mediated decarboxylative nitration involving sp^2 carbon

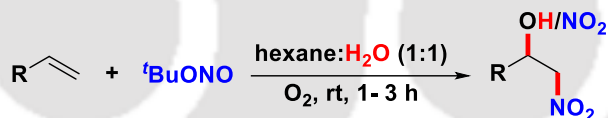
Maiti and co-workers reported decarboxylative nitration of α,β -unsaturated carboxylic acids. This decarboxylative nitration that was achieved in the presence of *tert*-butyl nitrite and TEMPO leads to the formation of a wide variety of nitrolefins via a radical pathway (Scheme III.2.3).^[9d]



Scheme III.2.3. TBN mediated decarboxylative nitration involving sp^2 carbon

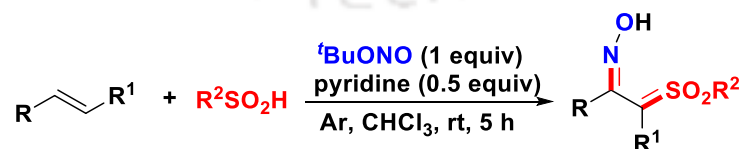
(ii) Di-functionalizations

In this context, Taniguchi *et al.* reported the oxidative nitration of alkenes using a combination of *tert*-butyl nitrite and molecular oxygen to give β -nitro alcohols and their nitrate derivatives (Scheme III.2.4).^[9e]



Scheme III.2.4. TBN mediated oxidative nitration involving sp^2 carbon

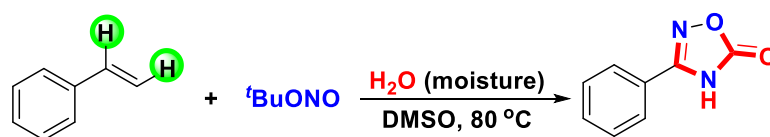
A vicinal sulfoximation of alkenes was achieved by Yu and co-workers by using sulfinic acid as the sulfonating agent and TBN as the NO source as well as an oxidant to access a variety of α -sulfonyl ketoximes (Scheme III.2.5).^[9f]



Scheme III.2.5. TBN-mediated sulfoximation involving sp^2 carbon

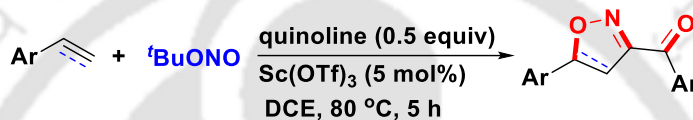
Our group reported *tert*-butyl nitrite mediated synthesis of 1,2,4-oxadiazole-5(4*H*)-ones from terminal alkenes. In this biradical pathway, TBN serves as a source of NO and N whereas

H₂O serves as a carbonyl oxygen source to furnish a variety of 1,2,4-oxadiazole-5(4*H*)-ones (Scheme III.2.6).^[9g]



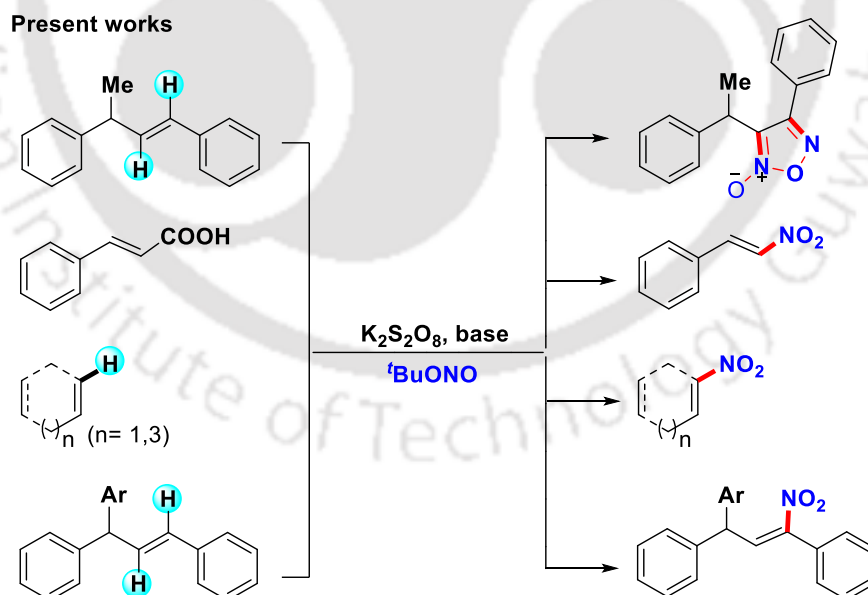
Scheme III.2.6. TBN-mediated 1,2,4-oxadiazole-5(4*H*)-ones synthesis involving *sp*² carbon

Recently our group has reported a *tert*-butyl nitrite-mediated domino synthesis of isoxazolines and isoxazoles from corresponding styrenes and phenylacetylenes. This Sc(OTf)₃ catalyzed strategy proceeds via a radical pathway to give isoxazolines and isoxazoles (Scheme III.2.7).^[9h]



Scheme III.2.7. TBN mediated domino synthesis of isoxazolines and isoxazoles

However, *tert*-butyl nitrite-mediated di-functionalization of any internal olefin is less explored so far.



Scheme III.2.8. Strategies for functionalization of internal alkenes using TBN

III.3. Present Work

Inspired by these developments on *tert*-butyl nitrite-mediated functionalizations particularly using styrenes and phenylacetylenes, we anticipated that if an internal alkene is

treated with TBN whether it may lead to the formation of similar isoxazoline^[9i] or a completely different reactivity may drive the formation of some other product? Therefore, we were curious to investigate the reaction of various internal alkenes with TBN (Scheme III.2.8).

Optimization of Reaction Conditions. To execute the above-envisaged strategy, our initial investigation started by reacting an internal alkene (**1**) with *tert*-butyl nitrite (**a**). Alkene (*E*)-1,3-diphenyl-1-butene (**1**) was chosen as the model substrate as this core unit contains an allylic carbon stereogenic center which represents a privileged and biologically important molecular scaffold.^[8a] Initially, alkene (**1**) was treated with *tert*-butyl nitrite (**a**) (2 equiv) in the presence of well explored FeCl₃ (2.5 mol%) catalyst, and base 1,4-diazabicyclo[2.2.2]octane (DABCO) (1 equiv) in 1,2-dichloroethane (DCE) (1.5 mL) at 85 °C for 5 h. A new product (**1a**) was isolated in 33% yield after column chromatographic separation (entry 1, Table III.3.1). Spectroscopic (¹H and ¹³C NMR) analysis of the product (**1a**) revealed the disappearance of both alkene protons at 6.40 ppm. However, the appearance of a doublet at 1.23 ppm and a multiplet at 3.27 ppm suggests that the PhCH(CH₃)- part is intact thereby confirming di-functionalization across the double bond of (**1**). Further, HRMS analysis of the product indicates the loss of two protons and the addition of two NO groups. Finally, the exact structure of the product was confirmed by X-ray crystallographic analysis of one of its derivative (**8a**) as shown in (Figure III.3.1). The

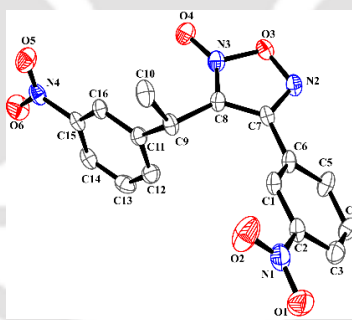
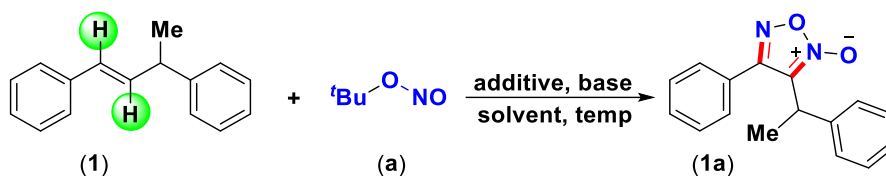


Figure III.3.1. ORTEP molecular diagram of (**8a**)

formation of this interesting furoxan skeleton fascinated us. Therefore, this reaction was further screened by varying various other Lewis acid catalysts. Among the catalysts screened such as AlCl₃ (37%), Fe(OTf)₃ (39%) and Sc(OTf)₃ (44%) (entries 2-4, Table III.3.1), it was observed that Sc(OTf)₃ provided better yield (44%). However, the use of other bivalent metal catalysts such as Cu(OTf)₂ and Zn(OTf)₂ provided the desired product (**1a**) in lesser yields 19% and 17% respectively (entries 5-6, Table IV.3.1). Interestingly, the use of organic base quinolone (entry 9, Table III.3.1) in place of DABCO, DBU, DMAP (entries 4, 7, 8, Table III.3.1) provided the product (**1a**) in an improved yield (56%). The reaction carried out in the absence

Table III.3.1. Screening of reaction conditions^[a-d]

Entry	Catalyst (mol %)	Base (equiv)	Solvent (mL)	Additive (equiv)	Yield (%) ^[b]
1	FeCl ₃ (2.5)	DABCO (1)	DCE		33
2	AlCl ₃ (2.5)	DABCO (1)	DCE		37
3	Fe(OTf) ₃ (2.5)	DABCO (1)	DCE		39
4	Sc(OTf) ₃ (2.5)	DABCO (1)	DCE		44
5	Cu(OTf) ₂ (2.5)	DABCO (1)	DCE		19
6	Zn(OTf) ₂ (2.5)	DABCO (1)	DCE		17
7	Sc(OTf) ₃ (2.5)	DBU (1)	DCE		44
8	Sc(OTf) ₃ (2.5)	DMAP (1)	DCE		27
9	Sc(OTf) ₃ (2.5)	Quinoline (1)	DCE		56
10		Quinoline (1)	DCE		23
11	Sc(OTf) ₃ (2.5)		DCE		39
12	Sc(OTf) ₃ (2.5)	Quinoline (1)	DCE	Oxone® (1)	59
13	Sc(OTf) ₃ (2.5)	Quinoline (1)	DCE	K ₂ S ₂ O ₈ (1)	62
14		Quinoline (1)	DCE	K ₂ S ₂ O ₈ (1)	64
15	Sc(OTf) ₃ (2.5)		DCE	K ₂ S ₂ O ₈ (1)	29
16	-		DCE	K ₂ S ₂ O ₈ (1)	51
17		Quinoline (1)	DCE	K ₂ S ₂ O ₈ (1)	64 ^[c]
18		Quinoline (1)	DCE	K ₂ S ₂ O ₈ (1)	52 ^[d]
19		Quinoline (1)	CH₃CN	K₂S₂O₈ (1)	73
20		Quinoline (1)	DMSO	K ₂ S ₂ O ₈ (1)	21
21		Quinoline (1)	DMF	K ₂ S ₂ O ₈ (1)	43
22		Quinoline (1)	AcOH	K ₂ S ₂ O ₈ (1)	51
23		Quinoline (1)		K ₂ S ₂ O ₈ (1)	27
24		Quinoline (2)	CH ₃ CN	K ₂ S ₂ O ₈ (1)	76
25		Quinoline (1)	CH ₃ CN	K ₂ S ₂ O ₈ (2)	60

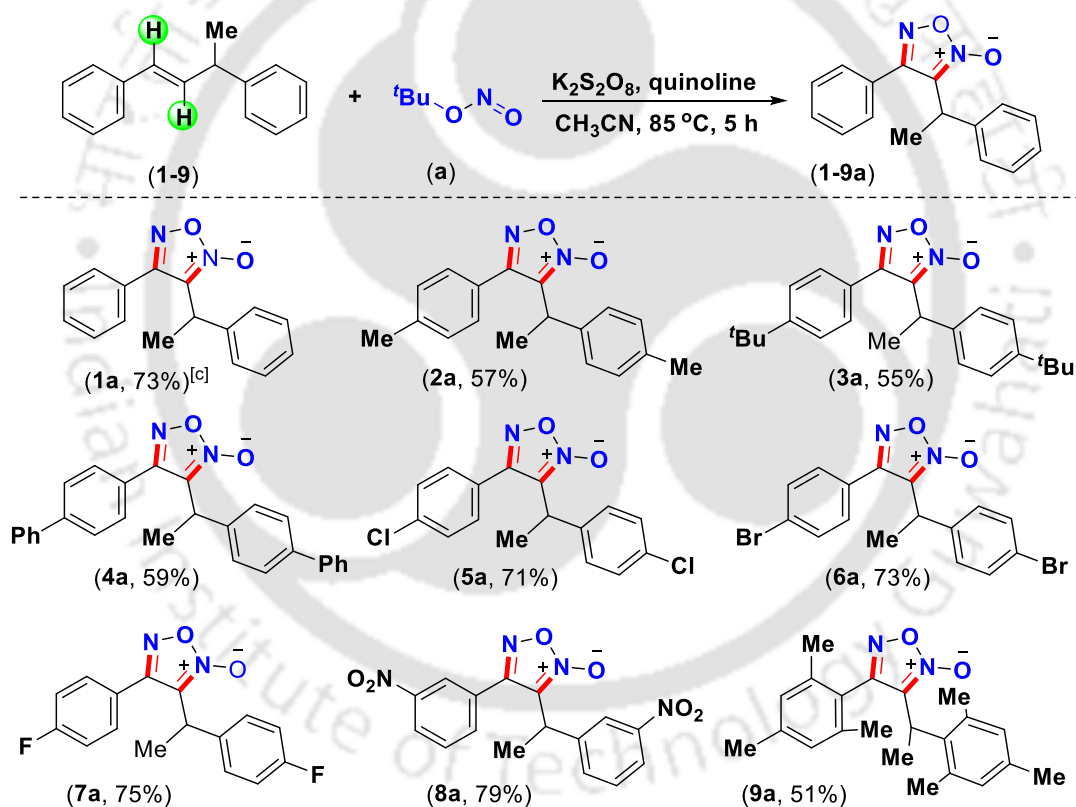
^[a]Reaction conditions: **1** (0.50 mmol), K₂S₂O₈ (0.50 mmol), base (0.50 mmol), *tert*-butylnitrite (1.0 mmol) at 85 °C. ^[b]Yield after 5 h. ^[c]Temperature 100 °C. ^[d]Temperature 70 °C.

of $\text{Sc}(\text{OTf})_3$ catalyst was detrimental to product formation (entry 10, Table III.3.1), suggesting the involvement of $\text{Sc}(\text{OTf})_3$ in facilitating the reaction. When the reaction was performed in the absence of base under otherwise identical conditions the yield of (**1a**) decreased to 39% (entry 11, Table III.3.1). These results suggest the active involvement of both catalyst and base in this reaction. To further improve the product yield, various oxidant/additive combinations were employed in instead of a single oxidant. It was found that the use of additive Oxone® along with TBN improved the product yield up to 59% (entry 12, Table III.3.1). By changing the additive from Oxone® to potassium persulphate ($\text{K}_2\text{S}_2\text{O}_8$) the product yield improved up to 62% (entry 13, Table III.3.1). Surprisingly, when the reaction was carried out in the absence of $\text{Sc}(\text{OTf})_3$ catalyst, but in the presence of TBN, $\text{K}_2\text{S}_2\text{O}_8$ and quinoline the yield of (**1a**) improved to 64% (entry 14, Table III.3.1). This observation suggests that the reaction is neither mediated by a redox process nor by a Lewis acid catalyst. However, when the reaction was carried out in the absence of base the product formation (**1a**) dropped to 29% (entry 15, Table III.3.1). In the presence of $\text{K}_2\text{S}_2\text{O}_8$ (1 equiv) alone *i.e* in the absence of any catalyst and base the reaction gave 51% yield (entry 16, Table III.3.1). When the reaction was carried out at 100 °C the yield remained unchanged (64%) of (**1a**) (entry 17, Table III.3.1) but a decrease in the reaction temperature to 70 °C provided reduced yield (52%) of the product (entry 18, Table III.3.1). Subsequently, screening of other solvents such as CH_3CN , DMSO, DMF, AcOH, solvent CH_3CN was found to give the best yield 73% (entries 19-22, Table III.3.1) under otherwise identical conditions. Since most of the reagents are liquid at room temperature the reaction was attempted under a neat condition, unfortunately, the reaction was unclean giving multitude of products and reducing the isolated yield to 27% (entry 23, Table III.3.1). A marginal improvement in the yield (76%) of the product was observed by increasing the quinoline amount to 2 equiv (entry 24, Table III.3.1). However, a twofold loading of $\text{K}_2\text{S}_2\text{O}_8$ was found to be counterproductive for the reaction giving only 60% yield (entry 25, Table III.3.1). After a series of screening, it was found that this bis-functionalization is best achieved using alkene (**1**) (0.5 mmol), TBN (2 equiv), quinoline (1 equiv), $\text{K}_2\text{S}_2\text{O}_8$ (1 equiv) at 85 °C for 5 h.

After establishing the optimized reaction condition for furoxan (**1a**) formation from internal alkene (**1**) as shown in (Table III.3.1), we explored the reaction between various (*E*)-1,3-diphenyl-1-butenes (**1-9**) with TBN (**a**). This reaction proceeded well with a variety of alkenes bearing electron-donating as well as electron-withdrawing groups in their phenyl rings. Phenyl rings of these alkenes possessing moderately electron-donating groups such as *p*-Me

(2) *p*-^tBu (3), *p*-Ph (4), gave their corresponding products (2a, 57%), (3a, 55%), (4a, 59%), in moderate yields (Scheme III.3.1). Alkene substrates having moderately electron-withdrawing groups such as *p*-Cl (5), *p*-Br (6), *p*-F (7) in the phenyl rings provided their corresponding products (5a, 71%), (6a, 73%), (7a, 75%) in good yields as shown in (Scheme III.3.1). Alkenes possessing strongly electron-withdrawing group such as *m*-NO₂ (8) also resulted in the formation of furoxan (8a) in good yield (79%). Internal alkene having tri-methyl (9) substitution in its phenyl ring reacted successfully and provided the corresponding furoxan (9a, 51%) in a relatively lesser yield (Scheme III.3.1). The lower yield of product obtained for the substrate (9) is possibly due to steric hindrance caused by *ortho*-substitutions.

Scheme III.3.1. Substrate scope for furoxan synthesis^[a-c]

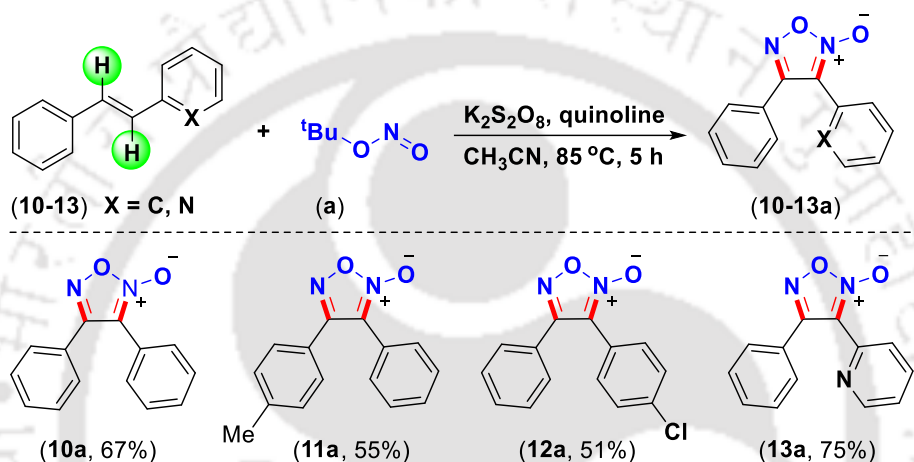


^[a]Reaction conditions: (1-9) (0.50 mmol), K₂S₂O₈ (0.50 mmol), quinoline (0.50 mmol), *tert* butyl nitrite (1.0 mmol) in CH₃CN (1.5 mL) at 85 °C for 5 h. ^[b]Isolated yields. ^[c]Gram scale yield (64%) TBN and K₂S₂O₈ was added in 4 equal lots over a period of 4 h.

In addition to these unsymmetrical benzylic internal alkenes, this method is equally amenable to 1,2-disubstituted symmetrical and unsymmetrical stilbenes. When *trans*-stilbene (10) was treated with TBN, it provided corresponding furoxan (10a) in 67% yield (Scheme III.3.2). Besides, unsymmetrical *trans*-stilbenes possessing moderately electron-donating *p*-Me

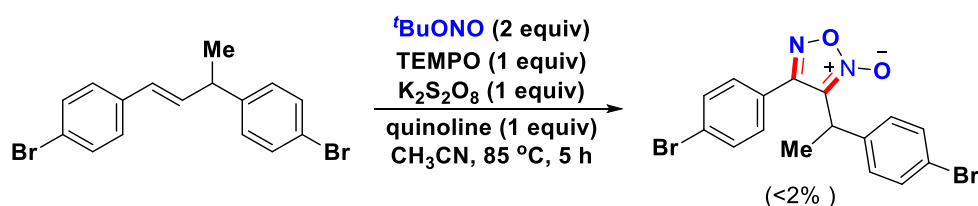
(11) and electron-withdrawing *p*-Cl (12) substituents in one of the phenyl ring reacted successfully providing their expected products (11a) and (12a) in 55% and 51% yields respectively. A heterocyclic *trans*-stilbene (13) also reacted successfully and provided the corresponding furoxan (13a) in good yield (75%). At present we are not sure about the position of *N*-oxide in *trans*-stilbenes as towards which phenyl ring it is oriented but based on the mechanism proposed in (Scheme III.3.4), the *N*-oxide is expected to be towards phenyl side in (11a), *p*-Cl phenyl side in (12a) and towards pyridine ring in (13a) (Scheme III.3.2).

Scheme III.3.2. Substrate scope for furoxan synthesis from *trans*-stilbenes^[a,b]



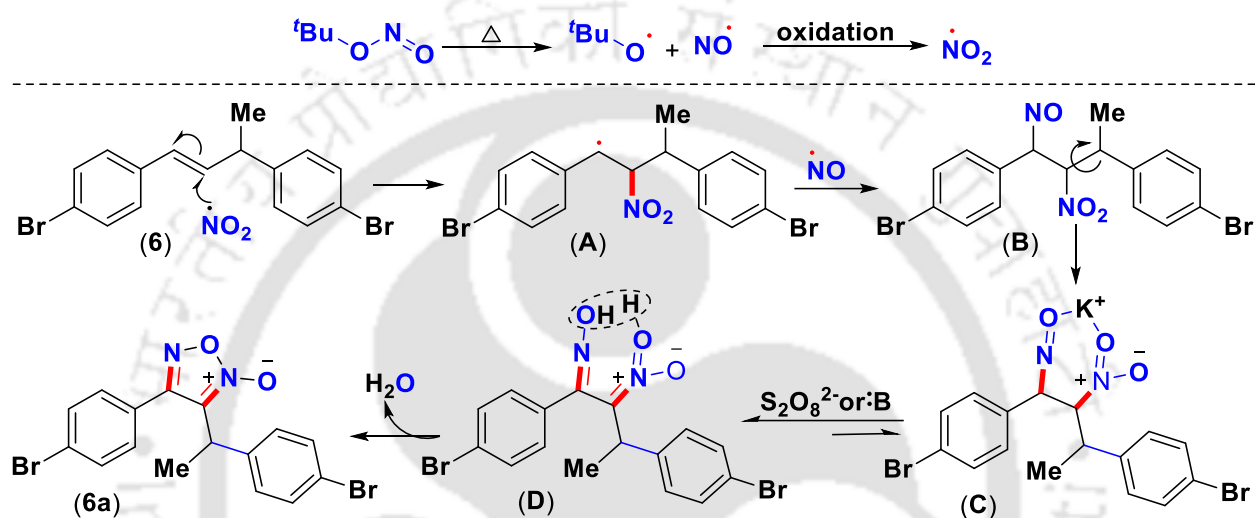
^[a]Reaction conditions: (10-13) (0.50 mmol), K₂S₂O₈ (0.50 mmol), quinoline (0.50 mmol), *tert*-butyl nitrite (1.0 mmol) in CH₃CN (1.5 mL) at 85 °C for 5 h. ^[b]Isolated yields.

To demonstrate the applicability of the reaction in large scale, internal alkene (1) (5 mmol, 1.04 g) was reacted with TBN (10 mmol) and K₂S₂O₈ (5 mmol) the product was obtained in 51% yield. Interestingly, when TBN and K₂S₂O₈ were added in four equal lots for 4 h the yield of the product (1a) improved up to 64% (Scheme III.3.1). To check whether the reaction is proceeding via a radical path, (*E*)-4,4'-(but-2-ene-1,3-diyl)bis(bromobenzene) (6) was reacted with *tert*-butyl nitrite (a) in the presence of an equimolar quantity of radical scavenger (2,2,6,6-tetramethylpiperidin-1-yl)oxidanyl (TEMPO). Formation of (<2%) of the product (6a) (Scheme III.3.3) suggests a possible radical pathway for this transformation.



Scheme III.3.3. Radical nature of furoxan synthesis

Based on the literature reports, intermediates detected by HRMS analysis of the reaction mixtures a plausible mechanism has been proposed for the furoxan formation. Initially, the homolytic cleavage of *tert*-butyl nitrite produces a NO radical and a *tert*-butoxy radical (Scheme III.3.4). The NO radical under an aerobic reaction condition gets converted to a NO₂ radical.^[10] Subsequently, the NO₂ radical attacks at the non-benzylic carbon of the olefin (**6**) to generate a nitroalkane benzyl radical intermediate (**A**) (Scheme III.3.4). The radical intermediate (**A**) then reacts with the NO• radical at its benzylic position to give a nitro-nitroso



Scheme IV.3.4. A plausible mechanism for furoxan synthesis

intermediate (**B**). Alternatively, the intermediate (**A**) loses a proton giving product (**A'**), which has been detected by HRMS analysis of the reaction aliquots (Figure III.3.2). This pattern of preferential attack of NO• at the benzylic position is consistent with our isoxazoline synthesis involving a terminal alkene and TBN.^[9i] The intermediate (**B**) then undergoes a C–C bond rotation which is perhaps facilitated by the co-ordination of K⁺ with two of the oxygen atoms from NO and NO₂ groups forming an intermediate (**C**). The nitroso intermediate (**C**) isomerizes to a *bis*-oxime type intermediate (**D**) in the presence of a base, from which furoxan (**6a**) is generated via the loss of a water molecule (Scheme III.3.4). Formation of intermediates (**B**) / (**D**) have been detected by HRMS analysis of the reaction mixture [Figure III.3.2] / [Figure III.3.3].

Sample Name	Unavailable	Position	Unavailable	Instrument Name	Unavailable	User Name	Unavailable
Inj Vol	Unavailable	InjPosition	Unavailable	SampleType	Unavailable	IRM Calibration Status	All Ions Missed
Data Filename	BM-DN-TEMPO.d	ACQ Method		Comment	Sample information is unavailable	Acquired Time	Unavailable

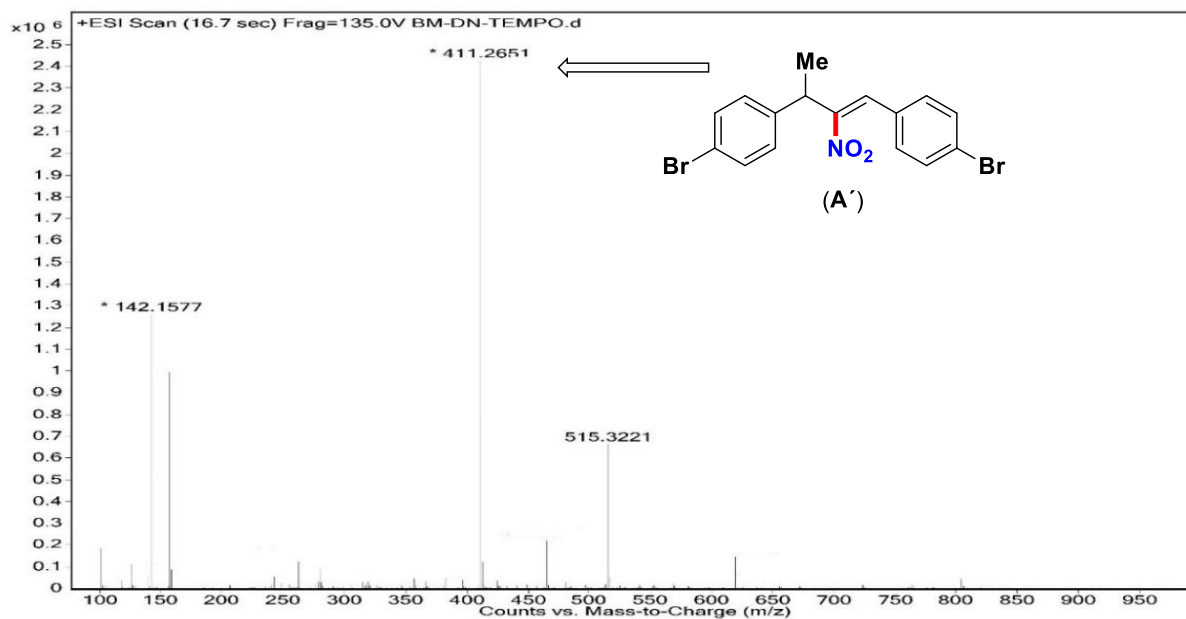


Figure III.3.2. HRMS spectrum of the reaction mixture after 15 minutes

Sample Name	Unavailable	Position	Unavailable	Instrument Name	Unavailable	User Name	Unavailable
Inj Vol	Unavailable	InjPosition	Unavailable	SampleType	Unavailable	IRM Calibration Status	All Ions Missed
Data Filename	BM-DN-TEMPO.d	ACQ Method		Comment	Sample information is unavailable	Acquired Time	Unavailable

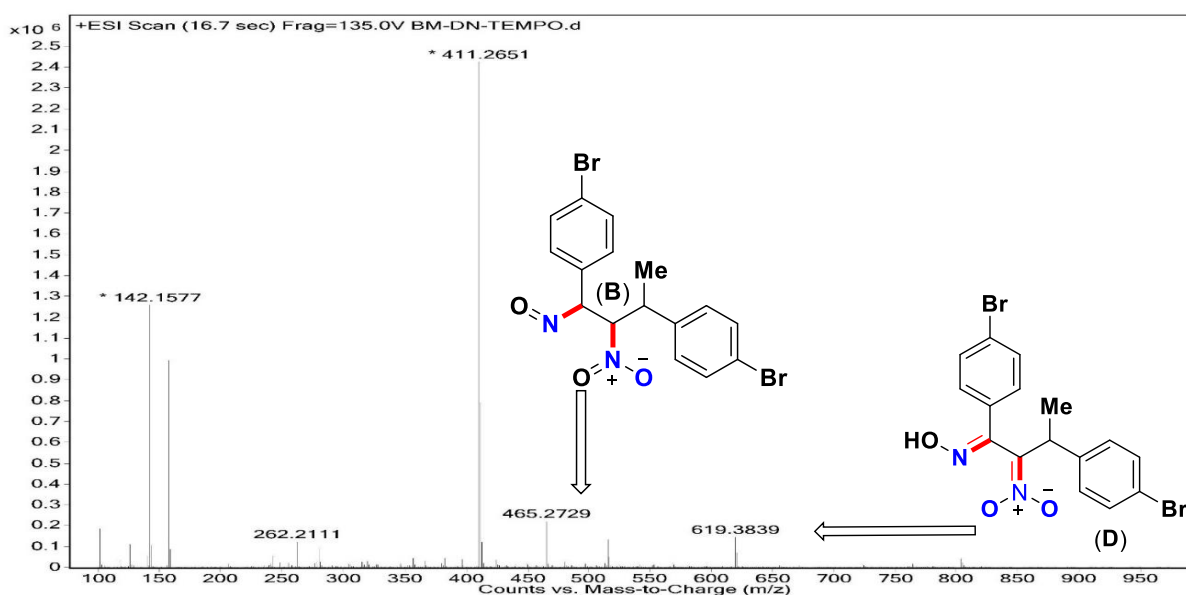
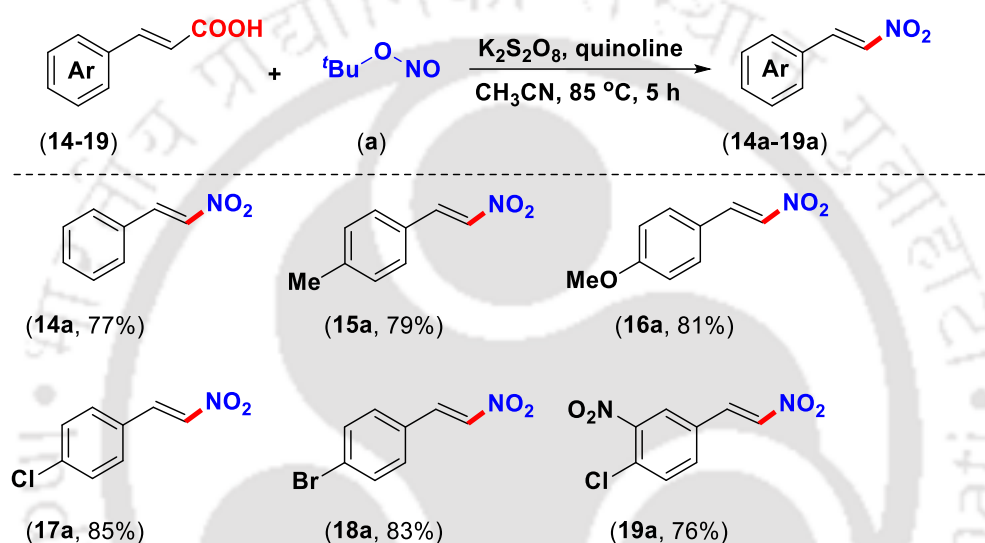


Figure III.3.3. HRMS spectrum of the reaction mixture after 30 minutes

Further, to check whether this strategy of furoxan synthesis applies to other internal alkenes such as α,β -unsaturated acids or not? *trans*-cinnamic acid (**14**) was reacted with TBN (**a**) under an identical reaction condition. The reaction proceeded well and provided product (**14a**) in good yield (77%). Spectroscopic (IR, ^1H and ^{13}C NMR) analysis of the isolated product (**14a**) showed the absence of the COOH group. The HRMS analysis of the new product

revealed the loss of a COOH group and incorporation of a NO₂ group. Here, perhaps *tert*-butyl nitrite (**a**) is serving as a decarboxylative nitrating agent because their corresponding ester did not yield any trace of the nitroalkene (nor even furoxan). To explore the generality of this strategy, the reaction of electron-donating such as *p*-Me (**15**), *p*-OMe (**16**) and electron-withdrawing such as *p*-Cl (**17**), *p*-Br (**18**), and *m*-NO₂-*p*-Cl (**19**) substituents present in the aryl ring of the cinnamic acids all afforded β -nitration products (**15a**, 79%), (**16a**, 81%), (**17a**, 85%), (**18a**, 83%) and (**19a**, 76%) (Scheme III.3.5) in good yields.

Scheme III.3.5. Nitration of α,β -unsaturated carboxylic acids^[a,b]



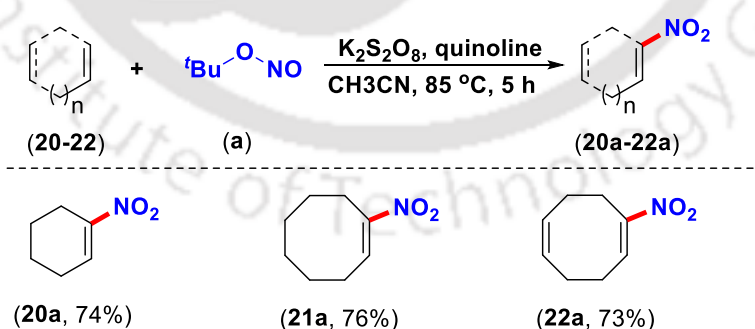
^[a]Reaction conditions: (**14-19**) (0.50 mmol), $K_2S_2O_8$ (0.50 mmol), quinoline (0.50 mmol), *tert*-butyl nitrite (1.0 mmol) in CH_3CN (1.5 mL) at 85 °C for 5 h. ^[b]Isolated yields.

Before this report, there are reports on decarboxylative nitration using HNO_3 ,^[11a-c] *tert*-BuONO in combination with $CuCl$ ^[9c] and TEMPO.^[9d] Few other methods such as Henry reaction involving nitroalkanes,^[11e] and direct nitration of alkenes using $AgNO_2$ ^[11f] have also been reported for the synthesis of nitroalkenes. Although few decarboxylative nitrations is reported, which have been achieved either using a metal catalyst or the use of harsh reaction conditions such as high temperature, highly acidic conditions or stoichiometric amounts of metal nitrates.^[11] It may be mentioned here that the nitro-olefins are a distinguished class of synthetic intermediates, which have been used in the preparation of a wide variety of biorelevant compounds and pharmaceuticals.^[12] Thus, the present metal-free decarboxylative nitration is an economical, safer and greener approach for the synthesis of nitroalkenes. The proposed mechanism for the reaction is expected to be similar to the one proposed by Prabhu

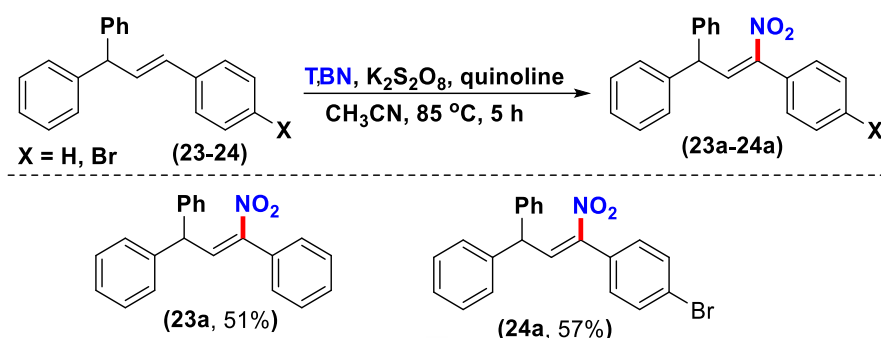
et.al. using TBN and CuCl^[9c] and Maiti *et.al.* using TEMPO and TBN^[9d] as shown in (Scheme III.3.8).

Encouraged by the above differential reactivity of *tert*-butyl nitrite (TBN) with two classes of alkenes, one leading to furoxans and the other decarboxylative nitration giving nitroalkenes, this strategy was then applied to alicyclic alkenes to see the type of product it would result. To our delight, alicyclic alkenes such as cyclohexene (**20**), cyclooctene (**21**) and cyclooctadiene (**22**) yielded nitroalkenes under an identical reaction condition affording products (**20a**, 74%), (**21a**, 76%) and (**22a**, 73%) respectively in good yields as shown in (Scheme III.3.6). Surprisingly, none of the substrates (**20-22**) gave any trace of their furoxan products. Here the reaction stops at the mono-nitration stage, however, for the furoxan synthesis generation of avicinal nitro-nitroso intermediate is essential (Scheme III.3.4). All the substrates in (Scheme III.3.2) and (Scheme III.3.3) form stable benzyl radical after initial mono nitration (Scheme III.3.4), but in alicyclic alkenes formation of such stable benzylic radical is not possible as a result none of the substrates gave furoxan as their products. Nevertheless, formation of similar nitro alkenes have been reported using TBN in the presence of TEMPO but only from terminal alkenes.^[9c] Acyclic *trans*-alkenes (γ -aryl styrenes) such as prop-2-ene-1,1,3-triyltribenzene (**23**) and 3-(4-bromophenyl)prop-2-ene-1,1-diyl)dibenzene (**24**) provided their α -nitro products (**23a**) and (**24a**) in 51% and 57% yields respectively rather than the expected β -nitro products.

Scheme III.3.6. Nitration of alicyclic alkenes^[a,b]



^[a]Reaction conditions: (**20-22**) (0.50 mmol), $K_2S_2O_8$ (0.50 mmol), quinoline (0.50 mmol), *tert*-butyl nitrite (1.0 mmol) in CH_3CN (1.5 mL) at $85\text{ }^\circ\text{C}$ for 5 h. ^[b]Isolated yields.

Scheme III.3.7. α -Nitration of γ -aryl styrenes^[a,b]

^[a]Reaction conditions: (23-25) (0.50 mmol), $\text{K}_2\text{S}_2\text{O}_8$ (0.50 mmol), quinoline (0.50 mmol), *tert*-butyl nitrite (1.0 mmol) in CH_3CN (1.5 mL) at 85°C for 5 h. ^[b]Isolated yields.

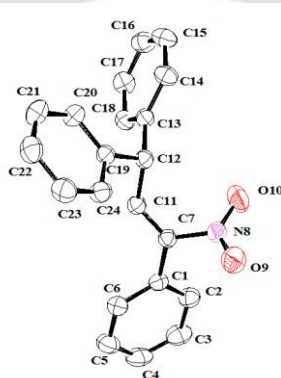
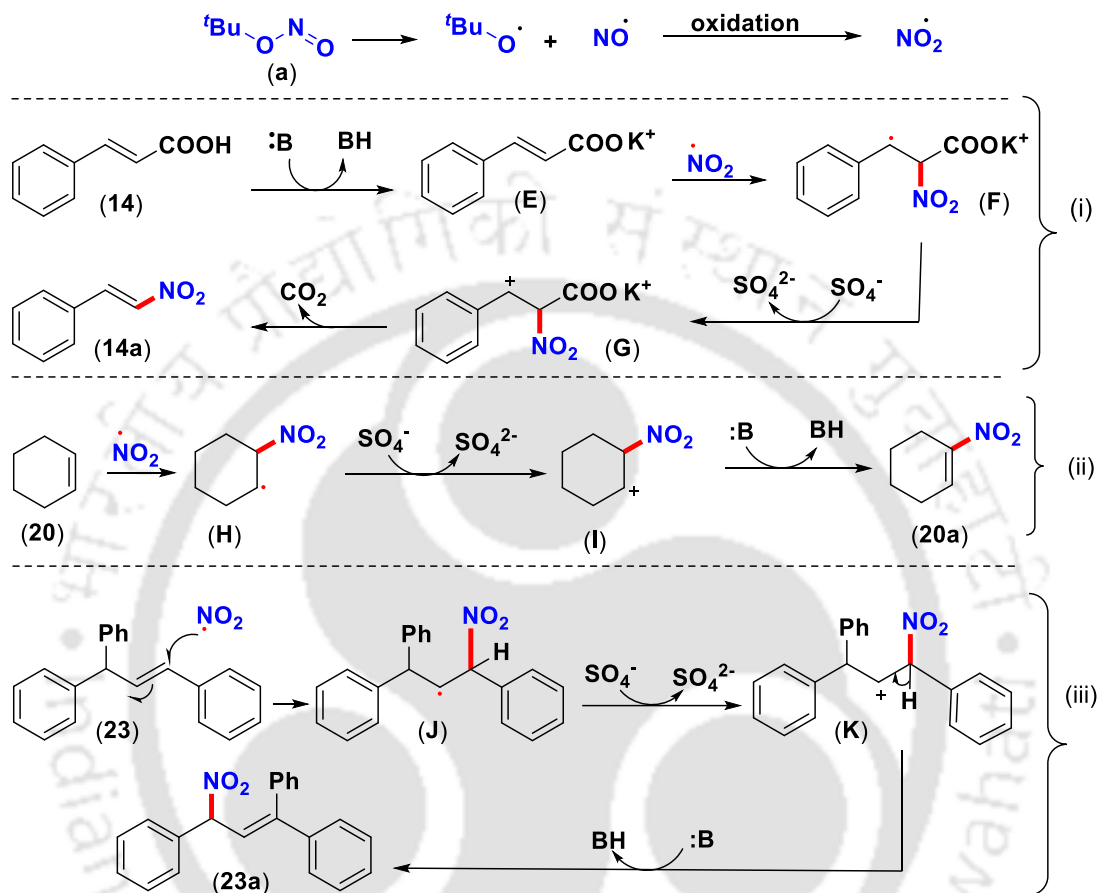


Figure III.3.5. ORTEP Molecular diagram of (23a)

The structure of the product (23a) is 3-nitro and not 2-nitro has been confirmed by X-ray crystallographic analysis (Figure III.3.5). Similarly, the structure of (24a) is ascertained by NOE experiments. Interestingly, under the present reaction condition terminal alkene *viz.* allyl cyclopentane (25) afforded the isoxazoline product (25a, 59%). This result is not surprising since we have recently reported the formation of isoxazoline from terminal alkenes using TBN, quinoline in the presence of catalyst $\text{Sc}(\text{OTf})_3$.^[9i]

To account for the formation of nitroalkenes from α,β -unsaturated carboxylic acids and alicyclic alkenes, the following mechanism has been proposed. The carboxylic acid reacts with the base and forms its potassium salt (E) [Scheme III.3.8 (i)]. The NO_2 radical generated via heterolytic cleavage of TBN and subsequent oxidation reacts with (E) to form a radical intermediate (F), the intermediate (F) undergoes oxidation to give intermediate (G), which upon decarboxylation gives (14a) [Scheme III.3.8 (i)]. An analogous mechanism has been proposed for the formation of nitroalkenes from alicyclic alkenes. The NO_2 radical reacts with alicyclic alkene (20) to form a radical intermediate (H) [Scheme III.3.8 (ii)], one-electron

oxidation of (**H**) gives rise to the carbocation intermediate (**I**). In the presence of a base, the intermediate (**I**) loses a proton to give (**20a**) [Scheme III.3.8 (ii)]. Mechanism for the formation of the unexpected 3-nitroprop-1-ene-1,1,3-triyltribenzene (**23a**) is shown in [Scheme III.3.8 (iii)].



Scheme III.3.8. Plausible mechanism for the synthesis of nitralkenes

In conclusion, we have demonstrated the differential reactivity of various alkenes with *tert*-butyl nitrite (TBN). Internal benzylic alkenes such as (*E*)-1,3-diphenyl-1-butene gave furoxan as the exclusive product in the presence of $K_2S_2O_8$, base and TBN. While α,β -unsaturated esters are inert to TBN but α,β -unsaturated acids under an identical condition undergo a rapid decarboxylation giving nitroalkenes. On the other hand, acyclic internal alkenes yielded nitro alkenes as the sole product, whereas terminal aliphatic alkenes gave isoxazolines as their product. In the furoxan formation, TBN is serving as a NO_2 cum NO synthon and as a decarboxylative nitrating agent when the substrates are α,β -unsaturated acids.

III.4. Experimental Section

III.4.1. General Information: All the reagents were commercial grade and purified according to the established procedures. Organic extracts were dried over anhydrous sodium sulphate. Solvents were removed in a rotary evaporator under reduced pressure. Silica gel (60-120 mesh size) was used for the column chromatography. Reactions were monitored by TLC on silica gel 60 F₂₅₄ (0.25mm). NMR spectra were recorded in CDCl₃ with tetramethylsilane as the internal standard for ¹H NMR (400 MHz and 600 MHz), hexafluorobenzene ¹⁹F NMR (400 MHz), CDCl₃ solvent as the internal standard for ¹³C NMR (151 MHz). HRMS spectra were recorded using ESI mode. IR spectra were recorded in KBr or neat.

III.4.2. Crystallographic Description:

Single crystal X-ray data were collected using a Rigaku Super Nova, single source offset, Eos diffractometer.¹ the structures were solved by direct methods and refined by full-matrix least-squares calculations using SHELXTL software.^{2,3} All the non-H atoms were refined in the anisotropic approximation against F² of all reflections. The H-atoms were placed at their calculated positions and refined in the isotropic approximation.

1. CrysAlispro, Oxford Diffraction Ltd., version 1, 171. 33.34d [release 27-02-2009 CrysAlis 171. NET]
2. SMART and SAINT, Siemens Analytical X-ray Instruments Inc., Madison, WI, **1996**.
3. G. M. Sheldrick, **2008**, *64*, 112-122.

CCDC Number for Compound 8a: CCDC 1812965. This data can be obtained free of charge from the Cambridge Crystallographic Data Centre via www.ccdc.cam.ac.uk/datarequest/cif.

CCDC Number for Compound 23a: CCDC 1854783. This data can be obtained free of charge from the Cambridge Crystallographic Data Centre via www.ccdc.cam.ac.uk/datarequest/cif.

Crystallographic Description of 23a: Crystal dimension (mm): 0.27 x 0.22 x 0.18 C₂₁H₁₇NO₂, Mr = 315.3720, triclinic, space group 'p -1'; a = 10.2644(3) Å, b = 10.2809(3) Å, c = 10.4984(3) Å; α = 61.091(4), β = 61.846(4), γ = 65.664(4), V = 830.42(6) Å³; Z = 2; ρ_{cal} = 1.261 g/cm³; μ (mm⁻¹) = 0.645; F(000) = 332.0; Refinement method = Full-matrix least-squares on F²; Final R indices [I > 2σ(I)] R1 = 0.0454, wR2 = 0.1223, goodness of fit = 1.036.

III.4.3. Synthesis of Furoxans and Nitrolefins

III.4.3. General Procedure for the Synthesis of 4-Phenyl-3-(1-phenylethyl)-1,2,5-oxadiazole 2-oxide (1a): To an oven-dried 25.0 mL round bottom flask fitted with a reflux condenser were added (*E*)-but-1-ene-1,3-diyl dibenzene (104 mg, 0.5 mmol), $K_2S_2O_8$ (135 mg, 0.5 mmol), quinoline (0.059 mL, 0.5 mmol), *tert*-butyl nitrite (0.119 mL, 1.0 mmol) and acetonitrile (1.5 mL). Then the reaction mixture was stirred in an oil bath at 85 °C for 5 h. After the completion of the reaction excess solvent was evacuated under reduced pressure. The reaction mixture was admixed with ethyl acetate 20.0 mL and washed with water (2.0 x 10.0 mL). The separated organic layer was dried over anhydrous sodium sulphate (Na_2SO_4), and evaporated under reduced pressure. The resulting crude product was purified by silica gel column chromatography using hexane as the eluent to give pure 4-phenyl-3-(1-phenylethyl)-1,2,5-oxadiazole 2-oxide (**1a**, 98 mg, 73% yield). The identity and purity of the product were confirmed by spectroscopic analysis.

III.4.3. General Procedure for the Synthesis of *E*-(2-Nitrovinyl)benzene (14a): To an oven-dried 25.0 mL round bottom flask fitted with a reflux condenser were added *trans*-cinnamic acid (74 mg, 0.5 mmol), $K_2S_2O_8$ (135 mg, 0.5 mmol), quinoline (0.059 mL, 0.5 mmol), *tert*-butyl nitrite (0.119 mL, 1.0 mmol) and acetonitrile (1.5 mL). Then the reaction mixture was stirred in an oil bath at 85 °C for 5 h. After the completion of the reaction excess solvent was evacuated under reduced pressure. The reaction mixture was admixed with ethyl acetate 20.0 mL washed with water (2.0 x 10.0 mL). The separated organic layer was dried over anhydrous sodium sulphate (Na_2SO_4), and evaporated under reduced pressure. The resulting crude product was purified by silica gel column chromatography using hexane as the eluent to give pure *E*-(2-nitrovinyl)benzene (**14a**, 57 mg, 77% yield). The identity and purity of the product were confirmed by spectroscopic analysis.

III.4.3. General Procedure for the Synthesis of 1-Nitrocyclohex-1-ene (20a): To an oven-dried 25.0 mL round bottom flask fitted with a reflux condenser were added cyclohexene (41 mg, 0.5 mmol), $K_2S_2O_8$ (135 mg, 0.5 mmol), quinoline (0.059 mL, 0.5 mmol), *tert*-butyl nitrite (0.119 mL, 1.0 mmol) and acetonitrile (1.5 mL). Then the reaction mixture was stirred in an oil bath at 85 °C for 5 h. After completion of the reaction excess solvent was evacuated under reduced pressure. The reaction mixture was admixed with ethyl acetate 20.0 mL and water (2.0 x 10.0 mL) and the separated organic layer was dried over anhydrous sodium sulphate

(Na₂SO₄), and evaporated under reduced pressure. The resulting crude product was purified by silica gel column chromatography using hexane as the eluent to give pure 1-nitrocyclohex-1-ene (**20a**, 47 mg, 74% yield). The identity and purity of the product were confirmed by spectroscopic analysis.

III.4.4. Mechanistic Investigation:

V.4.4 Reaction of (1) with Radical Scavenger TEMPO: To an oven-dried 25.0 mL round bottom flask fitted with a reflux condenser were added (*E*)-but-1-ene-1,3-diylidibenzene (104 mg, 0.5 mmol), K₂S₂O₈ (135 mg, 0.5 mmol), quinoline (0.059 mL, 0.5 mmol), TEMPO (0.078 g, 0.5 mmol) *tert*-butyl nitrite (0.119 mL, 1.0 mmol) and acetonitrile (1.5 mL). Then the reaction mixture was stirred in an oil bath at 85 °C for 5 h. After completion of the reaction desired product (**1a**) was isolated only in trace amount (<2%). This experiment supports the radical nature of the mechanism.

III.5. References

- [1] C. Medana, G. Ermondi, R. Fruttero, A. Di Stilo, C. Ferretti, A. Gasco, *J. Med. Chem.* **1994**, 37, 4412-4416.
- [2] a) S. Guglielmo, D. Cortese, F. Vottero, B. Rolando, V. P. Kommer, D. L. Williams, R. Fruttero, A. Gasco, *Eur. J. Med. Chem.* **2014**, 84, 135-145; b) R. A. M. Serafim, J. E. Goncalves, F. P. de Souza, A. P. de Melo Loureiro, S. Storpirtis, R. Krogh, A. D. Andricopulo, L. C. Dias, E. I. Ferreira, *Eur. J. Med. Chem.* **2014**, 82, 418-425; c) D. J. L. Santos, C. Lanaro, R. C. Chelucci, S. Gambero, P. L. Bosquesi, J. S. Reis, L. M. Lima, H. Cerecetto, M. González, F. F. Costa, M. C. Chung, *J. Med. Chem.* **2012**, 55, 7583-7592; d) P. Hernandez, M. Cabrera, M. L. Lavaggi, L. Celano, I. Tiscornia, T. R. D. Costa, L. Thomson, M. B. Fogolín, A. L. P. Miranda, L. M. Lima, E. J. Barreiro, M. González, H. Cerecetto, *Bioorganic Med. Chem.* **2012**, 20, 2158-2171; e) L. Lazzarato, C. Cena, B. Rolando, E. Marini, M. L. Lolli, S. Guglielmo, E. Guaita, G. Morini, G. Coruzzi, R. Fruttero, A. Gasco, *Bioorganic Med. Chem.* **2011**, 19, 5852-5860; f) Y. Ling, X. Ye, Z. Zhang, Y. Zhang, Y. Lai, H. Ji, S. Peng, J. Tian, *J. Med. Chem.* **2011**, 54, 3251-3259; g) M. Bertinaria, S. Guglielmo, B. Rolando, M. Giorgis, C. Aragno, R. Fruttero, A. Gasco, S. Parapini, D. Taramelli, Y. C. Martins, L. J. Carvalho, *Eur. J. Med. Chem.* **2011**, 46, 1757-1767; h) R. Fruttero, M. Crosetti, K. Chegaev, S. Guglielmo, A. Gasco, F. Berardi, M. Niso, R. Perrone, M. A. Panaro, N. A. Colabufo, *J. Med. Chem.* **2010**, 53, 5467-5475; i) G.

- Barriga, C. O. Azar, E. Norambuena, A. Castro, W. Porcal, A. Gerpe, M. Gonzalez, H. Cerecetto, *Bioorganic Med. Chem.* **2010**, *18*, 795-802; j) X. Dong, L. Du, Z. Pan, T. Liu, B. Yang, Y. Hua, *Eur. J. Med. Chem.* **2010**, *45*, 3986-3992; k) C. Cena, K. Chegaev, S. Balbo, L. Lazzarato, B. Rolando, M. Giorgis, E. Marini, R. Fruttero, A. Gasco, *Bioorganic Med. Chem.* **2008**, *16*, 5199-6006; l) L. Chen, Y. Zhang, X. Kong, E. Lan, Z. Huang, S. Peng, D. L. Kaufman, J. Tian, *J. Med. Chem.* **2008**, *51*, 4834-4838; m) W. F. Nirode, J. M. Luis, F. J. Wicker, N. M. Wachter, *Bioorganic Med. Chem. Lett.* **2006**, *16*, 2299-3001; n) M. L. Lolli, C. Cena, C. Medana, L. Lazzarato, G. Morini, G. Coruzzi, S. Manarini, R. Fruttero, A. Gasco, *J. Med. Chem.* **2001**, *44*, 3463-3468.
- [3] a) M. F. Buonsanti, M. Bertinaria, A. Di Stilo, C. Cena, R. Fruttero, A. Gasco, *J. Med. Chem.* **2007**, *50*, 5003-5011; b) I. T. Schiefer, L. Vande Vrede, M. Fa, O. Arancio, G. R. J. Thatcher, *J. Med. Chem.* **2012**, *55*, 3076-3087; c) H. Cerecetto, M. González, S. Onetto, M. Risso, A. Rey, J. Giglio, E. León, A. León, P. Pilatti, M. Fernández, *Arch. Pharm. Chem. Life Sci.* **2006**, *339*, 59-66; d) P. Tosco, M. Bertinaria, A. Di Stilo, C. Cena, G. Sorba, R. Fruttero, A. Gasco, *Bioorganic Med. Chem.* **2005**, *13*, 4750-4759; e) H. Takayama, S. Shirakawa, M. Kitajima, N. Aimi, K. Yamaguchi, Y. Hanasaki, T. Ide, K. Katsuura, M. Fujiwara, K. Ijichi, K. Konno, S. Sigeta, T. Yokota, M. Baba, *Bioorganic Med. Chem. Lett.* **1996**, *6*, 1993-1996.
- [4] a) M. Amir, A. M. Waseem, T. Sana, K. Somakala, *Int. Res. J. Pharm.* **2015**, *6*, 585-599; b) W. Tang, J. Xie, S. Xu, H. Lv, M. Lin, S. Yuan, J. Bai, Q. Hou, S. Yu, *J. Med. Chem.* **2014**, *57*, 7600-7612; c) J. Zhang, Y. Gao, F. Su, Z. Gong, Y. Zhang, *Chem. Pharm. Bull.* **2011**, *59*, 734-741; d) G. R. J. Thatcher, A. C. Nicolescu, B. M. Bennett, V. Toader, *Free Radic. Biol. Med.* **2004**, *37*, 1122-1143.
- [5] a) R. Calvino, R. Fruttero, D. Ghigo, A. Bosia, G. P. Pescarmona, A. Gasco, *J. Med. Chem.* **1992**, *35*, 3296-3300; b) R. Fruttero, D. Boschi, A. D. Stilo, A. Gasco, *J. Med. Chem.* **1995**, *38*, 4944-4949; c) C. Cena, M. L. Lolli, L. Lazzarato, E. Guaita, G. Morini, G. Coruzzi, S. P. McElroy, I. L. Megson, R. Fruttero, A. Gasco, *J. Med. Chem.* **2003**, *46*, 747-754; d) E. D. Grosso, D. Boschi, L. Lazzarato, C. Cena, A. D. Stilo, R. Fruttero, S. Moro, A. Gasco, *Chem. Biodivers.* **2005**, *2*, 886-900; e) G. Rai, A. A. Sayed, W. A. Lea, H. F. Luecke, H. Chakrapani, S. Prast-Nielsen, A. Jadhav, W. Leister, M. Shen, J. Inglese, C. P. Austin, L. Keefer, E. S. J. Arnér, A. Simeonov, D. J. Maloney, D. L. Williams, C. J. Thomas, *J. Med. Chem.* **2009**, *52*, 6474-6483; f) R. Fruttero, M. Crosetti, K. Chegaev, S. Guglielmo, A.

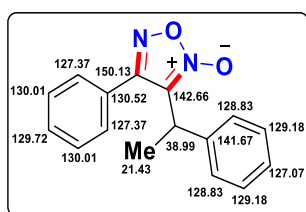
- Gasco, F. Berardi, M. Niso, R. Perrone, M. A. Panaro, N. A. Colabufo, *J. Med. Chem.* **2010**, *53*, 5467-5475.
- [6] U. Galli, L. Lazzarato, M. Bertinaria, G. Sorba, A. Gasco, S. Parapini, D. Taramelli, *Eur. J. Med. Chem.* **2005**, *40*, 1335-1340.
- [7] a) M. Curini, F. Epifano, M. C. Marcotullio, O. Rosati, R. Ballini, G. Bosica, *Tetrahedron Lett.* **2000**, *41*, 8817-8820; b) R. H. Wiley, B. J. Wakefield, *J. Org. Chem.* **1960**, *25*, 546-551; c) G. Alimenti, M. Grifantini, F. Gualteri, M. L. Stein, *Tetrahedron* **1968**, *24*, 395-402; d) R. Matsubara, Y. Saeki, J. Li, K. Eda, *Synthesis* **2013**, *45*, 1524-1528.
- [8] a) M. Feelisch, K. Schonafinger, E. Noack, *Biochem. Pharmacol.* **1992**, *44*, 1149-1157; b) M. Rueping, B. J. Nachtsheim, T. Scheidt, *Org. Lett.* **2006**, *8*, 3717-3719; c) J. Kischel, I. Jovel, K. Mertins, A. Zapf, M. Beller, *Org. Lett.* **2006**, *8*, 19-22.
- [9] a) P. Li, X. Jia, *Synthesis* **2018**, *50*, 711-722; b) S. Prateptongkum, I. Jovel, R. Jackstell, N. Vogl, C. Weckbeckerb, M. Beller, *Chem. Commun.* **2009**, 1990-1992; c) B. V. Rokade and K. R. Prabhu, *Org. Biomol. Chem.* **2013**, *11*, 6713-6716; d) S. Manna, S. Jana, T. Saboo, A. Maji, D. Maiti, *Chem. Commun.*, **2013**, *49*, 5286-5288; e) T. Taniguchi, A. Yajima, H. Ishibashi, *Adv. Synth. Catal.* **2011**, *353*, 2643-2647; f) F. Chen, N. -N. Zhou, J. L. Zhan, B. Han, W. Yu, *Org. Chem. Front.* **2017**, *4*, 135-139; g) P. Sau, A. Rakshit, T. Alam, H. K. Srivastava, B. K. Patel, *Org. Lett.* **2019**, *21*, 4966-4970; h) P. Sau, S. K. Santra, A. Rakshit, B. K. Patel, *J. Org. Chem.* **2017**, *82*, 6358-6365.
- [10] a) K. Muñiz, *Chem. Soc. Rev.* **2004**, *33*, 166-174; b) B. Kilpatrick, M. Heller, S. Arns, *Chem. Commun.* **2013**, *49*, 514-516; c) T. Taniguchi, Y. Sugiura, T. Hatta; A. Yajima, H. Ishibashi, *Chem. Commun.* **2013**, *49*, 2198-2200; d) X. F. Wu, J. Schranck, H. Neumann, M. Beller, *Chem. Commun.* **2011**, *47*, 12462-12463; e) B. Galliker, R. Kissner, T. Nauser, W. H. Koppenol, *Chem. Eur. J.* **2009**, *15*, 6161-6168.
- [11] a) J. P. Das, P. Sinha, S. A. Roy, *Org. Lett.* **2002**, *4*, 3055-3058; b) A. K. Bose, S. N. Ganguly, M. S. Manhas, W. He, and J. Speck, *Tetrahedron. Lett.* **2006**, *47*, 3213-3215; c) K. C. Rajanna, K. Ramesh, S. Ramgopal, S. Shylaja, P. G. Reddy, P. K. Saiprakash, *Green Sustainable Chem.* **2011**, *1*, 132-148; e) L. C. R. Henry, *Acad. Sci. Ser. C*, **1895**, *120*, 1265-1268; f) S. Maity, S. Manna, S. Rana, T. Naveen, A. Mallick, D. Maiti, *J. Am. Chem. Soc.* **2013**, *135*, 3355-3358; g) G. Bachman and T. Biermann, *J. Org. Chem.* **1970**, *35*, 4229-4231; h) M. S. Kumar, P. Venkanna, S. Ramgopal, K. Ramesh, M. Venkateswarlu, K. C. Rajanna, *Org. Commun.* **2012**, *5*, 42-49; i) A. Messere, A. Gentili, I. Garella, F. Temussi, B. D. Blasio, A. Fiorentino, *Synth. Commun.* **2004**, *34*, 3317-3324; j) S. Ramgopal, K. A.

Ramesh, N. Chakradhar, Reddy, Maasi and K. C. Rajanna, *Tetrahedron Lett.* **2007**, *48*, 4043-4045; k) A. S. Rao, P. V. Srinivas, K. S. Babu, J. M. Rao, *Tetrahedron Lett.* **2005**, *46*, 8141-8143; l) G. I. Nikishin, L. L. Sokova, V. D. Makhaev and N. I. Kapustina, *Russ. Chem. Bull.* **2008**, *57*, 118-123.

[12] a) A. G. M. Barrett, G. G. Graboski, *Chem. Rev.* **1986**, *86*, 751-762; b) T. A. Alston, D. J. T. Porter, H. J. Bright, *Bioorg. Chem.* **1985**, *13*, 375-403; c) P. Cheng, Z. Y. Jiang, R. R. Wang, X. M. Zhang, Q. Wang, Y. T. Zheng, J. Zhou, J. J. Chen, *Bioorganic Med. Chem. Lett.* **2007**, *17*, 4476-4480; d) H. Uehara, R. Imashiro, G. Hernández-Torres, C. F. Barbas, *Proc. Natl. Acad. Sci. U.S.A.* **2010**, *107*, 20672-20677; e) M. A. Reddy, N. Jain, D. Yada, C. Kishore, V. J. Reddy, P. S. Reddy, A. Addlagatta, S. V. Kalivendi, B. Sreedhar, *J. Med. Chem.* **2011**, *54*, 6751-6760; f) L. Q. Lu, J. R. Chen, W. J. Xiao, *Acc. Chem. Res.* **2012**, *45*, 1278-1293.

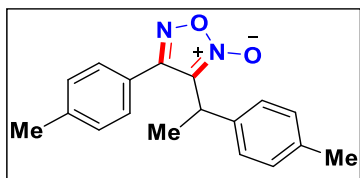
III.6. Spectral Data

4-Phenyl-3-(1-phenylethyl)-1,2,5-oxadiazole 2-oxide (1a):



Gummy, (97 mg, 73%). ^1H NMR (CDCl_3 , 400 MHz): δ 7.49–7.46 (m, 3H), 7.35–7.27 (m, 5H), 7.14 (d, 2H, $J = 8.0$ Hz), 3.50–3.45 (m, 1H), 1.44 (d, 3H, $J = 8.0$ Hz) ppm. ^{13}C NMR (CDCl_3 , 151 MHz): δ 150.13, 142.66, 141.67, 130.52, 130.01, 129.72, 129.18, 128.83, 127.37, 127.07, 38.99, 21.43 ppm. IR (KBr, cm^{-1}): 3427, 2923, 2853, 1629, 1384, 1121, 749; HRMS (ESI/Q-TOF) (m/z): calcd for $\text{C}_{16}\text{H}_{15}\text{N}_2\text{O}_2$ [$\text{M} + \text{H}$] $^+$: 267.1128, found 267.1129.

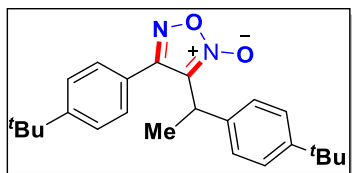
4-(*p*-Tolyl)-3-(1-(*p*-tolyl)ethyl)-1,2,5-oxadiazole 2-oxide (2a):



Yellowish gummy, (84 mg, 57%). ^1H NMR (CDCl_3 , 400 MHz): δ 7.43 (d, 1H, $J = 12.0$ Hz), 7.28 (d, 2H, $J = 8.0$ Hz), 7.18–7.12 (m, 3H), 7.04 (d, 2H, $J = 8.0$ Hz), 3.47–3.43 (m, 1H), 2.43 (s, 3H), 2.33 (s, 3H), 1.40 (d, 3H, $J = 4.0$ Hz) ppm. ^{13}C NMR (CDCl_3 , 151 MHz): δ 149.98, 141.63, 140.09, 139.72, 136.99, 130.38, 129.81, 129.51, 126.92, 126.77, 124.91, 38.65, 21.64, 21.47, 21.20 ppm. IR (KBr, cm^{-1}): 3412, 2921, 2853, 1525, 1513, 1450, 1331,

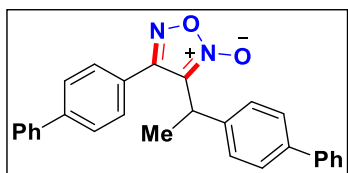
1275, 1260, 815, 764, 749; HRMS (ESI/Q-TOF) (m/z): calcd for C₁₈H₁₈N₂ KO₂ [M + K]⁺ 333.1000, found 333.1004.

4-(4-(*tert*-Butyl)phenyl)-3-(1-(4-(*tert*-butyl)phenyl)ethyl)-1,2,5-oxadiazole 2-oxide. (3a):



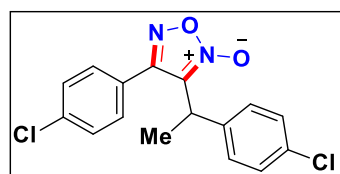
Gummy, (104 mg, 55%). ¹H NMR (CDCl₃, 600 MHz): δ 7.48 (d, 1H, *J* = 12.0 Hz), 7.43 (d, 1H, *J* = 12.0 Hz), 7.35 (d, 2H, *J* = 6.0 Hz), 7.22 (d, 2H, *J* = 6.0 Hz), 7.10 (d, 2H, *J* = 12.0 Hz) 3.51–3.48 (m, 1H), 1.42 (d, 3H, *J* = 6.0 Hz), 1.37 (s, 9H), 1.31 (s, 9H) ppm. ¹³C NMR (CDCl₃, 151 MHz): δ 153.02, 150.21, 150.02, 141.69, 139.56, 130.20, 126.74, 126.02, 125.73, 38.39, 35.04, 31.50, 31.43, 21.31 ppm. IR (KBr, cm⁻¹): 3411, 2963, 2869, 2873, 1527, 1268, 1110, 835, 742; HRMS (ESI/Q-TOF) (m/z): calcd for C₂₄H₃₁N₂O₂ [M + H]⁺: 379.2380, found 379.2386.

4-([1,1'-Biphenyl]-4-yl)-3-(1-([1,1'-biphenyl]-4-yl)ethyl)-1,2,5-oxadiazole 2-oxide (4a):



Gummy, (123 mg, 59%). ¹H NMR (CDCl₃, 600 MHz): δ 7.72 (d, 2H, *J* = 6.0 Hz), 7.65 (d, 2H, *J* = 6.0 Hz), 7.58–7.54 (m, 5H), 7.54 (s, 1H), 7.49 (t, 2H, *J* = 9.0 Hz), 7.45 (t, 2H, *J* = 9.0 Hz), 7.39 (d, 2H, *J* = 6.0 Hz), 7.35 (t, 2H, *J* = 9.0 Hz), 7.25 (s, 1H), 3.63–3.58 (m, 1H) 1.51 (d, 3H, *J* = 6.0 Hz) ppm. ¹³C NMR (CDCl₃, 151 MHz): 150.00, 142.90, 141.68, 141.65, 140.73, 140.40 140.28, 130.98, 129.12, 128.99, 128.47, 128.10, 127.92, 127.55, 127.52, 127.40, 127.22, 38.78, 21.56 ppm. IR (KBr, cm⁻¹): 3437, 2924, 2854, 1634, 1525, 1378, 1333, 1265, 1014, 737, 697; HRMS (ESI/Q-TOF) (m/z): calcd for C₂₈H₂₃N₂O₂ [M + H]⁺: 419.1754, found 419.1766.

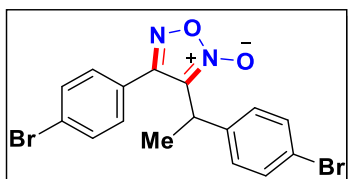
4-(4-Chlorophenyl)-3-(1-(4-chlorophenyl)ethyl)-1,2,5-oxadiazole 2-oxide (5a):



Yellowish gummy, (119 mg, 71%). ¹H NMR (CDCl₃, 600 MHz): δ 7.46 (t, 2H, *J* = 9.0 Hz), 7.30 (d, 2H, *J* = 12.0 Hz), 7.20 (d, 2H, *J* = 6.0 Hz), 7.05 (d, 2H, *J* = 6.0 Hz),

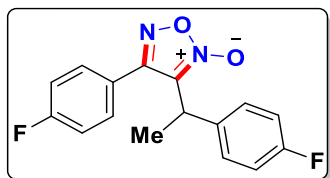
3.43–3.40 (m, 1H), 1.42 (d, 3H, $J = 6.0$ Hz) ppm. ^{13}C NMR (CDCl_3 , 151 MHz): δ 149.30, 141.46, 140.90, 136.42, 133.27, 131.81, 129.37, 129.24, 128.33, 127.87, 38.50, 21.49 ppm. IR (KBr, cm^{-1}): 3434, 2926, 1631, 1529, 1383, 1350, 1092, 828; HRMS (ESI/Q-TOF) (m/z): calcd for $\text{C}_{16}\text{H}_{13}\text{Cl}_2\text{N}_2\text{O}_2$ [$\text{M} + \text{H}$] $^+$: 335.0349, found 335.0357.

4-(4-Bromophenyl)-3-(1-(4-bromophenyl)ethyl)-1,2,5-oxadiazole 2-oxide (6a):

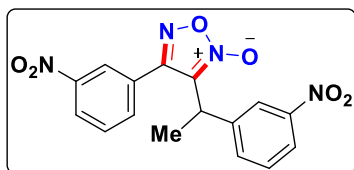


Gummy, (155 mg, 73%). ^1H NMR (CDCl_3 , 400 MHz): δ 7.62 (d, 2H, $J = 8.0$ Hz), 7.46–7.43 (m, 2H), 7.13 (d, 2H, $J = 8.0$ Hz), 7.00 (d, 2H, $J = 8.0$ Hz), 3.43–3.38 (m, 1H), 1.42 (d, 3H, $J = 8.0$ Hz) ppm. ^{13}C NMR (CDCl_3 , 151 MHz): δ 149.31, 141.40, 141.37, 132.33, 132.21, 132.02, 128.69, 128.30, 124.72, 121.32, 38.58, 21.46 ppm. IR (KBr, cm^{-1}): 3421, 2968, 2931, 2857, 1589, 1527, 1333, 1073, 1009, 825; HRMS (ESI/Q-TOF) (m/z): calcd for $\text{C}_{16}\text{H}_{13}\text{Br}_2\text{N}_2\text{O}_2$ [$\text{M} + \text{H}$] $^+$: 424.9318, found 424.9328.

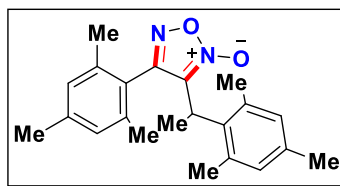
4-(4-Fluorophenyl)-3-(1-(4-fluorophenyl)ethyl)-1,2,5-oxadiazole 2-oxide (7a):



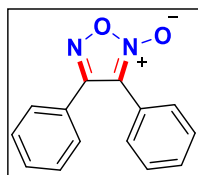
Gummy, (113 mg, 75%). ^1H NMR (CDCl_3 , 600 MHz): δ 7.45 (d, 1H, $J = 12.0$ Hz), 7.25 (d, 1H, $J = 6.0$ Hz), 7.18 (t, 2H, $J = 9.0$ Hz), 7.09–7.07 (m, 2H), 7.02 (t, 2H, $J = 9.0$ Hz), 3.45–3.42 (m, 1H), 1.43 (d, 3H, $J = 6.0$ Hz) ppm. ^{13}C NMR (CDCl_3 , 151 MHz): δ 164.48, 162.84 (d, $J = 8.4$ Hz), 161.22, 149.30, 141.70, 138.23 (d, $J = 3.2$ Hz), 132.54 (d, $J = 8.6$ Hz), 128.51 (d, $J = 8.1$ Hz), 125.56 (d, $J = 3.6$ Hz), 116.12 (dd, $J = 21.7, 8.0$ Hz), 38.38, 21.62 ppm. ^{19}F ($\text{CDCl}_3 + \text{Hexafluorobenzene}$, 400 MHz): 111.22, 116.28 ppm. IR (KBr, cm^{-1}): 3426, 2972, 2928, 1889, 1741, 1603, 1510, 1378, 1231, 1161, 839, 785; HRMS (ESI/Q-TOF) (m/z): calcd for $\text{C}_{16}\text{H}_{13}\text{F}_2\text{N}_2\text{O}_2$ [$\text{M} + \text{H}$] $^+$: 303.0940, found 303.0951.

4-(3-Nitrophenyl)-3-(1-(3-nitrophenyl)ethyl)-1,2,5-oxadiazole 2-oxide (8a):

Solid, (141 mg, 79%), m. p. 268–272 °C. ^1H NMR (CDCl_3 , 600 MHz): δ 8.41 (d, 1H, $J = 12.0$ Hz), 8.24 (s, 1H), 8.16 (d, 1H, $J = 12.0$ Hz), 8.12 (s, 1H), 7.85 (d, 1H, $J = 6.0$ Hz), 7.74 (t, 1H, $J = 6.0$ Hz), 7.65 (d, 1H, $J = 6.0$ Hz), 7.56 (t, 1H, $J = 6.0$ Hz), 4.42–4.38 (m, 1H), 1.80 (d, 3H, $J = 6.0$ Hz) ppm. ^{13}C NMR (CDCl_3 , 151 MHz): 155.08, 140.90, 134.12, 134.08, 133.59, 133.55, 130.88, 125.98, 123.43, 122.31, 116.61, 39.98, 15.95 ppm. IR (KBr, cm^{-1}): 3402, 2923, 1599, 1530, 1350, 1025, 1002, 764, 749; HRMS (ESI/Q-TOF) (m/z): calcd for $\text{C}_{16}\text{H}_{13}\text{N}_4\text{O}_6$ [$\text{M} + \text{H}$] $^+$: 357.0830, found 357.0843.

4-Mesityl-3-(1-mesitylethyl)-1,2,5-oxadiazole 2-oxide (9a):

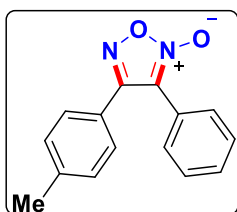
Yellowish gummy, (89 mg, 51%). ^1H NMR (CDCl_3 , 400 MHz): δ 7.97 (d, 1H, $J = 8.0$ Hz), 6.95 (s, 1H), 6.73 (s, 1H), 6.69 (s, 1H), 3.69–3.65 (m, 1H), 2.37 (s, 3H), 2.29 (s, 3H), 2.24 (s, 3H), 2.21 (s, 6H), 1.40 (d, 3H, $J = 8.0$ Hz), 1.35 (s, 3H) ppm. ^{13}C NMR (CDCl_3 , 151 MHz): δ 149.52, 143.36, 139.90, 138.95, 136.90, 136.11, 128.60, 128.42, 126.37, 33.86, 21.39, 20.82, 19.91, 18.95, 18.52 ppm. IR (KBr, cm^{-1}): 3416, 2921, 2851, 1644, 1524, 1384, 1275, 1261, 764, 749; HRMS (ESI/Q-TOF) (m/z): calcd for $\text{C}_{22}\text{H}_{25}\text{N}_2\text{NaO}_2$ [$\text{M} + \text{Na}$] $^+$: 373.1886, found 373.1896.

3,4-Diphenyl-1,2,5-oxadiazole 2-oxide (10a):

Yellowish gummy, (80 mg, 67%). ^1H NMR (CDCl_3 , 600 MHz): δ 7.98 (d, 2H, $J = 12.0$ Hz), 7.67 (t, 1H, $J = 7.6$ Hz), 7.53–7.51 (m, 4H), 7.47–7.43 (m, 3H) ppm. ^{13}C NMR (CDCl_3 , 151 MHz): δ 135.10, 131.19, 130.75, 130.10, 129.22, 129.21, 129.15, 128.88, 128.49 ppm. IR (KBr, cm^{-1}): 3423, 2923, 2852, 1672, 1593, 1578, 1506, 1449, 1422, 1211, 771, 716, 693, 643; HRMS (ESI/Q-TOF) (m/z):

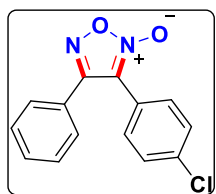
calcd for $C_{14}H_{11}N_2O_2$ $[M + H]^+$: 239.0815, found 239.0829.

3-Phenyl-4-(*p*-tolyl)-1,2,5-oxadiazole 2-oxide(11a):



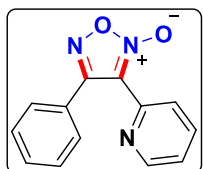
Gummy, (69 mg, 55%). 1H NMR ($CDCl_3$, 600 MHz): δ 8.08 (d, 1H, $J = 12.0$ Hz), 7.91 (d, 1H, $J = 6.0$ Hz), 7.54–7.48 (m, 4H), 7.32–7.30 (m, 2H), 7.25 (d, 1H, $J = 6.0$ Hz), 2.53 (s, 3H) ppm. ^{13}C NMR ($CDCl_3$, 151 MHz): δ 139.72, 138.51, 137.88, 137.56, 133.55, 130.44, 129.94, 129.86, 118.17, 110.91, 29.88 ppm. IR (KBr, cm^{-1}): 2925, 2854, 2231, 1636, 1524, 1341, 1263, 1091, 1016, 825, 739; HRMS (ESI/Q-TOF) (m/z): calcd for $C_{15}H_{16}N_3O_2$ $[M + NH_4]^+$: 270.1237, found 270.1250.

4-(4-Chlorophenyl)-3-phenyl-1,2,5-oxadiazole 2-oxide (12a):



Yellowish gummy, (70 mg, 51%). 1H NMR ($CDCl_3$, 600 MHz): δ 8.31 (s, 1H), 7.52(d, 1H, $J = 6.0$ Hz), 7.34–7.31 (m, 4H), 7.17 (d, 2H, $J = 12.0$ Hz), 7.02 (d, 2H, $J = 6.0$ Hz) ppm. ^{13}C NMR ($CDCl_3$, 151 MHz): δ 148.54, 136.47, 135.65, 133.66, 132.38, 132.24, 131.28, 131.24, 130.62, 129.80, 129.54, 129.26, 129.08, 129.05 ppm. IR (KBr, cm^{-1}): 2924, 1636, 1593, 1430, 1320, 1091, 832, 739; HRMS (ESI/Q-TOF) (m/z): calcd for $C_{14}H_{10}ClN_2O_2$ $[M + H]^+$: 273.0425, found 273.0438.

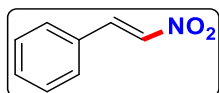
4-Phenyl-3-(pyridin-2-yl)-1,2,5-oxadiazole 2-oxide (13a):



Yellowish gummy, (90 mg, 75%). 1H NMR ($CDCl_3$, 600 MHz): δ 8.82 (d, 1H, $J = 6.0$ Hz), 8.20 (d, 1H, $J = 6.0$ Hz), 7.94 (d, 1H, $J = 12.0$ Hz), 7.88–7.85 (m, 1H), 7.82–7.79 (m, 1H), 7.58 (d, 1H, $J = 12.0$ Hz), 7.47–7.44 (m, 3H) ppm. ^{13}C NMR ($CDCl_3$, 151 MHz): δ 167.80, 162.08, 157.31, 150.16, 149.12, 136.78, 136.01, 126.00, 125.54, 125.50, 125.00, 120.79, 116.56 ppm. IR (KBr, cm^{-1}): 2923, 1672, 1612, 1585, 1460, 1295, 938, 755; HRMS

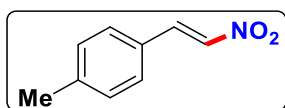
(ESI/Q-TOF) (m/z): calcd for $C_{13}H_{13}N_4O_2$ $[M + NH_4]^+$: 257.1033, found 257.1160.

(E)-(2-Nitrovinyl)benzene (14a):



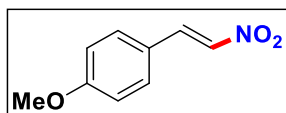
Yellow solid, (57 mg, 77%), m. p. 57–60 °C. 1H NMR ($CDCl_3$, 600 MHz): δ 8.01 (d, 1H, $J = 12.0$ Hz), 7.59 (d, 1H, $J = 12.0$ Hz), 7.56 (s, 1H), 7.54 (d, 1H, $J = 6.0$ Hz), 7.50 (d, 1H, $J = 6.0$ Hz), 7.47–7.44 (m, 2H) ppm. ^{13}C NMR ($CDCl_3$, 151 MHz): δ 139.25, 137.28, 132.31, 130.23, 129.56, 129.31 ppm. IR (KBr, cm^{-1}): 3109, 2923, 1632, 1577, 1513, 1449, 1344, 1262, 967, 764, 750; HRMS (ESI/Q-TOF) (m/z): calcd for $C_8H_7NNaO_2$ $[M + Na]^+$: 172.0369, found 172.0382.

(E)-1-Methyl-4-(2-nitrovinyl)benzene (15a):

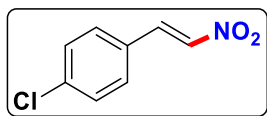


Yellow solid, (64 mg, 79%), m. p. 106–109 °C. 1H NMR ($CDCl_3$, 600 MHz): δ 7.98 (d, 1H, $J = 12.0$ Hz), 7.57 (d, 1H, $J = 18.0$ Hz), 7.44 (d, 2H, $J = 12.0$ Hz), 7.25 (d, 2H, $J = 6.0$ Hz), 2.41 (s, 3H) ppm. ^{13}C NMR ($CDCl_3$, 151 MHz): δ 143.29, 139.37, 136.40, 132.31, 130.30, 129.36, 127.39, 21.84 ppm. IR (KBr, cm^{-1}): 3109, 2923, 2853, 1632, 1496, 1341, 1265, 965, 810, 741; HRMS (ESI/Q-TOF) (m/z): calcd for $C_9H_{10}NO_2$ $[M + H]^+$: 164.0706, found 164.0712.

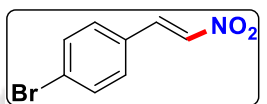
(E)-1-Methoxy-4-(2-nitrovinyl)benzene (16a):



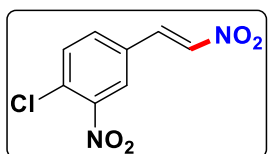
Yellow solid, (73 mg, 81%), m. p. 85–88 °C. 1H NMR ($CDCl_3$, 600 MHz): δ 7.96 (d, 1H, $J = 12.0$ Hz), 7.52–7.49 (m, 3H), 6.95 (d, 2H, $J = 12.0$ Hz), 3.86 (s, 3H); ^{13}C NMR ($CDCl_3$, 151 MHz): δ 163.07, 139.22, 135.11, 131.33, 122.63, 115.04, 55.68; IR (KBr, cm^{-1}): 2925, 1605, 1498, 1339, 1256, 1176, 1031, 973, 809; HRMS (ESI/Q-TOF) (m/z): calcd for $C_9H_{10}NO_3$ $[M + H]^+$: 180.0655, found 180.0669.

(E)-1-Chloro-4-(2-nitrovinyl)benzene (17a):

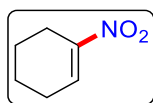
Yellow solid, (78 mg, 85%), m. p. 102–105 °C. ^1H NMR (CDCl_3 , 600 MHz): δ 7.96 (d, 1H, $J = 12.0$ Hz), 7.56 (d, 1H, $J = 18.0$ Hz), 7.49 (d, 2H, $J = 12.0$ Hz), 7.43 (d, 2H, $J = 12.0$ Hz) ppm. ^{13}C NMR (CDCl_3 , 151 MHz): δ 138.49, 137.89, 137.55, 130.44, 129.92, 128.65 ppm. IR (KBr, cm^{-1}): 3107, 2924, 2852, 1721, 1642, 1601, 1529, 1344, 1201, 1048, 965, 832, 753, 677; HRMS (ESI/Q-TOF) (m/z): calcd for $\text{C}_8\text{H}_6\text{ClNNaO}_2$ [$\text{M} + \text{Na}$] $^+$: 205.9979, found 205.9991.

(E)-1-Bromo-4-(2-nitrovinyl)benzene (18a):

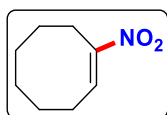
Yellow solid, (95 mg, 83%), m. p. 151–154 °C. ^1H NMR (CDCl_3 , 600 MHz): δ 7.97 (dd, 1H, $J_1 = 12.0$ Hz, $J_2 = 6.0$ Hz), 7.62–7.59 (m, 3H), 7.58–7.42 (m, 2H) ppm. ^{13}C NMR (CDCl_3 , 151 MHz): δ 137.98, 137.59, 132.89, 130.56, 129.07, 126.95 ppm. IR (KBr, cm^{-1}): 2923, 2849, 1633, 1517, 1341, 1073, 812; HRMS (ESI/Q-TOF) (m/z): calcd for $\text{C}_8\text{H}_6\text{BrNNaO}_2$ [$\text{M} + \text{Na}$] $^+$: 249.9474, found 249.9478.

(E)-1-Chloro-2-nitro-4-(2-nitrovinyl)benzene (19a):

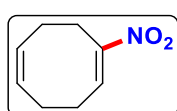
Yellow solid, (87 mg, 76%), m. p. 131–135 °C. ^1H NMR (CDCl_3 , $\text{DMSO}-d_6$, 600 MHz): δ 8.33 (d, 1H, $J = 6.0$ Hz), 8.06–8.00 (m, 2H), 7.91–7.89 (m, 1H), 7.71–7.68 (m, 1H) ppm. ^{13}C NMR (CDCl_3 , 151 MHz): δ 138.49, 137.89, 137.55, 130.44, 129.92, 130.00, 128.65 ppm. IR (KBr, cm^{-1}): 3103, 3039, 2924, 2852, 1734, 1633, 1591, 1518, 1404, 1339, 1259, 1086, 970, 819, 742; HRMS (ESI/Q-TOF) (m/z): calcd for $\text{C}_8\text{H}_5\text{ClN}_2\text{KO}_2$ [$\text{M} + \text{K}$] $^+$: 266.9569, found 266.9579.

1-Nitrocyclohex-1-ene (20a):

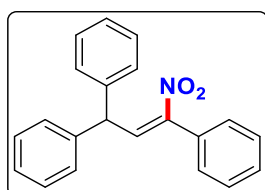
Yellow gummy, (47 mg, 74%). ^1H NMR (CDCl_3 , 600 MHz): δ 7.32–7.30 (m, 1H), 2.58–2.55 (m, 2H), 2.34–2.31 (m, 2H), 1.79–1.75 (m, 2H), 1.65–1.61 (m, 2H) ppm. ^{13}C NMR (CDCl_3 , 151 MHz): δ 149.89, 134.47, 24.96, 24.08, 21.96, 20.84 ppm. IR (KBr, cm^{-1}): 3434, 2927, 2857, 1636, 1517, 1337, 927, 696; HRMS (ESI/Q-TOF) (m/z): calcd for $\text{C}_6\text{H}_{10}\text{NO}_2$ [$\text{M} + \text{H}$] $^+$: 128.0706, found 128.0714.

1-Nitrocyclooct-1-ene (21a):

Brownish gummy, (59 mg, 76%). ^1H NMR (CDCl_3 , 600 MHz): δ 7.30 (t, 1H, $J = 9.0$ Hz), 2.75–2.73 (m, 2H), 2.34–2.31 (m, 4H), 1.74–1.69 (m, 4H), 1.51–1.50 (m, 2H) ppm. ^{13}C NMR (CDCl_3 , 151 MHz): δ 152.43, 136.46, 29.19, 28.44, 26.81, 26.56, 25.81, 24.96 ppm. IR (KBr, cm^{-1}): 3417, 2929, 2856, 1518, 1447, 1330, 821, 1746; HRMS (ESI/Q-TOF) (m/z): calcd for $\text{C}_8\text{H}_{14}\text{NO}_2$ [$\text{M} + \text{H}$] $^+$: 156.1019, found 156.1031.

1-Nitrocycloocta-1,5-diene (22a):

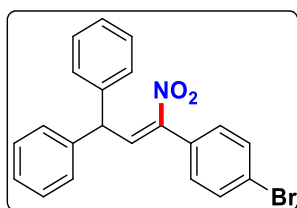
Reddish gummy, (56 mg, 73%). ^1H NMR (CDCl_3 , 600 MHz): δ 7.36 (t, 1H, $J = 12.0$ Hz), 5.59–5.55 (m, 2H), 3.03 (t, 2H, $J = 12.0$ Hz), 2.62–2.57 (m, 2H), 2.54–2.46 (m, 4H) ppm. ^{13}C NMR (CDCl_3 , 151 MHz): δ 135.39, 128.85, 127.85, 27.27, 26.89, 26.52, 25.86 ppm. IR (KBr, cm^{-1}): 3421, 2921, 2851, 2873, 1633, 1519, 1384, 1331, 1260, 1093, 1021, 799; HRMS (ESI/Q-TOF) (m/z): calcd for $\text{C}_8\text{H}_{12}\text{NO}_2$ [$\text{M} + \text{H}$] $^+$: 164.0863, found 164.0857.

(E)-(2-Nitroprop-2-ene-1,1,3-triyl)tribenzene (23a):

Light yellow solid, (80 mg, 51%), m. p. 118–123 °C. ^1H NMR (CDCl_3 , 600 MHz): δ 7.39 (bs, 6H), 7.34 (t, 3H, $J = 9.0$ Hz), 7.27 (t, 2H, $J = 6.0$ Hz), 7.23 (d, 4H, $J = 6.0$ Hz), 6.47 (d, 1H, $J = 12.0$ Hz), 5.14 (d, 1H, $J = 12.0$ Hz) ppm.

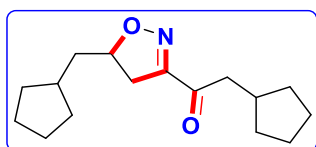
^{13}C NMR (CDCl_3 , 151 MHz): δ 151.73, 141.50, 131.20, 130.11, 129.08, 129.05, 128.99, 128.40, 128.34, 127.38, 127.02, 49.29 ppm. IR (KBr, cm^{-1}): 3438, 2925, 1741, 1526, 1491, 1448, 1265, 1027, 696; HRMS (ESI/Q-TOF) (m/z): calcd for $\text{C}_{21}\text{H}_{18}\text{NO}_2$ $[\text{M} + \text{H}]^+$: 316.1332, found 316.1352.

(3-(4-Bromophenyl)-3-nitroprop-1-ene-1,1-diyl)dibenzene (24a):



Brown solid, (112 mg, 57%), m. p. 152–157 °C. ^1H NMR (CDCl_3 , 600 MHz): δ 7.53(d, 2H, $J = 12.0$ Hz), 7.35(t, 4H, $J = 6.0$ Hz), 7.29 (d, 2H, $J = 6.0$ Hz), 7.26 (d, 2H, $J = 12.0$ Hz), 7.22(d, 4H, $J = 12.0$ Hz), 6.48 (d, 1H, $J = 6.0$ Hz), 5.16 (d, 1H, $J = 12.0$ Hz) ppm. ^{13}C NMR (CDCl_3 , 151 MHz): δ 150.67, 141.25, 132.29, 130.22, 129.44, 129.11, 128.38, 128.29, 127.49, 124.49, 49.33 ppm. IR (KBr, cm^{-1}): 3128, 1523, 1400, 1071, 829, 751, 701; HRMS (ESI/Q-TOF) (m/z): calcd for $\text{C}_{21}\text{H}_{17}\text{BrNO}_2$ $[\text{M} + \text{H}]^+$: 394.0437, found 394.0452.

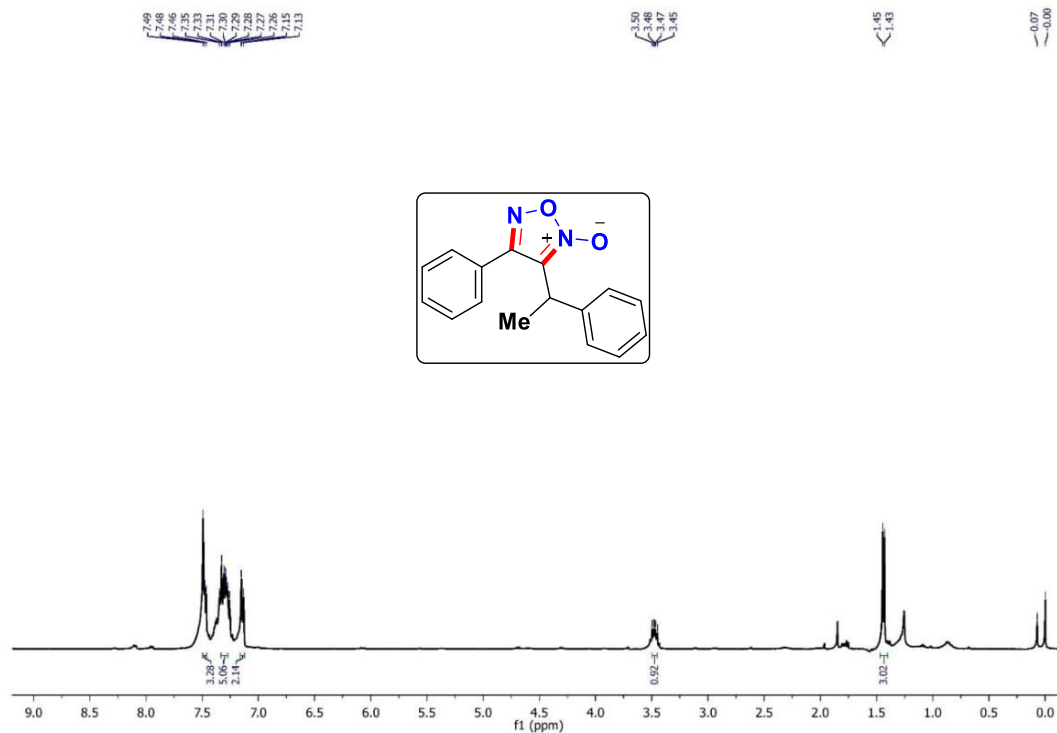
2-Cyclopentyl-1-(5-(cyclopentylmethyl)-4,5-dihydroisoxazol-3-yl)ethan-1-one (25a):



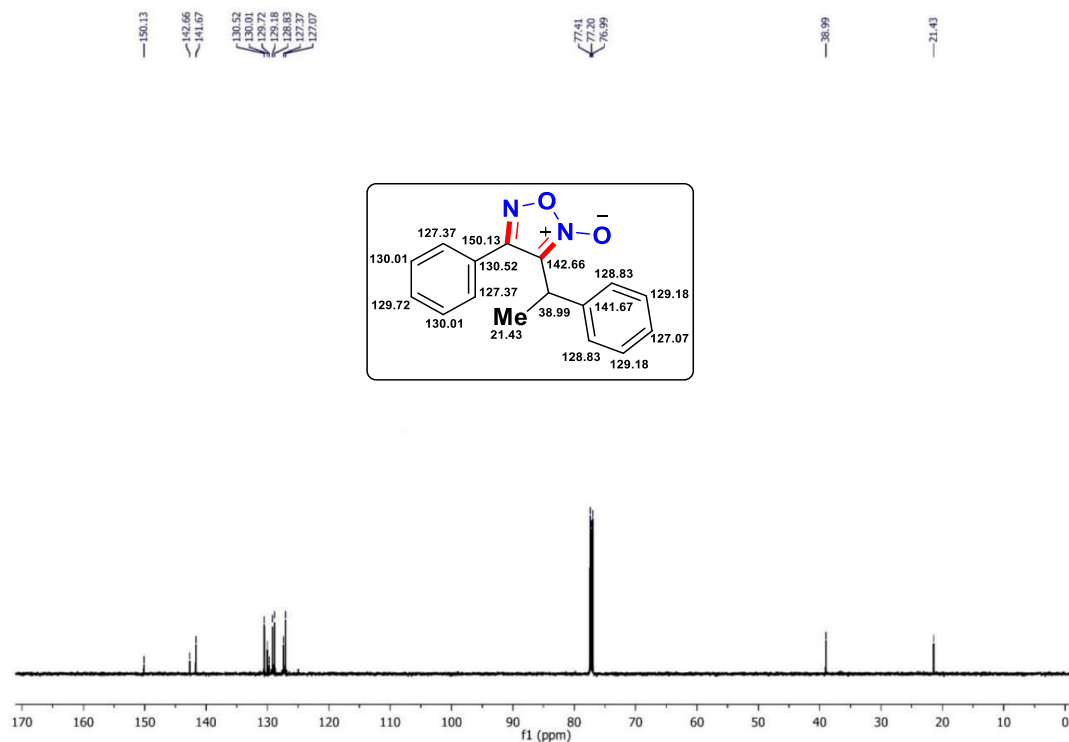
Gummy, (78 mg, 59%). ^1H NMR (CDCl_3 , 600 MHz): δ 4.80–4.75 (m, 1H), 3.17 (dd, 1H, $J = 18.0$ Hz, 12.0 Hz), 2.90 (d, 2H, $J = 6.0$ Hz), 2.75 (dd, 1H, $J = 18.0$, 6.0 Hz), 2.32–2.28 (m, 1H), 1.94–1.87 (m, 1H), 1.85–1.80 (m, 4H), 1.64–1.62 (m, 3H), 1.57–1.53 (m, 7H), 1.16–1.13 (m, 4H) ppm. ^{13}C NMR (CDCl_3 , 151 MHz): δ 196.21, 158.27, 84.34, 45.35, 41.58, 37.58, 37.02, 36.10, 32.96, 32.84, 32.72, 32.70, 25.15, 25.09 ppm. IR (KBr, cm^{-1}): 3416, 2952, 2867, 1685, 1629, 1572, 1384, 1201, 933, 764, 750; HRMS (ESI/Q-TOF) (m/z): calcd for $\text{C}_{16}\text{H}_{26}\text{NO}_2$ $[\text{M} + \text{H}]^+$: 264.1958, found 264.1970.

III.7. Spectra

4-Phenyl-3-(1-phenylethyl)-1,2,5-oxadiazole 2-oxide (1a): ^1H NMR (CDCl_3 , 400 MHz)



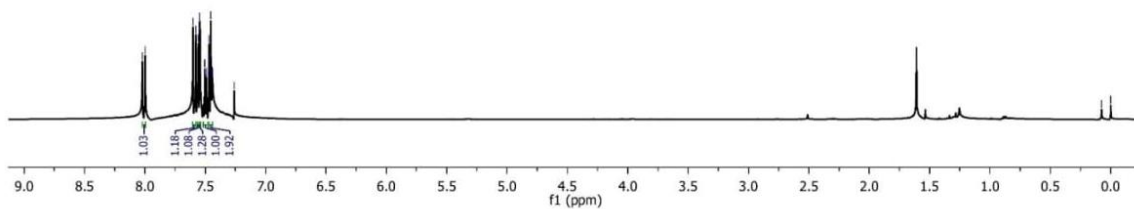
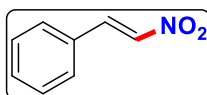
4-Phenyl-3-(1-phenylethyl)-1,2,5-oxadiazole 2-oxide (1a): ^{13}C NMR (CDCl_3 , 151 MHz)



(E)-(2-Nitrovinyl)benzene (14a): ^1H NMR (CDCl_3 , 600 MHz)

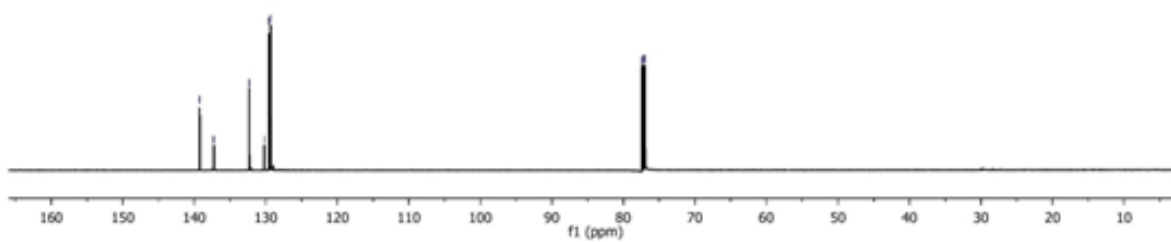
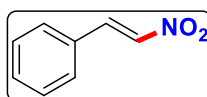
8.02
8.00
7.98
7.56
7.55
7.54
7.49
7.48
7.46
7.45
7.44
7.26

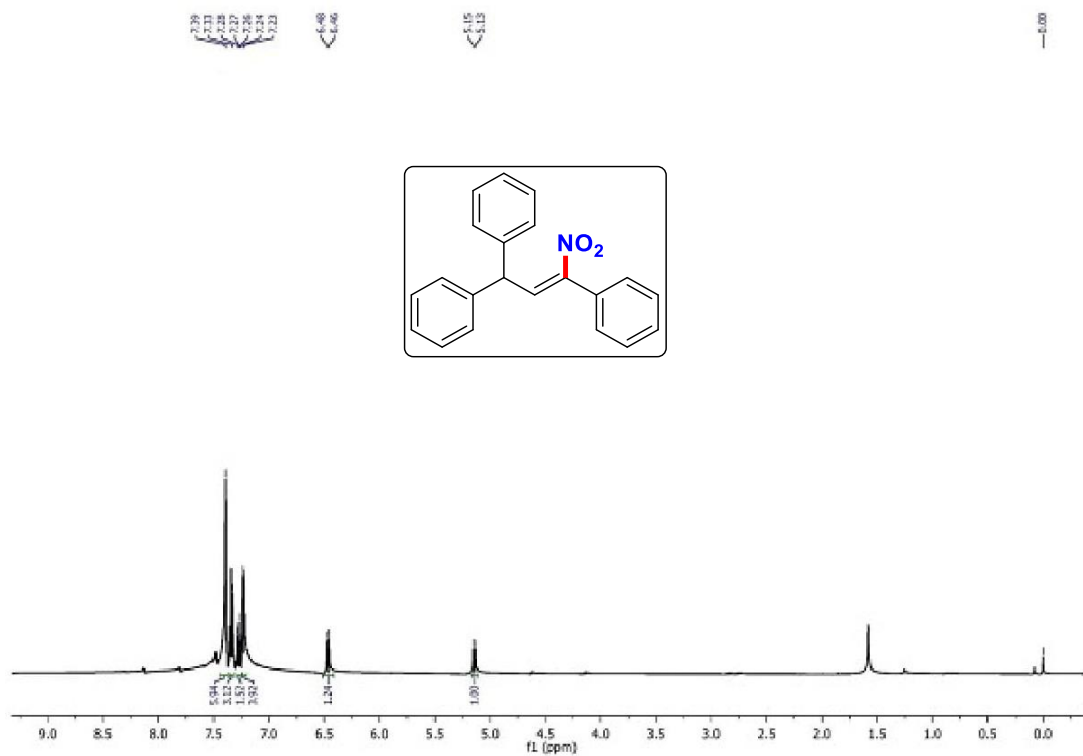
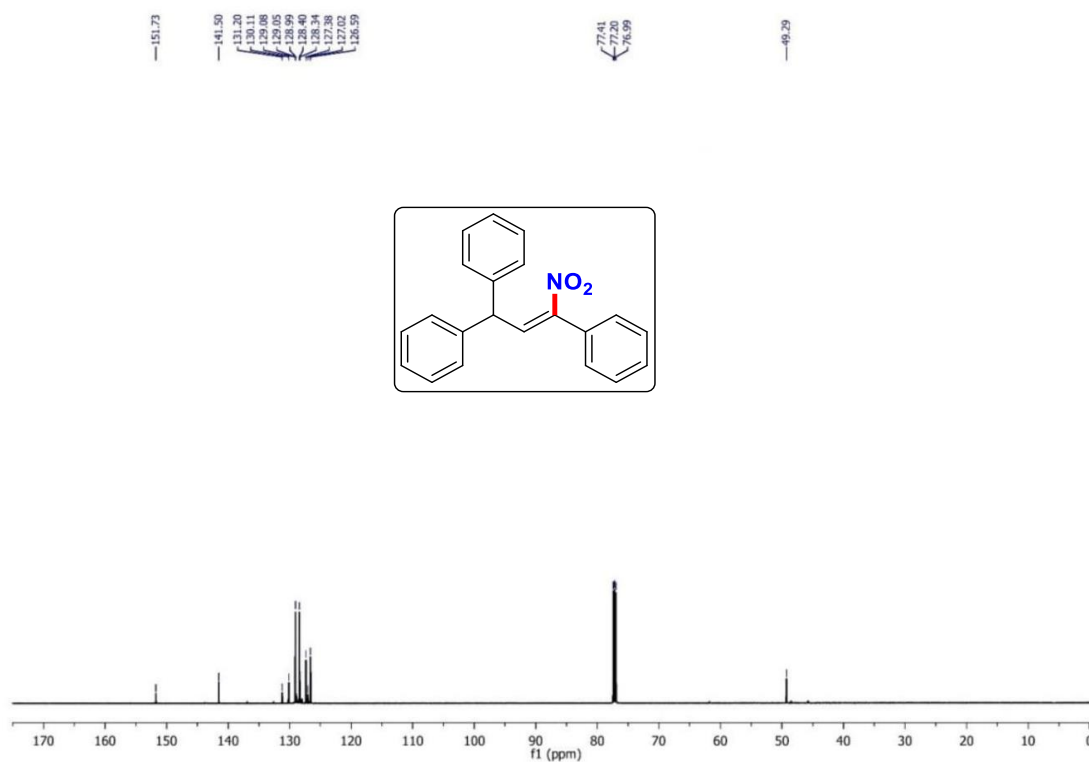
0.07
0.00

**(E)-(2-Nitrovinyl)benzene (14a): ^{13}C NMR (CDCl_3 , 151 MHz)**

138.25
137.28
132.31
130.23
128.56
128.31

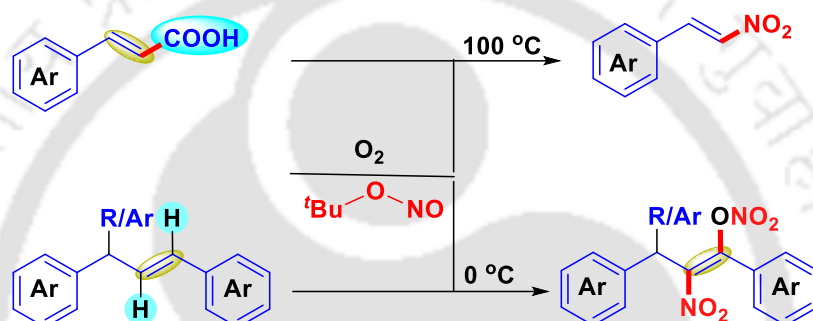
77.41
77.20
76.99



(2-Nitroprop-2-ene-1,1,3-triyl)tribenzene (23a): ^1H NMR (CDCl_3 , 600 MHz)**(2-Nitroprop-2-ene-1,1,3-triyl)tribenzene (23a): ^{13}C NMR (CDCl_3 , 151 MHz)**

CHAPTER IV

tert-Butyl Nitrite Mediated Nitro-Nitratosation of Internal Alkenes



ABSTRACT: In an oxygen atmosphere tert-butyl nitrite (TBN) reacts with unsymmetrical internal benzylic alkenes giving nitro-nitratosation product exclusively. The γ -diaryl substituted styrenes provided better yields compared to γ -alkyl-aryl substituted styrenes. The higher yields for the former type of substrates is possible dictated by the additional stability of benzylic radical due to the anchimeric assistance imparted by the γ -substituted phenyl ring. During oxidative nitration, the nitro (NO₂) group adds at the non-benzylic site, whereas the nitrato group (ONO₂) is attached at the relatively stable benzylic position. Under an identical reaction condition, α,β -unsaturated carboxylic acids, afforded nitroalkenes as the sole product.

CHAPTER IV

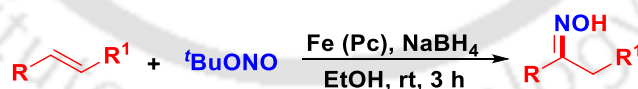
IV. *tert*-Butyl Nitrite Mediated Nitro-Nitratation of Internal Alkenes

IV.1. Introduction

The metal-free reagent, *tert*-butyl nitrite (TBN) is emerging as a multi-tasking reagent in various synthetic applications because of its easy availability, easy handling, low cost, and stability.^[1] Thermolysis of TBN provides NO and ^tBuO radicals. The former can directly participate in a reaction, whereas both these radicals can initiate several reactions. Due to the intrinsic ability of TBN to activate molecular oxygen it captures dioxygen generating a NO₂ radical, which prompts nitration and many other oxidation processes. Interestingly, the NO radical is a good acceptor of transient radicals thus serving as an efficient radical trapper and source of N and N-O synthons.^[1]

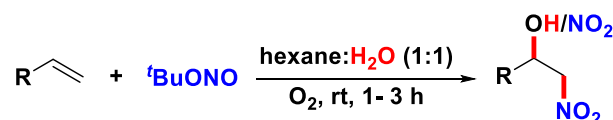
IV.2. Strategies for *tert*-Butyl Nitrite (TBN) Mediated Functionalizations of Alkenes

tert-Butyl nitrite reacts differently with alkenes depending upon the presence of other additives present in the reaction system. Therefore, it has been widely employed for different types of alkene functionalizations. In this context, Beller group reported Fe(II)-catalyzed synthesis of oximes from vinylarenes. This synthesis was accomplished in the presence of *tert*-butyl nitrite and NaBH₄ to access different oxime analogues in moderate to good yields (Scheme IV.2.1).^[2]



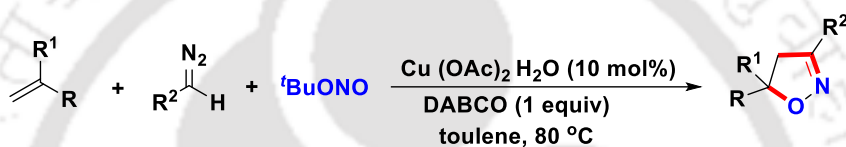
Scheme IV.2.1. TBN-mediated oximation of alkenes

Taniguchi *et al.* reported the synthesis of β -nitro alcohols along with nitrated products by treating vinylarenes with TBN. This synthesis was achieved under the oxygen atmosphere, where β -nitro alcohols were obtained as the main product and oxidative nitration product as a minor one (Scheme IV.2.2).^[3]



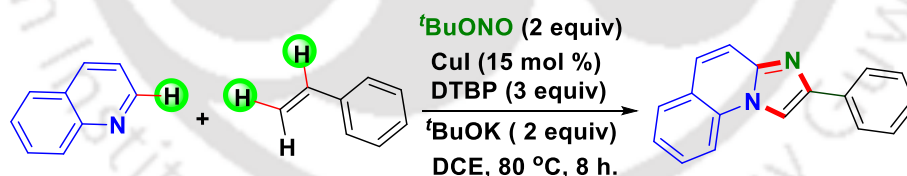
Scheme IV.2.2. TBN-mediated oxidative nitration of alkenes

Wan group developed a Cu (II)-catalyzed synthesis of isoxazolines. These isoxazolines were constructed in the presence of TBN as a NO-synthon, DABCO as base and diazoacetate as a carbene progenitor. In this process, styrene serves as a dienophile and undergo [3+2] cycloaddition with nitrile oxide intermediate to furnish the desired isoxazolines (Scheme IV.2.3).^[4] Following the analogous [3+2] cycloaddition strategy our group obtained symmetrical isoxazolines from styrenes in the presence of TBN as NO, NO₂-synthon, Sc(OTf)₃ as a catalyst and quinoline as a base.^[5]



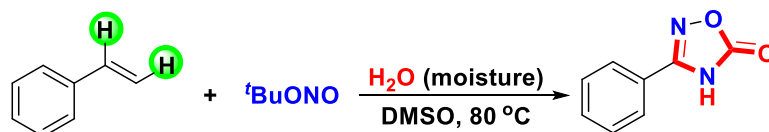
Scheme IV.2.3. TBN-mediated oximation of alkenes

Later on, our group reported a Cu-catalyzed imidazo[1,2-*a*]quinolines synthesis. In this process, quinoline takes part along with styrene and TBN providing imidazo[1,2-*a*]quinolones via a three-component process. Here, TBN serves the dual role of an N1 synthon as well as an oxidant (Scheme IV.2.4).^[6]



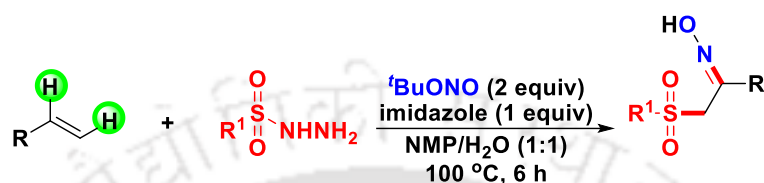
Scheme IV.2.4. TBN-mediated di-functionalization of alkenes

Recently our group reported *tert*-butyl nitrite mediated synthesis of 1,2,4-oxadiazole-5(4*H*)-ones from terminal alkenes. In this biradical pathway, TBN serves as a source of NO and N whereas H₂O serves as carbonyl oxygen source (Scheme IV.2.5).^[7]



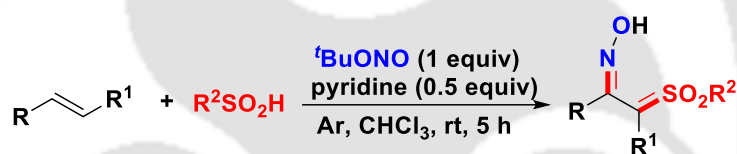
Scheme IV.2.5. TBN-mediated 1,2,4-oxadiazole-5(4*H*)-ones synthesis involving *sp*² carbon

A base-mediated bi-functionalization of alkenes for the synthesis of α -sulfonylethanone oximes was developed in water by Wang and co-workers. In this process, sulfonyl hydrazide as sulfonyl radical and TBN as the NO source adds across styrene double bond to give a bi-functionalized product α -sulfonylethanone oximes, which is mediated by a base (Scheme IV.2.6).^[8] Similarly, α -sulfonylethanone oxime is obtained from styrene, where TOsMIC acts as the sulfonyl source and TBN as the NO source as well as an oxidant.^[9]



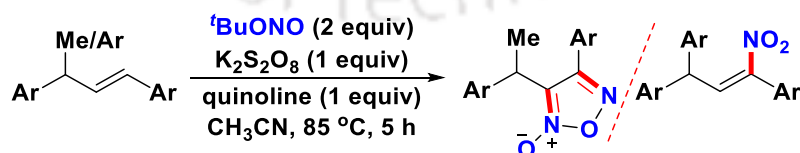
Scheme IV.2.6. TBN-mediated α -sulfonylethanone oxime synthesis involving sp^2 carbon

A vicinal sulfoximation of alkenes was achieved by Yu and co-workers by using sulfinic acid as the sulfonating agent and TBN as the NO source as well as an oxidant to access a variety of α -sulfonyl ketoximes (Scheme IV.2.7).^[10]



Scheme IV.2.7. TBN-mediated sulfoximation involving sp^2 carbon

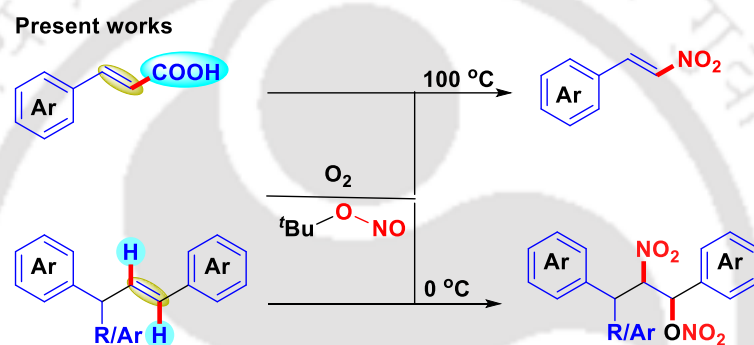
From the above literature reports, it is evident that TBN reacts with styrenes in many ways depending on the reaction conditions and other additives present. On the other hand, internal benzylic and non-benzylic alkenes also react differently with TBN. An interesting synthesis of furoxan is accomplished from benzylic internal alkene using TBN, quinoline and $K_2S_2O_8$ (Scheme IV.2.8). Under a similar condition α,β -unsaturated carboxylic acids and cyclic internal alkene afforded nitroalkenes (Scheme IV.2.8).^[11]



Scheme IV.2.8. TBN-mediated functionalizations of internal alkenes

During the formation of isoxazoline,^[4,5] imidazo[1,2-*a*]quinolines,^[6] and 1,2,4-oxadiazole-5(4*H*)-ones^[7] from styrenes and TBN, the *in situ* generated NO_2 radical attacks at the β -carbon while the NO radical attacks at the α -carbon even though both the radicals co-

exist in the medium. From the computational calculation, it was found that the attack of NO_2 radical at the terminal carbon that is at the β -carbon is stabilised by around 6 kcal/mole than the attack by NO radical at the same site.^[7] During the furoxan formation from internal alkenes *viz.* (*E*)-1,3-diphenyl-1-butenes, the NO_2 radical again attacks at the β -carbon while the NO radical at the benzylic position (i.e α -carbon) leading to the formation of furoxan (Scheme IV.2.8).^[11] However, in an analogous internal alkene *viz.* prop-2-ene-1,1,3-triyltriaryl system gave exclusively a mono nitro product where the nitro group is at the benzylic position (α -carbon) (Scheme IV.2.8). Surprisingly, compared to all other previous results^[5-7] this is an unusual attacking position for the nitro group as it always prefers to attack at the β -position (Scheme IV.2.1,2,5,8).^[2, 7, 11]



Scheme IV.2.8. Nitro-nitratosation of internal alkenes

IV.3. Present Work

Inspired by these developments on *tert*-butyl nitrite-mediated functionalizations particularly formation of β -nitro alcohols and their nitrate derivatives, where the exclusive attack of the NO_2 group is at the terminal carbon of the styrene (Scheme IV.2.2),^[3] we anticipated that instead of a terminal if an internal alkene such as γ -diaryl substituted or γ -alkyl-aryl-substituted styrene is treated with TBN under an oxygen atmosphere will they react similarly or behave differently giving different products? Further, if mono-nitration takes place will it be at the α or the β -position of the internal benzylic alkenes? Therefore, we were curious to investigate the reaction of various internal alkenes with TBN in an oxygen atmosphere (Scheme IV.2.8).

Optimization of Reaction Conditions. To implement the above-envisaged strategy, our initial investigation started by reacting γ -diaryl substituted internal alkene (**1**) with *tert*-butyl nitrite (**a**). Initially, alkene (**1**) was treated with *tert*-butyl nitrite (**a**) (2 equiv) in chlorobenzene (2.0 mL) at room temperature for 24 h in an air atmosphere. A new product (**1a**) was isolated in

39% yield after column chromatographic separation (entry 1, Table IV.3.1). Spectroscopic (IR, ^1H and ^{13}C NMR) analysis of the product (**1a**) revealed the disappearance of both alkene protons at 6.60 ppm and 6.40 ppm. However, the appearance of two doublets one at 5.87 ppm and another at 4.88 ppm along with a multiplet at 5.69 ppm suggests that the PhCH(Ph)- part is intact thereby confirming di-functionalization across the double bond of (**1**). Further, HRMS analysis of the product indicates the loss of two protons and the addition of NO_2 and ONO_2 groups. Eventually, the exact structure of the product was confirmed by X-ray crystallographic analysis of one of its derivative (**10a**) as shown in Figure IV.3.1. Fascinated by the formation

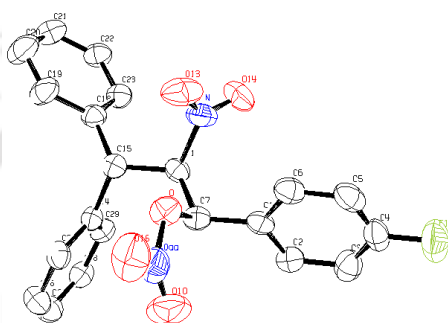
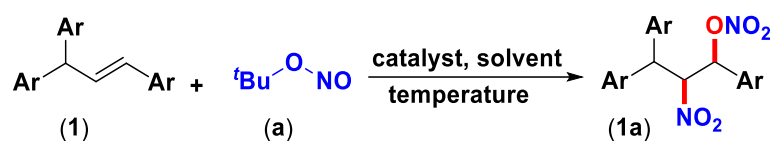


Figure IV.3.1. ORTEP molecular diagram of (**10a**)

of this oxidative nitration product (**1a**), this reaction was further screened by varying various other solvents. Among the solvents screened such as CH_3CN , DCE, DMSO, DMF, MeOH and THF (entries 2-6, Table IV.3.1) the polar aprotic solvent CH_3CN (entry 2, Table IV.3.1) was found to give the best yield of (**1a**) in 48% under otherwise identical condition. Gratifyingly, when the same reaction was performed in an oxygen atmosphere, the product (**1a**) was obtained in an improved yield of 65% (entry 7, Table IV.3.1). To see if the use of a metal catalyst can help improve the yield, various metal catalysts such as $\text{Cu}(\text{OAc})_2$, CuCl_2 , $\text{Cu}(\text{acac})_2$, CuO , Cu_2O , FeCl_3 were employed but none provided any improved yield of the product (**1a**) compared to the uncatalyzed reaction (entries 8-14, Table IV.3.1). Interestingly, when the reaction was performed at $0\text{ }^\circ\text{C}$ under otherwise identical reaction conditions provided the desired product (**1a**) in an improved yield of 74% (entry 15, Table IV.3.1). On the other hand, when the reaction was performed at $50\text{ }^\circ\text{C}$, the yield of (**1a**) dropped drastically to 11%, possibly due to competitive side reactions among various radicals (entry 16, Table IV.3.1).

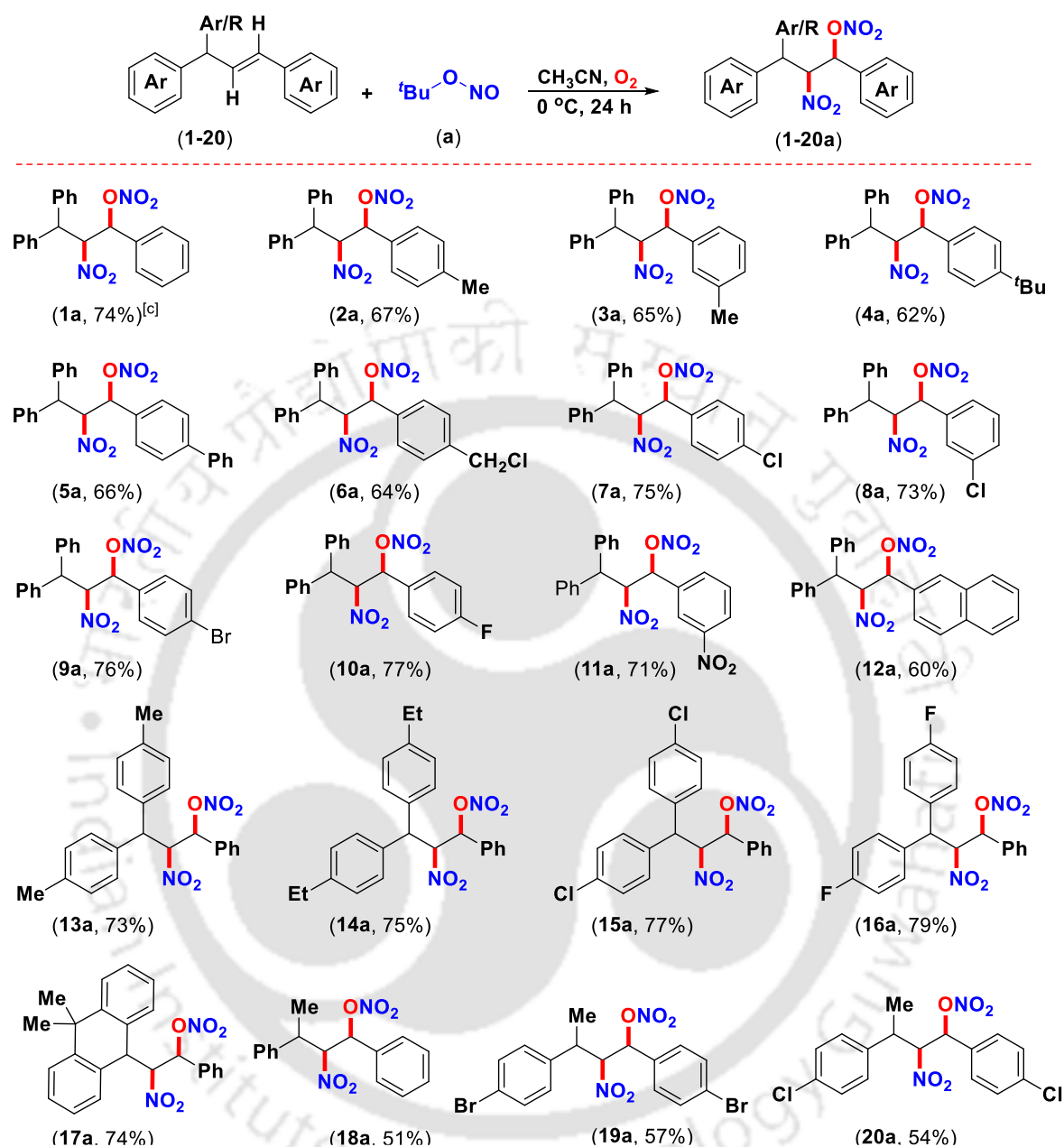
Table IV.3.1. Screening of reaction conditions^[a-c]

Entry	Catalyst (10 mol %)	Solvent (mL)	Temperature (°C)	Yield (%) ^[b]
1		PhCl	rt	39
2		CH ₃ CN	rt	48
3		DCE	rt	23
4		DMSO	rt	38
5		DMF	rt	14
6		MeOH	rt	18
7		CH ₃ CN	rt	65 ^[c]
8	Cu(OAc) ₂	CH ₃ CN	rt	27 ^[c]
9	CuCl ₂	CH ₃ CN	rt	23 ^[c]
10	Cu(acac) ₂	CH ₃ CN	rt	24 ^[c]
11	CuO	CH ₃ CN	rt	22 ^[c]
12	Cu(OTf) ₂	CH ₃ CN	rt	45 ^[c]
13	Cu ₂ O	CH ₃ CN	rt	34 ^[c]
14	FeCl ₃	CH ₃ CN	rt	11 ^[c]
15		CH₃CN	0	74^[c]
16		CH ₃ CN	50	11 ^[c]

^[a]Reaction conditions: **1** (0.5 mmol), *tert*-butyl nitrite (1.0 mmol) solvent (2.0 mL). ^[b]Yield after 24 h. ^[c]In the presence of O₂ (balloon).

After a series of screening experiments, it was found that this *bis*-functionalization is best achieved using alkene (**1**) (0.5 mmol), TBN (2 equiv) at 0 °C for 24 h. After establishing the optimized reaction condition for this oxidative nitration as shown in (Table IV.3.1), we explored the reaction of various (*E*)-prop-2-ene-1,1,3-triyltribenzenes (**1-20**) with TBN (**a**). This reaction proceeds well with a variety of internal alkenes (**1-20**) bearing electron-donating as well as electron-withdrawing groups in their phenyl ring attached directly to the double bond. Phenyl rings of these internal benzylic alkenes possessing moderately electron-donating groups such as *p*-Me (**2**), *m*-Me (**3**), *p*-^{*t*}Bu (**4**), *p*-Ph (**5**), *p*-CH₂Cl (**6**) gave their corresponding oxidative nitration products (**2a**, 67%), (**3a**, 65%), (**4a**, 62%), (**5a**, 66%), (**6a**, 64%) in moderate yields (Scheme IV.3.1). Internal benzylic alkenes bearing moderately electron-withdrawing groups such as *p*-Cl (**7**), *m*-Cl (**8**), *p*-Br (**9**) and *p*-F (**10**) in their phenyl rings, provided their corresponding products (**7a**, 75%), (**8a**, 73%), (**9a**, 76%) and (**10**, 77%), in good yields as shown in (Scheme IV.3.1). Alkene possessing strongly electron-withdrawing group such as *m*-NO₂ (**11**) also underwent oxidative nitration and provided the corresponding product (**11a**) in good yield (71%). As can be seen from the pattern in the yield obtained, phenyl ring possessing

moderately electron-withdrawing groups provided better yields than substrates having electron-donating groups. This yield trend is not pronounced for a substrate having strongly electron-withdrawing groups such as nitro suggesting some additional factors may be responsible for it. Alkene having a polycyclic ring such as 2-naphthyl (**12**) at the double also delivered the desired oxidative nitration product (**12a**) in moderate yield (Scheme IV.3.1). In addition to simple phenyl rings at the γ -position (**1-12**) substituted phenyl rings (**13-16**) all reacted efficiently. γ -Phenyl rings having electron-donating *p*-Me (**13**), *p*-Et (**14**) as well as electron-withdrawing *p*-Cl (**15**), *p*-F (**16**) all reacted successfully and provided their corresponding oxidative nitration products (**13a**, 73%), (**14a**, 75%) and (**15a**, 77%), (**16a**, 79%) in good yield (Scheme IV.3.1). An alkene (**17**) where both the γ -phenyl rings are locked through the $C(CH_3)_2$ unit also reacted successfully and provided the expected product (**17a**) in a good yield of (74%). As can be seen from Scheme IV.3.1, γ -diaryl substituted styrene (**1**) provided the better yield of the product compared to γ -alkyl-aryl-substituted styrene (**18**) even though the benzylic radical formed is away. The higher yield of the product (**1a**) obtained for the substrate (**1**) may be due to additional stability of the benzylic radical imparted by the γ -phenyl ring through anchimeric assistance. However, such over assistance is missing for substrate (**18**).

Scheme IV.3.1. Substrate scope for nitro-nitratosation^[a-c]

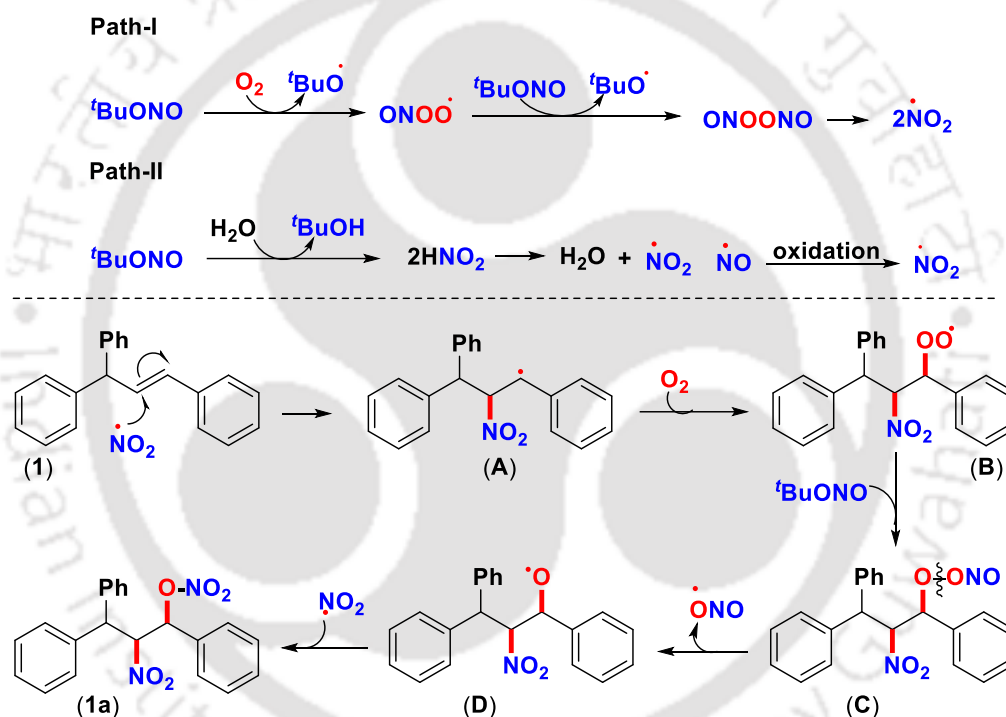
^[a]Reaction conditions: 1–20 (0.50 mmol), *tert*-butyl nitrite (1.0 mmol) in CH_3CN (2.0 mL) at $0\text{ }^\circ\text{C}$ for 24 h.

^[b]Isolated yields. ^[c]Gram scale yield (64%).

To check whether the reaction is proceeding *via* a radical path, alkene (1) was reacted with *tert*-butyl nitrite (a) in the presence of an equimolar quantity of radical scavenger (2,2,6,6-tetramethylpiperidin-1-yl)oxidanyl (TEMPO). Formation of (<8%) of the product (1a), suggests a possible radical pathway. To ascertain, whether molecular oxygen is involved in the product formation or not, a reaction was performed under an atmosphere of nitrogen keeping

all other parameters identical. The nitrogen atmosphere reaction provided the desired product (**1a**) in <5%, thereby suggesting the involvement of molecular oxygen in the product formation.

Taking cues from the above reactions and based on the literature reports,^[12] a plausible mechanism has been proposed for this nitro-nitrosation. Initially, *tert*-butyl nitrite reacts with molecular oxygen to generate NO₂ radical *via* peroxyxynitrite radical (ONOO[•]) intermediate (Scheme IV.3.2, path-I).^[12] Alternatively, the nitro radical can also be obtained by the reaction of TBN with water generating HNO₂, decomposition of which would give NO₂ radical (Scheme IV.3.2, path-II).^[3,12d-f] The NO₂ radical so generated then attacks at the non-benzylic carbon of the internal alkene (**1**) to form a nitroalkane benzyl radical intermediate (**A**) (Scheme IV.3.2). The benzylic radical intermediate (**A**) then reacts with the molecular O₂ to generate a



Scheme IV.3.2. A plausible mechanism for nitro-nitrosation

peroxy-radical intermediate (**B**). The intermediate (**B**) reacts further with TBN (**a**) to give intermediate (**C**) via the transfer of NO radical. The O–O bond cleavage of intermediate (**C**) generates an oxy-radical intermediate (**D**) via the loss of a NO₂ radical (Scheme IV.3.2). The intermediate (**D**) reacts with NO₂ radical where the electron is localized at the N-atom to give the product (**1a**) (Scheme IV.3.2). This proposed mechanism is well supported by DFT calculations as shown in Figure IV.3.2.

Based on experimental results, we have considered a credible mechanistic design which has been studied using density functional theory (DFT) to verify our findings. This plausible

mechanistic approach is depicted in Figure IV.3.2. All DFT calculations have been accomplished using 6-31+G(d,p) basis set for the atoms present in the system at M06^[13a] level

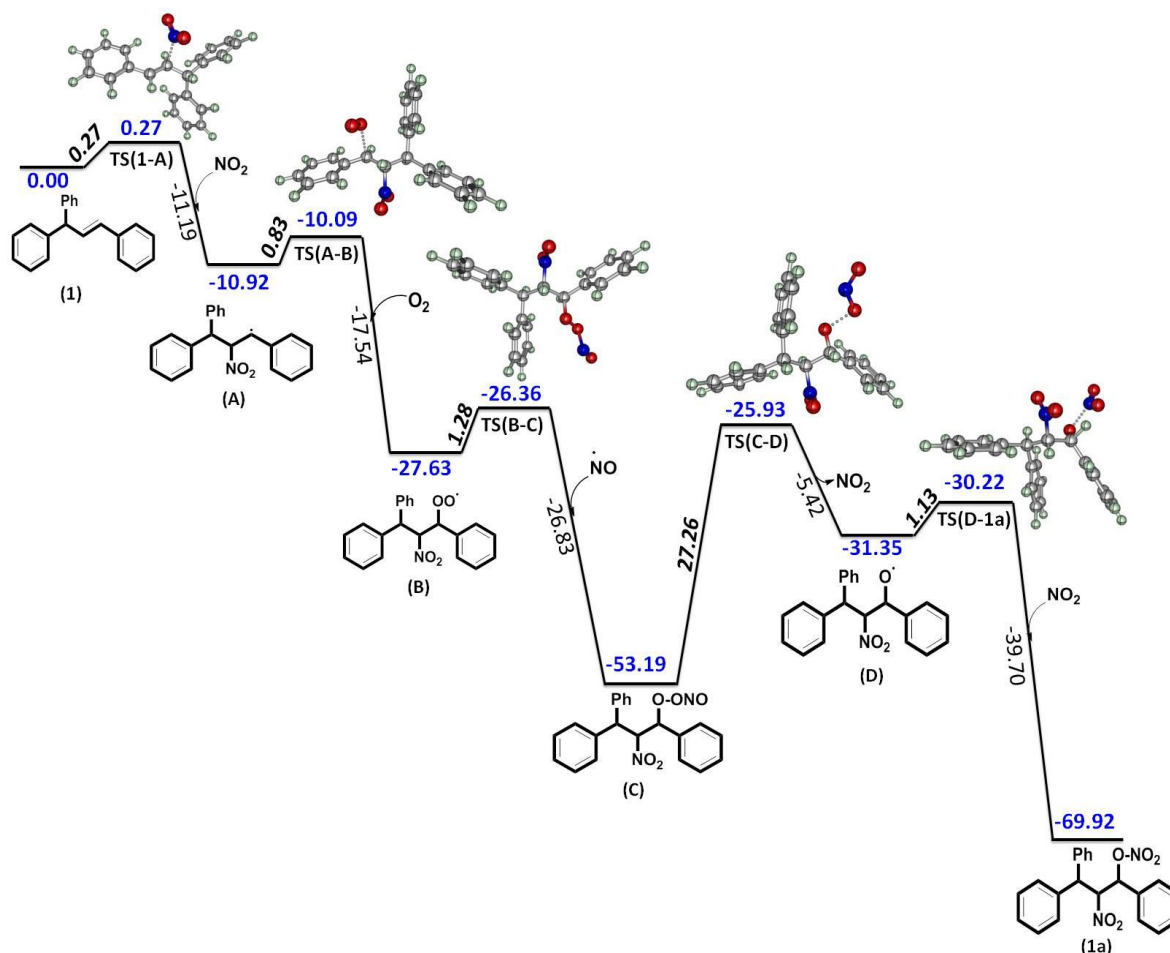


Figure IV.3.2. Calculated energy profile diagram for the nitro-nitratosation reaction. The relative energies from DFT calculations are in kcal mol⁻¹ at M06/6-31g+(d,p) level of theory. The relative energies are shown in blue colour, activation barrier in *italic bold* and stabilization energy in *normal font* are given in kcal mol⁻¹.

of theory. GAUSSIAN 09 program package has been utilized to perform the calculation.^[13b,c] Frequency calculations have been done on all modelled structures with the same level of theory. The reaction coordinates of all the species involved {i.e. reactants, intermediates, transition states (TSs) and products} along with the energy values are shown in Figure IV.3.3. The optimized geometries of the various structures involved in the reaction, as well as selected bond lengths, are also shown in Figure IV.3.3. The reaction starts with the attack of NO₂ radical at

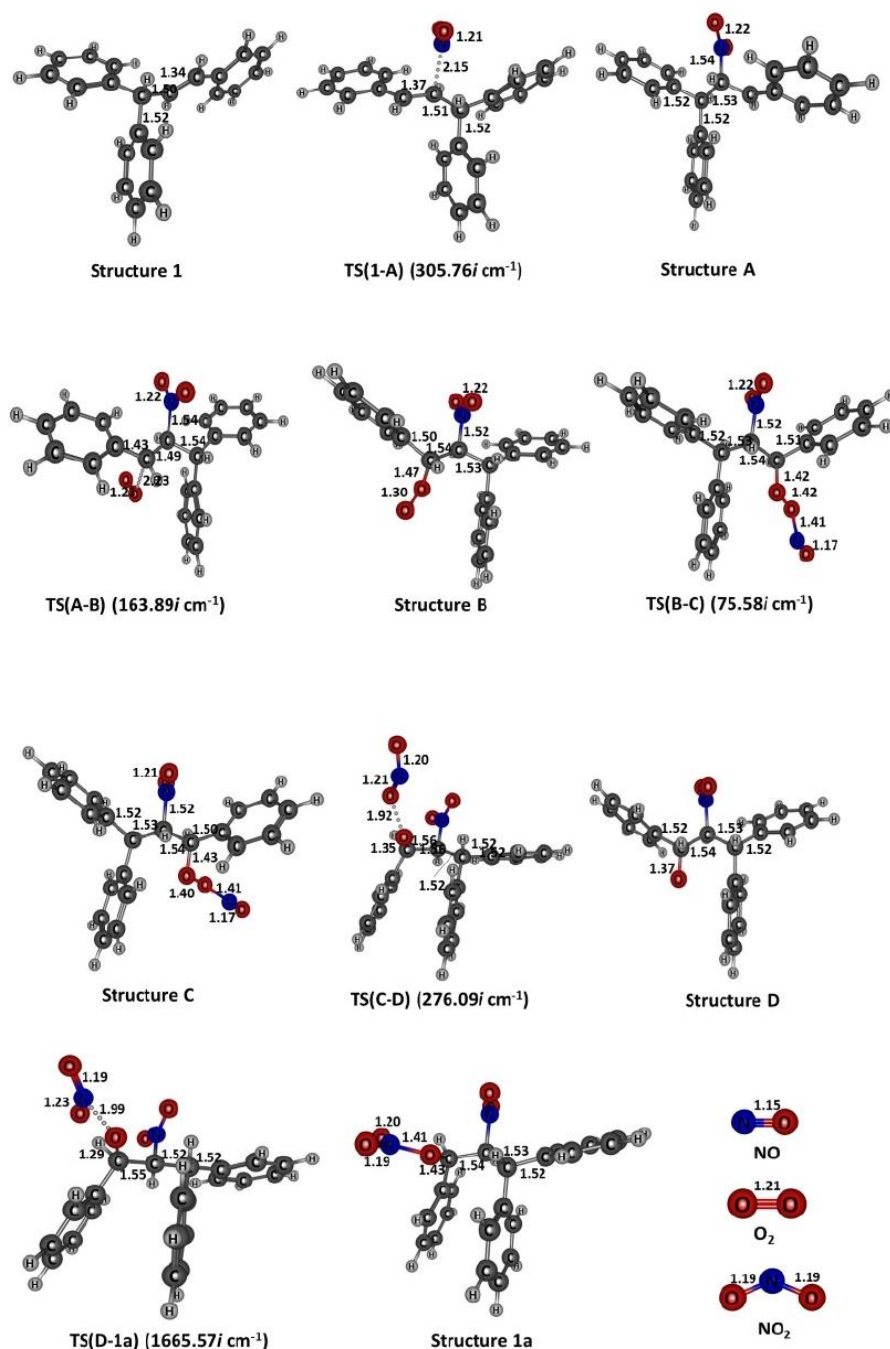
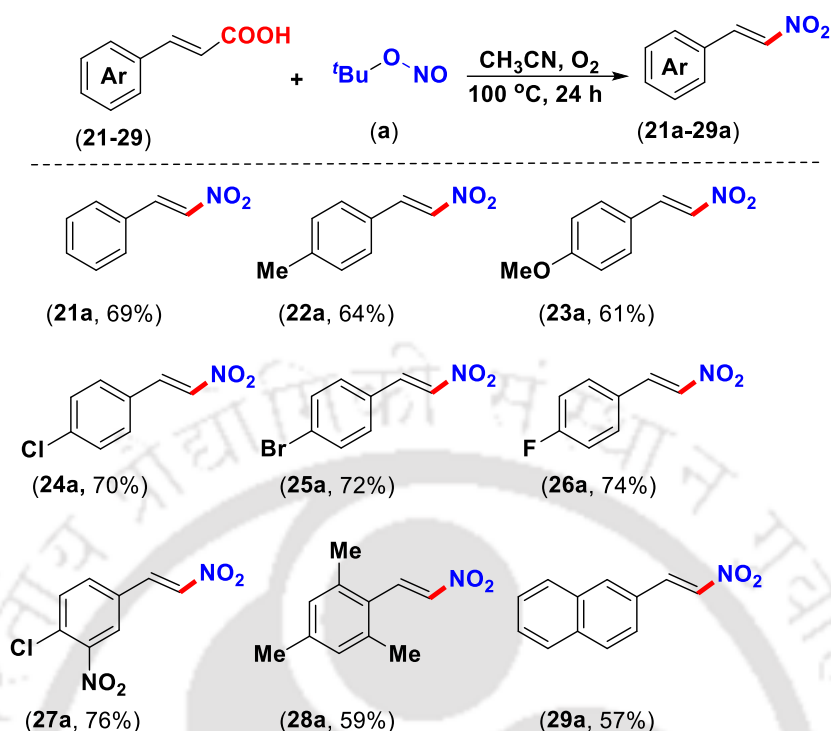


Figure IV.3.3. Optimized geometries of all species involved in the reaction along with selected bond lengths (in Å) at M06/6-31+G(d,p) level of theory

the internal C=C thereby generating another free radical (**A**) at the benzylic position; which is stabilized by releasing energy of 11.19 kcal mol⁻¹ and formed by crossing a barrier height of 0.27 kcal mol⁻¹. The intermediate benzylic radical attack molecular oxygen forming a peroxy radical intermediate (**B**) involving a barrier of 0.83 kcal mol⁻¹ and releasing 17.54 kcal mol⁻¹ of energy. At this stage, the NO radical generated from TBN attacks the intermediate (**B**) forming

an intermediate (**C**) in which the transition state is associated with a barrier of 1.28 kcal mol⁻¹ and releases energy of 26.83 kcal mol⁻¹. The radical intermediate (**D**) readily gets attached to the *N*-site of the NO₂ radical and the process is stabilized by releasing 39.70 kcal.mol⁻¹ of energy and formed by crossing height of 1.13 kcal mol⁻¹. In the case of intermediate (**C**), the NO₂ is linked to the O-atom of the benzylic position with O-site of NO₂; whereas, in the final product (**1a**) the NO₂ group is attached through its *N*-site. Further, from the energy profile diagram, we could see that the final product (**1a**) is energetically more favourable as compared to intermediate (**C**) by 38.57 kcal mol⁻¹ of energy. The overall reaction is found to be exothermic in nature. Thus, the theoretical findings are in good agreement with the proposed mechanism.

Further, to check whether this nitro-nitratosation strategy applies to other internal alkenes such as α,β -unsaturated acids or not? *trans*-cinnamic acid (**21**) was reacted with TBN (**a**) at 100 °C otherwise under identical reaction conditions. The reaction proceeded well and provided a new product (**21a**) (Scheme IV.3.3). Spectroscopic (IR, ¹H and ¹³C NMR) analysis of the isolated product (**21a**) showed the absence of the COOH group. The HRMS analysis of the new product revealed the loss of a COOH group and incorporation of a NO₂ group. The reaction of the corresponding ester (ethyl cinnamate) with TBN did not yield any trace of the nitroalkene nor any oxidative nitration product. Thus the *tert*-butyl nitrite (**a**) is serving as a decarboxylative nitrating agent. Before this report, there are reports on decarboxylative nitration of *trans*-cinnamic acid using HNO₃^[14a-c] *t*BuONO in combination with CuCl,^[14d] TEMPO,^[14e] and K₂S₂O₈.^[11] These decarboxylations have been achieved either by using a metal catalyst or the use of harsh reaction conditions such as high temperature, highly acidic conditions stoichiometric amounts of metal nitrates or stoichiometric amounts of additives.^[14] Compared to all the methods reported our present method is the mildest as it is achieved in the absence of any other additives.

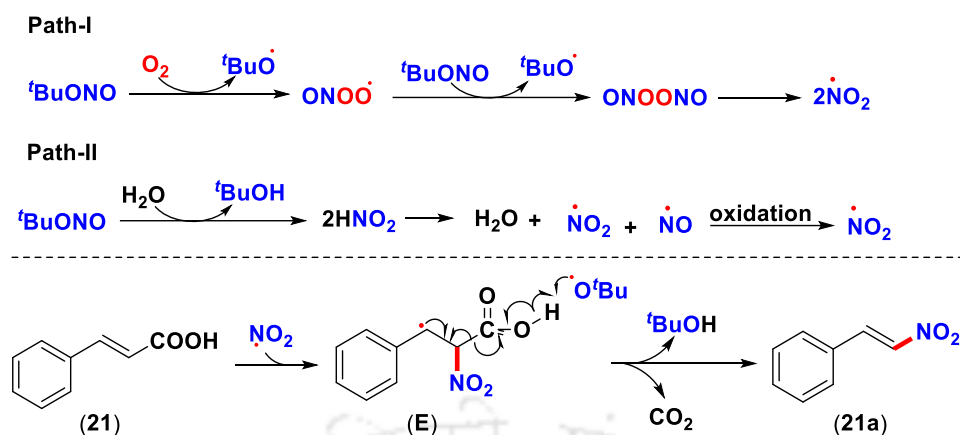
Scheme IV.3.3. Nitration of α,β -unsaturated carboxylic acids^[a-b]


^[a]Reaction conditions: **21–29** (0.50 mmol), *tert*-butyl nitrite (1.0 mmol) in CH_3CN (2.0 mL) at $100\text{ }^\circ\text{C}$ for 24 h.

^[b]Isolated yields.

To explore the generality of this strategy, the reaction of *trans*-cinnamic acid having moderately electron-donating such as *p*-Me (**22**) and strongly electron-donating group such as *p*-OMe (**23**) both provided their corresponding products (**22a**, 64%), (**23a**, 61%), in moderate yields. The moderately electron-withdrawing groups such as *p*-Cl (**24**), *p*-Br (**25**), *p*-F (**26**) and strongly electron-withdrawing such as *p*-Cl-*m*-NO₂ (**27**) cinnamic acids all reacted successfully and delivered their corresponding nitroalkenes (**24a**, 70%), (**25a**, 72%), (**26a**, 74%), (**27a**, 76%), in good yields. This strategy is equally successful even for a sterically crowded (**28**), and multinuclear (**29**) alkene carboxylic acids both provided their corresponding products (**28a**, 59%) and (**29a**, 57%) in moderate yields (Scheme IV.3.3).

To account for the formation of nitroalkenes from α,β -unsaturated carboxylic acids, the following mechanism has been proposed which is similar to previously proposed one. The *trans*-cinnamic acid reacts with *t*BuO radical and forms a nitro benzylic intermediate (**E**), which upon decarboxylation gives nitroalkene (**21a**) ((Scheme IV.3.4)).^[14e]



Scheme IV.3.4. A plausible mechanism for decarboxylative nitration

In conclusion, we have demonstrated the differential reactivity of TBN with internal benzylic alkenes in an oxygen atmosphere, which provided nitro-nitrosation products. This result is in contrast to the furoxan formation for the same substrate with TBN but in the presence of $\text{K}_2\text{S}_2\text{O}_8$. The γ -diaryl substituted styrenes provided better yields compared to γ -alkyl-aryl-substituted styrenes possible due to anchimeric assistance imparted by the γ -phenyl ring. While α,β -unsaturated esters are inert to TBN, α,β -unsaturated acids provided corresponding nitroalkenes via decarboxylation. Even though other radical species co-exist in the medium the nitro radical attacks exclusively at the β -carbon in internal benzylic alkenes. A plausible mechanism has been proposed which is supported by DFT calculation.

IV.4. Experimental Section

IV.4.1. General Information: All the reagents were commercial grade and purified according to the established procedures. Organic extracts were dried over anhydrous sodium sulphate. Solvents were removed in a rotary evaporator under reduced pressure. Silica gel (100-200 mesh size) was used for the column chromatography. Reactions were monitored by TLC on silica gel 60 F₂₅₄ (0.25 mm). NMR spectra were recorded in CDCl_3 with tetramethylsilane as the internal standard for ^1H NMR (400 and 600 MHz) and in for ^{13}C NMR (101 and 151 MHz) CDCl_3 as the internal standard. HRMS spectra were recorded using +ESI (TOF) mode. IR spectra were recorded in KBr or neat.

IV.4.2. Crystallographic Description:

Single crystal X-ray data were collected using a Rigaku Super Nova, single-source offset, Eos diffractometer.¹ the structures were solved by direct methods and refined by full-matrix least-squares calculations using SHELXTL software.^{2,3} All the non-H atoms were refined in the anisotropic approximation against F^2 of all reflections. The H-atoms were placed at their calculated positions and refined in the isotropic approximation.

1. CrysAlispro, Oxford Diffraction Ltd., version 1, 171. 33.34d [release 27-02-2009 CrysAlis 171. NET]
2. SMART and SAINT, Siemens Analytical X-ray Instruments Inc., Madison, WI, **1996**.
3. G. M. Sheldrick, **2008**, *64*, 112-122.

CCDC Number for Compound 10a: CCDC 1979947. This data can be obtained free of charge from the Cambridge Crystallographic Data Centre via www.ccdc.cam.ac.uk/datarequest/cif.

Crystallographic Description of 10a: Crystal dimension (mm): 0.27 x 0.22 x 0.18. 'C₂₁H₁₇FN₂O₅', Mr = 396.37. trigonal, space group 'p -32'; a = 12.8747(12) Å, b = 12.8739(15) Å, c = 10.1248(10) Å; $\alpha = 89.953(9)^\circ$, $\beta = 90.031(8)^\circ$, $\gamma = 120.005(11)$, V = 1453.2(3) Å³; Z = 3; $\rho_{\text{cal}} = 1.359 \text{ g/cm}^3$; $\mu (\text{mm}^{-1}) = 0.104$; $F(000) = 612.0$; Reflection collected / unique = 2734 / 1755; Refinement method = Full-matrix least-squares on F^2 ; Final R indices [$I > 2\sigma(I)$] R1 = 0.0518, wR2 = 0.1091, R indices (all data) R1 = 0.0906, wR2 = 0.1342; goodness of fit = 0.994.

IV.4.3. Synthesis of Oxidative Nitration and Decarboxylative Nitration Products

IV.4.3. General Procedure for the Synthesis of 2-Nitro-1,3,3-triphenylpropyl nitrate (1a):

To an oven-dried 25.0 mL round bottom flask was added (*E*)-prop-2-ene-1,1,3-triyltribenzene (135 mg, 0.5 mmol) and subjected to the vacuum for 10 minutes. Next, CH₃CN (2.0 mL) and *tert*-butyl nitrite (0.119 mL, 1.0 mmol) were introduced to the flask through a syringe under an oxygen atmosphere (balloon). Then the reaction mixture was stirred at 0 °C for 24 h. After the completion of the reaction excess solvent was evacuated under reduced pressure. The reaction mixture was admixed with dichloromethane (20.0 mL) and washed with water (2.0 x 10.0 mL) and the organic layer was separated. The separated organic layer was dried over anhydrous sodium sulphate (Na₂SO₄), and evaporated under reduced pressure. The resulting crude product was purified by silica gel column chromatography using hexane as the eluent to give pure 2-

nitro-1,3,3-triphenylpropyl nitrate (**1a**, 140 mg, 74% yield). The identity and purity of the product were confirmed by spectroscopic analysis.

IV.4.3. General Procedure for the Synthesis of *E*-(2-Nitrovinyl)benzene (24a**):** To an oven-dried 25.0 mL double-neck round bottom flask was added *trans*-cinnamic acid (74 mg, 0.5 mmol) and fitted with a reflux condenser. The reaction setup was subjected to the vacuum for 10 minutes. *tert*-Butyl nitrite (0.119 mL, 1.0 mmol) was purged into 2.0 mL of acetonitrile, then this *tert*-butyl nitrite containing acetonitrile was introduced into the reaction setup in an oxygen atmosphere. Then the reaction mixture was stirred in an oil bath at 100 °C for 24 h. After the completion of the reaction excess solvent was evacuated under reduced pressure. The reaction mixture was admixed with ethyl acetate 20.0 mL washed with water (2.0 x 10.0 mL). The separated organic layer was dried over anhydrous sodium sulphate (Na₂SO₄), and evaporated under reduced pressure. The resulting crude product was purified by silica gel column chromatography using hexane as the eluent to give pure *E*-(2-nitrovinyl)benzene (**21a**, 51 mg, 69% yield). The identity and purity of the product were confirmed by spectroscopic analysis.

IV.4.4. Mechanistic Investigation:

IV.4.4 Reaction of (1) with Radical Scavenger TEMPO: To an oven-dried 25.0 mL round fitted with a reflux condenser bottom flask was added (*E*)-prop-2-ene-1,1,3-triyltribenzene (135 mg, 0.5 mmol), TEMPO (0.078 g, 0.5 mmol) and subjected to the vacuum for 10 minutes. Next, CH₃CN (2.0 mL) and *tert*-butyl nitrite (0.119 mL, 1.0 mmol) were introduced to the flask through a syringe under an oxygen atmosphere (balloon). After the completion of the reaction excess solvent was evacuated under reduced pressure. The reaction mixture was admixed with dichloromethane (20.0 mL) and washed with water (2.0 x 10.0 mL) and the organic layer was separated. The separated organic layer was dried over anhydrous sodium sulphate (Na₂SO₄), and evaporated under reduced pressure. The resulting crude product was purified by silica gel column chromatography using hexane as the eluent to give pure 2-nitro-1,3,3-triphenylpropyl nitrate (**1a**, 13 mg, 7% yield). The identity and purity of the product was confirmed by spectroscopic analysis.

IV.5. References

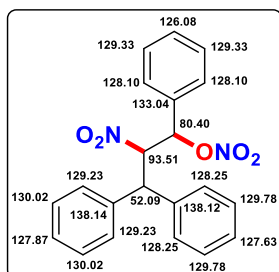
- [1] a) P. Li, X. Jia, *Synthesis* **2018**, *50*, 711-722; b) A. Dahiya, A. K. Sahoo, T. Alam, B. K. Patel, *Chem. Asian J.* **2019**, *14*, 4454-4492.
- [2] S. Prateptongkum, I. Jovel, R. Jackstell, N. Vogl, C. Weckbeckerb, M. Beller, *Chem. Commun.* **2009**, 1990-1992.
- [3] T. Taniguchi, A. Yajima, H. Ishibashi, *Adv. Synth. Catal.* **2011**, *353*, 2643-2647.
- [4] R. Chen, Y. Zhao, S. Fang, W. Long, H. Sun, X. Wan, *Org. Lett.* **2017**, *19*, 5896-5899.
- [5] P. Sau, S. K. Santra, A. Rakshit, B. K. Patel, *J. Org. Chem.* **2017**, *82*, 6358-6365.
- [6] P. Sau, A. Rakshit, A. Modi, A. Behera, B. K. Patel, *J. Org. Chem.* **2018**, *83*, 1056-1064.
- [7] P. Sau, A. Rakshit, T. Alam, H. K. Srivastava, B. K. Patel, *Org. Lett.* **2019**, *21*, 4966-4970.
- [8] B. Wang, L. Tang, L. Liu, J. Wang, Z. Zha, Z. Wang, *Green Chem.* **2017**, *19*, 5794-5799.
- [9] X. Q. Chu, D. Ge, T. P. Loh, Z. L. Shen, *Org. Chem. Front.* **2019**, *6*, 835-840.
- [10] F. Chen, N. N. Zhou, J. L. Zhan, B. Han, W. Yu, *Org. Chem. Front.* **2017**, *4*, 135-139.
- [11] B. A. Mir, S. J. Singh, R. Kumar, B. K. Patel, *Adv. Synth. Catal.* **2018**, *360*, 3801-3809.
- [12] For autoxidation of nitrogen monoxide: a) S. Goldstein, G. Czapski, *J. Am. Chem. Soc.* **1995**, *117*, 12078-12084; b) L. Grossi, S. Strazzari, *J. Org. Chem.* **1999**, *64*, 8076-8079; c) B. Galliker, R. Kissner, T. Nauser, W. H. Koppenol, *Chem. Eur. J.* **2009**, *15*, 6161-6168; d) M. P. Doyle, J. W. Terpstra, R. A. Pickering, D. M. LePoire, *J. Org. Chem.* **1983**, *48*, 3379-3382; e) J.- Y. Park, Y.- N. Lee, *J. Phy. Chem.* **1988**, *92*, 6294-6302; f) S. Ranganathan, S. K. Kar, *J. Org. Chem.* **1970**, *35*, 3962-3964.
- [13] a) Y. Zhao, D. G. Truhlar, The M06 suite of density functionals for main group thermochemistry, thermochemical kinetics, noncovalent interactions, excited states, and transition elements *Theor. Chem. Acc.* **2008**, *120*, 215-241; b) M. J. Frisch, G. W. Trucks, H. B. Schlegel, G. E. Scuseria, M. A. Robb, J. R. Cheeseman, G. Scalmani, V. Barone, B. Mennucci, G. A. Petersson, H. Nakatsuji, M. Caricato, X. Li, H. P. Hratchian, A. F. Izmaylov, J. Bloino, G. Zheng, J. L. Sonnenberg, M. Hada, M. Ehara, K. Toyota, R. Fukuda, J. Hasegawa, M. Ishida, T. Nakajima, Y. Honda, O. Kitao, H. Nakai, T. Vreven, J. A. Montgomery, Jr., J. E. Peralta, F. Ogliaro, M. Bearpark, J. J. Heyd, E. Brothers, K. N. Kudin, V. N. Staroverov, R. Kobayashi, J. Normand, K. Raghavachari, A. Rendell, J. C. Burant, S. S. Iyengar, J. Tomasi, M. Cossi, N. Rega, J. M. Millam, M. Klene, J. E. Knox, J. B. Cross, V. Bakken, C. Adamo, J. Jaramillo, R. Gomperts, R. E. Stratmann, O. Yazyev, A. J. Austin, R. Cammi, C. Pomelli, J. W. Ochterski, R. L. Martin, K. Morokuma, V. G.

Zakrzewski, G. A. Voth, P. Salvador, J. J. Dannenberg, S. Dapprich, A. D. Daniels, Ö. Farkas, J. B. Foresman, J. V. Ortiz, J. Cioslowski, D. J. Fox, Gaussian 09 (Gaussian, Inc., Wallingford CT, **2009**); c) Gaussian 09, Revision D.01, M. J. Frisch, G. W. Trucks, H. B. Schlegel, G. E. Scuseria, M. A. Robb, J. R. Cheeseman, G. Scalmani, V. Barone, B. Mennucci, G. A. Petersson, H. Nakatsuji, M. Caricato, X. Li, H. P. Hratchian, A. F. Izmaylov, J. Bloino, G. Zheng, J. L. Sonnenberg, M. Hada, M. Ehara, K. Toyota, R. Fukuda, J. Hasegawa, M. Ishida, T. Nakajima, Y. Honda, O. Kitao, H. Nakai, T. Vreven, J. A. Montgomery, Jr., J. E. Peralta, F. Ogliaro, M. Bearpark, J. J. Heyd, E. Brothers, K. N. Kudin, V. N. Staroverov, R. Kobayashi, J. Normand, K. Raghavachari, A. Rendell, J. C. Burant, S. S. Iyengar, J. Tomasi, M. Cossi, N. Rega, J. M. Millam, M. Klene, J. E. Knox, J. B. Cross, V. Bakken, C. Adamo, J. Jaramillo, R. Gomperts, R. E. Stratmann, O. Yazyev, A. J. Austin, R. Cammi, C. Pomelli, J. W. Ochterski, R. L. Martin, K. Morokuma, V. G. Zakrzewski, G. A. Voth, P. Salvador, J. J. Dannenberg, S. Dapprich, A. D. Daniels, Ö. Farkas, J. B. Foresman, J. V. Ortiz, J. Cioslowski, D. J. Fox, Gaussian, Inc., Wallingford CT, **2009**.

- [14] a) J. P. Das, P. Sinha, S. A. Roy, *Org. Lett.* **2002**, *4*, 3055-3058; b) A. K. Bose, S. N. Ganguly, M. S. Manhas, W. He, J. Speck, *Tetrahedron. Lett.* **2006**, *47*, 3213-3215; c) K. C. Rajanna, K. Ramesh, S. Ramgopal, S. Shylaja, P. G. Reddy, P. K. Saiprakash, *Green Sustainable Chem.* **2011**, *1*, 132-148; d) B. V. Rokade, K. R. Prabhu, *Org. Biomol. Chem.* **2013**, *11*, 6713-6716; e) S. Manna, S. Jana, T. Saboo, A. Maji, D. Maiti, *Chem. Commun.*, **2013**, *49*, 5286-5288; f) L. C. R. Henry, *Acad. Sci. Ser. C*, **1895**, *120*, 1265-1268; g) S. Maity, S. Manna, S. Rana, T. Naveen, A. Mallick, D. Maiti, *J. Am. Chem. Soc.* **2013**, *135*, 3355-3358; h) G. Bachman, T. Biermann, *J. Org. Chem.* **1970**, *35*, 4229-4231; i) M. S. Kumar, P. Venkanna, S. Ramgopal, K. Ramesh, M. Venkateswarlu, K. C. Rajanna, *Org. Commun.* **2012**, *5*, 42-49; j) A. Messere, A. Gentili, I. Garella, F. Temussi, B. D. Blasio, A. Fiorentino, *Synth. Commun.* **2004**, *34*, 3317-3324; k) S. Ramgopal, K. Ramesh, A. Chakradhar, N. M. Reddy, K. C. Rajanna, *Tetrahedron Lett.* **2007**, *48*, 4043-4045; l) A. S. Rao, P. V. Srinivas, K. S. Babu, J. M. Rao, *Tetrahedron Lett.* **2005**, *46*, 8141-8143.

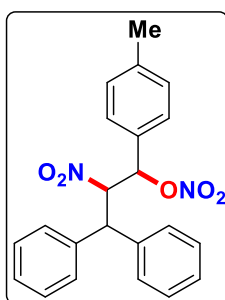
IV.6. Spectral Data

2-Nitro-1,3,3-triphenylpropyl nitrate (1a):



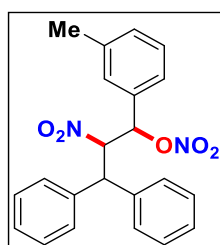
Yellow gummy, (140 mg, 61%). ^1H NMR (400 MHz, CDCl_3) δ 7.36–7.31 (m, 10H), 7.28 (bs, 1H), 7.25–7.19 (m, 4H), 5.87 (d, $J = 5.0$ Hz, 1H), 5.69 (dd, $J = 11.4, 5.0$ Hz, 1H), 4.88 (d, $J = 11.4$ Hz, 1H) ppm. ^{13}C NMR (101 MHz, CDCl_3) δ 138.14, 138.12, 133.04, 130.02, 129.78, 129.33, 129.23, 128.25, 128.10, 127.87, 127.63, 126.08, 93.51, 80.40, 52.09 ppm. IR (KBr, cm^{-1}): 3032, 2913, 1646, 1556, 1493, 1453, 1363, 1272, 1031, 903, 828, 746, 695; HRMS (ESI/Q-TOF) m/z : $[\text{M} + \text{Na}]^+$ Calcd for $\text{C}_{21}\text{H}_{18}\text{N}_2\text{NaO}_5$ 411.1108, found 411.1116.

2-Nitro-3,3-diphenyl-1-(*p*-tolyl)propyl nitrate (2a):



Yellow solid, (131 mg, 67%), m. p. 110–114 °C. ^1H NMR (400 MHz, CDCl_3) δ 7.35 (d, $J = 7.6$ Hz, 2H), 7.31 (d, $J = 4.4$ Hz, 5H), 7.28–7.21 (m, 4H), 7.11 (d, $J = 4.0$ Hz, 3H), 5.83 (d, $J = 5.2$ Hz, 1H), 5.67 (dd, $J = 11.6, 5.2$ Hz, 2H), 4.87 (d, $J = 11.6$ Hz, 1H), 2.30 (s, 3H) ppm. ^{13}C NMR (CDCl_3 , 101 MHz) δ 140.12, 138.16, 138.13, 130.10, 129.92, 129.73, 129.22, 128.15, 128.07, 127.86, 127.64, 126.00, 93.52, 80.41, 52.01, 21.35 ppm. IR (KBr, cm^{-1}): 3031, 2915, 1653, 1552, 1492, 1450, 1363, 1270, 1087, 1031, 823, 751, 704, 588, 532; HRMS (ESI/Q-TOF) m/z : $[\text{M} + \text{NH}_4]^+$ Calcd for $\text{C}_{22}\text{H}_{24}\text{N}_3\text{O}_5$ 410.1710, found 410.1739.

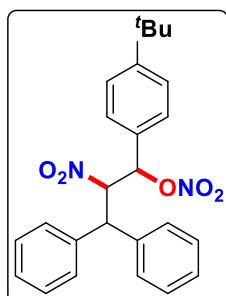
2-Nitro-3,3-diphenyl-1-(*m*-tolyl)propyl nitrate (3a):



Yellow solid, (128 mg, 65%), m. p. 116–119 °C. ^1H NMR (400 MHz, CDCl_3) δ 7.36 (d, $J = 7.5$ Hz, 2H), 7.31 (d, $J = 4.4$ Hz, 4H), 7.28–7.19 (m, 5H), 7.12 (d, $J = 7.6$ Hz, 1H), 7.03 (d, $J = 7.6$ Hz, 1H), 6.97 (s, 1H), 5.84 (d, $J = 5.1$ Hz, 1H), 5.68 (dd, $J = 11.4, 5.1$ Hz, 1H), 4.86 (d, $J = 11.4$ Hz, 1H), 2.29 (s, 3H) ppm. ^{13}C NMR (CDCl_3 , 101 MHz) δ 139.14, 138.15, 138.12, 132.86, 130.82, 129.69, 129.21, 128.18, 128.07, 127.84, 127.63, 126.72, 123.06, 93.43, 80.56, 52.13, 21.45 ppm. IR (KBr, cm^{-1}): 3031,

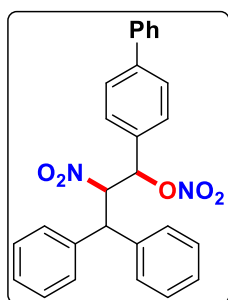
2915, 1645, 1556, 1492, 1452, 1364, 1272, 1036, 836, 748, 696, 613; HRMS (ESI/Q-TOF) m/z : $[M + NH_4]^+$ Calcd for $C_{22}H_{24}N_3O_5$ 410.1710, found 410.1735.

1-(4-(*tert*-Butyl)phenyl)-2-nitro-3,3-diphenylpropyl nitrate (4a):



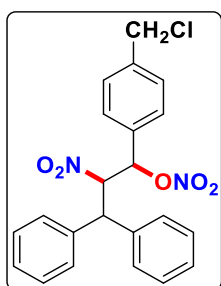
Yellow gummy, (135 mg, 62%). 1H NMR (400 MHz, $CDCl_3$) δ 7.35–7.26 (m, 11H), 7.23–7.19 (m, 2H), 7.12 (d, $J = 8.0$ Hz, 2H), 5.90 (d, $J = 5.6$ Hz, 1H), 5.69 (dd, $J = 11.2, 5.6$ Hz, 1H), 4.81 (d, $J = 11.2$ Hz, 1H), 1.26 (s, 9H) ppm. ^{13}C NMR ($CDCl_3$, 101 MHz) δ 153.12, 138.23, 138.14, 129.73, 129.62, 129.20, 128.08, 128.05, 127.88, 127.67, 126.19, 93.17, 80.94, 52.40, 31.26 ppm. IR (KBr, cm^{-1}): 3034, 2961, 1645, 1556, 1493, 1453, 1363, 1272, 1107, 1029, 831, 749, 698, 610; HRMS (ESI/Q-TOF) m/z : $[M + NH_4]^+$ Calcd for $C_{25}H_{30}N_3O_5$ 452.2180, found 452.2270.

1-([1,1'-Biphenyl]-4-yl)-2-nitro-3,3-diphenylpropyl nitrate (5a):



Yellow gummy, (150 mg, 66%). 1H NMR (400 MHz, $CDCl_3$) δ 7.44–7.42 (m, 2H), 7.35 (t, $J = 7.4$ Hz, 2H), 7.28 (d, $J = 7.2$ Hz, 3H), 7.22–7.18 (m, 9H), 7.14 (d, $J = 8.0$ Hz, 2H), 5.87 (d, $J = 5.6$ Hz, 1H), 5.66 (dd, $J = 11.2, 5.2$ Hz, 1H), 4.80 (d, $J = 11.6$ Hz, 3H) ppm. ^{13}C NMR (101 MHz, $CDCl_3$) δ 142.94, 140.09, 138.14, 138.08, 131.75, 129.72, 129.23, 129.00, 128.12, 127.97, 127.90, 127.65, 127.25, 126.75, 93.33, 80.61, 52.30 ppm. IR (KBr, cm^{-1}): 3035, 2961, 1646, 1556, 1489, 1451, 1362, 1270, 1025, 828, 749, 695; HRMS (ESI/Q-TOF) m/z : $[M + NH_4]^+$ Calcd for $C_{27}H_{26}N_3O_5$ 472.1768, found 472.1775.

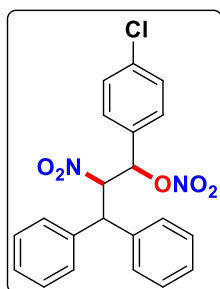
1-(4-(Chloromethyl)phenyl)-2-nitro-3,3-diphenylpropyl nitrate (6a):



Yellow solid, (137 mg, 64%), m. p. 120–125 °C. 1H NMR (400 MHz, $CDCl_3$) δ 7.36–7.33 (m, 4H), 7.31–7.28 (m, 5H), 7.27–7.20 (m, 5H), 5.87 (d, $J = 5.2$ Hz, 1H), 5.68 (dd, $J = 11.6, 5.2$ Hz, 1H), 4.87 (d, $J = 11.6$ Hz, 1H), 4.52 (s, 2H) ppm. ^{13}C NMR ($CDCl_3$, 101 MHz) δ 140.94, 138.09, 136.14, 136.08, 129.75, 127.72, 127.23, 127.00, 126.12, 125.97, 125.90, 125.65, 125.25, 124.75, 91.33, 78.61, 50.30, 27.83 ppm. IR (KBr, cm^{-1}): 3032,

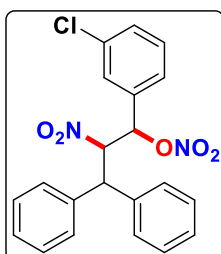
2960, 1654, 1554, 1492, 1451, 1360, 1275, 1032, 899, 828, 748, 698, 671, 617, 591, 552; HRMS (ESI/Q-TOF) m/z : $[M + NH_4]^+$
Calcd for $C_{22}H_{23}ClN_3O_5$ 444.1321, found 444.1334.

1-(4-Chlorophenyl)-2-nitro-3,3-diphenylpropyl nitrate (7a):



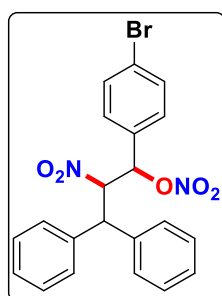
Yellow solid, (155 mg, 75%), m. p. 140–144 °C. 1H NMR (400 MHz, $CDCl_3$) δ 7.35 (d, $J = 8.0$ Hz, 2H), 7.31–7.27 (m, 8H), 7.25–7.22 (m, 2H), 7.14 (d, $J = 8.4$ Hz, 2H), 5.83 (d, $J = 5.2$ Hz, 1H), 5.66 (dd, $J = 11.6, 5.6$ Hz, 1H), 4.86 (d, $J = 11.6$ Hz, 1H) ppm. ^{13}C NMR (101 MHz, $CDCl_3$) δ 137.94, 137.88, 136.15, 131.52, 129.83, 129.61, 129.28, 128.30, 128.18, 127.83, 127.54, 93.29, 79.77, 52.11 ppm. IR (KBr, cm^{-1}): 3029, 2912, 1658, 1598, 1554, 1491, 1452, 1410, 1365, 1273, 1196, 1091, 1033, 900, 826, 755, 707, 674; HRMS (ESI/Q-TOF) m/z : $[M + NH_4]^+$
Calcd for $C_{21}H_{21}ClN_3O_5$ 430.1164, found 430.1180.

1-(3-Chlorophenyl)-2-nitro-3,3-diphenylpropyl nitrate (8a):



Yellow solid, (151 mg, 73%), m. p. 116–119 °C. 1H NMR (400 MHz, $CDCl_3$) δ 7.36 (d, $J = 7.6$ Hz, 2H), 7.32–7.22 (m, 10H), 7.17 (s, 1H), 7.12 (d, $J = 7.6$ Hz, 1H), 5.83 (d, $J = 5.2$ Hz, 1H), 5.67 (dd, $J = 11.6, 5.2$ Hz, 1H), 4.86 (d, $J = 11.6$ Hz, 1H) ppm. ^{13}C NMR ($CDCl_3$, 101 MHz) δ 139.14, 138.15, 138.12, 132.86, 130.82, 129.69, 129.21, 128.18, 128.07, 127.84, 127.63, 126.72, 123.06, 93.43, 80.56, 52.13, 21.45 ppm. IR (KBr, cm^{-1}): 3029, 2958, 1658, 1554, 1491, 1361, 1275, 1098, 1079, 1032, 820, 787, 747, 696, 614; HRMS (ESI/Q-TOF) m/z : $[M + NH_4]^+$ Calcd for $C_{21}H_{21}ClN_3O_5$ 430.1164, found 430.1176.

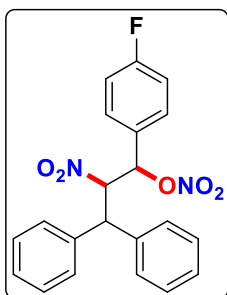
1-(4-Bromophenyl)-2-nitro-3,3-diphenylpropyl nitrate (9a):



Yellow gummy, (174 mg, 76%). 1H NMR (400 MHz, $CDCl_3$) δ 7.45 (d, $J = 8.4$ Hz, 2H), 7.36–7.26 (m, 10H), 7.08 (d, $J = 8.4$ Hz, 2H), 5.82 (d, $J = 5.2$ Hz, 1H), 5.65 (dd, $J = 11.6, 5.2$ Hz, 1H), 4.85 (d, $J = 11.2$ Hz, 1H) ppm. ^{13}C NMR ($CDCl_3$, 101 MHz) δ 137.94, 137.89, 132.57, 129.84, 129.29, 128.31, 128.19,

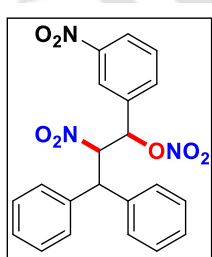
127.84, 127.78, 127.56, 124.38, 93.24, 79.83, 52.12 ppm. IR (KBr, cm^{-1}): 3029, 2958, 1658, 1554, 1491, 1361, 1275, 1098, 1079, 1032, 820, 787, 747, 698, 616; HRMS (ESI/Q-TOF) m/z : $[\text{M} + \text{NH}_4]^+$ Calcd for $\text{C}_{21}\text{H}_{21}\text{BrN}_3\text{O}_5$ 474.0659, found 474.0668.

1-(4-Fluorophenyl)-2-nitro-3,3-diphenylpropyl nitrate (10a):

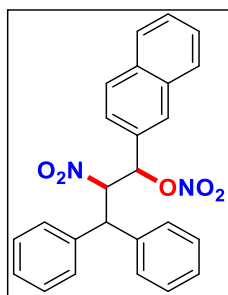


Colourless solid, (153 mg, 77 %), m. p. 128–131 °C. ^1H NMR (400 MHz, CDCl_3) δ 7.35 (d, $J = 7.2$ Hz, 2H), 7.31–7.29 (m, 5H), 7.27–7.18 (m, 5H), 7.00 (t, $J = 8.6$ Hz, 2H), 5.86 (d, $J = 5.2$ Hz, 1H), 5.66 (dd, $J = 11.2, 5.2$ Hz, 1H), 4.85 (d, $J = 11.2$ Hz, 1H) ppm. ^{13}C NMR (101 MHz, CDCl_3) δ 163.49 (d, $J = 251.49$ Hz), 137.97 (d, $J = 5.1$ Hz), 129.80, 129.27, 128.87 (d, $J = 3.3$ Hz), 128.28, 128.20, 128.17, 127.83, 127.57, 116.5 (d, $J = 22.2$ Hz), 93.39, 79.89, 52.17 ppm. ^{19}F NMR (CDCl_3 , 377 MHz) δ -110.42. IR (KBr, cm^{-1}): 3031, 2958, 1654, 1601, 1551, 1508, 1492, 1364, 1270, 1228, 1158, 1092, 1031, 825, 752, 703, 674; HRMS (ESI/Q-TOF) m/z : $[\text{M} + \text{NH}_4]^+$ Calcd for $\text{C}_{21}\text{H}_{21}\text{FN}_3\text{O}_5$ 414.1460, found 414.1480.

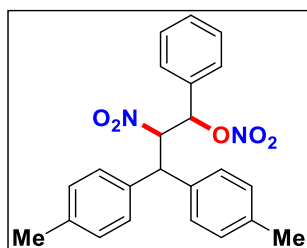
2-Nitro-1-(3-nitrophenyl)-3,3-diphenylpropyl nitrate (11a):



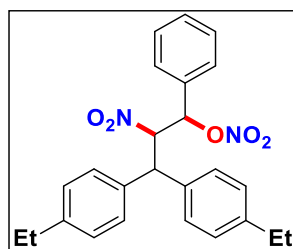
Yellow gummy, (150 mg, 71%). ^1H NMR (400 MHz, CDCl_3) δ 8.18 (d, $J = 8.0$ Hz, 1H), 8.05 (s, 1H), 7.60 (d, $J = 7.6$ Hz, 1H), 7.53 (t, $J = 8.0$ Hz, 1H), 7.36 (d, $J = 7.2$ Hz, 2H), 7.32–7.28 (m, 6H), 7.26–7.22 (m, 3H), 5.98 (d, $J = 5.2$ Hz, 1H), 5.74 (dd, $J = 11.6, 5.6$ Hz, 1H), 4.88 (d, $J = 11.6$ Hz, 1H) ppm. ^{13}C NMR (CDCl_3 , 101 MHz) δ 148.48, 137.74, 137.56, 135.34, 131.82, 130.65, 129.93, 129.36, 129.11, 128.44, 128.31, 127.82, 127.48, 124.91, 121.86, 92.95, 79.48, 52.34 ppm. IR (KBr, cm^{-1}): 3032, 2922, 1658, 1554, 1524, 1451, 1349, 1274, 1090, 1031, 825, 736, 700, 592, 551; HRMS (ESI/Q-TOF) m/z : $[\text{M} + \text{Na}]^+$ Calcd for $\text{C}_{21}\text{H}_{17}\text{N}_3\text{NaO}_7$ 446.0959, found 446.0965.

1-(Naphthalen-2-yl)-2-nitro-3,3-diphenylpropyl nitrate (12a):

Yellow gummy, (129 mg, 60%). ^1H NMR (400 MHz, CDCl_3) δ 7.81 (d, $J = 8.8$ Hz, 3H), 7.68 (s, 1H), 7.52–7.50 (m, 2H), 7.38–7.24 (m, 12H), 6.04 (d, $J = 4.8$ Hz, 1H), 5.79 (dd, $J = 11.6, 5.2$ Hz, 1H), 4.92 (d, $J = 11.2$ Hz, 1H) ppm. ^{13}C NMR (101 MHz, CDCl_3) δ 138.12, 138.10, 133.05, 129.73, 129.50, 129.25, 128.35, 128.20, 128.13, 127.94, 127.88, 127.67, 127.32, 127.05, 126.16, 122.74, 93.37, 80.69, 52.21 ppm. IR (KBr, cm^{-1}): 2921, 2853, 1646, 1555, 1493, 1453, 1364, 1273, 1029, 824, 747, 698; HRMS (ESI/Q-TOF) m/z : $[\text{M} + \text{Na}]^+$ Calcd for $\text{C}_{25}\text{H}_{20}\text{N}_2\text{NaO}_5$ 451.1264, found 451.1273.

2-Nitro-1-phenyl-3,3-di-*p*-tolylpropyl nitrate (13a):

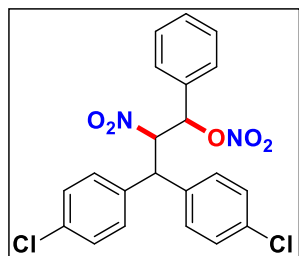
Yellow gummy, (148 mg, 73%). ^1H NMR (400 MHz, CDCl_3) δ 7.33–7.31 (m, 3H), 7.23–7.18 (m, 6H), 7.11–7.06 (m, 4H), 5.85 (d, $J = 4.8$ Hz, 1H), 5.64 (dd, $J = 11.6, 4.8$ Hz, 1H), 4.82 (d, $J = 11.6$ Hz, 1H), 2.28 (s, 3H), 2.25 (s, 3H) ppm. ^{13}C NMR (101 MHz, CDCl_3) δ 137.96, 137.71, 135.34, 135.31, 133.20, 130.42, 129.87, 129.30, 127.40, 126, 93.74, 80.32, 51.28, 21.13, 21.11 ppm. IR (KBr, cm^{-1}): 3030, 2919, 1646, 1656, 1511, 1365, 1273, 1037, 906, 832, 732, 697; HRMS (ESI/Q-TOF) m/z : $[\text{M} + \text{NH}_4]^+$ Calcd for $\text{C}_{23}\text{H}_{26}\text{N}_3\text{O}_5$ 424.1867, found 424.1875.

3,3-bis(4-Ethylphenyl)-2-nitro-1-phenylpropyl nitrate (14a):

Yellow gummy, (163 mg, 75%). ^1H NMR (400 MHz, CDCl_3) δ 7.24–7.21 (m, 3H), 7.18 (d, $J = 8.4$ Hz, 2H), 7.44–7.12 (m, 4H), 7.03 (t, $J = 8.2$ Hz, 4H), 5.79 (d, $J = 4.8$ Hz, 1H), 5.58 (dd, $J = 11.6, 4.8$ Hz, 1H), 4.75 (d, $J = 11.2$ Hz, 1H), 2.53–2.44 (m, 4H), 1.12–1.05 (m, 6H) ppm. ^{13}C NMR (CDCl_3 , 101 MHz) δ 144.17, 143.92, 135.57, 135.48, 133.21, 129.89, 129.26, 129.18, 128.64, 127.73, 127.47, 126.08, 93.70, 80.49, 51.48, 28.49, 28.45, 15.41, 15.41 ppm. IR (KBr, cm^{-1}): 3031, 2966, 1646, 1557, 1510, 1455, 1365, 1273, 1125, 1034, 905, 829, 744, 696; HRMS (ESI/Q-

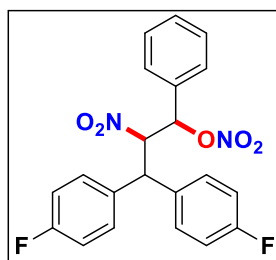
TOF) m/z : $[M + NH_4]^+$ Calcd for $C_{25}H_{30}N_3O_5$ 452.2180, found 452.2192.

3,3-bis(4-Chlorophenyl)-2-nitro-1-phenylpropyl nitrate (15a):



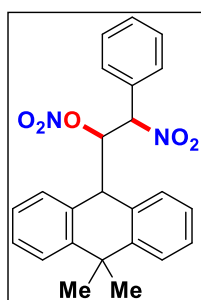
Yellow gummy, (171 mg, 77%). 1H NMR (400 MHz, $CDCl_3$) δ 7.33 (d, $J = 8.0$ Hz, 3H), 7.28–7.25 (m, 6H), 7.22–7.17 (m, 4H), 5.89 (d, $J = 5.6$ Hz, 1H), 5.60 (dd, $J = 10.8, 5.6$ Hz, 1H), 4.79 (d, $J = 11.2$ Hz, 1H) ppm. ^{13}C NMR (101 MHz, $CDCl_3$) δ 136.15, 136.05, 134.45, 134.41, 132.59, 130.26, 129.99, 129.58, 129.43, 129.11, 128.95, 126.34, 92.83, 80.62, 50.95 ppm. IR (KBr, cm^{-1}): 3030, 2916, 1900, 1654, 1648, 1557, 1490, 1410, 1364, 1273, 1091, 1013, 906, 819, 730, 696; HRMS (ESI/Q-TOF) m/z : $[M + NH_4]^+$ Calcd for $C_{21}H_{20}Cl_2N_3O_5$ 464.0775, found 464.0782.

3,3-bis(4-Fluorophenyl)-2-nitro-1-phenylpropyl nitrate (16a):



Yellow solid, (164 mg, 79%), m. p. 130–135 °C. 1H NMR (400 MHz, $CDCl_3$) δ 7.34–7.19 (m, 9H), 7.02–6.96 (m, 4H), 5.89 (d, $J = 5.6$ Hz, 1H), 5.60 (dd, $J = 11.2, 5.6$ Hz, 1H), 4.82 (d, $J = 11.2$ Hz, 1H) ppm. ^{13}C NMR ($CDCl_3$, 101 MHz) δ 162.46 (d, $J = 248.46$ Hz), 162.35 (d, $J = 249.47$ Hz), 133.72 (d, $J = 3.8$ Hz), 132.70, 130.22, 129.51, 129.42, 129.41, 129.35, 129.27, 126.33, 116.68 (d, $J = 47.47$ Hz), 116.45 (d, $J = 47.47$ Hz), 93.29, 80.63, 50.72 ppm. ^{19}F NMR (377 MHz, $CDCl_3$) δ -113.10, -113.61 IR (KBr, cm^{-1}): 3065, 2917, 1661, 1603, 1564, 1508, 1453, 1418, 1366, 1230, 1161, 1109, 1033, 905, 833, 777, 750, 700, 677; HRMS (ESI/Q-TOF) m/z : $[M + NH_4]^+$ Calcd for $C_{21}H_{20}F_2N_3O_5$ 432.1366, found 432.1371.

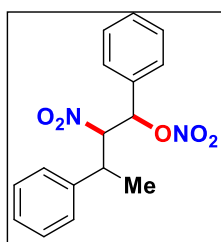
1-(10,10-Dimethyl-9,10-dihydroanthracen-9-yl)-2-nitro-2-phenylethyl nitrate (17a):



Gummy, (155 mg, 74%). 1H NMR (400 MHz, $CDCl_3$) δ 7.60 (dd, $J = 15.2, 8.0$ Hz, 2H), 7.44–7.33 (m, 7H), 7.26 (d, $J = 4.4$ Hz, 3H), 7.18 (d, $J = 7.6$ Hz, 1H), 6.02 (d, $J = 7.2$ Hz, 1H), 5.02 (t, $J = 6.9$ Hz, 1H), 4.72 (d, $J = 6.8$ Hz, 1H), 1.68 (s, 3H), 1.65 (s, 3H) ppm. ^{13}C NMR ($CDCl_3$, 101 MHz) δ 145.60, 144.86,

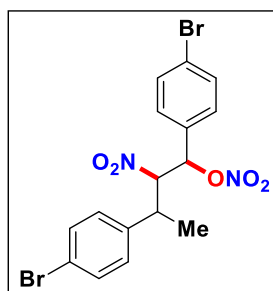
132.92, 131.54, 130.57, 130.40, 129.70, 128.70, 128.67, 128.04, 127.99, 127.40, 127.15, 127.08, 126.67, 97.10, 80.83, 45.18, 38.87, 35.53, 32.77 ppm. IR (KBr, cm^{-1}): 3036, 2971, 1658, 1599, 1448, 1322, 1264, 1167, 1039, 932, 735, 700; HRMS (ESI/Q-TOF) m/z : $[\text{M} + \text{Na}]^+$ Calcd for $\text{C}_{24}\text{H}_{22}\text{NaN}_2\text{O}_5$ 441.1421, found 441.1432.

2-Nitro-1,3-diphenylbutyl nitrate (18a):



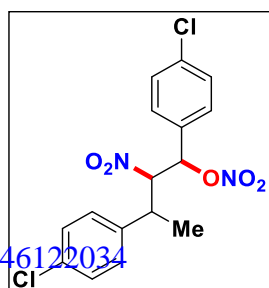
Gummy, (81 mg, 51%). ^1H NMR (400 MHz, CDCl_3) δ 7.45–7.42 (m, 3H), 7.38–7.36 (m, 2H), 7.27–7.25 (m, 3H), 7.01–6.99 (m, 2H), 6.20 (d, $J = 9.6$ Hz, 1H), 5.11 (dd, $J = 9.6, 6.0$ Hz, 1H), 3.27–3.17 (m, 1H), 1.33 (d, $J = 7.2$ Hz, 3H) ppm. ^{13}C NMR (101 MHz, CDCl_3) δ 138.45, 132.29, 130.68, 129.45, 128.78, 128.30, 128.18, 127.84, 92.88, 82.29, 40.17, 18.86 ppm. IR (KBr, cm^{-1}): 3037, 2979, 1694, 1640, 1552, 1494, 1452, 1270, 1199, 1084, 1040, 745, 695; HRMS (ESI/Q-TOF) m/z : $[\text{M} + \text{Na}]^+$ Calcd for $\text{C}_{16}\text{H}_{16}\text{NaN}_2\text{O}_5$ 339.0951, found 339.0959.

1,3-bis(4-Bromophenyl)-2-nitrobutyl nitrate (19a):



Yellow solid, (135 mg, 57%), m. p. 183–187 °C. ^1H NMR (600 MHz, CDCl_3) δ 7.52 (d, $J = 8.4$ Hz, 2H), 7.35 (d, $J = 8.4$ Hz, 2H), 7.15 (d, $J = 8.4$ Hz, 2H), 6.79 (d, $J = 8.4$ Hz, 2H), 6.05 (d, $J = 9.0$ Hz, 1H), 4.96 (dd, $J = 9.0, 6.0$ Hz, 1H), 3.17–3.11 (m, 1H), 1.28 (d, $J = 7.2$ Hz, 3H) ppm. ^{13}C NMR (151 MHz, CDCl_3) δ 137.27, 132.86, 132.11, 131.20, 129.81, 129.53, 125.32, 122.43, 92.44, 81.16, 39.74, 18.61 ppm. IR (KBr, cm^{-1}): 3049, 2925, 2854, 1644, 1555, 1460, 1375, 1274, 1016, 801, 723; HRMS (ESI/Q-TOF) m/z : $[\text{M} + \text{NH}_4]^+$ Calcd for $\text{C}_{16}\text{H}_{18}\text{Br}_2\text{NaN}_3\text{O}_5$ 489.9608, found 489.9615.

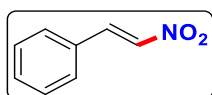
1,3-bis(4-Chlorophenyl)-2-nitrobutyl nitrate (20a):



Gummy, (104 mg, 54 %). ^1H NMR (600 MHz, CDCl_3) δ 7.37 (d, $J = 6.6$ Hz, 2H), 7.30 (dd, $J = 6.0, 2\text{H}$), 7.20 (d, $J = 6.0$ Hz, 2H), 6.92 (dd, $J = 6.4, 2.8$ Hz, 8H), 6.12 (d, $J = 9.0$ Hz, 2H), 5.03 (dd,

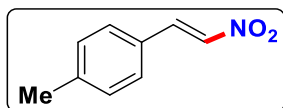
$J = 9.0, 5.4$ Hz, 1H), 3.17–3.11 (m, 1H) ppm. ^{13}C NMR (151 MHz, CDCl_3) δ 138.47, 132.40, 130.74, 129.51, 128.84, 128.39, 128.26, 127.90, 92.90, 82.29, 40.23, 18.95 ppm. IR (KBr, cm^{-1}): 3036, 2924, 2848, 1653, 1558, 1449, 1366, 1275, 1092, 1014, 749; HRMS (ESI/Q-TOF) m/z : $[\text{M} + \text{NH}_4]^+$ Calcd for $\text{C}_{16}\text{H}_{18}\text{Cl}_2\text{NaN}_3\text{O}_5$ 402.0618, found 402.0625.

(E)-(2-Nitrovinyl)benzene (21a):



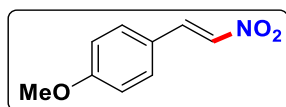
Yellow solid, (51 mg, 69%), m. p. 57–61 °C. ^1H NMR (600 MHz, CDCl_3) δ 8.01 (d, $J = 13.7$ Hz, 1H), 7.59 (d, $J = 13.7$ Hz, 1H), 7.56–7.54 (m, 2H), 7.52–7.49 (m, 1H), 7.47–7.44 (m, 2H) ppm. ^{13}C NMR (151 MHz, CDCl_3) δ 139.21, 137.24, 132.27, 130.19, 129.52, 129.27 ppm. IR (KBr, cm^{-1}): 3109, 2923, 1632, 1577, 1513, 1449, 1344, 1262, 967, 764, 750; HRMS (ESI/Q-TOF) Calcd for $\text{C}_8\text{H}_7\text{NaNO}_2$ $[\text{M} + \text{Na}]^+$ 172.0369, found 172.0382.

(E)-1-Methyl-4-(2-nitrovinyl)benzene (22a):



Yellow solid, (52 mg, 64%), m. p. 106–109 °C. ^1H NMR (600 MHz, CDCl_3) δ 7.98 (d, $J = 13.6$ Hz, 1H), 7.57 (d, $J = 13.6$ Hz, 1H), 7.44 (d, $J = 7.8$ Hz, 2H), 7.26 (d, $J = 7.9$ Hz, 2H), 2.41 (s, 3H) ppm. ^{13}C NMR (151 MHz, CDCl_3) δ 143.25, 139.33, 136.36, 130.26, 129.32, 127.35, 21.80 ppm. IR (KBr, cm^{-1}): 3109, 2923, 2853, 1632, 1496, 1341, 1265, 965, 810, 741; HRMS (ESI/Q-TOF) m/z : Calcd for $\text{C}_9\text{H}_{10}\text{NO}_2$ $[\text{M} + \text{H}]^+$ 164.0706, found 164.0712.

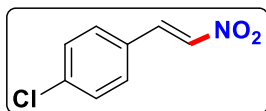
(E)-1-Methoxy-4-(2-nitrovinyl)benzene (23a):



Yellow solid, (55 mg, 61%), m. p. 85–88 °C. ^1H NMR (600 MHz, CDCl_3) δ 7.97 (d, $J = 13.6$ Hz, 1H), 7.54–7.48 (m, 3H), 6.96 (d, $J = 8.8$ Hz, 2H), 3.87 (s, 3H) ppm. ^{13}C NMR (151 MHz, CDCl_3) δ 163.03, 139.18, 135.07, 131.29, 122.60, 115.01, 55.64 ppm. IR (KBr, cm^{-1}): 2925, 1605, 1498, 1339, 1256, 1176, 1031,

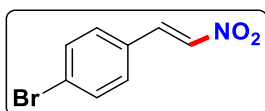
973, 809; HRMS (ESI/Q-TOF) m/z : Calcd for $C_9H_{10}NO_3$ [$M + H$]⁺ 180.0655, found 180.0669.

(E)-1-Chloro-4-(2-nitrovinyl)benzene (24a):



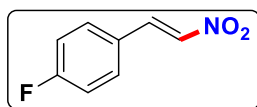
Yellow solid, (64 mg, 70%), m. p. 102–105 °C. ¹H NMR (600 MHz, CDCl₃) δ 7.97 (d, $J = 13.7$ Hz, 1H), 7.57 (d, $J = 13.7$ Hz, 1H), 7.52–7.48 (m, 2H), 7.44 (d, $J = 8.5$ Hz, 2H) ppm. ¹³C NMR (151 MHz, CDCl₃) δ 138.45, 137.85, 137.51, 130.40, 129.88, 128.61 ppm. IR (KBr, cm⁻¹): 3107, 2924, 2852, 1721, 1642, 1601, 1529, 1344, 1201, 1048, 965, 832, 753, 677; HRMS (ESI/Q-TOF) m/z : calcd for $C_8H_6ClNaNO_2$ [$M + Na$]⁺ 205.9979, found 205.9991.

(E)-1-Bromo-4-(2-nitrovinyl)benzene (25a):

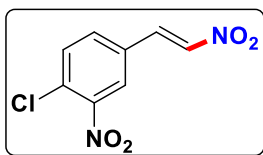


Yellow solid, (82 mg, 72%), m. p. 151–154 °C. ¹H NMR (600 MHz, CDCl₃) δ 7.98–7.94 (m, 1H), 7.64–7.56 (m, 3H), 7.47–7.39 (m, 2H) ppm. ¹³C NMR (151 MHz, CDCl₃) δ 137.94, 137.55, 132.85, 130.52, 129.03, 126.91 ppm. IR (KBr, cm⁻¹): 2923, 2849, 1633, 1517, 1341, 1073, 812; HRMS (ESI/Q-TOF) m/z : Calcd for $C_8H_6BrNaNO_2$ [$M + Na$]⁺ 249.9474, found 249.9480.

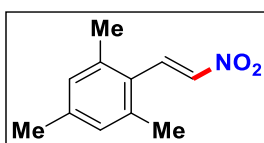
(E)-1-Fluoro-4-(2-nitrovinyl)benzene (26a):



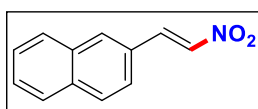
Yellow solid, (62 mg, 74%), m. p. 102–105 °C. ¹H NMR (400 MHz, CDCl₃) δ 8.02–7.97 (m, 1H), 7.60–7.53 (m, 3H), 7.19–7.14 (m, 2H) ppm. ¹³C NMR (101 MHz, CDCl₃) δ 165.06 (d, $J = 255.83$ Hz), 137.96, 136.99, 131.41 (d, $J = 8.9$ Hz), 126.46, 116.91 (d, $J = 22.32$ Hz) ppm. ¹⁹F NMR (377 MHz, CDCl₃) δ -105.81. IR (KBr, cm⁻¹): 3109, 2973, 1630, 1554, 1514, 1449, 1338, 1261, 1189, 1072, 964, 762, 699; HRMS (ESI/Q-TOF) m/z : Calcd for $C_8H_6FNaN_2O_2$ [$M + Na$]⁺ 190.0275, found 190.0287.

(E)-1-Chloro-2-nitro-4-(2-nitrovinyl)benzene (27a):

Yellow solid, (87 mg, 76%), m. p. 131–135 °C. ^1H NMR (600 MHz, $\text{CDCl}_3 + \text{DMSO-}d_6$) δ 8.33 (d, $J = 6.0$ Hz, 1H), 8.10–7.96 (m, 2H), 7.93–7.83 (m, 1H), 7.73–7.61 (m, 1H) ppm. ^{13}C NMR (151 MHz, $\text{CDCl}_3 + \text{DMSO-}d_6$) δ 147.68, 139.39, 134.85, 132.77, 132.10, 129.96, 128.80, 125.34 ppm. IR (KBr, cm^{-1}): 3103, 3039, 2924, 2852, 1734, 1633, 1591, 1518, 1404, 1339, 1259, 1086, 970, 819, 742; HRMS (ESI/Q-TOF) m/z : Calcd for $\text{C}_8\text{H}_5\text{ClNaN}_2\text{O}_2$ [$\text{M} + \text{Na}$] $^+$ 250.983, found 250.989.

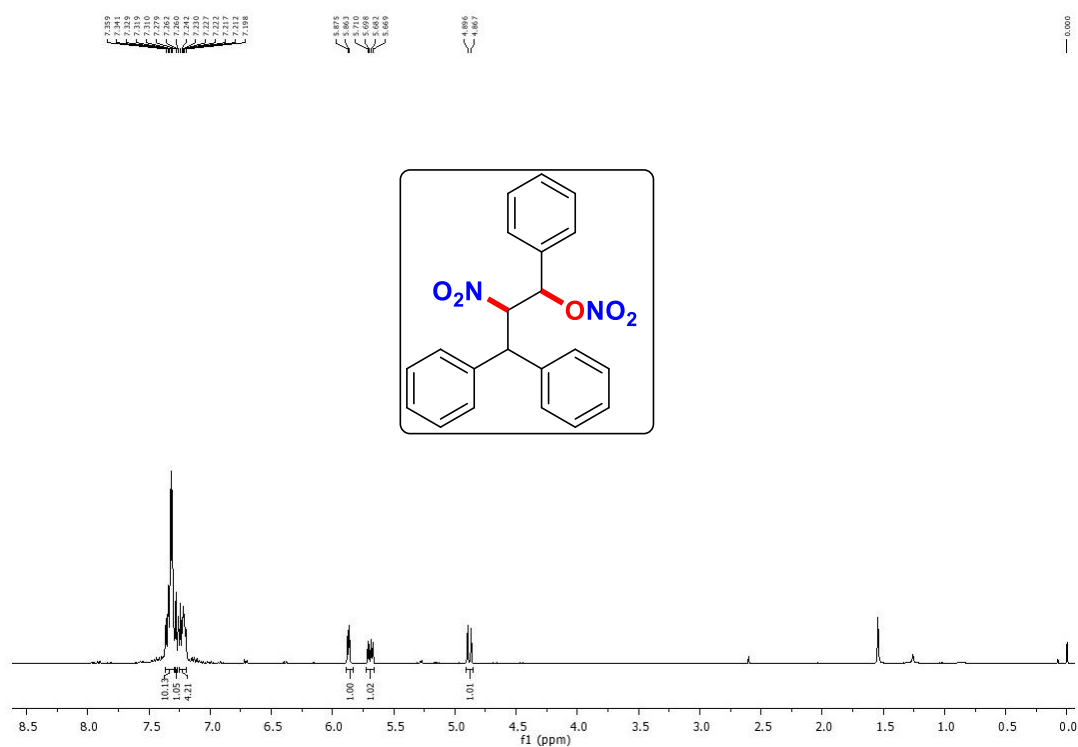
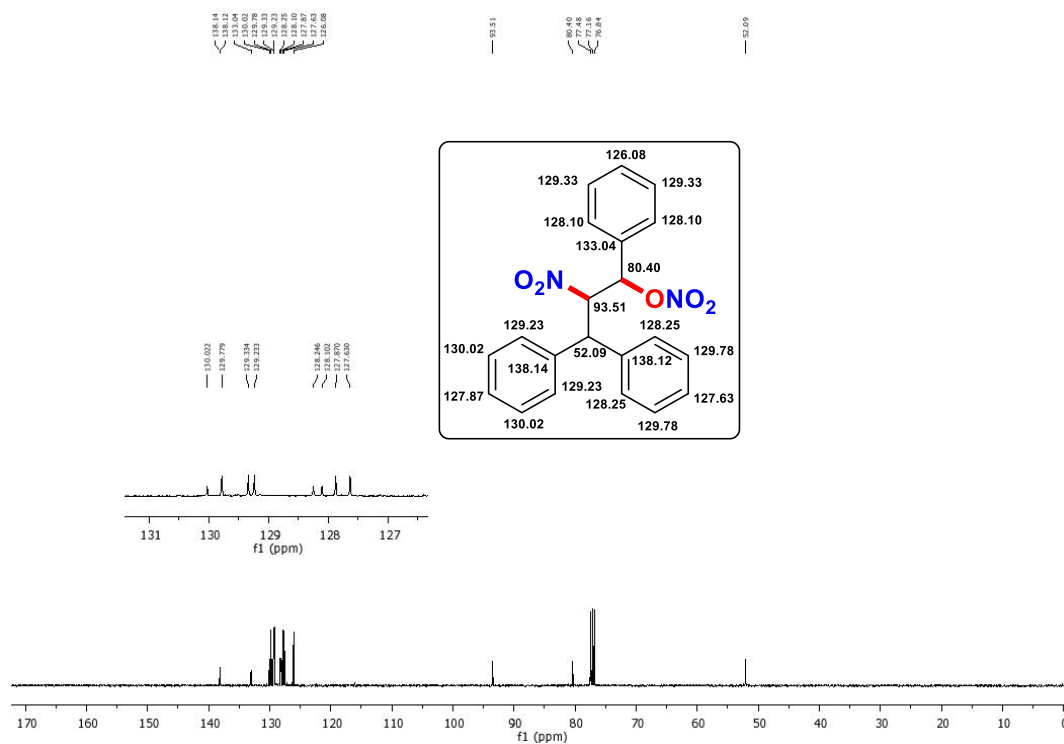
(E)-1,3,5-Trimethyl-2-(2-nitrovinyl)benzene (28a):

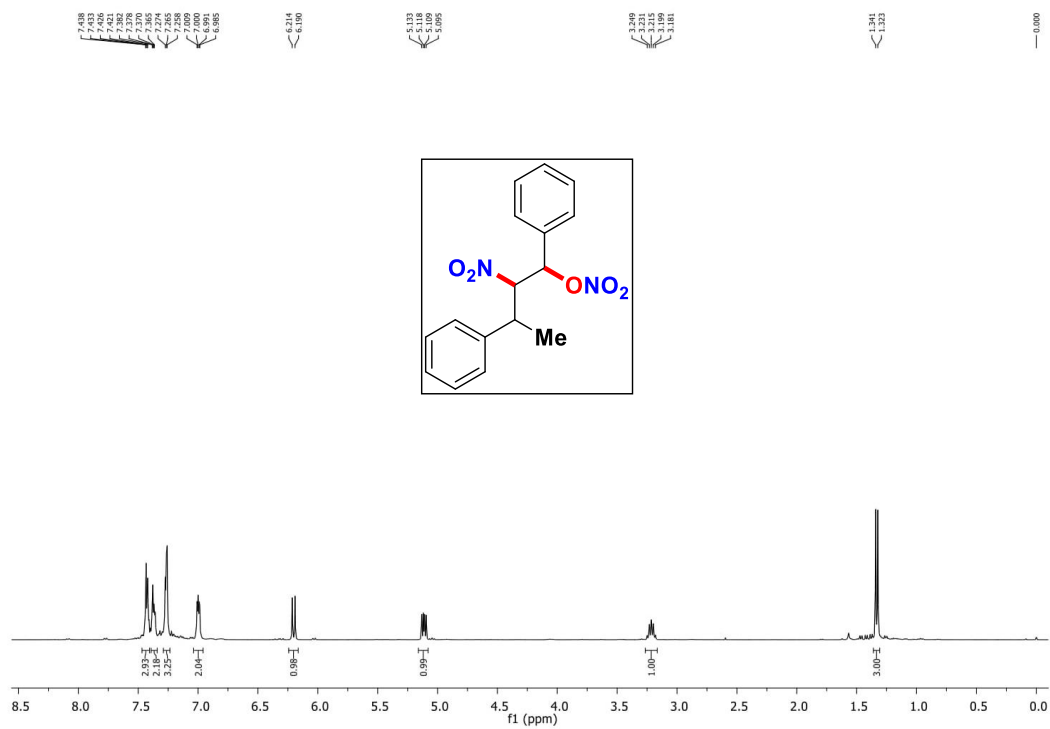
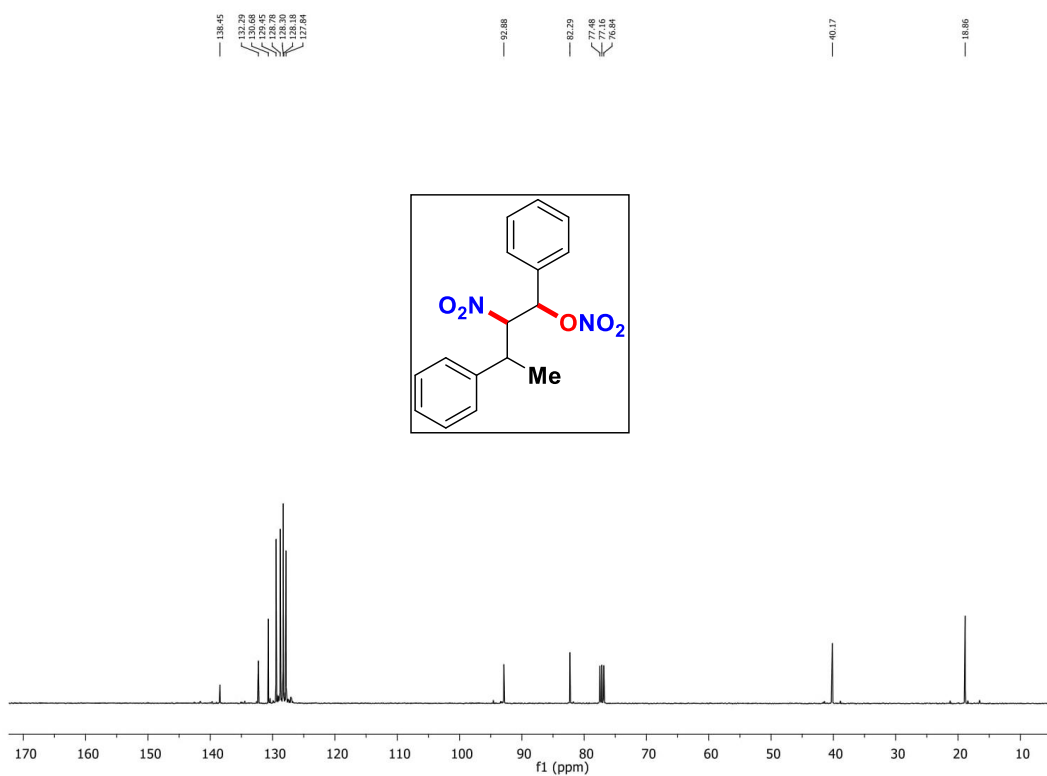
Yellow solid, (56 mg, 59%), m. p. 122–125 °C. ^1H NMR (400 MHz, CDCl_3) δ 8.27 (d, $J = 13.9$ Hz, 1H), 7.31 (d, $J = 13.9$ Hz, 1H), 6.95 (s, 2H), 2.39 (s, 6H), 2.31 (s, 3H) ppm. ^{13}C NMR (101 MHz, CDCl_3) δ 141.01, 139.82, 138.61, 136.72, 130.02, 125.88, 21.67, 21.34 ppm. IR (KBr, cm^{-1}): 2918, 1627, 1604, 1500, 1329, 1149, 1032, 967, 922, 799, 751, 716; HRMS (ESI/Q-TOF) m/z : Calcd for $\text{C}_{11}\text{H}_{13}\text{NaNO}_2$ [$\text{M} + \text{Na}$] $^+$ 214.0838, found 214.0847.

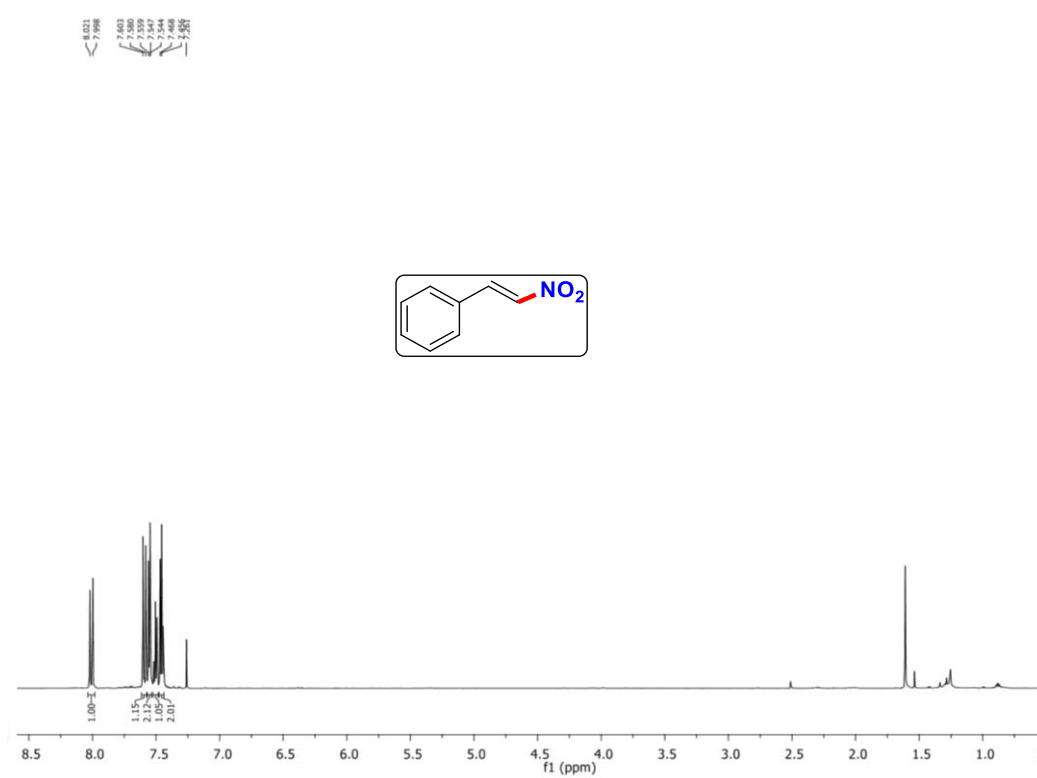
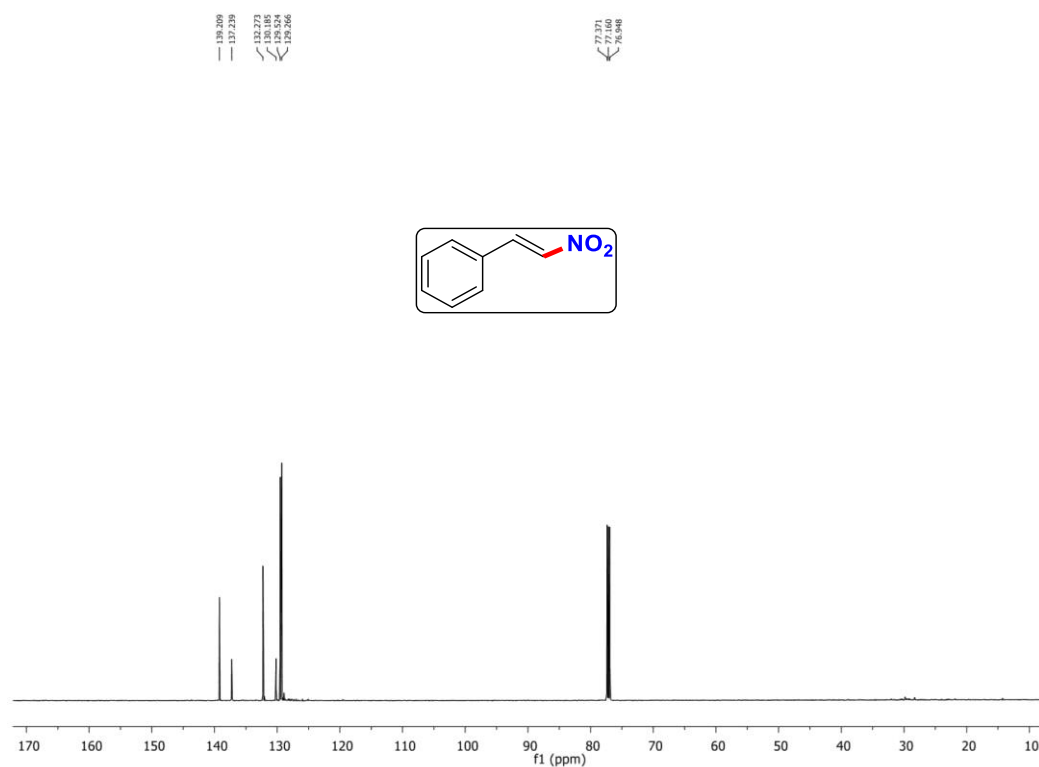
(E)-2-(2-Nitrovinyl)naphthalene (29a):

Yellow solid, (57 mg, 57%), m. p. 129–132 °C. ^1H NMR (400 MHz, CDCl_3) δ 8.14 (d, $J = 13.6$ Hz, 1H), 7.99 (s, 1H), 7.89–7.85 (m, 3H), 7.68 (d, $J = 13.6$ Hz, 1H), 7.63–7.53 (m, 3H) ppm. ^{13}C NMR (101 MHz, CDCl_3) δ 139.34, 137.25, 135.03, 133.26, 132.39, 129.48, 128.95, 128.51, 128.06, 127.66, 127.40, 123.44 ppm. IR (KBr, cm^{-1}): 3106, 1625, 1503, 1328, 1267, 1169, 960, 872, 821, 750, 710; HRMS (ESI/Q-TOF) m/z : Calcd for $\text{C}_{12}\text{H}_9\text{NaNO}_2$ [$\text{M} + \text{Na}$] $^+$ 222.0525, found 222.0531.

IV.7. Spectra

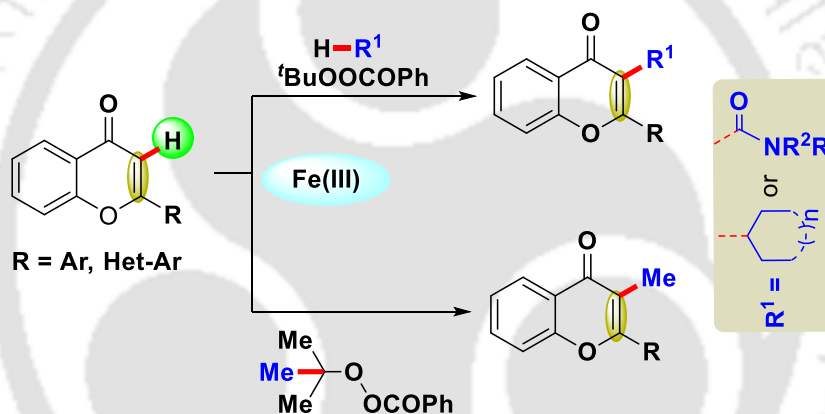
2-Nitro-1,3,3-triphenylpropyl nitrate (1a): ^1H NMR (CDCl_3 , 400 MHz)2-Nitro-1,3,3-triphenylpropyl nitrate (1a): ^{13}C NMR (CDCl_3 , 101 MHz)

2-Nitro-1,3-diphenylbutyl nitrate (18a): ^1H NMR (CDCl_3 , 400 MHz)**2-Nitro-1,3-diphenylbutyl nitrate (18a): ^{13}C NMR (CDCl_3 , 151 MHz)**

(E)-(2-Nitrovinyl)benzene (21a): ^1H NMR (CDCl_3 , 600 MHz)**(E)-(2-Nitrovinyl)benzene (21a): ^{13}C NMR (CDCl_3 , 151 MHz)**

CHAPTER V

Iron(III) Catalyzed Peroxide Mediated C-3 Functionalizations of Flavones



ABSTRACT: An iron(III) catalyzed C-3 functionalization of flavones has been achieved using tert-butyl peroxybenzoate (TBPB) / potassium persulphate ($\text{K}_2\text{S}_2\text{O}_8$) oxidant combinations with a suitable solvent. In the presence of iron(III) / tert-butyl peroxybenzoate / potassium persulphate, the reaction of flavones in cycloalkanes afforded exclusive C-3 cycloalkylation via $\text{C}_{\text{sp}2}\text{-C}_{\text{sp}3}$ coupling, whereas the solvent *N,N*-dialkylformamide provided C-3 amidation via $\text{C}_{\text{sp}2}\text{-C}_{\text{sp}2}$ coupling. Under identical reaction conditions just by switching the solvent to chlorobenzene, C-3 methylated flavones were obtained where tert-butyl peroxybenzoate (TBPB) served as the source of the methyl group.

CHAPTER V

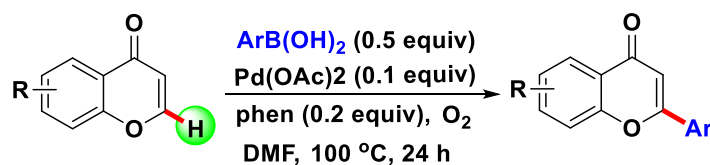
V. Iron(III) Catalyzed Peroxide Mediated C-3 Functionalizations of Flavones

V.1. Introduction

Transition metal-catalyzed C–H functionalization has undergone a renaissance in the past decade for the construction of carbon–carbon (C–C) and carbon–heteroatom (C–X) bonds.^[1] In this context, cross dehydrogenative coupling (CDC) protocols have emerged as a promising and powerful tool towards the formation of C_{sp}–C_{sp}, C_{sp}–C_{sp}² and C_{sp}²–C_{sp}² bonds.^[2] In recent times, this CDC protocol has even made progress for the formation of C_{sp}³–C bonds.^[3] In this context, cycloalkanes have been employed for CDC reactions in the absence^[4a-b] or presence of transition metal catalysts^[4c-g] albeit with limited examples. Aliphatic C_{sp}³–H bonds are the most available natural resource. Thus, methodologies for the direct functionalization of aliphatic C_{sp}³–H bonds will expand the synthetic toolbox, allowing access to value-added products with various important applications.

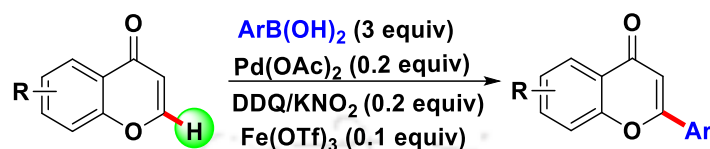
V.2. Strategies for α/β -Functionalizations of Chromones

Flavone (a type of chromone) is an important structural motif, present in many natural products and pharmaceutical molecules having a wide range of biological and pharmaceutical applications.^[5] Thus, any further derivatization on this moiety may generate potentially important candidates. To date, there are many examples where chromones have been employed as the coupling partner for regioselective β -functionalization (sp^2 -functionalization). In this context, Shafiee group reported the palladium-catalyzed β -arylation of chromones by coupling of chromones with arylboronic acids. This coupling was achieved by using a combination of ligand (1,10-phenanthroline) and O₂ along with Pd(OAc)₂ catalyst to yield a variety of flavones [Scheme V.2.1].^[6a]



Scheme V.2.1. β -Functionalization of chromones involving sp^2 carbon

Hong group also reported a palladium-catalyzed β -functionalization of chromones by coupling chromones with arylboronic acids. This functionalization proceeds via conjugate addition of arylboronic acids to chromones (Scheme V.2.2). This coupling was achieved by using catalytic amounts of $\text{Fe}(\text{OTf})_3$ as a Lewis acid and DDQ and KNO_2 as oxidants to yield a variety of flavones as major products (Scheme V.2.2).^[6b]



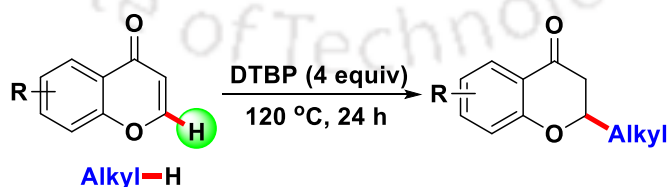
Scheme V.2.2. β -Functionalization of chromones involving sp^2 carbon

Latter on Antonchick group reported the β -alkylation of chromones and (thio) chromones by using both acyclic as well as cyclic alkanes. This 1,4-radical addition of alkyl radicals to chromones was achieved by using a combination hypervalent iodine ($\text{PhI}(\text{O}_2\text{CCF}_3)_2$) oxidant and sodium azide (NaN_3) additive to access a variety of flavones and (thio) flavones (Scheme V.2.3).^[4b]



Scheme V.2.3. β -Functionalization of chromones and thio-chromones

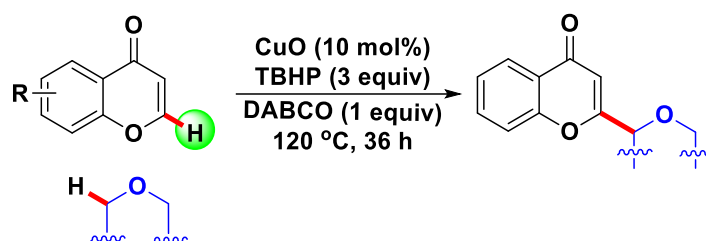
Han and coworkers also reported the β -alkylation of chromones. This alkylation was achieved via 1,4-conjugate radical addition of alkanes to chromones. This coupling was done by using both cyclic as well as acyclic alkanes in combination with di-tertiary butyl peroxide (DTBP) to yield a variety of β -alkylated chromanones (Scheme V.2.4).^[6c]



Scheme V.2.4. β -Functionalization of chromones involving sp^2 carbon

Recently, Ge group reported the copper-catalyzed β -cross dehydrogenative coupling (CDC) of chromones by using both cyclic and acyclic ethers. This β -CDC was achieved by

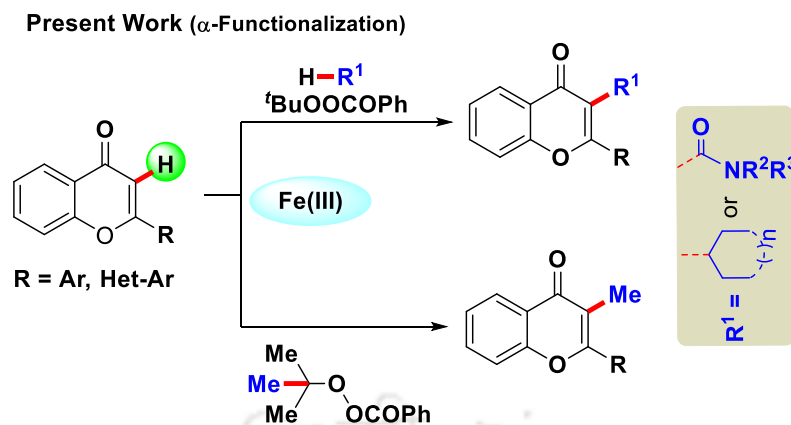
using a combination of oxidant (TBHP), base (DABCO) to yield a variety of β -alkylated chromones (Scheme V.2.5).^[6d]



Scheme V.2.5. β -Functionalization of chromones with ethers involving sp^2 C-H bond

Up to now, we have seen the alkylation of chromone where the source of an alkyl group is either cycloalkanes or cyclic ethers. In contrast, there are reports regarding peroxide mediated α -methylation although not on the chromone moiety but on other moieties such as methylation on pyrimidinones and pyridinones with dicumyl peroxide (DCP)^[7a] and *tert*-butyl peroxybenzoate (TBPB)-promoted direct α -methylation of 1,3-dicarbonyl compounds.^[7b] Both cycloalkanes and the cyclic ethers in presence of peroxides form radicals and act as a source of an alkyl group. Similar to this, formamides such as dimethylformamide are also known to generate formamide radical in presence of peroxides and act as a source of formamide. In this connection, peroxide mediated formamidation has been reported with some important moieties such as azoles,^[8a] 2-picolinamides,^[8b] α -oxocarboxylic.^[8c] Thus, in order to expand the scope of chromone functionalizations, alkylation and formamidation of chromones can be tried with peroxides and formamides respectively.

If both α and β -positions are available as in the case of chromone, regioselective functionalization can occur at its β -position (previous reports) but not at the more nucleophilic α -position. We speculated that if the β -position is substituted with a stabilizing group such as aryl as in flavones, the functionalization might occur at the nucleophilic α -position of flavone via a radical pathway (present work, Scheme V.2.6).



Scheme V.2.6. Strategies for α -functionalization of flavones

V.3. Present Work

Herein, we have developed conditions for the selective α -cycloalkylation, formamidation and methylation of flavones. Some of these α -functionalized flavones such as flavoxate (brand name: urispas), dimeflin and bisflavone possessing potential pharmaceutical applications are shown in Figure V.3.1.^[9]

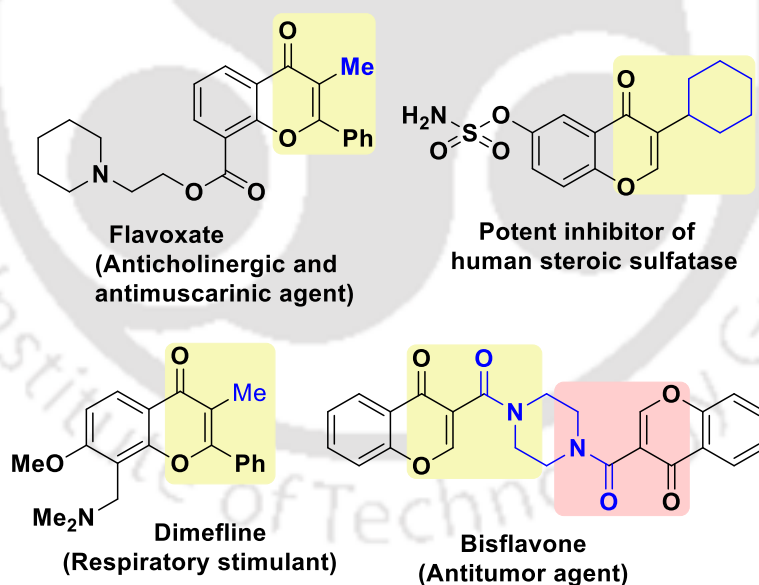


Figure V.3.1. α -Functionalized bioactive flavones

Optimization of Reaction Conditions. Taking cues from the functionalization of chromone derivatives with cyclic ethers as reported by Ge *et al.*,^[6d] a coupling reaction between flavone (**1**) and cyclohexane (**a**) was carried out. Our initial investigation started with the evaluation of reaction conditions for oxidative α -functionalization of flavone (**1**) with cyclohexane (**a**).

Flavone (**1**) was chosen as the model substrate as this core represents a highly privileged and biologically important molecular scaffold.^[5] Initially flavone (**1**) was treated with cyclohexane (**a**) in the presence of a well-explored iron(III) acetylacetonate [Fe(acac)₃] (20 mol%) catalyst, *tert*-butyl hydroperoxide (TBHP) (1.5 equiv) as the oxidant and 1,4-diazabicyclo[2.2.2]octane (DABCO) (1 equiv) as the base in 1,2-dichloroethane (DCE) (2.0 mL). A new product was isolated in a mere yield of 16%, after column chromatographic separation. Spectroscopic (¹H and ¹³C NMR) analysis of the product (**1a**) revealed the presence of a cyclohexyl unit in flavone and disappearance of the α -proton at 6.84 ppm (entry 1, Table V.3.1). This confirmed the α -functionalization of flavone to a 3-cyclohexylflavone along with the retention of α,β -double C=C bond. The structure of the compound (**1a**) was further ascertained by X-ray crystallographic analysis as shown in (Fig. V.3.2).

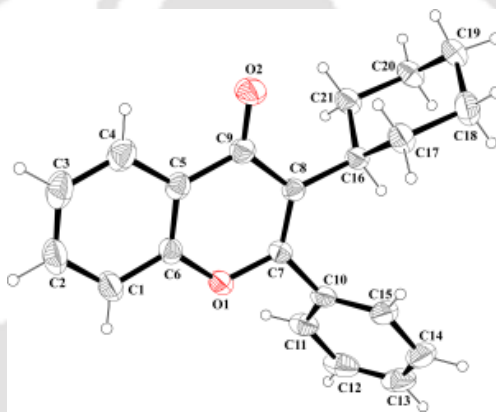
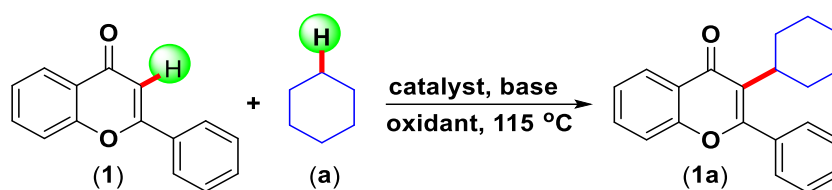


Figure. V.3.2. ORTEP molecular diagram of (**1a**)

This reaction was further screened by varying the oxidants from TBHP to di-*tert*-butylperoxide (DTBP), benzoyl peroxide (BP) and *tert*-butyl peroxybenzoate (TBPB) using only cyclohexane as the solvent cum reagent (entries 2-4, Table V.3.1). It was observed that TBPB provided better yield (28%) compared to other oxidants tested. To further improve the product yield, various oxidant combinations were employed in place of a single oxidant. It was found that the use of co-oxidant (additive) oxone® along with TBPB improved the product yield up to 41% (entry 5, Table V.3.1). By changing the additive from oxone® to potassium persulphate (K₂S₂O₈) the product yield improved up to 69% (entry 6, Table V.3.1). Again the use of other iron catalysts such as FeCl₃ and FeCl₂ was found inferior (entries 7-8, Table V.3.1). Switching to copper catalysts from iron catalysts such as Cu(OAc)₂ and CuCl₂ did not afford any trace of the desired product (**1a**) (entries 9-10, Table V.3.1). The use of organic bases such as bicyclo[2.2.1]hept-2-ene (DBU), 4-dimethylamino-pyridine (DMAP) or pyridine instead of

Table V.3.1. Screening of the reaction conditions^[a-c]

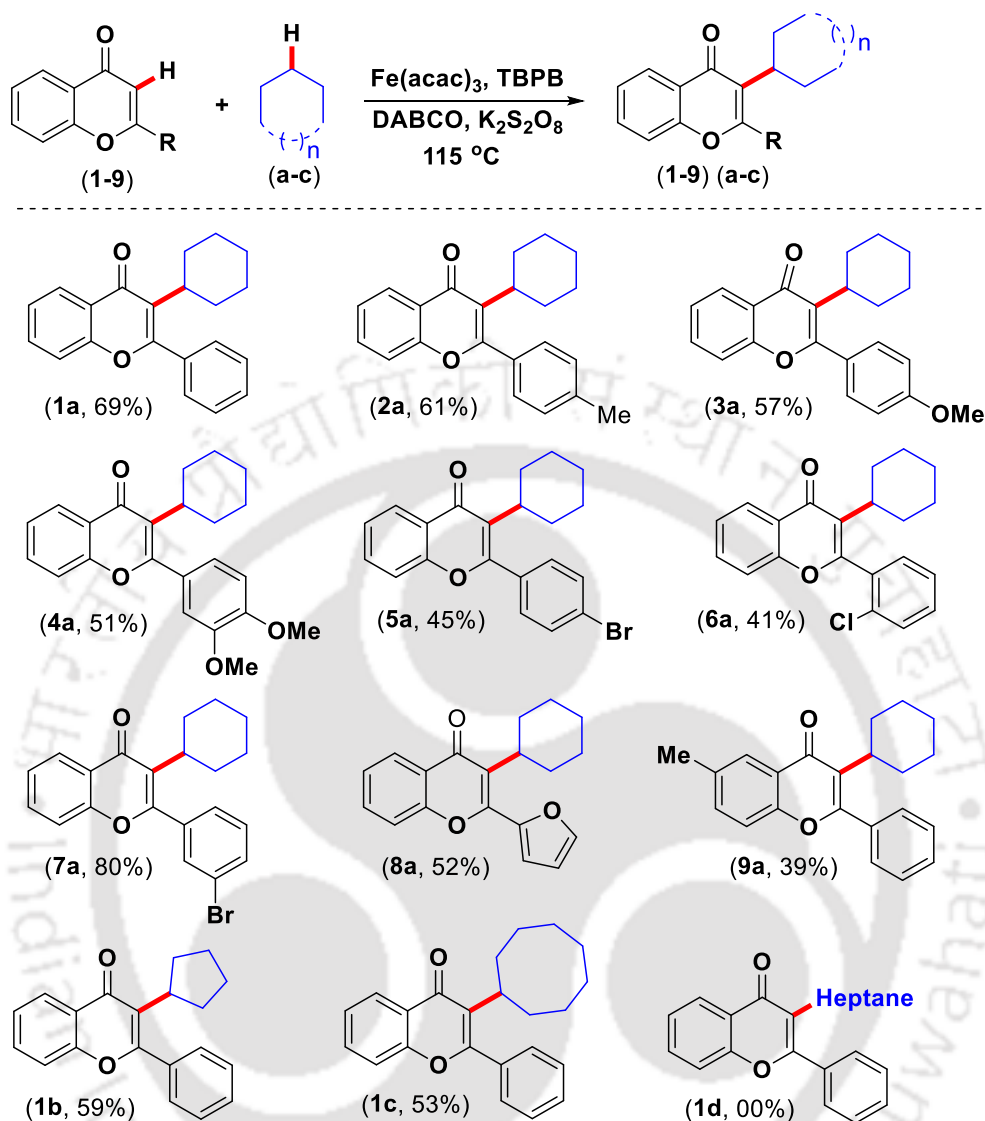
Entry	Catalyst (mol%)	Base (1 equiv)	Oxidant/Additive (3/1 equiv)	Yield (%) ^[a,b]
1	Fe(acac) ₃ (20)	DABCO	TBHP	16 ^[c]
2	Fe(acac) ₃ (20)	DABCO	DTBP	10
3	Fe(acac) ₃ (20)	DABCO	BP	13
4	Fe(acac) ₃ (20)	DABCO	TBPB	28
5	Fe(acac) ₃ (20)	DABCO	TBPB/Oxone [®]	41
6	Fe(acac)₃ (20)	DABCO	TBPB/K₂S₂O₈	69
7	FeCl ₃ (20)	DABCO	TBPB/K ₂ S ₂ O ₈	35
8	FeCl ₂ (20)	DABCO	TBPB/K ₂ S ₂ O ₈	00
9	Cu(OAc) ₂ (20)	DABCO	TBPB/K ₂ S ₂ O ₈	00
10	CuCl ₂ (20)	DABCO	TBPB/K ₂ S ₂ O ₈	00
11	Fe(acac) ₃ (20)	DBU	TBPB/K ₂ S ₂ O ₈	12
12	Fe(acac) ₃ (20)	DMAP	TBPB/K ₂ S ₂ O ₈	29
13	Fe(acac) ₃ (20)	Pyridine	TBPB/K ₂ S ₂ O ₈	27
14	Fe(acac) ₃ (10)	DABCO	TBPB/K ₂ S ₂ O ₈	54
15	Fe(acac) ₃ (30)	DABCO	TBPB/K ₂ S ₂ O ₈	71
16	-	-	TBPB/K ₂ S ₂ O ₈	<5

^[a]Reaction conditions: (1) (0.50 mmol), catalyst (20 mol%), base (0.50 mmol), oxidant (1.50 mmol) additive (0.50 mmol) in cyclohexane (a) (2.0 mL) at 115 °C for 12 h. ^[b]Isolated yield. ^[c]1,2-dichloroethane (2.0 mL).

DABCO provided the desired α -cycloalkylated product (**1a**) in lower yields (entries 11-13, Table V.3.1). Furthermore, decreasing the catalyst loading [Fe(acac)₃] to 10 mol% lowered the product yield to 54%. However, an increase in the catalyst loading to 30 mol% did not improve the yield (**1a**, 71%) significantly (entries 14 and 15, Table V.3.1). In the absence of iron(III) catalyst only a trace (<5%) of the desired cycloalkylated product (**1a**) (entry 16, Table V.3.1) was obtained thereby confirming the active involvement of iron(III) in this reaction.

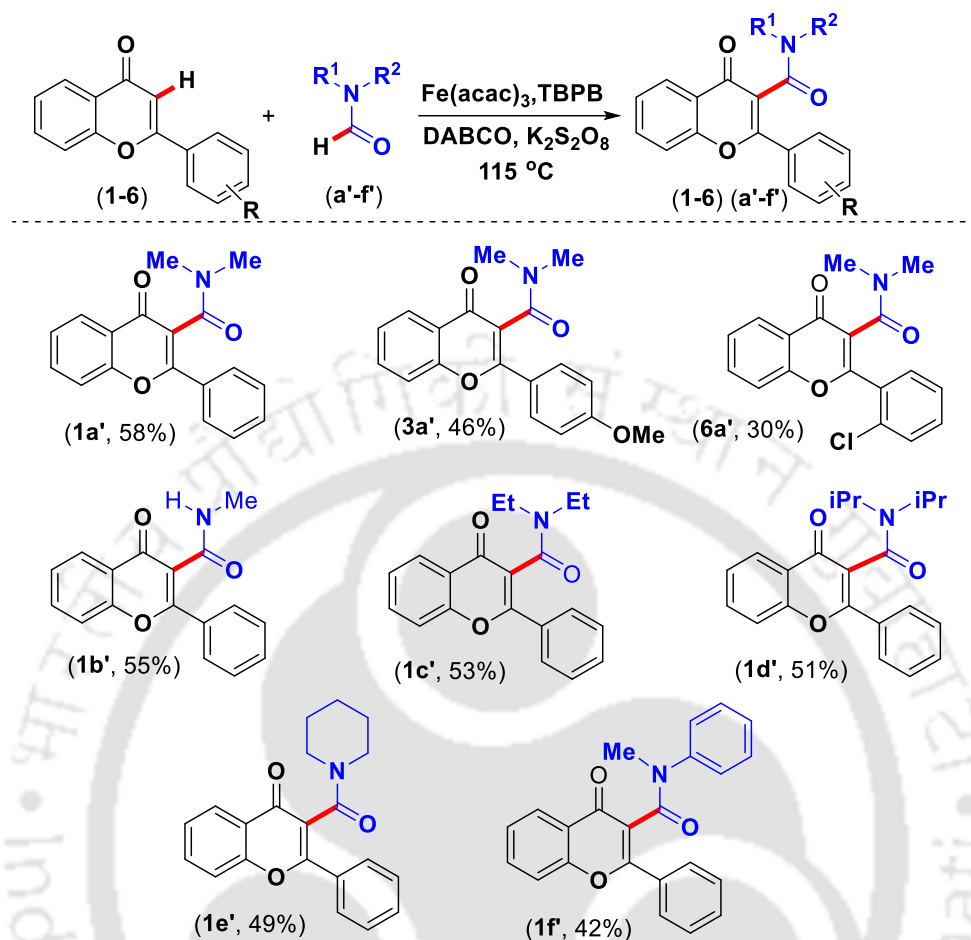
Substrate Scope for α -Cycloalkyl Flavones. After establishing the optimized reaction conditions for α -cycloalkylation, we explore the coupling between various flavones (**1-9**) with other cycloalkanes (**a-c**). The 2-Aryl rings of flavone bearing electron-donating as well as electron-withdrawing substituents, were all compatible providing their desired α -cycloalkylated products. Flavones containing electron-donating substituents such as *p*-Me (**2**), *p*-OMe (**3**) in their 2-aryl rings provided the desired products (**2a**) and (**3a**) in 61% and 57% yields respectively (Scheme V.3.1). The 2-Aryl ring of flavones bearing two electron-donating groups such as 3,4-di-OMe (**4**) when reacted with cyclohexane (**a**) to afforded α -cycloalkylated product (**4a**) in moderate yield (51%). Electron-withdrawing substituents such as *p*-Br (**5**), *o*-Cl (**6**) and *m*-Br (**7**) present in the 2-aryl ring of flavones also underwent oxidative functionalization giving their corresponding products (**5a**, 45%), (**6a**, 41%) and (**7a**, 80%) (Scheme V.3.1). In addition to this, flavone possessing 2-heteroaryl ring and methyl substitution in the fused aromatic ring also reacted successfully and provided their corresponding products (**8a**, 52%) and (**9a**, 39%). To evaluate the scope and generality of this strategy, reactions of flavone (**1**) with other cycloalkanes such as cyclopentane (**b**) and cyclooctane (**c**) were investigated. Cyclopentane (**b**) and cyclooctane (**c**) when coupled with flavone (**1**) under the optimized reaction conditions resulted in α -cycloalkylated products (**1b**, 59%) and (**1c**, 53%) in moderate yields (Scheme V.3.1). When flavone (**1**) was coupled with an open chain alkane such as heptane under the optimized reaction conditions it did not afford any trace of the desired product (**1d**).

Scheme V.3.1. α -Cycloalkylation of flavone using cycloalkane^[a,b]



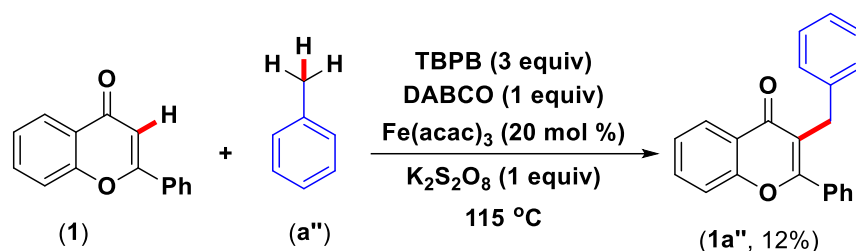
^[a]Reaction conditions: (1-9) (0.50 mmol), $[\text{Fe}(\text{acac})_3]$ (20 mol%), DABCO (0.50 mmol), TBPB (1.50 mmol), $\text{K}_2\text{S}_2\text{O}_8$ (0.50 mmol) in cycloalkane (a-c) (2.0 mL) at $115\text{ }^\circ\text{C}$ for 12 h. ^[b]Isolated yields.

Analogous to cycloalkane, formamide can also form a stable radical at the carbonyl carbon in the presence of a peroxide oxidant.^[8] Thus the idea is to generate α -amidation in place of α -cycloalkylation of flavones (1-9) under similar reaction conditions. After a series of screening runs it was found that chlorobenzene was the best solvent giving the expected α -amidated flavone in moderate yield (1a', 58%) during the reaction of flavone (1) with *N,N*-dimethyl formamide (a') (Scheme V.3.2). Flavones containing electron-donating as well as electron-withdrawing substituents present in their 2-aryl rings were functionalized efficiently

Scheme V.3.2. α -Amidation of flavone using *N,N*-dialkylformamides^[a,b]


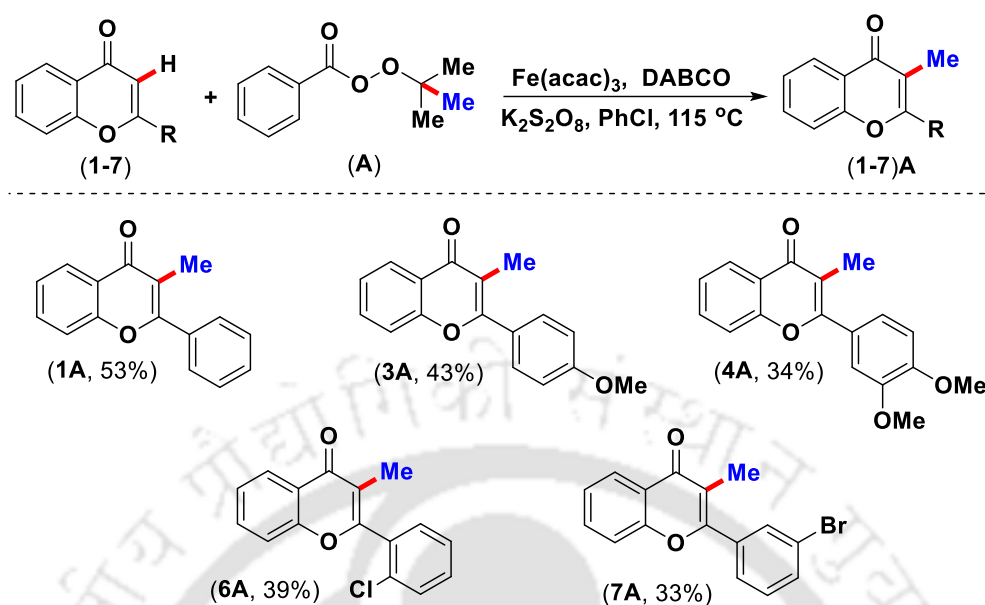
^[a]Reaction conditions: (1-6) (0.50 mmol), (a'-f') (1.0 mL), $[\text{Fe}(\text{acac})_3]$ (20 mol%), DABCO (0.50 mmol), TBPB (1.50 mmol), $\text{K}_2\text{S}_2\text{O}_8$ (0.50 mmol) at $115\text{ }^\circ\text{C}$ for 12 h. ^[b]Isolated yields.

with formamide (a') providing their respective α -amidated products (3a') and (6a') in 46% and 30% yields. The lower yield (30%) of the product obtained in the case of *o*-chloro substituted flavone (6) is possibly due to steric hindrance. Switching the amide from *N,N*-dimethylformamide (a') to *N*-methyl formamide (b'), *N,N*-diethylformamide (c') and *N,N*-diisopropyl-formamide (d') all afforded their desired α -amidated flavones in moderate yields (51-55%) when reacted with (1). Even the reactions of *N*-formylpiperidine (e') and *N*-methyl-*N*-phenylformamide (f') with flavone (1) provided their respective amidated products (1e') and (1f') in 49% and 42% yields respectively (Scheme V.3.2). Again, the reaction of alkylbenzene *viz.* toluene (a'') in instead of cycloalkane (a) or *N,N*-dialkylformamide (a') with flavone (1) under the present reaction conditions provided only a trace amount of α -benzylated flavone (1a''), 12% (Scheme V.3.3) along with a multitude of other side products.



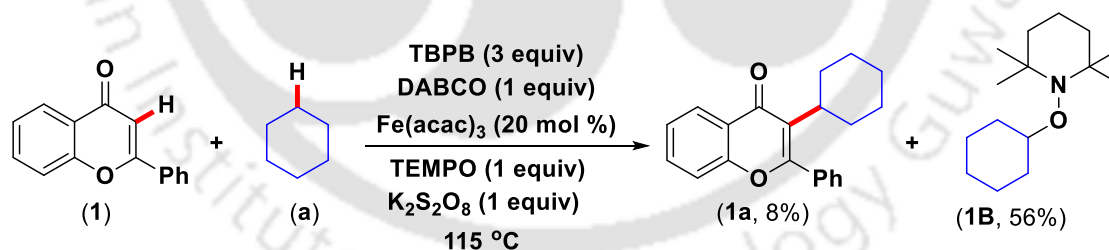
Scheme V.3.3. The reaction of flavone with alkylbenzene (toluene)

Furthermore, to check whether this reaction is feasible with an active methylene compound such as ethyl acetoacetate, the reaction of flavone (**1**) with ethyl acetoacetate was carried out in the presence of the Fe(III)/TBPB/K₂S₂O₈ combination. Spectroscopic analysis of the new isolated product (**1A**) showed the absence of the ethyl acetoacetate group. However, the product (**1A**, 22%) was found to have a singlet (–CH₃) at 2.17 ppm in its ¹H NMR and a peak at 11.9 ppm in its ¹³C NMR spectra confirming the presence of a methyl group at the α-site of the flavone (Scheme V.3.4). When the same reaction was carried out in the absence of ethyl acetoacetate, again the same α-methylated product was isolated (**1A**) in 27% yield. This confirms that the methyl group is originating from the *tert*-butyl peroxybenzoate (TBPB) (**A**). It may be mentioned here that such α-methylated flavones are present in drugs such as flavoxate (brand name: urispas) and dimeflin as shown in Figure V.3.1. After a series of screening runs, the reaction of flavone (**1**) under Fe(III)/TBPB/K₂S₂O₈ combinations in chlorobenzene afforded the optimum yield of α-methylated flavone (**1A**, 53%). Homolytic cleavage of TBPB provides a methyl radical and acetone from the *in situ* generated *tert*-butoxy radical which is the source of the methyl group.^[7b,10] To explore the generality of the strategy, the reaction of flavone containing both electron-donating and electron-withdrawing substituents present in its 2-aryl ring smoothly afforded α-methylated products (**3A**, 43%), (**4A**, 34%), (**6A**, 39%) and (**7A**, 33%) (Scheme V.3.4).

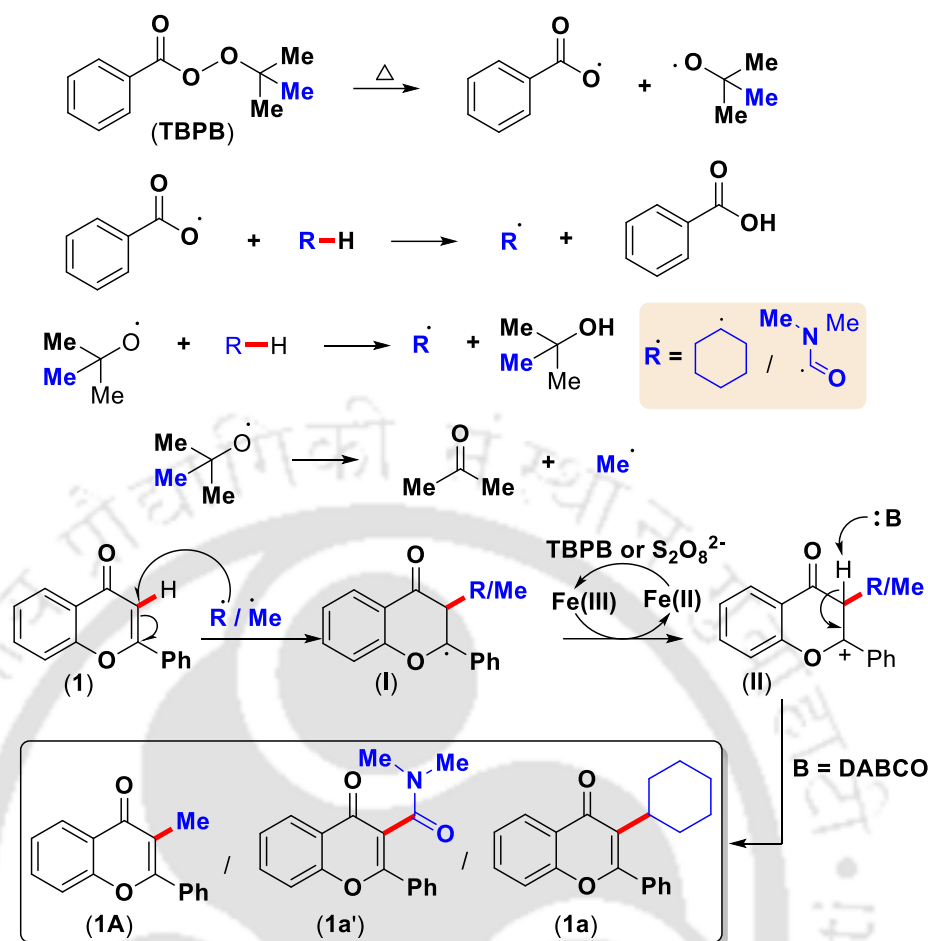
Scheme V.3.4. α -Methylation of flavone with *tert*-butyl peroxybenzoate (TBPB)^[a,b]

^[a]Reaction conditions: (1-7) (0.50 mmol), $[\text{Fe}(\text{acac})_3]$ (20 mol%), DABCO (0.50 mmol), TBPB (1.50 mmol), $\text{K}_2\text{S}_2\text{O}_8$ (0.50 mmol), in chlorobenzene (2.0 mL) at 115 °C for 12 h. ^[b]Isolated yields.

To check the radical nature of this reaction when flavone (**1**) was reacted with cyclohexane (**a**) in the presence of a radical scavenger TEMPO (**B**), only a trace of the α -cycloalkylated product (**1a**, 8%) was formed. However, the formation of TEMPO-cyclohexyl adduct (**1B**, 56%) confirms the radical nature for this reaction (Scheme V.3.5.).

**Scheme V.3.5.** Radical trapping experiment of flavone with cyclohexane

Based on experiments performed and from earlier literature reports, a plausible mechanism is depicted for this α -functionalization of flavone (**1**). This reaction is initiated by the thermal homolytic cleavage of the peroxide oxidant *tert*-butyl peroxybenzoate (TBPB) at 115 °C to peroxybenzoate radical and *tert*-butoxy radical. Both these radicals can abstract a proton from cyclohexane (**a**) or N,N-dimethylformamide (**a'**). Radical addition of any of these species (**R** or **Me**) across the α,β -C=C double bond of flavone (**1**) afforded stable benzyl radical species (**I**). This radical species (**I**) further generates a cationic intermediate (**II**) via the



Scheme V.3.6. A plausible mechanism for α -functionalizations

reduction of a Fe(III) catalyst to Fe(II). This Fe(II) species is converted to active Fe(III) catalyst via peroxide or persulphate mediated one-electron oxidation. In the final step, base (DABCO) abstracts the α -proton to reinstall the α,β -C=C double bond affording the α -functionalized flavones (**1a**) or (**1a'**) (Scheme V.3.6). In the absence of any radical forming active coupling solvents such as cyclohexane (**a**) or N,N-dimethylformamide (**a'**), TBPB generates a methyl radical from *tert*-butoxy radical along with the formation of acetone. This methyl radical adds across the α,β -C=C double bond of flavone providing the α -methylated flavone (**1A**) in a similar manner (Scheme V.3.6).

In summary, we have for the first time demonstrated a Fe(III) catalyzed α -cycloalkylation, amidation and methylation of flavones using suitable oxidant/solvent combinations. A broad range of flavones, cycloalkanes and dialkyl-formamides are tolerated under the reaction conditions. The practical advantages of this strategy are the use of solvents such as cyclohexane, dimethylformamide as the reactive coupling partners with flavones. This method

offers a novel and convenient route for the synthesis of α -functionalized flavones, which can be extended for the synthesis of drugs such as flavoxate and dimeflin.

V.4. Experimental Section

V.4.1. General Information. All the reagents were commercial grade and purified according to the established procedures. Organic extracts were dried over anhydrous sodium sulphate. Solvents were removed in a rotary evaporator under reduced pressure. Silica gel (60-120 mesh size) was used for the column chromatography. Reactions were monitored by TLC on silica gel 60 F₂₅₄ (0.25mm). NMR spectra were recorded in CDCl₃ with tetramethylsilane as the internal standard for ¹H NMR (400 and 600 MHz) CDCl₃ solvent as the internal standard for ¹³C NMR (100 and 151 MHz). HRMS spectra were recorded using +ESI (TOF) mode. IR spectra were recorded in KBr or neat. All the reagents and solvents were procured either from Sigma Aldrich, Alfa aesar or Merck. Starting flavones were prepared by reacting 2-hydroxyacetophenone derivatives with benzaldehyde derivatives following the literature procedure (M. Cabrera *et.al.* / *Bioorg. Med. Chem.* **2007**, *15*, 3356-3367). The catalyst iron(III)acetylacetonate (97% pure) was procured from Sigma Aldrich [CAS NO: 14024-18-1, Product code 101490459, Lot # MKBP3040V]. Further purity of the catalyst was checked ICP analysis. As per the ICP analysis, an amount of 0.028 mg/L of Pd is found to be coexisting with the catalyst having Fe 555.7 mg/L. No trace of any other metals could be detected.

V.4.2. Crystallographic Description:

Crystal data were collected with Bruker Smart Apex-II CCD diffractometer using graphite monochromated MoK α -radiation ($\lambda = 0.71073 \text{ \AA}$) at 298 K. Cell parameters were retrieved using SMART^[a] software and refined with SAINT^[a] on all observed reflections. Data reduction was performed with the SAINT software and corrected for Lorentz and polarization effects. Absorption corrections were applied with the program SADABS^[b]. The structure was solved by direct methods implemented in SHELX-97^[c] program and refined by full-matrix least-squares methods on F₂. All non-hydrogen atomic positions were located in difference Fourier maps and refined anisotropically. The hydrogen atoms were placed in their geometrically generated positions. Colourless crystals were isolated in a rectangular shape from acetonitrile at room temperature.

[a] SMART V 4.043 Software for the CCD Detector System; Siemens Analytical Instruments Division: Madison, WI, 1995.

[b] SAINT V 4.035 Software for the CCD Detector System; Siemens Analytical Instruments Division: Madison, WI, 1995.

[c] Sheldrick, G. M. SHELXL-97, Program for the Refinement of Crystal Structures; University of Göttingen: Göttingen (Germany), 1997.

CCDC Number for Compound 1a: CCDC 1476816. This data can be obtained free of charge from the Cambridge Crystallographic Data Centre via www.ccdc.cam.ac.uk/datarequest/cif.

Crystallographic Description of 1a: Crystal dimension (mm): 0.28 x 0.23 x 0.19. C₂₁H₂₀O₂, Mr = 304.37. triclinic, space group 'p -1'; a = 9.1619(17) Å, b = 10.216(2) Å, c = 10.489(2) Å; $\alpha = 67.76(2)^\circ$, $\beta = 83.945(16)^\circ$, $\gamma = 68.57(2)^\circ$, V = 845.4(3) Å³; Z = 2; $\rho_{\text{cal}} = 1.196 \text{ g/cm}^3$; $\mu (\text{mm}^{-1}) = 0.075$; $F(000) = 324.0$; Reflection collected / unique = 3817 / 1917; Refinement method = Full-matrix least-squares on F^2 ; Final R indices [$I > 2\sigma(I)$] R1 = 0.0601, wR2 = 0.1727, R indices (all data) R1 = 0.1232, wR2 = 0.2476; goodness of fit = 0.896.

V.4.3. Synthesis of α -functionalized flavones:

V.4.3. General Procedure for the Synthesis of 3-Cyclohexyl-2-phenyl-4H-chromen-4-one (1a) from 2-Phenyl-4H-chromen-4-one (1): To an oven-dried 10.0 mL round bottom flask were added sequentially 2-phenyl-4H-chromen-4-one (**1**) (0.111 g, 0.5 mmol), DABCO (0.056 g, 0.5 mmol), Fe(acac)₃ (0.035 g, 0.01 mmol), K₂S₂O₈ (0.135 g, 0.5 mmol), and TBPB (0.291 g, 1.5 mmol) in cyclohexane (2.0 mL). The reaction mixture was then stirred in an oil bath at 115 °C. After completion of the reaction (12 h) the crude product was admixed with ethyl acetate (25.0 mL) and the organic layer was washed with saturated sodium bicarbonate solution (2.0 x 10.0 mL), dried over anhydrous sodium sulphate (Na₂SO₄) and evaporated under reduced pressure. The resulting crude product was purified by silica gel column chromatography (hexane / ethyl acetate, 99.5:0.5) to give pure 3-cyclohexyl-2-phenyl-4H-chromen-4-one (**1a**); 0.105 g, yield: (69%). The identity and purity of the product were confirmed by spectroscopic analysis.

V.4.3. General Procedure for the Synthesis of N,N-Dimethyl-4-oxo-2-phenyl-4H-chromene-3-carboxamide (1a') from 2-Phenyl-4H-chromen-4-one (1): To an oven-dried 10.0 mL round bottom flask were added sequentially 2-phenyl-4H-chromen-4-one (**1**) (0.111 g, 0.5 mmol), DABCO (0.056 g, 0.5 mmol), Fe(acac)₃ (0.035 g, 0.01 mmol), TBPB (0.291 g, 1.5 mmol) and K₂S₂O₈ (0.135 g, 0.5 mmol), in DMF (1.0 mL). The reaction mixture was further stirred in an oil bath at 115 °C. After completion of the reaction (12 h) the crude product was

admixed with ethyl acetate (25.0 mL) and the organic layer was washed with saturated sodium bicarbonate solution (2.0 x 10.0 mL), dried over anhydrous sodium sulphate (Na_2SO_4) and evaporated under reduced pressure. The resulting crude product was purified by silica gel column chromatography (hexane / ethyl acetate, 30:70) to give pure *N,N*-dimethyl-4-oxo-2-phenyl-4*H*-chromene-3-carboxamide (**1a'**); yield: 0.085 g (58%). The identity and purity of the product were confirmed by spectroscopic analysis.

V.4.3. General Procedure for the Synthesis of 3-Methyl-2-phenyl-4*H*-chromen-4-one (1A) from 2-Phenyl-4*H*-chromen-4-one (1): To an oven-dried 10.0 mL round bottom flask were added sequentially 2-phenyl-4*H*-chromen-4-one (**1**) (0.111 g, 0.5 mmol), DABCO (0.056 g, 0.5 mmol), $\text{Fe}(\text{acac})_3$ (0.035 g, 0.01 mmol), $\text{K}_2\text{S}_2\text{O}_8$ (0.135 g, 0.5 mmol), TBPB (0.291 g, 1.5 mmol) in chlorobenzene (2.0 mL). The reaction mixture was then stirred in an oil bath at 115 °C. After completion of the reaction (12 h) the crude product was admixed with ethyl acetate (25.0 mL) and the organic layer was washed with saturated sodium bicarbonate solution (2.0 x 10.0 mL), dried over anhydrous sodium sulphate (Na_2SO_4) and evaporated under reduced pressure. The resulting crude product was purified by silica gel column chromatography (hexane / ethyl acetate, 99:1) to give pure 3-methyl-2-phenyl-4*H*-chromen-4-one (**1A**); yield: 0.063 g (53%). The identity and purity of the product were confirmed by spectroscopic analysis.

V.4.4. Mechanistic Investigation:

V.4.4. Trapping of Radical Intermediates with Radical Scavenger TEMPO: An oven-dried 10.0 mL round bottom flask was charged with 2-phenyl-4*H*-chromen-4-one (**1**) (0.111 g, 0.5 mmol), DABCO (0.056 g, 0.5 mmol), $\text{Fe}(\text{acac})_3$ (0.035 g, 0.01 mmol), $\text{K}_2\text{S}_2\text{O}_8$ (0.135 g, 0.5 mmol), TEMPO (0.078 g, 0.5 mmol), TBPB (0.291g, 1.5 mmol) in cyclohexane (**a**) (2.5 mL). The flask was fitted to a reflux condenser and the reaction mixture was stirred in an oil bath at 115 °C for 12 h. After completion of the reaction, the crude product was admixed with ethyl acetate (25.0 mL) and the organic layer was washed with saturated sodium bicarbonate solution (2.0 x 10.0 mL), dried over anhydrous sodium sulphate (Na_2SO_4) and evaporated under reduced pressure. The resulting crude product was purified by silica gel column chromatography (hexane) to give cyclohexyl-TEMPO adduct 1-(cyclohexyloxy)-2,2,6,6-tetramethylpiperidine (**1B**) in (56%) yield and the desired product only in trace amount (8%) (**1a**). This experiment supports the *in situ*

generation of cyclohexyl radical from cyclohexane (**a**) induced by TBPB and also the radical nature of the reaction mechanism.

V.5. References

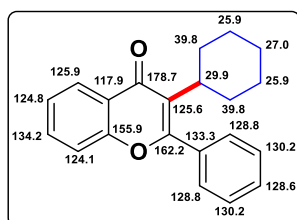
- [1] a) G. Dyker, *Handbook of C–H Transformations: Applications in Organic Synthesis*, Wiley-VCH: Weinheim, **2005**; b) T. W. Lyons, M. S. Sanford, *Chem. Rev.* **2010**, *110*, 1147-1169; c) D. A. Colby, R. G. Bergman, J. A. Ellman, *Chem. Rev.* **2010**, *110*, 624-655; d) J. Wencel-Delord, T. Droge, F. Liu, F. Glorius, *Chem. Soc. Rev.* **2011**, *40*, 4740-4761; e) S. H. Cho, J. Y. Kim, J. Kwak, S. Chang, *Chem. Soc. Rev.* **2011**, *40*, 5068-5083; f) C. L. Sun, B.-J. Li, Z.-J. Shi, *Chem. Rev.* **2011**, *111*, 1293-1314; g) L. Ackermann, *Chem. Rev.* **2011**, *111*, 1315-1345; h) S. A. Girard, T. Knauber, C. J. Li, *Angew. Chem. Int. Ed.* **2014**, *53*, 74-100; i) Z. Chen, B. Wang, J. Zhang, W. Yu, Z. Liu, Y. Zhang, *Org. Chem. Front.* **2015**, *2*, 1107-1295; j) F. Chen, T. Wang, N. Jiao, *Chem. Rev.* **2014**, *114*, 8613-8661.
- [2] a) C.-J. Li, *Acc. Chem. Res.* **2009**, *42*, 335-344; b) C. S. Yeung, V. M. Dong, *Chem. Rev.* **2011**, *111*, 1215-1292; c) C. Liu, H. Zhang, W. Shi, A. Lei, *Chem. Rev.* **2011**, *111*, 1780-1824; d) K. Hirano, M. Miura, *Chem. Commun.* **2012**, *48*, 10704-10714; e) S. I. Kozhushkov, L. Ackermann, *Chem. Sci.* **2013**, *4*, 886-896; f) C. Liu, J. Yuan, M. Gao, S. Tang, W. Li, R. Shi, A. Lei, *Chem. Rev.* **2015**, *115*, 12138-12204.
- [3] a) Z. Li, L. Cao, C.-J. Li, *Angew. Chem. Int. Ed.* **2007**, *46*, 6505-6507; b) A. J. Young, M. C. White, *J. Am. Chem. Soc.* **2008**, *130*, 14090-14091; c) Y. Z. Li, B. J. Li, X.-Y. Lu, S. Lin, Z.-J. Shi, *Angew. Chem. Int. Ed.* **2009**, *48*, 3817-3820; d) C. A. Correia, C. J. Li, *Adv. Synth. Catal.* **2010**, *352*, 1446-1450; e) E. Shi, Y. Shao, S. Chen, H. Hu, Z. Liu, J. Zhang, X. Wan, *Org. Lett.* **2012**, *14*, 3384-3387; f) H. Liu, G. Shi, S. Pan, Y. Jiang, Y. Zhang, *Org. Lett.* **2013**, *15*, 4098-5101; g) Z. Li, C. J. Li, *J. Am. Chem. Soc.* **2004**, *126*, 11810-11811; h) Z. Li, H. Li, X. Guo, L. Cao, R. Yu, H. Li, S. Pan, *Org. Lett.* **2008**, *10*, 803-805; i) T. Sugiishi, H. Nakamura, *J. Am. Chem. Soc.* **2012**, *134*, 2504-2507; j) Z. Xie, Y. Cai, H. Hu, C. Lin, J. Jiang, Z. Chen, L. Wang, Y. Pan, *Org. Lett.* **2013**, *15*, 4600-4603; k) G. Qin, X. Chen, L. Yang, H. Huang, *ACS Catal.* **2015**, *5*, 2882-2885; l) S. K. Rout, S. Guin, W. Ali, A. Gogoi, B. K. Patel, *Org. Lett.* **2014**, *16*, 3086-3089; m) G. Majji, S. Guin, A. Gogoi, S. K. Rout, B. K. Patel, *Chem. Commun.* **2013**, *49*, 3031-3033; n) A. Banerjee, S. K. Santra, A. Mishra, N. Khatun, B. K. Patel, *Org. Biomol. Chem.* **2015**, *13*, 1307-1312; o) A. Banerjee, S. K. Santra, N. Khatun, W. Ali, B. K. Patel, *Chem. Commun.* **2015**, *51*, 15422-

- 15425; p) S. K. Santra, A. Banerjee, S. Rajamanickam, N. Khatun, B. K. Patel, *Chem. Commun.* **2016**, 52, 4501-4504.
- [4] a) J. Ji, P. Liu, P. Sun, *Chem. Commun.* **2015**, 51, 7546-7549; b) R. Narayan, A. P. Antonchick, *Chem. Eur. J.* **2014**, 20, 4568-4572; c) G. Deng, L. Zhao, C. J. Li, *Angew. Chem. Int. Ed.* **2008**, 47, 6278-6282; d) Y. Zhang, C.-J. Li, *Eur. J. Org. Chem.* **2008**, 4654-4657; e) Y. Zhu, Y. Wei, *Chem. Sci.* **2014**, 5, 2379-2382; f) B. L. Tran, B. Li, M. Driess, J. F. Hartwig, *J. Am. Chem. Soc.* **2014**, 136, 2555-2563; g) B. L. Tran, M. Driess, J. F. Hartwig, *J. Am. Chem. Soc.* **2014**, 136, 17292-17301.
- [5] a) E. Middleton, C. Kandaswani, T. C. Theoharides, *Pharmacol. Rev.* **2000**, 52, 673-751; b) D. F. Birt, S. Hendrich, W. Wang, *Pharmacol. Ther.* **2001**, 90, 157-177; c) M. Wang, *Toxicol. Sci.* **2007**, 96, 203-205; d) J. M. Patel, *Lethbridge Underg. Res. J.* **2008**, 3, 1-5; e) B. H. Havsteen, *Pharmacol. Ther.* **2002**, 96, 67-202; f) A. K. Verma, R. Pratap, *Nat. Prod. Rep.* **2010**, 27, 1571-1593; g) M. Cárdenas, M. Marder, V. C. Blank, L. P. Roguin, *Bioorg. Med. Chem.* **2006**, 14, 2966-2971; h) Y. P. Lin, F.-L. Hsu, C.-S. Chen, J.-W. Chern, M.-H. Lee, *Phytochemistry* **2007**, 68, 1189-1199; i) J. T. Zhu, R. C. Choi, G. K. Chu, A. W. Cheung, Q. T. Gao, J. Li, Z. Y. Jiang, T. T. Dong, K. W. Tsim, *J. Agric. Food Chem.* **2007**, 55, 2438-2445.
- [6] a) M. Khoobi, M. Alipour, S. Zarei, F. Jafarpour, A. Shafiee, *Chem. Commun.* **2012**, 48, 2985-2987; b) D. Kim, K. Ham, S. Hong, *Org. Biomol. Chem.* **2012**, 10, 7305-7315; c) J. Zhao, H. Fang, P. Qian, J. Han, Y. Pan, *Org. Lett.* **2014**, 16, 5342-5345; d) B. Niu, W. Zhao, Y. Ding, Z. Bian, C. U. Pittman, A. Zhou, H. Ge, *J. Org. Chem.* **2015**, 80, 7251-7257.
- [7] a) P. Z. Zhang, J. A. Li, L. Zhang, A. Shoberu, J. P. Zou, W. Zhang, *Green Chem.* **2017**, 19, 919-923; b) S. Guo, Q. Wang, Y. Jiang, J. T. Yu, *J. Org. Chem.* **2014**, 79, 11285-11289.
- [8] a) T. He, H. Li, P. Lia, L. Wang, *Chem. Commun.* **2011**, 47, 8946-8948; b) X. Li, B. Li, J. You, J. Lan, *Org. Biomol. Chem.* **2013**, 11, 1925-1928; c) D. Li, M. Wang, J. Liu, Q. Zhao, L. Wang, *Chem. Commun.* **2013**, 49, 3640-3642.
- [9] a) X.-F. Wu, H. Neumann, M. Beller, *Chem. Eur. J.* **2012**, 18, 12595-12598; b) P. Nussbaumer, P. Lehr, A. Billich, *J. Med. Chem.* **2002**, 45, 4310-4320; c) M. Miliutina, S. A. Ejaz, V. O. Iaroshenko, A. Villinger, J. Iqbal, P. Langer, *Org. Biomol. Chem.* **2016**, 14, 495-502.
- [10] a) Y. Zhang, J. Feng, C.-J. Li, *J. Am. Chem. Soc.* **2008**, 130, 2900-3001; b) Q. Dai, J.-T. Yu, X. Feng, Y. Jiang, H. Yang, J. Cheng, *Adv. Synth. Catal.* **2014**, 356, 3341-3346; c)

Q. Xia, X. Liu, Y. Zhang, C. Chen, W. Chen, *Org. Lett.* **2013**, *15*, 3326-3329; d) Y. Bao, Y. Yan, K. Xu, J. Su, Z. Zha, Z. Wang, *J. Org. Chem.* **2015**, *80*, 4736-4742.

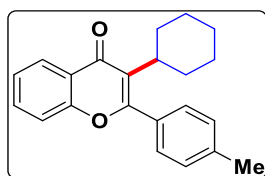
V.6. Spectral Data

3-Cyclohexyl-2-phenyl-4*H*-chromen-4-one (1a):



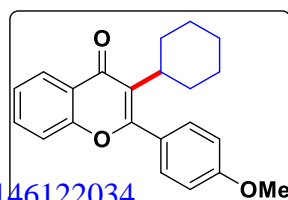
Solid, (105 mg, 69%), m. p. 102–104 °C. ¹H NMR (CDCl₃, 400 MHz): δ 8.22 (d, 1H, *J* = 8.0 Hz), 7.62 (t, 1H, *J* = 8.0 Hz), 7.53 (bs, 5H), 7.39–7.35 (m, 2H), 2.56–2.49 (m, 1H), 2.39–2.29 (m, 2H), 1.96–1.69 (m, 3H), 1.58–1.55 (m, 2H), 1.33–1.25 (m, 1H), 1.16–1.07 (m, 2H) ppm. ¹³C NMR (CDCl₃, 101 MHz): δ 178.7, 162.2, 155.9, 134.2, 133.3, 130.2, 128.8, 128.6, 125.9, 125.6, 124.8, 124.1, 117.9, 39.8, 29.9, 27.0, 25.9 ppm. IR (KBr, cm⁻¹): 3056, 2926, 2845, 1635, 1619, 1566, 1468, 1449, 1379, 1313, 1224, 1144, 1096, 1007, 999, 902, 774, 756, 702; HRMS (ESI/Q-TOF) *m/z*: calcd for C₂₁H₂₁O₂ (M + H)⁺ 305.1543, found 305.1550.

3-Cyclohexyl-2-(*p*-tolyl)-4*H*-chromen-4-one (2a):



Gummy, (97 mg, 61%). ¹H NMR (CDCl₃, 600 MHz): δ 8.21 (d, 1H, *J* = 8.1 Hz), 7.61 (t, 1H, *J* = 8.1 Hz), 7.44 (d, 2H, *J* = 7.8 Hz), 7.39–7.35 (m, 2H), 7.32 (d, 2H, *J* = 7.8 Hz), 2.58–2.53 (m, 1H), 2.46 (s, 3H), 2.39–2.32 (m, 2H), 1.76–1.71 (m, 3H), 1.63–1.54 (m, 2H), 1.33–1.25 (m, 1H), 1.15–1.11 (m, 2H) ppm. ¹³C NMR (CDCl₃, 151 MHz): δ 178.7, 162.4, 155.9, 140.4, 133.3, 131.3, 129.3, 128.7, 125.9, 125.5, 124.7, 124.1, 117.9, 39.8, 29.9, 27.0, 25.9, 21.7 ppm. IR (KBr, cm⁻¹): 2923, 2851, 1732, 1638, 1617, 1572, 1509, 1466, 1451, 1375, 1225, 1185, 1143, 1093, 1021, 1006, 905, 817, 758; HRMS (ESI/Q-TOF) *m/z*: calcd for C₂₂H₂₃O₂ (M + H)⁺ 319.1699, found 319.1706.

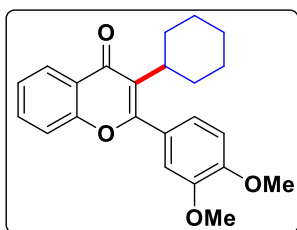
3-Cyclohexyl-2-(4-methoxyphenyl)-4*H*-chromen-4-one (3a):



Gummy, (95 mg, 57%). ¹H NMR (CDCl₃, 400 MHz): δ 8.20 (d, 1H, *J* = 8.0 Hz), 7.61 (t, 1H, *J* = 8.0 Hz), 7.50 (d, 2H, *J* = 8.0

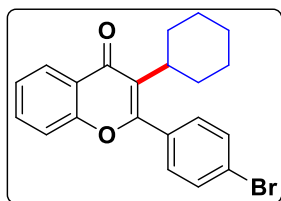
Hz), 7.39–7.34 (m, 2H), 7.03 (d, 2H, $J = 8.0$ Hz), 3.90 (s, 3H), 2.57 (t, 1H, $J = 8.0$ Hz), 2.41–2.31 (m, 2H), 1.64–1.54 (m, 3H), 1.77–1.74 (m, 2H), 1.25–1.09 (m, 3H) ppm. ^{13}C NMR (CDCl_3 , 101 MHz): δ 178.7, 162.2, 155.9, 134.1, 133.4, 130.3, 130.2, 128.8, 128.6, 125.9, 124.8, 117.9, 113.9, 55.6, 39.8, 29.9, 27.0, 25.9 ppm. IR (KBr, cm^{-1}): 2923, 2851, 1638, 1618, 1568, 1509, 1466, 1378, 1314, 1251, 1225, 1175, 1143, 1109, 1095, 1029, 1006, 904, 833, 760; HRMS (ESI/Q-TOF) m/z : calcd for $\text{C}_{22}\text{H}_{23}\text{O}_3$ ($\text{M} + \text{H}$) $^+$ 335.1648, found 335.1653.

3-Cyclohexyl-2-(3,4-dimethoxyphenyl)-4H-chromen-4-one (4a):



Gummy, (93 mg, 51%). ^1H NMR (CDCl_3 , 400 MHz): δ 8.20 (d, 1H, $J = 8.0$ Hz), 7.62 (t, 1H, $J = 8.0$ Hz), 7.41–7.34 (m, 2H), 7.16 (d, 1H, $J = 8.0$ Hz), 7.07 (s, 1H), 6.99 (d, 1H, $J = 8.0$ Hz), 3.97 (s, 3H), 3.94 (s, 3H), 2.64–2.58 (m, 1H), 2.42–2.33 (m, 2H), 1.78–1.75 (m, 2H), 1.61–1.55 (m, 2H), 1.34–1.23 (m, 2H), 1.16–1.12 (m, 2H) ppm. ^{13}C NMR (CDCl_3 , 101 MHz): δ 178.7, 162.0, 155.8, 150.5, 148.8, 133.3, 126.5, 125.9, 125.3, 124.7, 124.0, 121.9, 117.8, 111.7, 110.9, 56.2, 56.1, 39.9, 29.9, 27.1, 25.9 ppm. IR (KBr, cm^{-1}): 2923, 2850, 1636, 1617, 1564, 1512, 1466, 1416, 1374, 1330, 1262, 1236, 1169, 1097, 1025, 895, 861, 811, 761; HRMS (ESI/Q-TOF) m/z : calcd for $\text{C}_{23}\text{H}_{25}\text{O}_4$ ($\text{M} + \text{H}$) $^+$ 365.1754, found 365.1749.

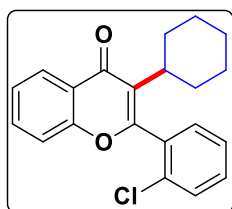
2-(4-Bromophenyl)-3-cyclohexyl-4H-chromen-4-one (5a):



Gummy, (86 mg, 69%). ^1H NMR (CDCl_3 , 400 MHz): δ 8.21 (d, 1H, $J = 8.0$ Hz), 7.68–7.61 (m, 3H), 7.43–7.36 (m, 4H), 2.50–2.44 (m, 1H), 2.38–2.28 (m, 2H), 1.77–1.74 (m, 2H), 1.59–1.52 (m, 2H), 1.37–1.25 (m, 2H), 1.21–1.07 (m, 2H) ppm. ^{13}C NMR (CDCl_3 , 151 MHz): δ 178.5, 160.9, 155.9, 133.5, 131.9, 130.7, 130.4, 126.1, 125.9, 124.9, 124.7, 124.1, 117.9, 39.9, 29.9, 26.9, 25.9 ppm. IR (KBr, cm^{-1}): 2923, 2849, 1640, 1617, 1571, 1487, 1467, 1397, 1225, 1183, 1144, 1108, 1094,

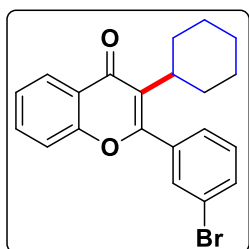
1069, 1011, 905, 823, 759; HRMS (ESI/Q-TOF) m/z : calcd for $C_{21}H_{20}BrO_2$ ($M + H$)⁺ 383.0647, found 383.0647.

2-(2-Chlorophenyl)-3-cyclohexyl-4*H*-chromen-4-one (6a):



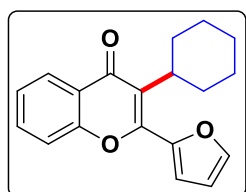
Gummy, (69 mg, 41%). ¹H NMR (CDCl₃, 400 MHz): δ 8.23 (d, 1H, $J = 8.0$ Hz), 7.63 (t, 1H, $J = 8.0$ Hz), 7.55 (d, 1H, $J = 8.0$ Hz), 7.49–7.47 (m, 1H), 7.41–7.37 (m, 3H), 7.36 (bs, 1H) 2.20–2.10 (m, 3H), 1.70–1.49 (m, 5H), 1.30–1.20 (m, 1H), 1.10–1.00 (m, 2H) ppm. ¹³C NMR (CDCl₃, 151 MHz): δ 178.5, 159.6, 156.1, 133.7, 133.5, 133.3, 131.4, 130.5, 130.2, 126.98, 126.93, 126.1, 124.9, 124.3, 117.9, 40.1, 29.8, 27.0, 25.9 ppm. IR (KBr, cm⁻¹): 2923, 2851, 1641, 1572, 1463, 1450, 1379, 1223, 1144, 1111, 1055, 1033, 1006, 906, 759; HRMS (ESI/Q-TOF) m/z : calcd for $C_{21}H_{20}ClO_2$ ($M + H$)⁺ 339.1153, found 339.1156.

2-(3-Bromophenyl)-3-cyclohexyl-4*H*-chromen-4-one (7a):



Gummy, (153 mg, 80%). ¹H NMR (CDCl₃, 400 MHz): δ 8.19 (d, 1H, $J = 7.6$ Hz), 7.69 (s, 1H), 7.65–7.59 (m, 2H), 7.46 (d, 1H, $J = 7.6$ Hz), 7.39–7.33 (m, 3H), 2.50–2.44 (m, 1H), 2.38–2.28 (m, 2H), 1.77–1.73 (m, 2H), 1.63–1.53 (m, 3H), 1.33–1.24 (m, 1H), 1.17–1.07 (m, 2H) ppm. ¹³C NMR (CDCl₃, 101 MHz): δ 178.3, 160.2, 155.7, 135.8, 133.4, 133.2, 131.7, 130.1, 127.4, 125.93, 125.86, 124.9, 123.9, 122.6, 117.8, 39.8, 29.8, 26.9, 25.8 ppm. IR (KBr, cm⁻¹): 2923, 2849, 1640, 1619, 1569, 1558, 1465, 1450, 1375, 1313, 1224, 1185, 1143, 1109, 1005, 962, 887, 788, 759; HRMS (ESI/Q-TOF) m/z : calcd for $C_{21}H_{20}BrO_2$ ($M + H$)⁺ 383.0647, found 383.0656.

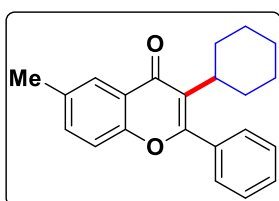
3-Cyclohexyl-2-(furan-2-yl)-4*H*-chromen-4-one (8a):



Gummy, (77 mg, 52%). ¹H NMR (CDCl₃, 400 MHz): δ 8.16 (d, 1H, $J = 8.0$ Hz), 7.66–7.59 (m, 2H), 7.41 (d, 1H, $J = 8.8$ Hz), 7.34 (t, 1H, $J = 7.8$ Hz), 6.98–6.94 (m, 1H), 6.61 (bs, 1H) 3.10–3.04 (m, 1H), 2.39–2.30 (m, 2H), 1.84–1.81 (m, 3H),

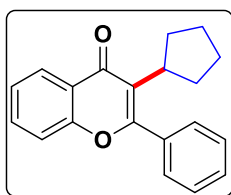
1.72–1.61 (m, 2H), 1.42–1.24 (m, 3H) ppm. ^{13}C NMR (CDCl_3 , 101 MHz): δ 178.7, 155.4, 151.5, 147.2, 144.7, 133.4, 125.9, 125.3, 124.8, 123.9, 117.7, 114.6, 111.9, 38.7, 29.7, 27.2, 26.1 ppm. IR (KBr, cm^{-1}): 2925, 2853, 1724, 1639, 1621, 1580, 1466, 1451, 1401, 1370, 1145, 1089, 1068, 1025, 759, 711; HRMS (ESI/Q-TOF) m/z : calcd for $\text{C}_{19}\text{H}_{19}\text{O}_3$ ($\text{M} + \text{H}$) $^+$ 295.1135, found 295.1341.

3-Cyclohexyl-6-methyl-2-phenyl-4*H*-chromen-4-one (9a):

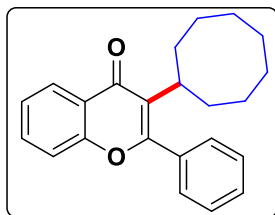


Gummy, (62 mg, 39%). ^1H NMR (CDCl_3 , 400 MHz): δ 7.99 (s, 1H), 7.55–7.50 (m, 5H), 7.43 (d, 1H $J = 8.0$ Hz), 7.29 (bs, 1H), 2.55–2.48 (m, 1H), 2.45 (s, 3H), 2.35–2.28 (m, 2H), 1.76–1.72 (m, 2H), 1.59–1.54 (m, 2H), 1.33–1.28 (m, 2H), 1.16–1.06 (m, 2H) ppm. ^{13}C NMR (CDCl_3 , 101 MHz): δ 178.7, 162.0, 154.1, 134.6, 134.5, 134.2, 130.1, 128.7, 128.6, 125.3, 125.2, 123.7, 117.6, 39.8, 29.8, 26.9, 25.9, 21.2 ppm. IR (KBr, cm^{-1}): 2625, 2851, 1633, 1617, 1603, 1571, 1493, 1485, 1445, 1430, 1367, 1279, 1262, 1227, 1207, 1145, 1131, 1094, 1025, 962, 821, 802, 787, 756; HRMS (ESI/Q-TOF) m/z : calcd for $\text{C}_{22}\text{H}_{23}\text{O}_2$ ($\text{M} + \text{H}$) $^+$ 319.1699, found 319.1704.

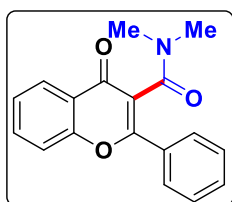
3-Cyclopentyl-2-phenyl-4*H*-chromen-4-one (1b):



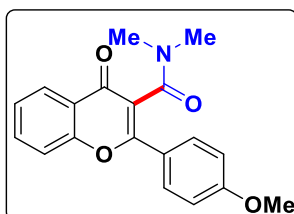
Gummy, (86 mg, 59%). ^1H NMR (CDCl_3 , 400 MHz): δ 8.23 (d, 1H, $J = 8.0$ Hz), 7.65–7.61 (m, 1H), 7.55–7.52 (m, 5H), 7.40–7.37 (m, 2H), 2.56–2.46 (m, 1H), 2.39–2.29 (m, 1H), 1.76–1.73 (m, 2H), 1.62–1.55 (m, 2H), 1.33–1.24 (m, 2H), 1.16–1.06 (m, 1H) ppm. ^{13}C NMR (CDCl_3 , 101 MHz): δ 178.7, 162.2, 155.9, 134.2, 133.4, 130.2, 129.1, 128.8, 128.7, 126.0, 125.7, 124.8, 117.9, 39.9, 30.8, 29.9, 27.0, 25.9 ppm. IR (KBr, cm^{-1}): 2922, 2849, 1638, 1619, 1568, 1466, 1445, 1379, 1312, 1225, 1143, 1023, 1006, 760; HRMS (ESI/Q-TOF) m/z : calcd for $\text{C}_{20}\text{H}_{19}\text{O}_2$ ($\text{M} + \text{H}$) $^+$ 291.1386, found 291.1390.

3-Cyclooctyl-2-phenyl-4H-chromen-4-one (1c):

Gummy, (88 mg, 53%). ^1H NMR (CDCl_3 , 400 MHz): δ 8.22 (d, 1H, $J = 8.0$ Hz), 7.63 (t, 1H, $J = 7.8$ Hz), 7.57–7.55 (m, 5H), 7.41–7.35 (m, 2H), 2.79–2.74 (m, 1H), 2.32–2.27 (m, 2H), 1.76–1.68 (m, 2H), 1.62–1.56 (m, 3H), 1.47–1.42 (m, 3H), 1.39–1.34 (m, 1H), 1.33–1.26 (m, 3H) ppm. ^{13}C NMR (CDCl_3 , 101 MHz): δ 178.5, 161.1, 156.0, 134.1, 133.4, 130.2, 128.8, 128.59, 128.55, 125.9, 124.7, 124.2, 117.9, 38.0, 32.2, 26.8, 26.7, 26.5 ppm. IR (KBr, cm^{-1}): 2921, 2849, 1639, 1621, 1570, 1463, 1383, 1224, 1180, 1102, 1019, 894, 769; HRMS (ESI/Q-TOF) m/z : calcd for $\text{C}_{23}\text{H}_{25}\text{O}_2$ ($\text{M} + \text{H}^+$) 333.1856, found 333.1850.

***N,N*-Dimethyl-4-oxo-2-phenyl-4H-chromene-3-carboxamide (1a')**

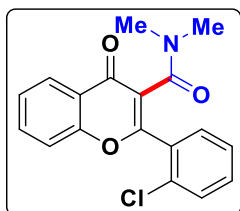
Gummy, (85 mg, 58%). ^1H NMR (CDCl_3 , 400 MHz): δ 8.26 (d, 1H, $J = 8.0$ Hz), 7.83 (d, 1H, $J = 7.6$ Hz), 7.72 (t, 1H, $J = 7.8$ Hz), 7.55–7.42 (m, 6H), 3.06 (s, 3H), 2.84 (s, 3H) ppm. ^{13}C NMR (CDCl_3 , 101 MHz): δ 175.6, 165.6, 160.8, 156.1, 134.4, 131.9, 131.7, 129.0, 128.2, 126.2, 125.7, 123.2, 119.8, 118.2, 38.0, 35.0 ppm. IR (KBr, cm^{-1}): 2925, 2846, 1637, 1565, 1494, 1465, 1446, 1400, 1376, 1111, 1076, 1025, 909, 871, 764; HRMS (ESI/Q-TOF) m/z : calcd for $\text{C}_{18}\text{H}_{16}\text{NO}_3$ ($\text{M} + \text{H}^+$) 294.1131, found 294.1133.

2-(4-Methoxyphenyl)-*N,N*-dimethyl-4-oxo-4H-chromene-3-carboxamide (3a')

Gummy, (74 mg, 46%). ^1H NMR (CDCl_3 , 400 MHz): δ 8.24 (d, 1H, $J = 7.8$ Hz), 7.81 (d, 1H, $J = 8.8$), 7.71 (t, 1H, $J = 7.0$ Hz), 7.53–7.41 (m, 3H), 6.99 (d, 2H, $J = 9.2$ Hz), 3.88 (s, 3H), 3.09 (s, 3H), 2.85 (s, 3H) ppm. ^{13}C NMR (CDCl_3 , 101 MHz): δ 175.6, 166.1, 162.3, 156.1, 134.2, 130.5, 129.9, 126.2, 125.5, 124.2, 123.2, 118.1, 114.6, 114.5, 55.7, 38.0, 35.1 ppm. IR (KBr, cm^{-1}): 2925, 2850, 1636, 1617, 1511, 1466, 1375, 1307, 1259, 1181,

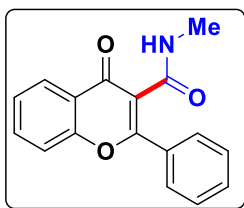
1109, 1076, 1025, 969, 912, 873, 840, 764; HRMS (ESI/Q-TOF) m/z : calcd for $C_{19}H_{18}NO_4$ ($M + H$)⁺ 324.1237, found 324.1243.

2-(2-Chlorophenyl)-*N,N*-dimethyl-4-oxo-4*H*-chromene-3-carboxamide (6a):



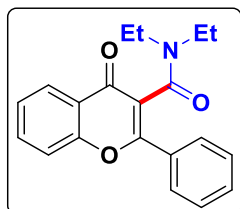
Gummy, (49 mg, 30%). ¹H NMR ($CDCl_3$, 400 MHz): δ 8.28 (d, 1H, $J = 8.0$ Hz), 7.75–7.67 (m, 2H), 7.53–7.44 (m, 4H), 7.38 (t, 1H, $J = 7.5$ Hz), 2.91 (s, 3H), 2.91 (s, 3H) ppm. ¹³C NMR ($CDCl_3$, 151 MHz): δ 175.2, 164.3, 160.4, 156.3, 134.6, 133.0, 132.2, 131.8, 130.9, 130.1, 128.5, 127.1, 126.3, 125.8, 123.5, 118.4, 38.2, 34.9 ppm. IR (KBr, cm^{-1}): 2925, 2853, 1718, 1644, 1573, 1463, 1441, 1401, 1376, 1261, 1216, 1110, 1082, 1057, 915, 875, 762; HRMS (ESI/Q-TOF) m/z : calcd for $C_{18}H_{15}ClNO_3$ ($M + H$)⁺ 328.0741, found 328.0736.

***N*-Methyl-4-oxo-2-phenyl-4*H*-chromene-3-carboxamide (1b):**



Gummy, (77 mg, 55%). ¹H NMR ($CDCl_3$, 400 MHz): δ 8.25 (d, 1H, $J = 8.0$ Hz), 8.08 (bs, 1H), 7.76–7.68 (m, 3H), 7.54–7.45 (m, 5H), 2.92 (d, 3H, $J = 8.0$ Hz) ppm. ¹³C NMR ($CDCl_3$, 151 MHz): δ 177.6, 168.5, 164.4, 155.6, 134.7, 133.7, 131.3, 128.7, 128.5, 126.3, 126.0, 123.5, 118.2, 116.6, 26.6 ppm. IR (KBr, cm^{-1}): 3278, 2925, 2853, 1636, 1570, 1493, 1467, 1446, 1393, 1261, 1171, 1130, 761; HRMS (ESI/Q-TOF) m/z : calcd for $C_{17}H_{14}NO_3$ ($M + H$)⁺ 280.0974, found 280.0977.

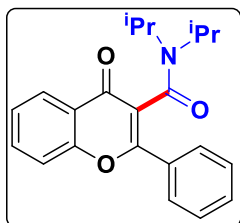
***N,N*-Diethyl-4-oxo-2-phenyl-4*H*-chromene-3-carboxamide (1c):**



Gummy, (85 mg, 53%). ¹H NMR ($CDCl_3$, 400 MHz): δ 8.25 (d, 1H, $J = 8.0$ Hz), 7.91 (d, 1H, $J = 8.6$ Hz), 7.72 (t, 1H, $J = 7.8$ Hz), 7.55–7.42 (m, 6H), 3.75–3.69 (m, 1H), 3.36–3.31 (m, 1H), 3.22–3.16 (m, 1H), 3.12–3.04 (m, 1H), 1.33 (t, 3H, $J = 7.2$ Hz), 0.86 (t, 3H, $J = 7.2$ Hz) ppm. ¹³C NMR ($CDCl_3$, 151 MHz): δ 175.9, 164.7, 160.3, 156.2, 134.3, 132.1, 131.6, 128.8, 128.5, 126.3, 125.6, 123.3, 120.3, 118.2, 43.3, 39.3, 13.9, 12.4 ppm. IR (KBr, cm^{-1}): 2975, 2932, 1718, 2907, 2163, 1565, 1465, 1446, 1378, 1270, 1220, 1180, 1151, 1111, 1028, 902, 852, 763;

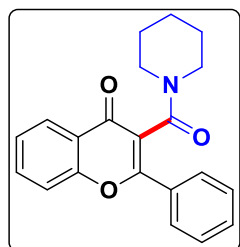
HRMS (ESI/Q-TOF) m/z : calcd for $C_{20}H_{20}NO_3$ ($M + H$)⁺
322.1444, found 322.1450.

***N,N*-Diisopropyl-4-oxo-2-phenyl-4*H*-chromene-3-carboxamide (1d):**



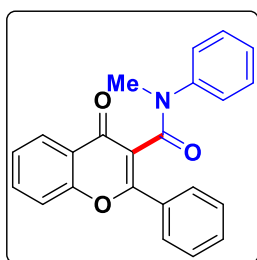
Gummy. (89 mg, 51%). ¹H NMR (CDCl₃, 600 MHz): δ 8.23 (d, 1H, $J = 7.8$ Hz), 7.95 (d, 2H, $J = 7.8$ Hz), 7.71 (t, 1H, $J = 7.8$ Hz), 7.54–7.42 (m, 5H), 3.80–3.76 (m, 1H), 3.38–3.34 (m, 1H), 1.61 (d, 3H, $J = 6.6$ Hz), 1.40 (d, 3H, $J = 6.6$ Hz), 1.12 (d, 3H, $J = 6.6$ Hz), 0.55 (d, 3H, $J = 6.6$ Hz) ppm. ¹³C NMR (CDCl₃, 151 MHz): δ 175.9, 164.2, 159.6, 156.2, 134.2, 132.1, 131.5, 128.7, 128.6, 126.2, 125.5, 123.4, 121.6, 118.2, 51.7, 46.3, 21.2, 20.6, 20.2, 19.8 ppm. IR (KBr, cm⁻¹): 2969, 2928, 1644, 1564, 1494, 1465, 1446, 1371, 1332, 1214, 1178, 1140, 1110, 1086, 1040, 907, 833, 791, 762; HRMS (ESI/Q-TOF) m/z : calcd for $C_{22}H_{24}NO_3$ ($M + H$)⁺ 350.1757, found 350.1761.

2-Phenyl-3-(piperidine-1-carbonyl)-4*H*-chromen-4-one (1e):



Gummy. (82 mg, 69%). ¹H NMR (CDCl₃, 400 MHz): δ 8.25 (d, 1H, $J = 8.0$ Hz), 7.90–7.87 (m, 2H), 7.72 (t, 1H, $J = 9.0$ Hz), 7.54–7.50 (m, 4H), 7.44 (t, 1H, $J = 7.0$ Hz), 3.90–3.84 (m, 1H), 3.53–3.47 (m, 1H), 3.23–3.20 (m, 2H), 1.52–1.47 (m, 3H), 1.38–1.34 (m, 1H), 0.88–0.81 (m, 2H) ppm. ¹³C NMR (CDCl₃, 101 MHz): δ 175.7, 163.7, 160.4, 156.2, 134.3, 132.1, 131.7, 128.9, 128.5, 126.3, 125.6, 123.3, 119.9, 118.2, 47.9, 42.7, 26.1, 25.3, 24.6 ppm. IR (KBr, cm⁻¹): 2925, 2853, 1644, 1621, 1563, 1466, 1457, 1446, 1377, 1256, 1228, 1123, 1097, 1028, 1007, 860, 786, 758; HRMS (ESI/Q-TOF) m/z : calcd for $C_{21}H_{20}NO_3$ ($M + H$)⁺ 334.1444, found 334.1440.

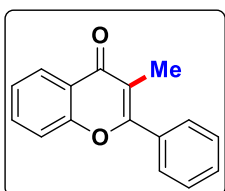
***N*-Methyl-4-oxo-*N*,2-diphenyl-4*H*-chromene-3-carboxamide (1f):**



Gummy. (75 mg, 42%). ¹H NMR (CDCl₃, 600 MHz): δ 8.26 (d, 1H, $J = 8.0$ Hz), 7.67–7.63 (m, 4H), 7.54–7.51 (m, 5H), 7.46 (d, 2H, $J = 8.0$ Hz), 7.42–7.35 (m, 2H), 2.17 (s, 3H) ppm. ¹³C NMR (CDCl₃, 151 MHz): δ 179.1, 161.3, 156.7, 154.4, 134.9, 133.7,

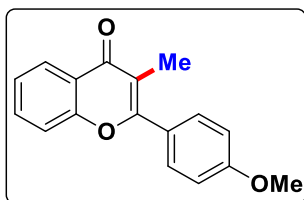
133.6, 130.4, 130.3, 129.2, 128.7, 128.6, 126.1, 125.3, 124.9, 118.1, 117.84, 117.76, 29.9 ppm. IR (KBr, cm^{-1}): 2923, 2850, 1723, 1639, 1572, 1468, 1449, 1372, 1285, 1233, 1132, 1110, 1015, 760.

3-Methyl-2-phenyl-4*H*-chromen-4-one (1A):



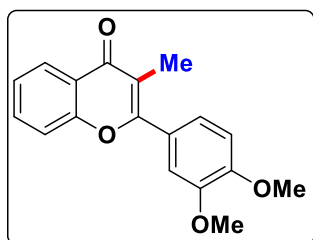
Gummy, (63 mg, 53%). ^1H NMR (CDCl_3 , 400 MHz): δ 8.26 (d, 1H, $J = 8.0$ Hz), 7.67–7.64 (m, 3H), 7.54–7.52 (m, 3H), 7.46 (d, 1H, $J = 8.4$ Hz), 7.40 (t, 1H, $J = 7.5$ Hz), 2.17 (s, 3H) ppm. ^{13}C NMR (CDCl_3 , 101 MHz): δ 179.1, 161.2, 156.3, 133.5, 130.4, 129.1, 128.6, 126.3, 126.1, 124.9, 122.7, 118.1, 117.7, 11.9 ppm. IR (KBr, cm^{-1}): 2923, 2850, 1739, 1639, 1571, 1494, 1467, 1450, 1389, 1372, 1232, 1132, 1109, 1079, 1015, 857, 761; HRMS (ESI/Q-TOF) m/z : calcd for $\text{C}_{16}\text{H}_{13}\text{O}_2$ ($\text{M} + \text{H}$) $^+$ 237.0917, found 237.0923.

2-(4-Methoxyphenyl)-3-methyl-4*H*-chromen-4-one (3A):



Gummy, (57 mg, 43%). ^1H NMR (CDCl_3 , 400 MHz): δ 8.25 (d, 1H, $J = 8.0$ Hz), 7.67–7.61 (m, 3H), 7.45 (d, 1H, $J = 8.0$ Hz), 7.39 (t, 1H, $J = 8.0$ Hz), 7.04 (d, 2H, $J = 12.0$ Hz), 3.90 (s, 3H), 2.19 (s, 3H) ppm. ^{13}C NMR (CDCl_3 , 151 MHz): δ 179.2, 161.2, 156.3, 133.4, 130.8, 126.1, 126.0, 124.8, 122.7, 117.9, 117.1, 114.6, 114.0, 55.6, 12.1 ppm. IR (KBr, cm^{-1}): 2920, 2850, 1640, 1622, 1610, 1577, 1515, 1469, 1391, 1369, 1310, 1263, 1181, 1116, 1020, 836, 753; HRMS (ESI/Q-TOF) m/z : calcd for $\text{C}_{17}\text{H}_{15}\text{O}_3$ ($\text{M} + \text{H}$) $^+$ 267.1022, found 267.1020.

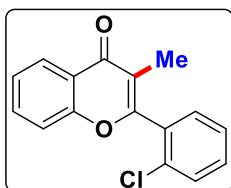
2-(3,4-Dimethoxyphenyl)-3-methyl-4*H*-chromen-4-one (4A):



Gummy, (50 mg, 34%). ^1H NMR (CDCl_3 , 400 MHz): δ 8.26 (d, 1H, $J = 8.0$ Hz), 7.66 (t, 1H, $J = 8.0$ Hz), 7.47 (t, 1H, $J = 8.0$ Hz), 7.40 (t, 1H, $J = 8.0$ Hz), 7.24 (s, 1H), 7.18 (s, 1H), 7.00 (d, 1H, $J = 8.0$ Hz), 3.97 (s, 3H), 3.96 (s, 3H), 2.20 (s, 3H) ppm. ^{13}C NMR (CDCl_3 , 151 MHz): δ 179.1, 161.2, 156.2, 150.8, 148.9, 133.5, 126.13, 126.09, 124.9, 122.7, 118.0, 117.2, 111.9, 110.9,

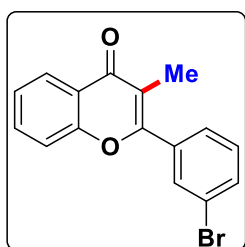
56.3, 56.2, 12.2 ppm. IR (KBr, cm^{-1}): 2923, 2848, 1638, 1606, 1572, 1519, 1477, 1469, 1444, 1392, 1369, 1343, 1281, 1266, 1247, 1226, 1172, 1147, 1128, 1108, 1022, 993, 894, 870, 850, 823, 752; HRMS (ESI/Q-TOF) m/z : calcd for $\text{C}_{18}\text{H}_{17}\text{O}_4$ ($\text{M} + \text{H}$)⁺ 297.1128, found 297.1130.

2-(2-Chlorophenyl)-3-methyl-4H-chromen-4-one (6A):



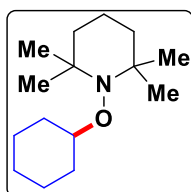
Gummy, (53 mg, 39%). ¹H NMR (CDCl_3 , 400 MHz): δ 8.28 (d, 1H, $J = 8.0$ Hz), 7.69–7.62 (m, 1H), 7.54 (t, 1H, $J = 8.0$ Hz), 7.49–7.46 (m, 1H), 7.48–7.39 (m, 4H), 1.94 (s, 3H) ppm. ¹³C NMR (CDCl_3 , 151 MHz): δ 178.8, 159.3, 156.5, 133.7, 131.5, 130.9, 130.3, 127.1, 126.1, 125.1, 122.9, 119.7, 118.2, 116.4, 114.4, 11.5 ppm. IR (KBr, cm^{-1}): 2924, 2848, 1643, 1575, 1467, 1440, 1390, 1373, 1230, 1138, 1110, 1066, 1014, 857, 759; HRMS (ESI/Q-TOF) m/z : calcd for $\text{C}_{16}\text{H}_{12}\text{ClO}_2$ ($\text{M} + \text{H}$)⁺ 271.0527, found 271.052.

2-(3-Bromophenyl)-3-methyl-4H-chromen-4-one (7A):



Gummy, (52 mg, 33%). ¹H NMR (CDCl_3 , 600 MHz): δ 8.26 (d, 1H, $J = 6.0$ Hz), 7.81 (s, 1H), 7.69–7.65 (m, 2H), 7.58 (d, 1H, $J = 6.0$ Hz), 7.47 (d, 1H, $J = 6.0$ Hz), 7.42–7.39 (m, 2H), 2.16 (s, 3H) ppm. ¹³C NMR (CDCl_3 , 151 MHz): δ 178.9, 159.5, 156.3, 135.5, 133.8, 133.4, 132.0, 130.2, 127.9, 126.1, 125.1, 122.7, 122.6, 118.2, 118.1, 11.9 ppm. IR (KBr, cm^{-1}): 2923, 2848, 1646, 1607, 1574, 1559, 1467, 1384, 1368, 1252, 1231, 1132, 1112, 1073, 1021, 790, 778, 754, 717; HRMS (ESI/Q-TOF) m/z : calcd for $\text{C}_{16}\text{H}_{12}\text{BrO}_2$ ($\text{M} + \text{H}$)⁺ 315.0021, found 315.0016.

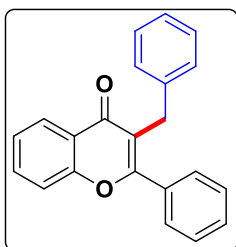
1-(Cyclohexyloxy)-2,2,6,6-tetramethylpiperidine (1B):



Gummy, (67 mg, 56%). ¹H NMR (CDCl_3 , 400 MHz): δ 3.59 (bs, 1H), 2.06 (bs, 2H), 1.76 (bs, 2H), 1.62–1.45 (m, 6H), 1.29–1.12 (m, 18H) ppm. ¹³C NMR (CDCl_3 , 101 MHz): δ 81.9, 59.8, 40.4, 34.6, 33.1, 26.1, 25.3, 17.5 ppm. IR (KBr, cm^{-1}): 2932, 2855, 1453, 1374, 1359, 1257, 1242, 1208, 1181, 1132, 1058, 1044,

1020, 993, 966, 913, 890, 786, 711; HRMS (ESI/Q-TOF) m/z :
calcd for $C_{15}H_{27}NO$ ($M + H$)⁺ 240.2328, found 240.2333.

3-Benzyl-2-phenyl-4*H*-chromen-4-one (1a''):

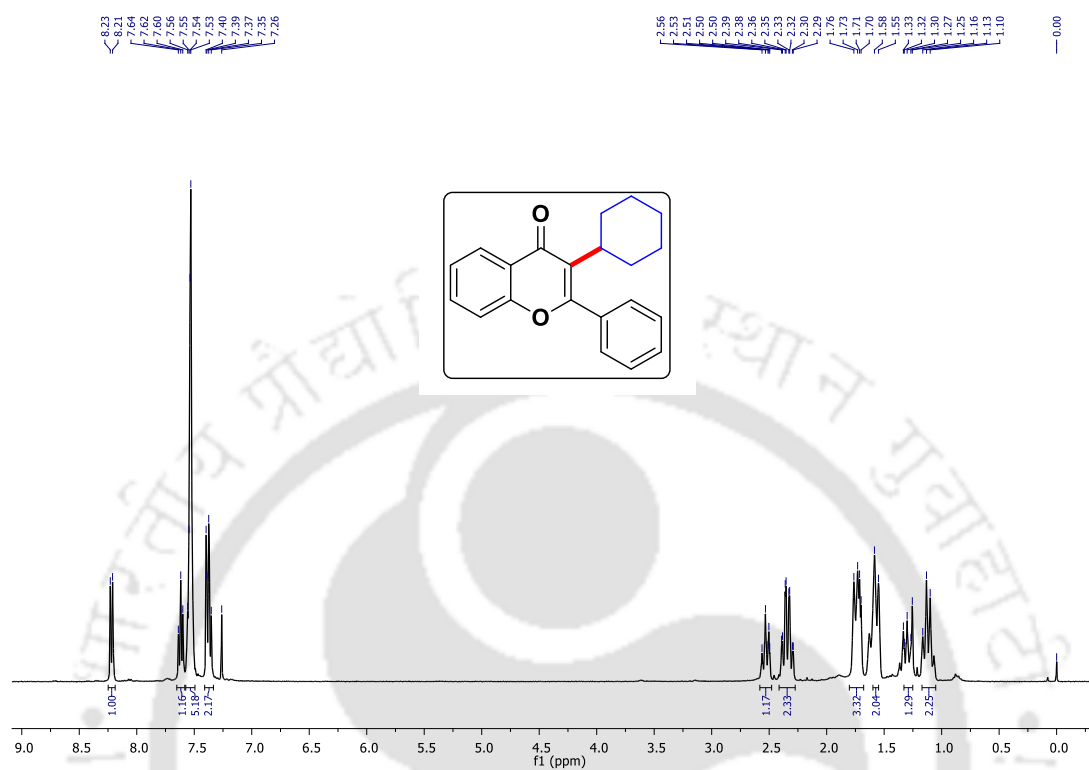


Gummy, (19 mg, 12%). ¹H NMR (CDCl₃, 400 MHz): δ 8.27 (d, 1H, $J = 8.0$ Hz), 7.93–7.90 (m, 1H), 7.67–7.65 (m, 3H), 7.56–7.52 (m, 4H), 7.47 (t, 2H, $J = 8.0$ Hz), 7.40 (t, 1H, $J = 8.0$ Hz), 7.23–7.21 (m, 2H), 2.18 (s, 2H) ppm. HRMS (ESI/Q-TOF) m/z : calcd for $C_{22}H_{17}O_2$ ($M + H$)⁺ 313.1229, found 313.1238.

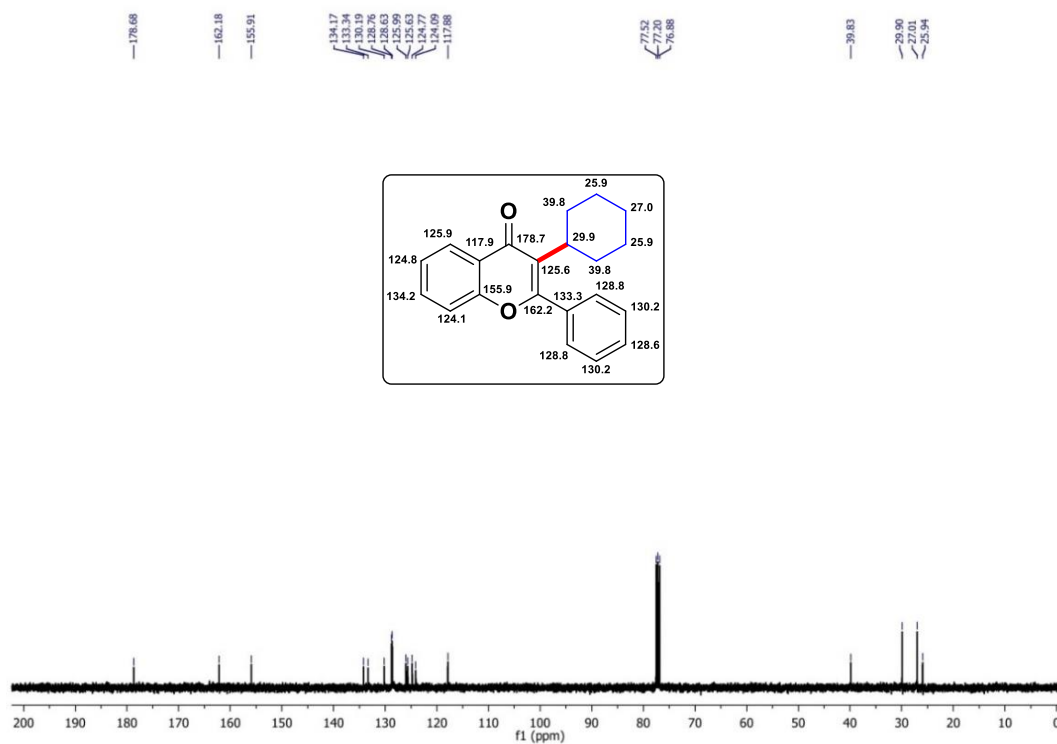


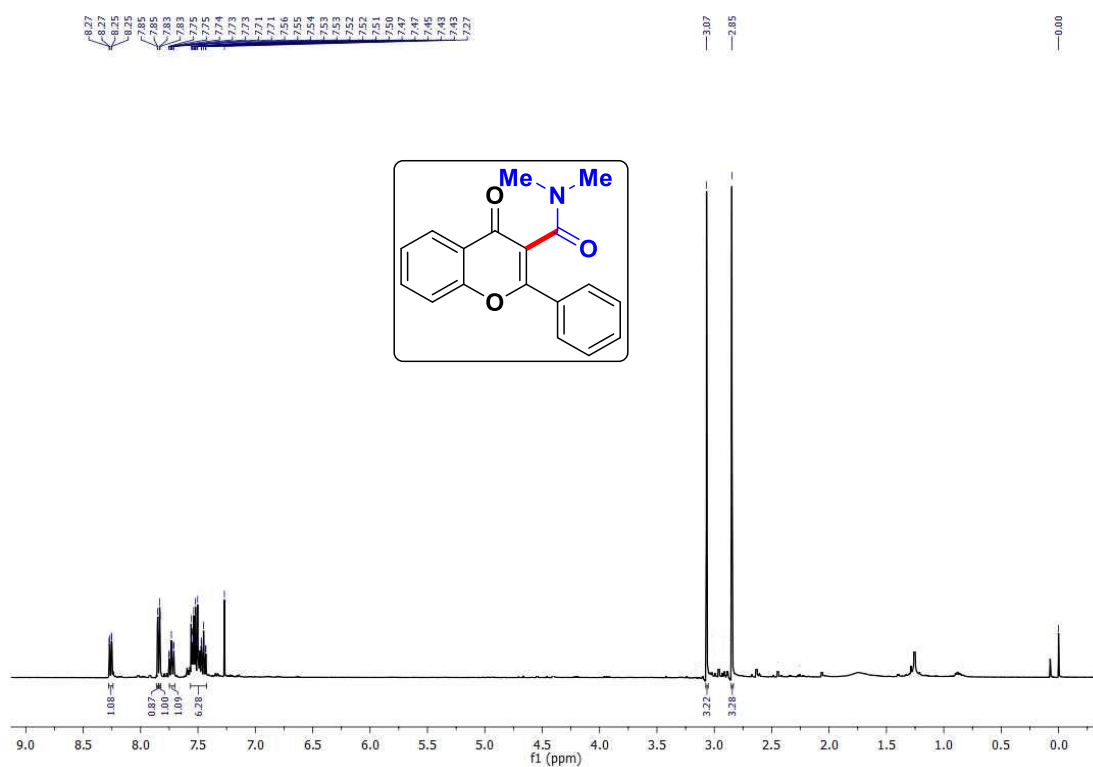
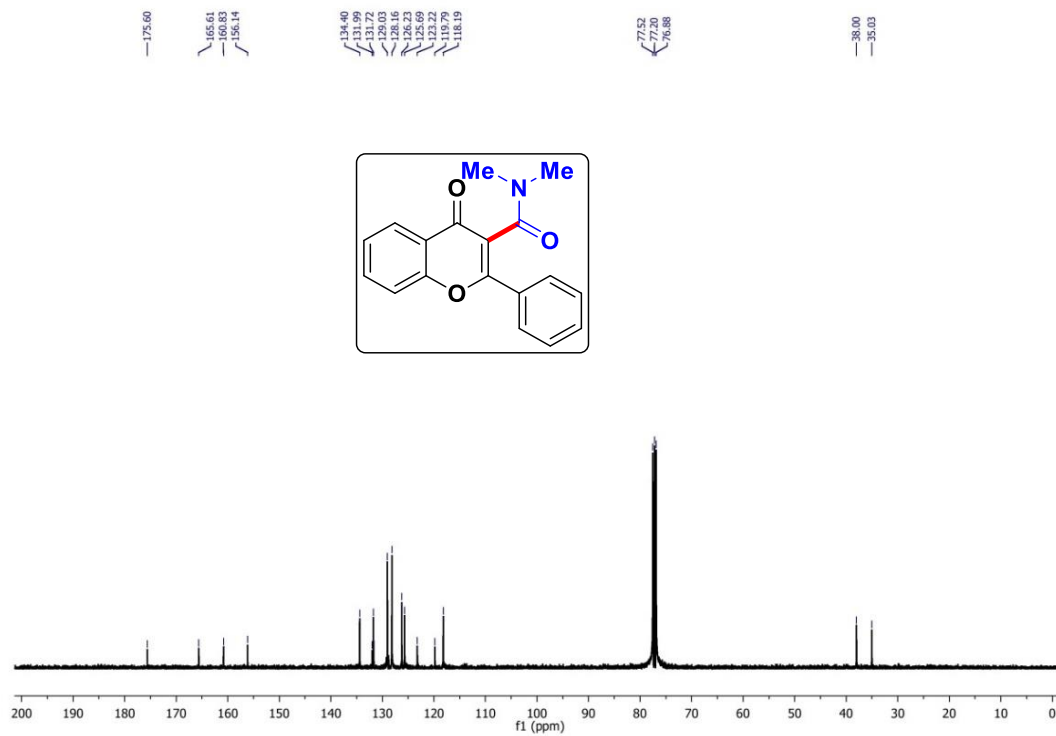
V.7. Spectra

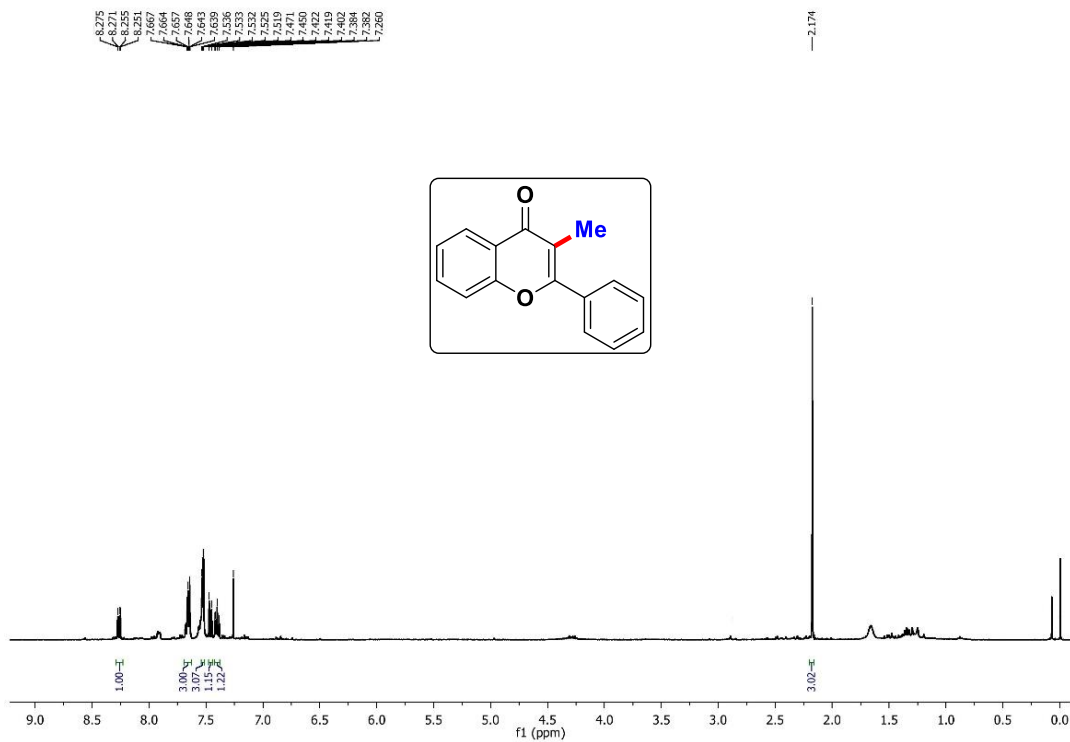
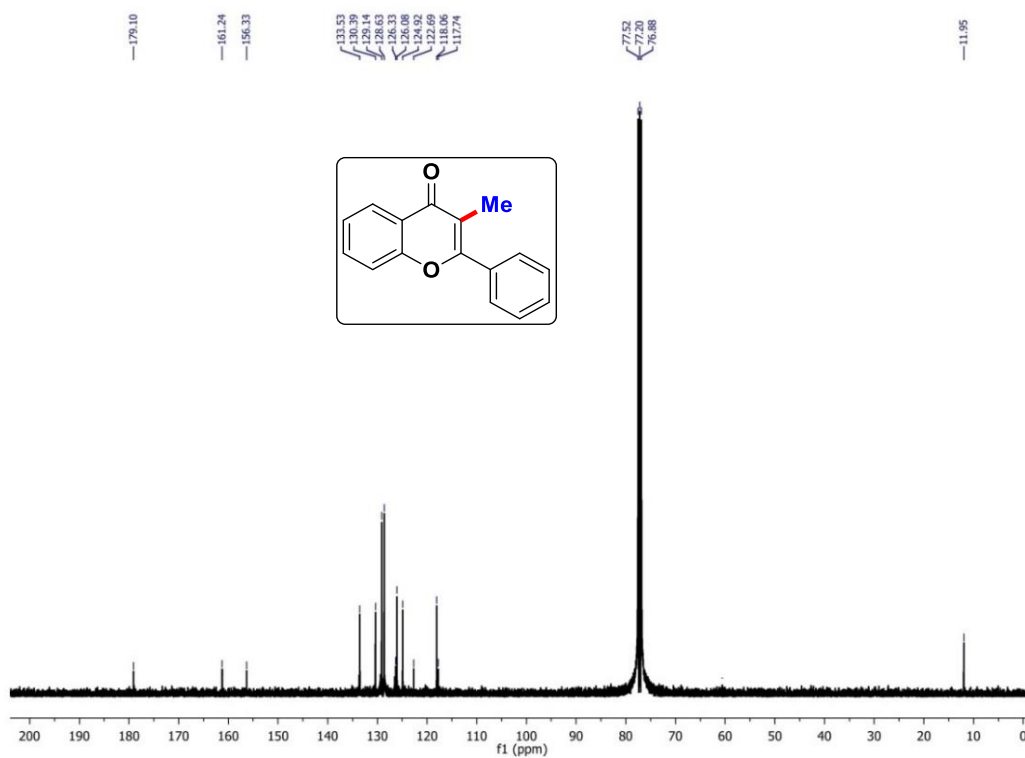
3-Cyclohexyl-2-phenyl-4H-chromen-4-one (1a): ^1H NMR (CDCl_3 , 400 MHz)



3-Cyclohexyl-2-phenyl-4H-chromen-4-one (1a): ^{13}C NMR (CDCl_3 , 101 MHz)



N,N*-Dimethyl-4-oxo-2-phenyl-4*H*-chromene-3-carboxamide (1a')**: ^1H NMR (CDCl_3 , 400 MHz)N,N*-Dimethyl-4-oxo-2-phenyl-4*H*-chromene-3-carboxamide (1a')**: ^{13}C NMR (CDCl_3 , 101 MHz)

3-Methyl-2-phenyl-4H-chromen-4-one (1A): ^1H NMR (CDCl_3 , 400 MHz)**3-Methyl-2-phenyl-4H-chromen-4-one (1A): ^{13}C NMR (CDCl_3 , 101 MHz)**

List of Publications:

1. Iron(III) catalyzed peroxide mediated C-3 functionalizations of flavones
Mir, B. A., Banerjee, A., Santra S. K., Rajamanickam, S. Patel, B. K. *Adv. Synth. Catal.* **2016**, 358, 3471.
2. *tert*-Butyl nitrite mediated different functionalizations of internal alkenes: paths to furoxans and nitroalkenes
Mir, B. A., Singh, S. J., Kumar, R., Patel, B. K. *Adv. Synth. Catal.* **2018**, 360, 3801.
3. Cu(I) Catalyzed differential peroxidation of terminal and internal alkenes using TBHP
Mir, B. A., Rajamanickam, S., Begum, P., Patel, B. K. *Eur. J. Org. Chem.* **2020**, 252.
4. *tert*-Butyl Nitrite Mediated Nitro-Nitratation of Internal Alkenes
Mir, B. A., Rajamanickam, S., Begum, P., Patel, B. K. *under communication.*
5. A TBPB-mediated C-3 cycloalkylation and formamidation of 4-arylcoumarin
Singh, S. J., **Mir, B. A.,** Patel, B. K. *Eur. J. Org. Chem.* **2018**, 1026.
6. Bu₄Ni-Catalyzed, radical-induced regioselective *N*-alkylations and arylations of tetrazoles using organic peroxides/peresters
Rajamanickam, S., Sah, C., **Mir, B. A.,** Ghosh, S., Sethi, G., Yadav, V., Venkataramani S., Patel, B. K. *J. Org. Chem.* DOI:10.1021/acs.joc.9b02875.